MITOCHONDRIAL DYSFUNCTION IN THE STRIATUM: IMPLICATIONS FOR L-DOPA INDUCED DYSKINESIA

By

Emily Booth Warren

Dissertation

Submitted to the Faculty of the

Graduate School of Vanderbilt University

in partial fulfillment of the requirements

for the degree of

DOCTOR OF PHILOSOPHY

in

Pharmacology

February 28, 2018

Nashville, TN

Approved:

Christine Konradi, Ph.D.

Aaron B. Bowman, Ph.D.

Joshua P. Fessel, M.D., Ph.D.

Eugenia Gurevich, Ph.D.

Qi Zhang, Ph.D.

To Kirti and Amy, who have endured.

ACKNOWLEDGEMENTS

I am profoundly grateful to the vast number of people who have supported me throughout my PhD program. First, I would like to thank my advisor, Christine Konradi, for her mentorship, guidance, and training. I am also indebted to the members of my committee, Qi Zhang, Eugenia Gurevich, Josh Fessel, and Aaron Bowman, for their patience and assistance throughout my graduate career. I am especially appreciative of Aaron's generosity over the last few months of my graduate work, by providing me a place in his own lab and a rare opportunity to continue to grow in a new setting.

I would like to thank the Department of Pharmacology for continuing to support me as I completed my dissertation, with an especial thanks to Karen Gieg for her tireless efforts. I am also grateful to Dehui Mi and Josh Bauer of the High Throughput Screening Core, Sean Schaffer and Bob Matthews of the Cell Imaging Shared Resource, and Donald Stec and Markus Voehler of the Small Molecule and Biomolecular NMR facilities. A large portion of the work in this dissertation depended on the expertise of these members of these core facilities, and all have been exceptionally willing to help and answer my endless questions.

I would also like to thank the friends that I have made here at Vanderbilt, and especially those that have been lab members as well, both at the beginning of this journey and at the end. Sharing this experience has been instrumental in completing it. I am grateful to my family for their belief in me and their unwavering support, and I would not be where I am today without them. Finally, I am intensely thankful to my friends, Kirti Sarkar and Amy Hassenberg, who have been there for me since before I even considered applying to graduate school. They have heard more about this project and this process than anyone, and I am more indebted to them than words can say.

TABLE OF CONTENTS

Page

LIST OF TABLES

Page

LIST OF FIGURES

Page

LIST OF ABBREVIATIONS

3-MT	3-Methoxytyramine
6-OHDA	6-Hydroxydopamine
6PGD	6-phosphogluconate dehydrogenase
6PGLS	6-phosphogluconolactonase
A2AR	Adenosine 2A Receptor
AADC/DDC	Aromatic L-Amino Acid Decarboxylase/Dopa Decarboxylase
ABAT	Aminobutyrate Transaminase
AC	Adenylyl Cyclase
ACO	Aconitase
AD	Alzheimer's Disease
AGAT	Arginine:Glycine Amidinotransferase
AGC	Aspartate-Glutamate Carrier
AIM	Abnormal Involuntary Movements
AKAP	A-kinase Anchoring Protein
ALAT	Alanine Transaminase
ALDO	Aldolase
AMPA(R)	α-Amino-3-Hydroxy-5-Methyl-4-Isoxazolepropionic Acid (Receptor)
AMPK	AMP Kinase
ANLS	Astrocyte-Neuron Lactate Shuttle
ANT	Adenine Nucleotide Translocase
AP2	Adaptor Protein Complex
APC/C-CDH1	Anaphase Promoting Complex-Cadherin 1
AraC	Cytosine Arabinoside
AST	Aspartate Transaminase
ATP	Adenosine Triphosphate
B-CK	Brain Cytosolic Creatine Kinase
Ca^{2+}	Calcium
CAC	Carnitine-Acylcarnitine Carrier
CaM	Calmodulin
CaMK	Ca^{2+} and CaM-Kinase
cAMP	3',5'-Cyclic Adenosine Monophosphate
CBP	CREB Binding Protein
CCDS	Creatine Deficiency Syndrome
CDK	Cyclin-Dependent Kinase
CI-V	RC Complexes I-IV
CMT2A	Charcot Marie Tooth Disease
COMT	Catechol-O-Methyl Transferase
CPEO	Chronic Progressive External Ophthalmoplegia
Cr	Creatine
CRE	cAMP Response Element
CREB	cAMP Response Element Binding Protein
CrT	Creatine Transporter
CS	Citrate Synthase
CytbR	Cytochrome b5 Reductase
CytC	Cytochrome C
D1R/D2R	DA D1 or D2 Receptor
DA	Dopamine
DAG	Diacylglycerol
DARPP32/ PPP1R1B	Dopamine- and cAMP-Regulated Neuronal Phosphoprotein (Protein Phosphatase 1 Regulatory Subunit 1B)
DAT	Dopamine Transporter
DBH	Dopamine-β-Hydroxylase
DBS	Deep Brain Stimulation
DCD	Delayed Calcium Dysregulation
DGK	Diacylglycerol Kinase
DGUOK	Deoxyguanosine Kinase
DHODH	Dihydroorotate Dehydrogenase
DIC	Dicarboxylate Carrier
DLD	Dihydrolipoamide Dehydrogenase
dMSNs	Direct Pathway MSN
DNC	Deoxynucleotide Carrier
DOPAL	3,4-Dihydroxyphenylacetaldehyde
Drp1/ Dnm1l	Dynamin Related Protein/ Dynamin-1-like
DUSP	Dual Specificity Phosphatase
EAAT	Excitatory Amino Acid Transporter
ECAR	Extracellular Acidification Rate
eCB	Endocannabinoid
eIF2	Eukaryotic Initiation Factor 2
EMRE	Essential MCU Regulator

ENO	Enolase
Epac	Exchange Protein Activated by cAMP
ER	Endoplasmic Reticulum
ERK	Extracellular Signal-Regulated Kinases
ERMES	Endoplasmic Reticulum-Mitochondria Encounter Structure
F6P	Fructose 6-Phosphate
FAD	Flavin Adenine Dinucleotide
FCCP	Carbonyl Cyanide-p-Trifluromethoxyphenylhydrazone
FeS	Iron-Sulfur Cluster
Fis1	Mitochondrial Fission Protein 1
FMN	Flavin Mononucleotide
Fms	Fumarase
G6P	Glucose 6-Phosphate
G6PD	Glucose 6-Phosphate Dehydrogenase
GAA	Guanidinoacetate
GABA	γ-Amino Butyric Acid (4-Aminobutyrate)
$GABA_AR$	Ionotropic GAB_AA Receptor
$GABA_BR$	Metabotropic $GABA_B$ Receptor
GAD	Glutamic Acid Decarboxylase
GAMT	Guanidinoacetate Methyltransferase
GAPDH	Glyceraldehyde Phosphate Dehydrogenase
GAT	GABA Transporter
GBA	Glucocerebrosidase
GDP	Guanosine Diphosphate
GEF	Guanine Nucleotide Exchange Factor
GFAP	Glial Fibrillary Acidic Protein
GIRK	G-Protein Coupled Inwardly Rectifying Potassium Channel
GLUT	Glucose Transporter
GP	Glycogen Phosphorylase
GPCR	G-Protein Coupled Receptor
GPe	External Globus Pallidus
GPi	Internal Globus Pallidus
GPx	Glutathione Peroxidase
GR	Glutathione Reductase
GRK	G-Protein Coupled Receptor Kinase
GS	Glutamine Synthetase
GSH	Glutathione
GSK3	Glycogen Synthase Kinase 3
GST	Glutathione-S-Transferase
GTP	Guanosine Triphosphate
H3	Histone 3
HAT/KAT	Histone Acetyltransferase
HDAC	Histone Deacetylase
HKII	Hexokinase II
HSP	Heavy Strand Promoter
ICDH/IDH	Isocitrate Dehydrogenase
IEG	Immediate Early Gene
IMM	Inner Mitochondrial Membrane
IMS	Intermembrane Space
iMSNs	Indirect Pathway MSN
IP_3(R)	Inositol Triphosphate (Receptor)
KSS	Kearns-Sayre Syndrome
L-DOPA	L-3,4-Dihydroxyphenylalanine
LAT1	Large Neutral Amino Acid Transporter
Letm1	H^+/Ca^{2+} exchanger
LHON	Leber's Hereditary Optic Neuropathy
LID	L-DOPA Induced Dyskinesia
LRRK2	Leucine-Rich Repeat Kinase 2
LS	Leigh Syndrome
LSP	Light Strand Promoter
LSU/ mtLSU	Mitochondrial Large Ribosomal Subunit
LTD	Long-Term Depression
LTP	Long-Term Potentiation
M1-5 R	Muscarinic 1-5 Receptor
MAM	Mitochondria-Associated ER Membranes
MAOA/B	Monoamine Oxidase A/B
MAOI	MAO Inhibitor
MAPK	Mitogen-Activated Protein Kinase
MAS	Malate-Aspartate Shuttle
MCU	Mitochondrial Calcium Uniporter

MDH/ME	Malate Dehydrogenase/Malic Enzyme
MDS/ MTDPS	mtDNA Depletion Syndrome
MELAS	Mitochondrial Encephalomyopathy, Lactic Acidosis, and Stroke-like Episodes
MERRF	Myoclonic Epilepsy with Ragged Red Fibers
MFF	Mitochondrial Fission Factor
MFN1/2	Mitofusin 1/2
MFRTA	Mitochondrial Free Radical Theory of Aging
MGE	Median Ganglionic Eminence
mGluR	Metabotropic Glutamate Receptor
mGPDH	Glycerol-3-Phosphate Dehydrogenase
MICU	Mitochondrial Calcium Uptake Protein
MiD49/51	Mitochondrial Dynamics Protein 49/51
MNGIE	Mitochondrial Neurogastrointestinal Encephalopathy Syndrome
mNHE1	Na^+/H^+ exchanger
MPC	Mitochondrial Pyruvate Carrier
MPTP	1-Methyl-4-Phenyl-1,2,3,6-Tetrahydropyridine
mPTP	Mitochondrial Permeability Transition Pore
MRS	Magnetic Resonance Spectroscopy
MSK	Mitogen and Stress Activated Protein Kinase
MSN	Medium Spiny Neuron
mtCK	Mitochondrial Creatine Kinase
mtDNA	Mitochondrial DNA
mTORC	Mammalian Target of Rapamycin Complex
mtRNA	mtDNA-encoded mRNA
MTS	Mitochondrial Targeting Sequence
N2a	Neuroblastoma 2a
nAChR	Nicotinic Acetylcholine Receptor
NADH	Nicotinamide Adenine Dinucleotide
NADPH	Nicotinamide Adenine Dinucleotide Phosphate
NARP	Neuropathy, Ataxia, and Retinitis Pigmentosa
NCLX	Na^+/Ca^{2+} Exchanger
NET	Norepinephrine Transporter
NMDA(R)/ GRIN1-4	N-Methyl-D-Aspartate (Receptor)
NMT	Non-Mammalian Target
NNT	NAD(P) transhydrogenase
O-GlcNAc	*O* -linked N-acetylglucosamine
OAA	Oxaloacetate
OCR	Oxygen Consumption Rate
ODC	Oxodicarboxylate Carrier
OGC	αKG Carrier
O_H	Origin of Heavy Strand Replication
O_L	Origin of Light Strand Replication
OMM	Outer Mitochondrial Membrane
OPA1	Optic Atrophy 1
ORC2	Ornithine Carrier
OXA1	Oxidase Assembly Translocase
PAG	Phosphate-Activated Glutaminase
PARL	Presenilins-Associated Rhomboid-Like Protein
PC	Pyruvate Carboxylase
PCr	Phosphocreatine
PD	Parkinson's Disease
PDE	Phosphodiesterase
PDH	Pyruvate Dehydrogenase
PERK (EIF2AK3)	Protein Kinase R-like Endoplasmic Reticulum Kinase (Eukaryotic Translation Initiation Factor 2-alpha Kinase 3
PET	Positron Emission Tomography
PFK	Phosphofructokinase
PGC	Peroxisome Proliferator-Activated Receptor Gamma Coactivator
PGI	Phosphoglucose Isomerase

PGK	Phosphoglycerate Kinase
PGM	Phosphoglycerate Mutase
PI3K	Phosphatidylinositol-4,5-Bisphosphate 3-Kinase
PiC	Phosphate carrier
PINK1	PTEN-Induced Putative Kinase 1
PIP2	Phosphatidylinositol 4,5-bisphosphate
PK	Pyruvate Kinase
PKA	Protein Kinase A
PLCβ	Phospholipase C β
PNC	Pyrimidine Nucleotide Carrier
POLG	p140 Subunit of POLγ
POLG2	p55 Accessory Subunit of POLγ
POLRMT	Mitochondrial RNA Polymerase
POLγ	mtDNA Polymerase Holoenzyme
PP2B	Protein Phosphatase 2B, Calcineurin
Ppd	Preprodynorphin
Ppe	Preproenkephalin
PPP	Pentose Phosphate Pathway
Ppt	Preprotachykinin
Prx	Peroxiredoxin
PTEN	Phosphatase and Tensin Homolog
PUFA	Polyunsaturated Fatty Acids
PVDF	Polyvinylidene Fluoride
RC	Respiratory Chain
Rhes	Ras Homolog Enriched in Striatum
ROS	Reactive Oxygen Species
RPE	Ribulose 5-Phosphate 3-Epimerase
RPI	Ribulose 5-Phospate Isomerase
RSK	Ribosomal S6 Kinase
RTK	Receptor Tyrosine Kinase
RyR	Ryanodine Receptor
SAMC	S-Adenosyl-Homocysteine-S-Adenosyl-Methionine Carrier
SCS	Succinyl-CoA Synthetase
SDH	Succinate Dehydrogenase
SERT	Serotonin Transporter
SFK	Src Family Kinase
SLC	Solute Carrier Protein
SNARE	Soluble N-Ethylmaleimide-Sensitive Factor Attachment Protein Receptor
SNAT1	System A Transporter, Neuron-Specific
SNAT2	System A Transporter, Ubiquitous
SNAT3/5	System N Transporter
SNc	Substantia Nigra pars compacta
SNr	Substantia Nigra pars reticulata
SOD	Superoxide Dismutase
SRF	Serum Response Factor
SSADH	Succinyl Semialdehyde Dehydrogenase
SSBP/ mtSSBP	Mitochondrial Single Strand Binding Protein
SSU/mtSSU	Mitochondrial Small Ribosomal Subunit
STEP	Striatal Enriched Protein Tyrosine Phosphatase
STN	Subthalamic Nucleus
TALDO	Transaldolase
TCA	Tricarboxylic Acid Cycle
TFAM	Mitochondrial Transcription Factor A
TFBM	Mitochondrial Transcription Factor B
TH	Tyrosine Hydroxylase
TIM	Translocase of the Inner Membrane
TK2	Thymidine Kinase
TKT	Transketolase
TMSP	Sodium Trimethylsilyl Propionate-d4
TOM	Translocase of the Outer Membrane
TP	Thymidine Phosphorylase
TPI	Triosephosphate Isomerase
TRAP	Tremor, Rigidity, Akinesia, Postural Instability
Trx	Thioredoxin
TrxR	Thioredoxin Reductase
UCP	Uncoupling Protein
UPDRS	Unified Parkinson Disease Rating Scale
UPR$^{mt/ER}$	Mitochondrial/ER Unforlded Protein Response

VDAC	Voltage Dependent Anion Channel
vGAT	Vesicular GABA Transporter
VGCC	Voltage Gated Ca^{2+} Channel
vGlut	Vesicular Glutamate Transporter
VMAT2	Vesicular Monoamine Transporter
VTA	Ventral Tegmental Area
αKG	α-Ketoglutarate
αKGDH	α-Ketoglutarate Dehydrogenase
Δψ	Membrane Potential

CHAPTER I

INTRODUCTION

N.B.: Portions of this chapter (including figures, tables, and text) have been reproduced with permission from previously published work. Relevant figures and tables have been annotated, but please see the end of this chapter for details.

As the U.S. population ages, the incidence of age-related diseases is rising rapidly (Dall et al., 2013). One of the most prevalent and debilitating classes of age-related diseases are neurodegenerative disorders, which include Alzheimer's Disease (AD) and Parkinson's Disease (PD). By 2013, over six million people were diagnosed with one of these two diseases, and that number is projected to rise to over 15 million by 2050 (Hebert et al., 2013; Kowal et al., 2013). Though PD is the less prevalent of these two diseases, current estimates have calculated an annual economic burden of over $15 billion (Kowal et al., 2013). Moreover, a recent study demonstrated that Medicare subscribers with PD both used more health care services and paid more out of pocket than all other elderly Medicare members (Noyes et al., 2007), suggesting a disproportionately high cost for this disorder. While a range of therapeutics are available for PD, none reduce or reverse its progression. Furthermore, the most commonly used therapeutic, L-3,4-dihydroxyphenylalanine (L-DOPA), causes its own set of debilitating motor side effects known as L-DOPA Induced Dyskinesia (LID), which severely reduce patient quality of life (Chapuis et al., 2005). Continued study into the pathogenesis of PD and LID is necessary to aid the development of new disease therapies and diagnostic approaches to improve both the economic and psychosocial burden of this disorder.

1. Physiology and pharmacology of Parkinson's Disease and L-DOPA Induced Dyskinesia

1.1. PD and LID in the clinic

First described 200 years ago by James Parkinson (Parkinson, 1817), PD is the second most common neurodegenerative disease afflicting the population today (de Lau and Breteler, 2006). Though the pathology of the disorder is complex, the canonical clinical hallmarks of PD are the degeneration of the dopaminergic neurons of the substantia nigra pars compacta (SNc), and the presence of Lewy bodies; intracellular inclusions comprised of α-synuclein aggregates (Gibb and Lees, 1988; Jankovic, 2008). However, these can only be identified through the use of positron emission tomography (PET) imaging (Loane and Politis, 2011), or post-mortem (Braak et al., 2003), so establishing clinical diagnostic criteria remains an important endeavor.

Parkinson initially described the disorder as the 'shaking palsy,' but PD is characterized today by (and typically diagnosed by the recognition of) four major symptoms: tremor, rigidity, akinesia, and postural instability (TRAP) (Jankovic, 2008). However, PD also involves a number of other symptoms that can severely impact patient quality of life, including more subtle motor symptoms such as difficulty writing and swallowing, as well as various postural abnormalities, but also non-motor symptoms including cognitive impairment, psychiatric problems, dysautonomia, and sleep disorders (Jankovic, 2008; Chaudhuri et al., 2011; Martinez-Martin et al., 2011). It is commonly accepted that motor problems appear relatively late in the course of the disease, and symptoms such as anosmia and shoulder stiffness or pain may be some of the first manifestations of the disease (Kalia and Lang, 2004; Berg et al., 2014).

Tracking the symptoms and development of PD has been standardized by the use of the Unified Parkinson's Disease Rating Scale (UPDRS) (Goetz et al., 2008; Martinez-Martin et al., 2015). The UPDRS groups symptoms into psychological symptoms, daily living activities, motor function, and treatment complications, and is particularly useful for quantitatively assessing the

performance of clinical trials. Currently, clinical diagnosis depends on recognition of the hallmark TRAP motor symptoms, and is typically supported by response to the most-commonly prescribed pharmacotherapy, L-DOPA (Jankovic, 2008). Studies with post-mortem follow-up have reported diagnostic accuracy ranging from 75-90%.

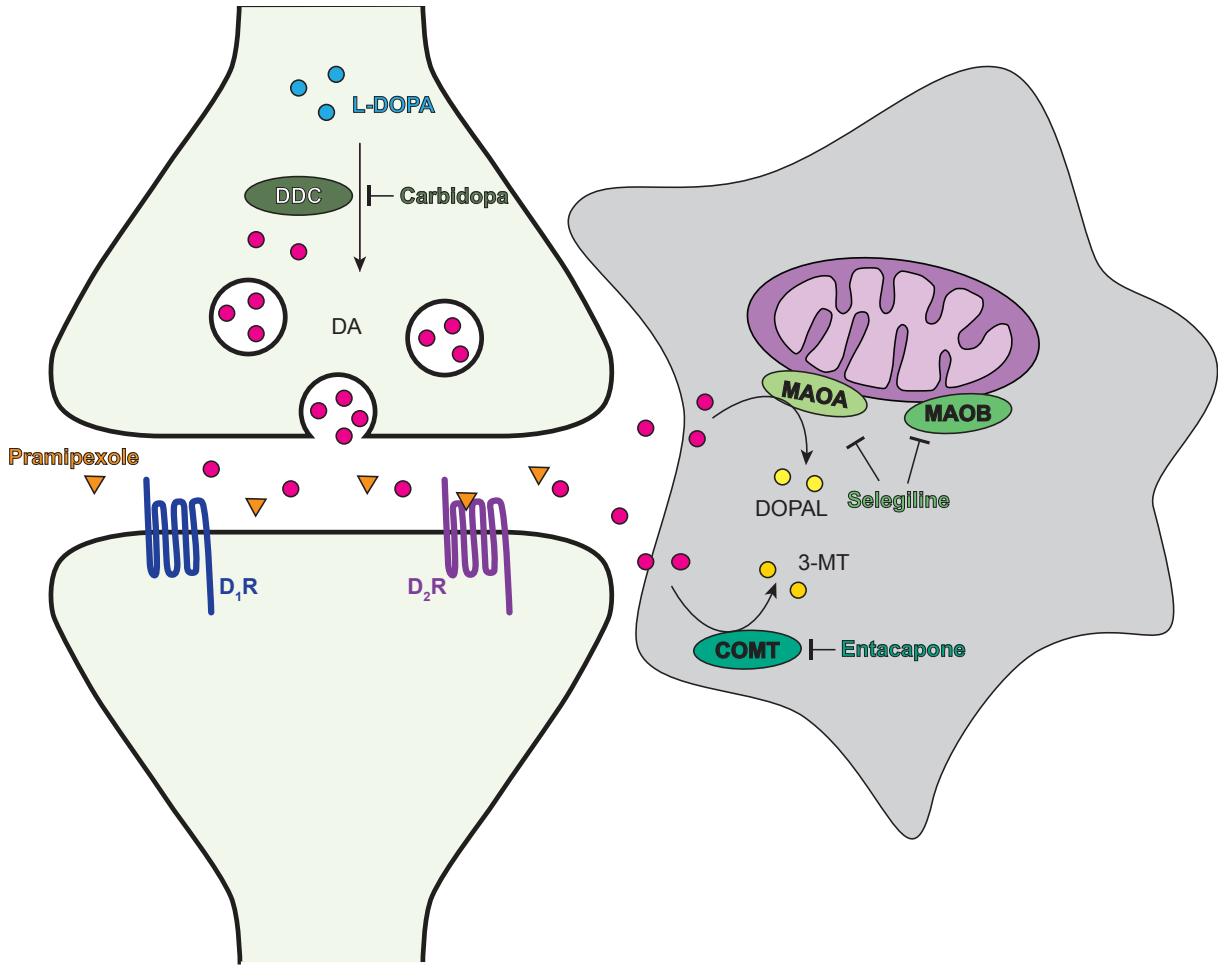

Figure 1. PD pharmacotherapy.
Representative diagram of the pharmacological agents used in PD therapy, and their sites of action, at the nigrostriatal interface in the presence of glia. Examples of the most commonly used drugs for each target are presented. Dopamine is released from the presynaptic terminal on onto the dendrites of the striatum, but can be metabolized into 3-methoxytyramine (3-MT) or 3,4-dihydroxyphenylacetaldehyde (DOPAL). DDC, Dopa decarboxylase (amino acid decarboxylase); MAOA/MAOB, monoamine oxidase; COMT, catechol-O-methyltransferase; $D_{1/2}R$, dopamine 1/2 receptor. Adapted from Wu and Fruct, 2005.

PD is predominantly treated pharmacologically (Wu and Frucht, 2005; Oertel and Schulz, 2016) (Figure 1), though deep brain stimulation (DBS) has also been used to treat an increasing number of cases (Bronstein et al., 2011; McIntyre and Anderson, 2016). Pharmacologic treatments can be divided into two broad categories – dopaminergic and non-dopaminergic,

though non-dopaminergic drugs are used almost exclusively as adjunct therapy to dopaminergic drugs (Oertel and Schulz, 2016). The dopaminergic category can be further sub-divided into L-DOPA (a metabolic precursor of dopamine (DA)), and other dopamimetic agonists. Despite the similar mechanisms of action of these drugs, an attempt to replace dopaminergic stimulation, there is considerable disagreement as to which is the more appropriate first-line therapy. In a recent clinical trial (Goudreau et al., 2016), a large patient cohort was examined, and patients were approximately evenly divided between receiving L-DOPA or DA receptor agonists as the primary therapeutic. This retrospective study revealed that patients receiving agonists are younger, more educated, and had fewer co-morbidities than those receiving L-DOPA. This discrepancy may be at least partially attributable to differential concerns about side effects, but as dopaminergic agonists are significantly more expensive than L-DOPA, patients with higher educational attainment and socioeconomic status likely have greater access to these drugs.

Three major classes of drugs are regularly prescribed as adjunct therapeutics to L-DOPA therapy: decarboxylase inhibitors, monoamine oxidase inhibitors (MAOIs), and catechol-O-methyl transferase (COMT) inhibitors. Decarboxylase inhibitors (e.g. carbidopa) are concurrently prescribed with L-DOPA, as they inhibit peripheral metabolism of the drug, dramatically increasing L-DOPA's bioavailability (Nutt et al., 1985). MAOIs (e.g. selegiline) and COMT inihibitors (e.g. entacapone) putatively perform similar roles, as they inhibit the enzymatic mechanisms of DA metabolism in the CNS (Ménnistó, 1994; Lyytinen et al., 1997; Kaakkola, 2000; Yamada and Yasuhara, 2004), though their utility has been recently called into question (Olanow et al., 2013).

A number of compounds with therapeutic potential for PD have entered stage 3 clinical trials, acting on the noradrenergic, adenosine, and serotonergic systems (see Oertel and Schulz, 2016 for review), but as of this writing the vast majority of approved drugs for PD function within the dopaminergic system. It is important to note that despite the variety of drugs available for PD, no treatment has been shown to have disease-modifying efficacy; i.e., to slow or reverse the

progression of the disease. In all cases, treatment is entirely symptomatic. The lack of disease-modifying therapy presents a large unmet need for the disorder (Chaudhuri et al., 2016).

Though the existing compounds do, at least initially, sufficiently address bradykinetic symptoms, prolonged L-DOPA and dopaminergic agonist therapy both have characteristic sets of side effects. Dopaminergic agonists tend to produce both autonomic dysregulation, such as orthostatic hypotension and nausea (Kujawa et al., 2000; Li et al., 2015), but also neuropsychiatric effects associated with other DA dysregulation disorders, including psychosis, compulsive behaviors, and punding (Giladi et al., 2007; Weintraub et al., 2010). Typically, these side effects are considered even more disabling in elderly patients, who may have a higher incidence of comorbid age-related cognitive decline.

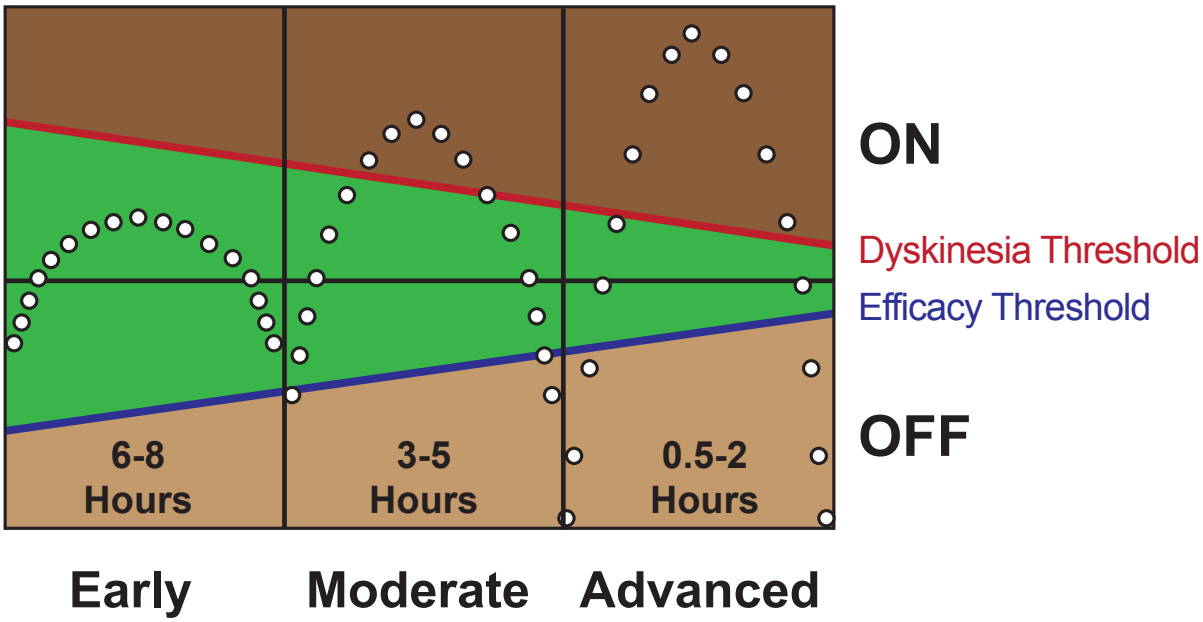

Figure 2. Overview of the shift in response to L-DOPA over the course of treatment.
The dotted line represents plasma L-DOPA concentration following an oral dose, the green window represents the therapeutic window, the red line represents the dyskinesia threshold, the blue line represents the efficacy threshold. Early in L-DOPA treatment, the oral dose maintains patients well within the therapeutic window. As treatment continues, the dyskinesia threshold is lowered, the efficacy threshold raises, and the therapeutic window narrows. Subsequent doses of L-DOPA cross both thresholds, causing dyskinesia and 'wearing-off' motor side effects. Redrawn with permission from Jankovic, 2005.

However, it is L-DOPA therapy that produces the best side effect of PD pharmacotherapy – LID. LID is characterized by uncontrolled, hyperkinetic and choreiform movements, and as these dyskinesias increase in severity, they can become as disabling as the parkinsonsian akinesia and

tremor. “Wearing off” is a related side effect associated with L-DOPA therapy, wherein an akinesia-alleviating dose of L-DOPA is increasingly less effective during its dose window. In the most severe cases, patients treated with L-DOPA may then oscillate between “ON” phases with disabling dyskinesia, and “OFF” phases where they return to a parkinsonian state (Jankovic, 2005) (Figure 2).

Based on a large meta-analysis of several long-term PD treatment studies, the risk of LID development increases over time, and affects about 40% of patients after 4-6 years of therapy, and about 90% of patients after 9+ years (Ahlskog and Muenter, 2001; Manson et al., 2012). Interestingly, “wearing off,” also referred to as motor fluctuations, affects nearly 50% of patients after only one year of treatment. However, this incidence doesn’t increase until >6 years of treatment, when approximately 70% of patients are affected. The two most frequently identified risk factors for LID are L-DOPA dose and age of PD onset (Grandas et al., 1999; Olanow et al., 2013). Higher L-DOPA doses, particularly when considered in relationship to the patient’s body weight, dramatically increase the risk of LID. Younger PD patients are also more susceptible, as nearly 90% of patients diagnosed below 40 years of age will develop LID within five years (Ahlskog and Muenter, 2001).

A persistent theory in clinical practice posits that initial treatment with DA agonists is an ‘L-DOPA sparing’ method to postpone the development of dyskinesia (Rascol et al., 2000). However, several studies have shown that initial agonist monotherapy is not, over time, superior to L-DOPA monotherapy. The initial advantage of reduced dyskinesia incidence is lost over time, as L-DOPA more effectively manages motor symptoms, and has a decreased risk of non-motor side effects (Rascol et al., 2006; Xie et al., 2015).

Regardless of the drug chosen for PD treatment, debilitating side effects remain inevitable for the vast majority of patients. Continuing to study the mechanisms underlying the side effects as well as developing improved therapeutics is an imperative for the field.

1.2. Physiology and pathophysiology of the basal ganglia in PD and LID

Disentangling the mechanisms of PD pathology has been a primary driver in understanding the function of the larger brain region it affects – the basal ganglia. The basal ganglia are a cluster of subcortical nuclei that encompass portions of the diencephalon, telencephalon, and mesencephalon. Particularly because of their role in PD pathogenesis, the basal ganglia are typically associated with their role in regulating motor function, but recent studies have highlighted their roles in motor learning, habit formation, executive function, and the selection of actions based on positive outcomes.

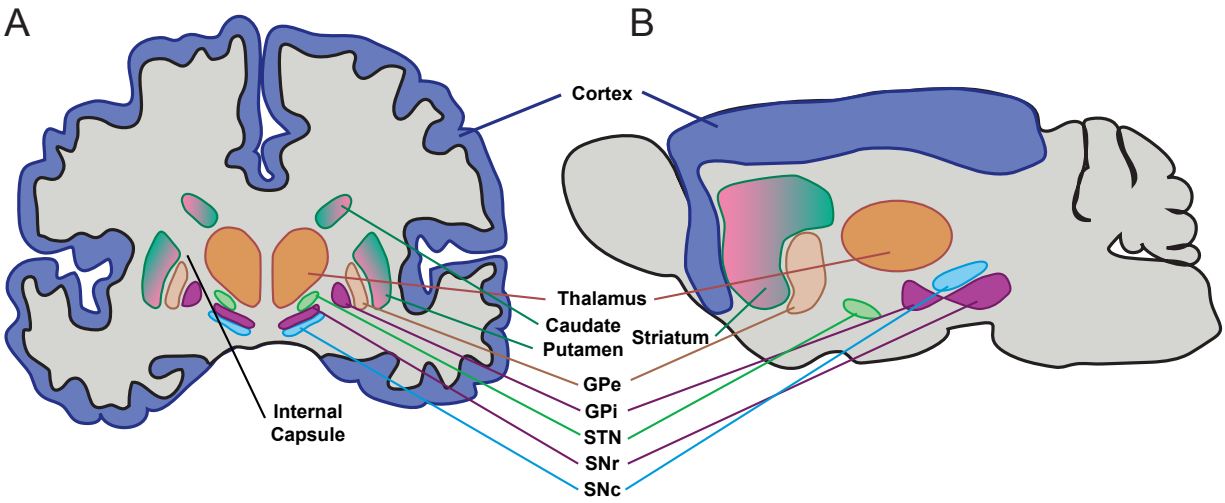

Figure 3. Schematic of the basal ganglia nuclei.
(A) Coronal section of primate basal ganglia. (B) Sagittal section of rodent basal ganglia. See Figure 4 for pathway connectivity. GPe, external globus pallidus; GPi, internal globus pallidus (entopeduncular nucleus); STN, subthalamic nucleus; SNr, substantia nigra pars reticulata; SNc, substantia nigra pars compacta. Adapted from Adams and Victor's Principles of Neurology, 2014, and Gerfen, 1992.

1.2.1. Functional Anatomy of the Basal Ganglia

Strictly defined, the basal ganglia only include the striatum and the globus pallidus, but most literature groups together the striatum, globus pallidus (internal (GPi) and external (GPe) segments), subthalamic nucleus (STN), substantia nigra pars reticulata (SNr), and SNc (Lanciego et al., 2012; Gerfen and Bolam, 2017) (Figure 3). Though these structures are largely conserved across species, humans and rodents have a few key differences. In humans, the striatum consists

of two separate regions – the caudate and putamen, divided by fiber tracts of the internal capsule, whereas in rodents the striatum is a single structure (Hardman et al., 2002). Despite this lack of division, the rodent striatum still preserves some of same functional topographical organization (Gerfen and Bolam, 2017). Additionally, in some studies, the rodent GPi is referred to as the entopeduncular nucleus (Benhamou and Cohen, 2014), but this chapter will use primate terminology.

Collectively, the basal ganglia filter and process information from the cerebral cortex, project to the thalamus (and other related motor nuclei, including the pedunculopontine nucleus), which applies additional filtering and processing, and relays back to the cortex. The major input nucleus of the basal ganglia is the striatum, which receives direct cortical input, while the major output nuclei are the GPi and SNr, which themselves predominantly project onto different thalamic nuclei (Lanciego et al., 2012). However, several recursive loops and alternative pathways between the different nuclei dramatically increase the complexity of this information processing system (Redgrave et al., 2010; Smith et al., 2011).

The classical model of basal ganglia function organizes information flow through the different nuclei into two major pathways (Bolam et al., 2000). Though newer studies have demonstrated that this organization is somewhat oversimplified, this classification still holds pharmacologically, for basic motor behaviors and in certain pathophysiological states (i.e., DA denervation). Nearly every region of the cerebral cortex projects onto the striatum (Lanciego et al., 2012), which is comprised almost entirely of medium spiny neurons (MSNs), with a small percentage of interneurons (Gerfen and Bolam, 2017). The MSNs are divided into two classes – “direct pathway” MSNs and “indirect pathway” MSNs, or dMSNs and iMSNs. Both MSN types are γ-amino butyric acid (GABA)ergic projection neurons, though dMSNs (also termed striatonigral neurons) project ‘directly’ to the SNr/GPi, while iMSNs (also termed striatopallidal neurons) project ‘indirectly’ to the GPe. The indirect pathway eventually converges onto the basal ganglia output nuclei, as the GPe projects to the STN, which then projects to the SNr/GPi (Figure 4). This

differential routing of these pathways means that despite using the same neurotransmitter, activation of dMSNs inhibits the activity of the output nuclei, while iMSNs activate them. As the output nuclei are themselves inhibitory, direct pathway activation results in a disinhibition of thalamic activity, promoting motor activity. In contrast, while the indirect pathway stimulates the output nuclei, this inhibits the thalamus and motor activity. This has led to the classification of the two pathways as “go” and “no-go” paths, which has been validated through optogenetic studies utilizing the independent stimulation of one or the other pathway (Kravitz et al., 2010).

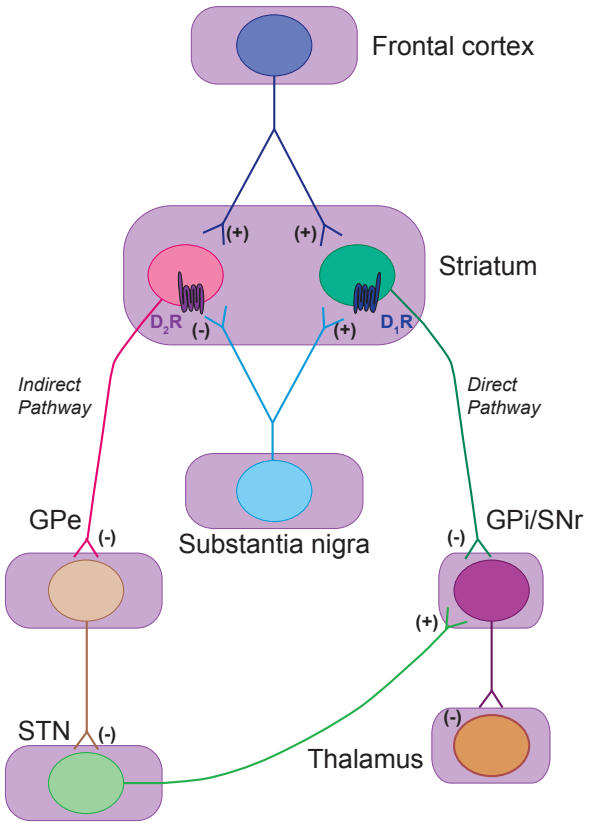

Figure 4. Direct and indirect pathways of the basal ganglia.
Glutamate is released from the cortex onto the medium spiny neurons (MSNs) of the striatum through the corticostriatal pathway, while DA is released from the substantia nigra onto the same neurons through the nigrostriatal pathway. Through the differential expression of D1 and D2 receptors, dopamine either stimulates the MSNs of the direct pathway or inhibits the MSNs of the indirect pathway. Through the direct pathway, MSN inhibition of the GPi/SNr disinhibits the thalamus, promoting motor function. In contrast, DAergic inhibition of the indirect pathway disinhibits the GPe, increasing inhibition of the STN, which reduces stimulation of the GPi/SNr. This has the net effect of inhibiting the thalamus and reducing motor activity. GPi, internal globus pallidus; SNr, substantia nigra pars reticulata; GPe, external globus pallidus; STN, subthalamic nucleus. Redrawn with permission from Jenner, 2008.

Intriguingly, dMSNs and iMSNs are also distinguished by their expression of different classes of DA receptors. dMSNs exclusively express D_1 DA receptors, while iMSNs exclusively express D_2 receptors. Though in the ventral striatum, these receptors are coexpressed in some MSNs, they appear to be completely segregated in the dorsal striatum (Frederick et al., 2015).

This means that dopaminergic input differentially regulates the activity of the direct pathway and indirect pathway, which has enormous implications for the pathophysiology of both PD and LID. Activation of D_1 receptors acts as an excitatory input, while activation of D_2 receptors is inhibitory (Beaulieu and Gainetdinov, 2011; Valjent, 2012). Consequently, normal DA input activates the direct pathway and inhibits the indirect pathway, which may be a mechanism by which the limbic pathway influences action selection and habit formation (Vicente et al., 2016; Graybiel, 2005).

1.2.2. Pathological Network Alterations of the Basal Ganglia in PD and LID

As PD is a consequence of dopaminergic degeneration in the SNc, many studies have examined the effects of DA denervation on the circuit function of the basal ganglia. The classical model of direct and indirect pathways continues to be particularly useful for this purpose. Removal of DA stimulation under-activates the direct pathway, as it eliminates the stimulatory effect of D_1 receptor activity, and over-activates the indirect pathway, as it eliminates the inhibitory effect of D_2 receptor activity. This deregulation carries through to the output nuclei, as the SNr/GPi become over-active following DA denervation, and reduce thalamic stimulation of motor activity, resulting in bradykinesia or akinesia (Crossman, 2000; Jenner, 2008) (Figure 3). Interestingly, this pathway deregulation can also explain the phenomenology of LID, which is characterized by supersensitization of the direct pathway (largely due to signaling changes from the D_1 receptor (Gerfen, 2003), see section 1.4). After the 'honeymoon' period of L-DOPA efficacy, its non-physiological spikes in extracellular DA over-activate the direct pathway, and over-inhibit the indirect pathway. As a result, the SNr/GPi are over-inhibited, which over-increases input to the thalamus and produces hyperkinetic movements (Carta et al., 2008; Jenner, 2008) (Figure 5). Though a large array of other pathological changes occurs within the basal ganglia during PD and LID, it is still clear that a large degree of dysfunction occurs at the level of the striatum, and can be modulated by dopaminergic function.

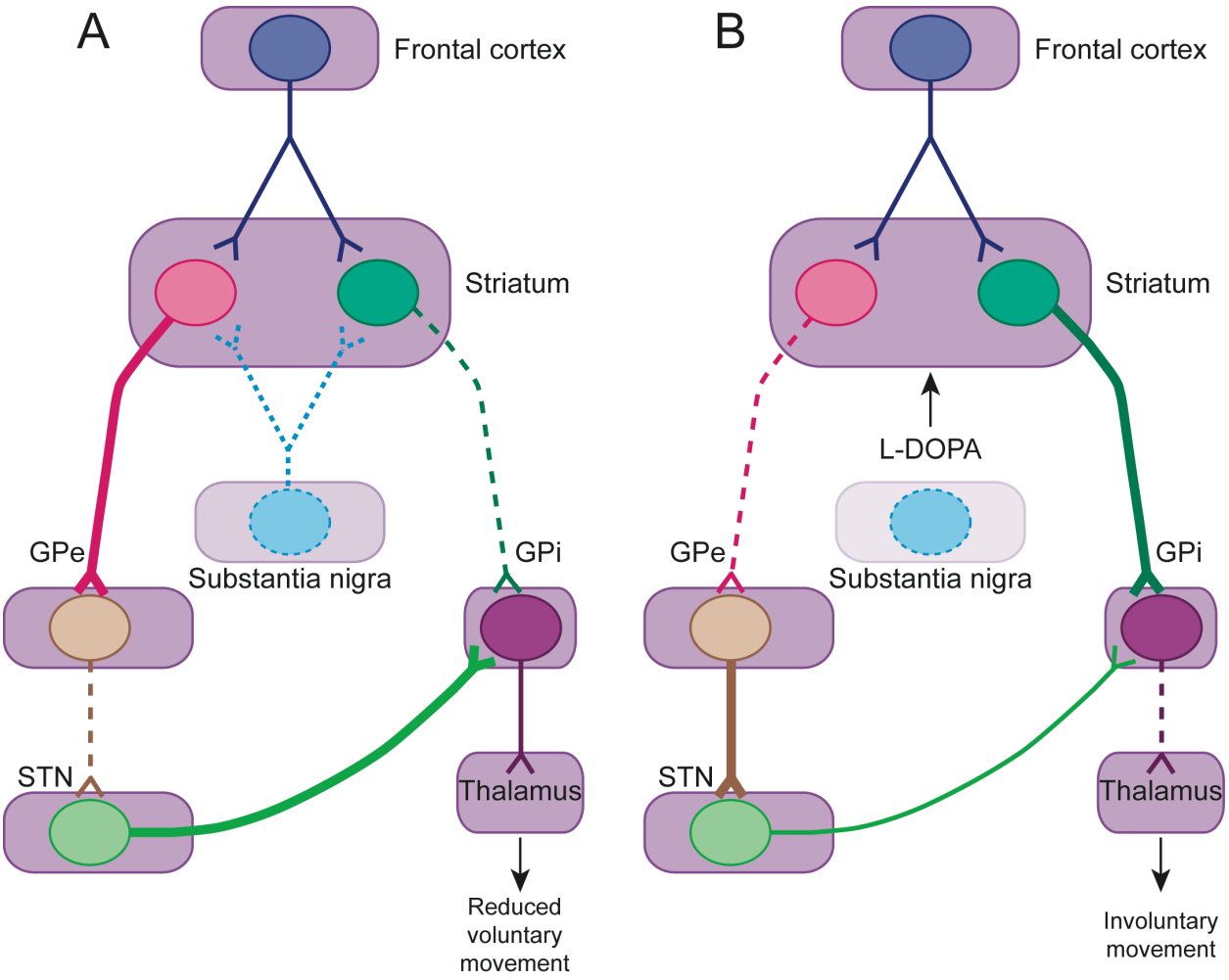

Figure 5. Pathological network alterations in the basal ganglia.
(A) In PD, degeneration of the substantia nigra reduces stimulation to dMSNs, which disinhibits the GPi, inhibiting the thalamus and suppressing movement. Concurrently, reduced inhibition of iMSNs inhibits the GPe, disinhibiting the STN, which activates the GPi, further inhibiting the thalamus. Consequently, dysfunction in both pathways causes parkinsonian bradykinesia. (B) In LID, maladaptive hyperactivation of dMSNs inhibits the GPi, activating the thalamus and promoting movement. Hypoactivation of iMSNs increases GPe activity, inhibiting the STN, reducing GPi stimulation. Together, these pathways disinhibit the thalamus, producing involuntary dyskinetic movements. Redrawn with permission from Jenner, 2008.

Nonetheless, some of the other pathophysiological changes that occur within the basal ganglia network following DA denervation and pharmacological DA replacement are informative to contextualize PD and LID pathogenesis. In particular, changes in network oscillations that occur between the different nuclei may help explain the efficacy of one of the alternatives to dopaminergic therapy – DBS (Okun, 2012; Walters, 2017). Animal studies have demonstrated that even at the normal physiological state, the basal ganglia are, to a degree, entrained by cortical

oscillations – for example, 1Hz cortical oscillations during sleep are transmitted to the striatum. DA denervation dramatically increases the degree to which these nuclei are entrained by these oscillations, and consequently this pathological state increases the degree to which the basal ganglia are synchronized with the cortex. It has been observed that following DA denervation, the STN and GPi have increased likelihood of forming synchronized oscillation patterns (Walters, 2017). Though a detailed discussion of changes in network oscillations is outside the scope of this chapter, it is useful to consider the functional information derived from these studies – that is, one of the principal physiological roles of DA in the striatum is to 'filter' cortical information and prevent 'nonsense' synchronization, and that DBS may work in part by similarly preventing pathological synchronization further downstream in the basal ganglia network.

1.3. Molecular physiology of the SNc and Striatum

As the majority of the biochemical changes observed in PD and LID occur at the nigrostriatal and corticostriatal interface, a characterization of the molecular substrates of these changes – neurotransmitters and their synthesis pathways, striatal receptors, and their respective signaling cascades – is useful to identify perturbations during pathogenesis. While cholinergic and GABAergic interneurons also play an important role in the function of the striatum, this chapter will focus exclusively on the interactions between corticostriatal and nigrostriatal afferents.

1.3.1. Neurotransmitters

Dopamine

As previously indicated, nigrostriatal afferents from the SNc are dopaminergic (Figure 6). The primary synthetic pathway for DA begins with phenylalanine, which is converted in the liver or kidneys by phenylalanine hydroxylase into tyrosine (Cansev and Wurtman, 2007). Tyrosine crosses the blood-brain barrier through the large neutral amino acid transporter (LAT1, a

heteromer of solute carrier transporters (SLC) SLC3A2 and SLC7A2) (Choi and Pardridge, 1986; Boado et al., 1999; Geier et al., 2013) and is subsequently taken up into neurons through the same mechanism (Lerner, 1987). Tyrosine is converted to L-DOPA by tyrosine hydroxylase, which is expressed in the brain by dopaminergic (and other catecholeminergic) neurons (Kumer and Vrana, 1996) and can be used as both a marker for immunohistochemistry studies or as a specific promoter for transgenic animals (Richfield et al., 2002; Liu et al., 2016). L-DOPA is then converted to DA by Dopa Decarboxylase (DDC), alternatively called aromatic L-amino acid decarboxylase (AADC) as it is expressed in other catecholeminergic neurons (Björklund and Dunnett, 2007). DA shares its metabolic pathway with the other catecholamine neurotransmitters, and it can be subsequently converted by dopamine beta hydroxylase (DBH) into norepinephrine, which can then be converted to epinephrine by phenylethanolamine N-methyltransferase. However, these enzymes are not expressed in dopaminergic neurons (Hoyle et al., 1994).

DA is packaged into vesicles by an isoform of the vesicular monoamine transporter (VMAT2) (Guillot and Miller, 2009), which has been another useful pharmacological target as it is irreversibly inhibited by reserpine (Schuldiner et al., 1993). Application of reserpine depletes dopaminergic vesicles, and produces parkinsonian phenotypes (Carlsson et al., 1959), which aided in the confirmation of the DA hypothesis of PD pathogenesis. Once released, the majority of DA is taken back up into DA neurons through the high affinity DA transporter (DAT) (Torres et al., 2003).

The routes of DA metabolism are exploited in therapeutic approaches to PD, as many of these enzymatic pathways are inhibited during PD pharmacotherapy. DA can be metabolized by monoamine oxidase A or B (MAOA/B), which is tethered to the outer mitochondrial membrane (OMM), which produces 3,4-dihydroxyphenylacetaldehyde (DOPAL). Alternately, released DA can be metabolized by COMT, which is has membrane-bound and cytosolic soluble forms, and which generates 3-methoxytyramine (3-MT). Both of these metabolites can then be converted in

subsequent steps with the alternate enzyme to homovanillic acid, one of the primary excreted metabolites of DA (Meiser et al., 2013).

All three of the major enzymes involved in DA synthesis and degradation (DDC/AADC, MAO, and COMT), also metabolize L-DOPA, and are consequently the targets of L-DOPA adjunct therapy. L-DOPA is always administered with a DDC inhibitor, as peripheral expression of this enzyme would prevent sufficient L-DOPA from reaching the brain. However, these inhibitors cannot cross the blood brain barrier, and consequently L-DOPA is freely metabolized to DA after uptake into a monoaminergic neuron (Kostrzewa, 2007).

Interestingly, DA can be oxidized into a DA quinone, which is a precursor of neuromelanin (Sulzer and Zecca, 2000; Sulzer et al., 2000; Napolitano et al., 2011), the “black substance” that characterizes the SNc. The function of this pathway has not been resolved *in vivo*, though it seems to be produced from the accumulation of extravesicular DA. The oxidation capacity of DA has led to multiple studies about neurotoxicity of DA, its metabolites, and its precursor L-DOPA, all of which have similar reactive oxidative potential (Meiser et al., 2013). This has led to the related hypothesis that L-DOPA treatment might be similarly neurotoxic. While DA oxidative toxicity has been demonstrated in a number of contexts (Napolitano et al., 2011), the therapeutic benefit of L-DOPA therapy (Oertel and Schulz, 2016), combined with findings that L-DOPA does not induce the same types of intracellular damage as DA (Naydenov et al., 2010), suggests that L-DOPA-induced neurotoxicity is not a primary mechanism for increased dopaminergic degeneration or LID pathogenesis.

Glutamate and GABA

Though these neurotransmitters are expressed in different neuron types (i.e., corticostriatal neurons are glutamatergic, and both iMSNs and dMSNs are GABAergic), the metabolism of these neurotransmitters are tightly interrelated (Figure 6). Glutamine is taken up

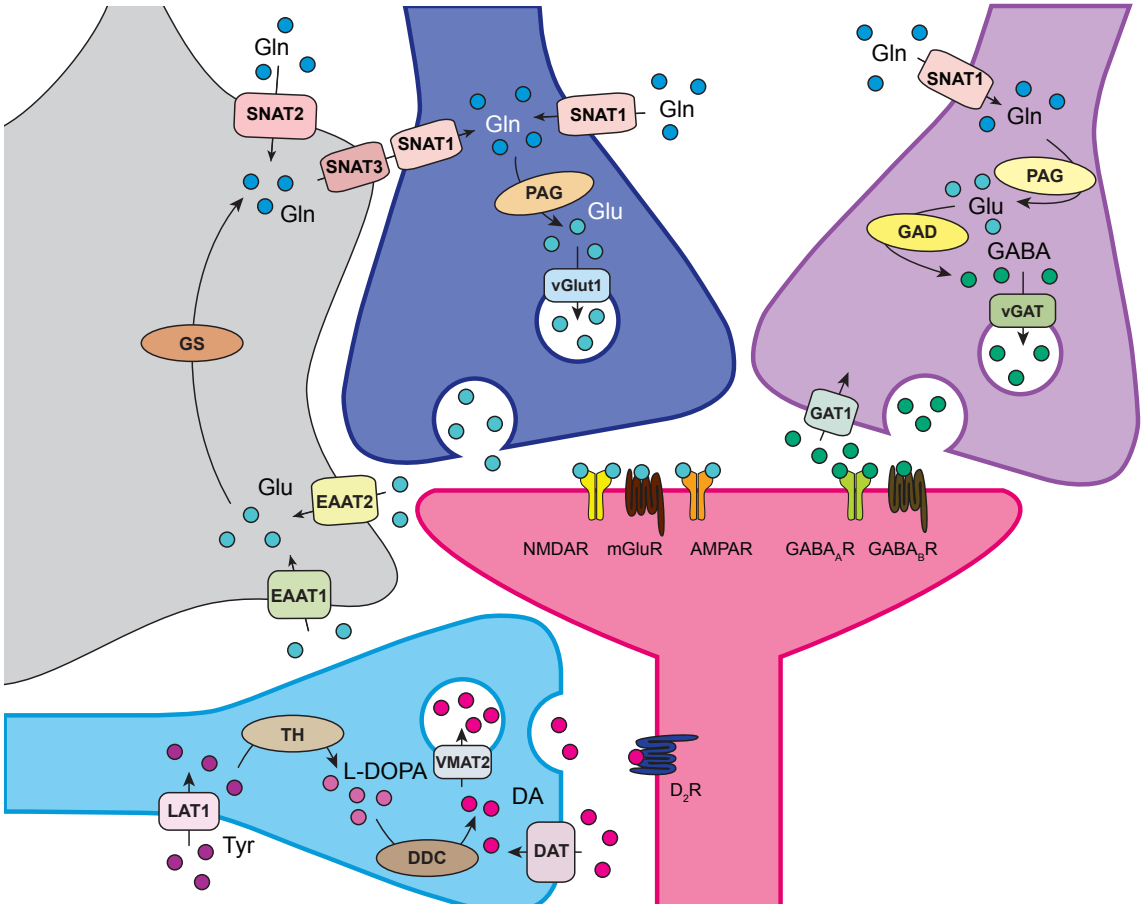

Figure 6. Neurotransmitter systems at a representative D2 striatal synapse, with representative receptors.
Nigrostriatal afferents (aqua) are dopaminergic; target D2 striatal spines are pink. Tyrosine is taken up into neurons through LAT1, and is converted through multiple enzymatic reactions to DA. DA is packaged into vesicles, released, and taken up through the DAT. Interneuron projections or MSN-MSN projections (purple) are GABAergic. Glutamine is taken up through system A transporters, converted into glutamate by glutaminase, then GABA by GAD. GABA is packaged into vesicles by vGAT, and predominantly cleared from the synapse by GAT1. Corticostriatal afferents are glutamatergic (blue). Here, glutamate is packaged into vesicles by vGlut2 and released, but no known neuronal reuptake mechanism has been identified. Glutamate is instead cleared from the synapse by glia (grey), using the EAAT1 and EAAT2 transporters. GS converts glutamate to glutamine, which is exported from glia via system N transporters. LAT1, large neutral amino acid transporter; TH, tyrosine hydroxylase; DDC, aromatic amino acid decarboxylase; VMAT2, vesicular monoamine transporter; DAT, dopamine transporter; D2R, D2 receptor; NMDAR, N-Methyl-D-Aspartic acid receptor; AMPAR, α-Amino-3-hydroxy-5-methyl-4-isoxazolepropionic acid receptor; mGluR, metabotropic glutamate receptor; $GABA_AR$, ionotropic GABA receptor; $GABA_BR$, metabotropic GABA receptor; EAAT1/2, excitatory amino acid transporter; GS, glutamine synthetase; SNAT1, neuron-specific system A transporter; SNAT2, ubiquitous system A transporter; SNAT3, system N transporter; PAG, phosphate-activated glutaminase; GAD, glutamic acid decarboxylase; vGlut2, vesicular glutamate transporter; vGAT, vesicular GABA transporter; GAT1, GABA transporter.

across the blood-brain barrier through system N amino acid transporters, which may involve SLC38A3 and/or SLC38A5 (Ennis et al., 1998; Nałęcz, 2016) and then taken up by neurons, likely through system A amino acid transporters (SNAT1/2) (Varoqui et al., 2000; Bak et al., 2006).

Neurons can convert glutamine to glutamate by selective expression of phosphate-activated glutaminase (PAG) (Kvamme et al., 2001; Bak et al., 2006). In glutamatergic neurons, glutamate is then packaged into vesicles by one of the vesicular glutamate transporter (vGlut) isoforms (in corticostriatal fibers, vGlut1 (SLC17A7), in thalamostriatal fibers, vGlut2 (SLC17A6) (Shen et al., 2017), and released. However, neuronal glutamate reuptake is low, so glutamate is predominantly taken up by neighboring glia through the excitatory amino acid transporters EAAT1 (GLAST) and EAAT2 (GLT-1). This glutamate can be transferred through a number of pathways, but in the

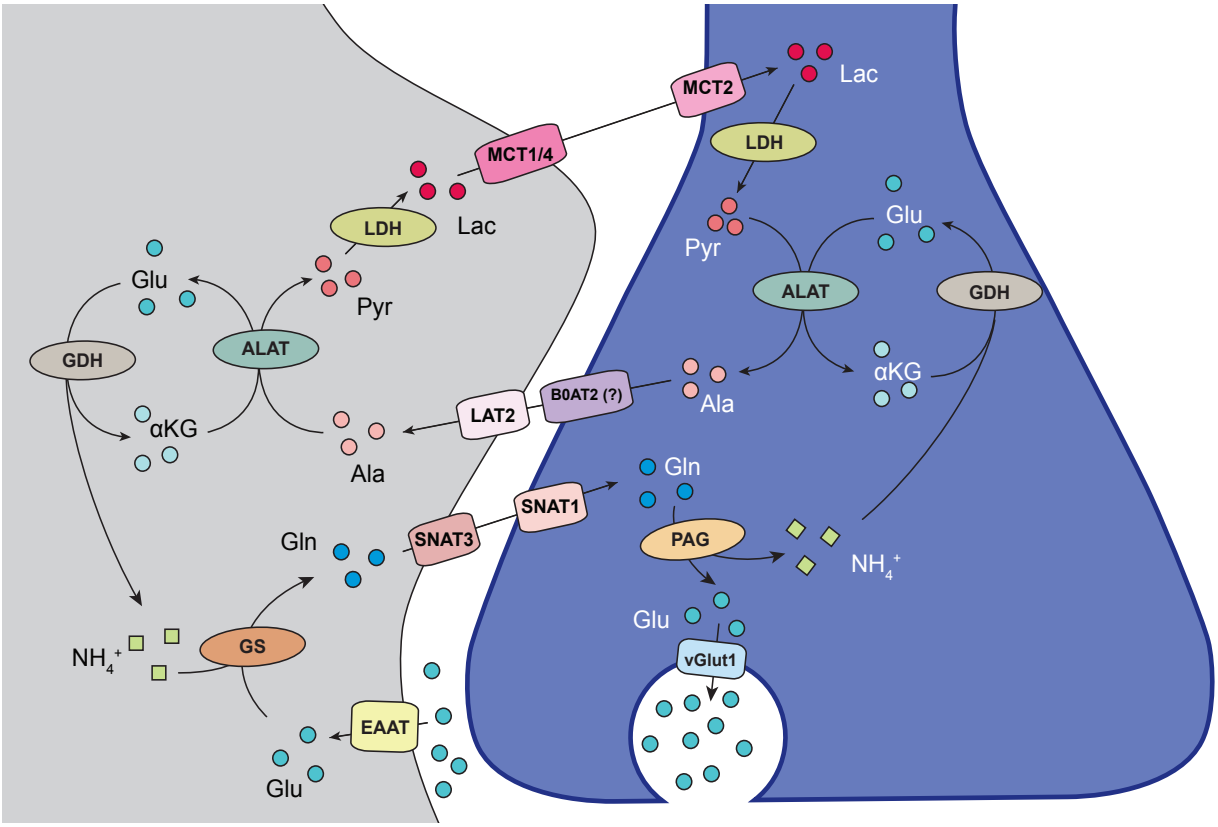

Figure 7. Putative ammonia exchange mechanisms at glutamatergic terminals.
The glutamate-glutamine cycle between neurons and glia requires a net transfer of ammonia from neurons to glia. While ammonia can diffuse across membranes, a link to amino acid metabolism and glycolysis has been suggested to facilitate this process. Lactate is transferred from glia to neurons through MCTs, which have differential affinities for lactate (Hertz 2005). Lactate can then be converted by LDH to pyruvate in neurons, which is transaminated with glutamate by ALAT into alanine and αKG. αKG can be reconverted into glutamate by GDH, which consumes an NH4+ molecule. Alanine can then be transported from neurons, likely through a system B transporter (B(0)AT2, putatively, Bröer 2007), and taken up by LAT2 into astrocytes. Here, the reverse transamination occurs, yielding pyruvate and glutamate. Glutamate conversion into αKG by GDH generates an additional NH4+, necessary for the GS reaction. ALAT, alanine transaminase; GDH, glutamate dehydrogenase; LDH, lactate dehydrogenase; MCT, monocarboxylate transporter. See Figure 6 and text for additional abbreviations. Adapted from Schousboe, 2014.

simplest version of the glutamate-glutamine cycle, glutamate is converted to glutamine by glutamine synthetase (GS), which is uniquely expressed in glia, and this glutamine is exported back to neurons, possibly through system N transporters (SNAT3/5) (Bak et al., 2006; McKenna et al., 2012).

The metabolic pathway for GABA in GABAergic neurons is very similar, as it is directly converted from glutamate into GABA by glutamate dehydrogenase (GAD). GAD comes in two isoforms – GAD67/GAD1 and GAD65/GAD2, but the division of labor between these two enzymes remains elusive (Soghomonian and Laprade, 1997; Schousboe et al., 2013). GABA is packaged into vesicles by vGAT (SLC32A1), released, and in contrast to glutamate, most released GABA is taken back up into neurons, through the plasma membrane GAT1 (Borden, 1996; Smith et al., 1996; Savtchenko et al., 2015), though some GABA is taken up into glia (Boddum et al., 2016). However, GABA is less easily transferred back into neurons, and instead converted into succinyl semialdehyde, and then succinate, which is incorporated into the tricarboxylic acid (TCA) cycle, which can then produce additional glutamate.

Metabolism through the TCA cycle in both glutamatergic and GABAergic neurons and their glia is likely a crucial aspect of neurotransmitter homeostasis. Glutamate can be converted into alpha ketoglutarate (αKG), an important TCA intermediate, and as previously mentioned, GABA can be converted into succinate, another TCA intermediate. Function of the TCA cycle is crucial for the regeneration of glutamate and GABA lost at the synapse. This relationship links mitochondrial function to neurotransmitter homeostasis, as the enzymes of the TCA cycle are located exclusively within the mitochondrial matrix (Hertz, 2013; Schousboe et al., 2013; Hertz and Rothman, 2017) (see Section 2.2.2).

Glutamate metabolism also creates a toxic byproduct for glutamatergic and GABAergic neurons, somewhat analogously to the toxicity produced by DA metabolism. The synthesis of glutamate from glutamine generates free ammonia, and synthesizing glutamine from glutamate requires ammonia. While some ammonia can diffuse across cell membranes, to reduce

alterations in local pH, neurons must shuttle ammonia to glia in order to maintain the glutamate/glutamine cycle. Most studies indicate that neurons do this through the exchange of other metabolites – the lactate/alanine shuttle is a promising candidate for this exchange. In this shuttle, neuronal pyruvate and glutamate are transaminated by alanine transaminase (ALAT) (abundantly expressed throughout the brain), which generates α-ketoglutarate and alanine. Alanine can then be shuttled into glia, which catalyzes the reverse reaction, resulting in the net transfer of an amino group (Figure 7). Importantly, the activity of this shuttle has not been shown to be directly coupled to the activity of the glutamine-glutamate cycle (Cooper, 2013; Schousboe et al., 2013).

1.3.2. Receptors Implicated in the pathogenesis of PD and LID

GPCRs

All G-protein coupled receptors (GPCRs) possess seven transmembrane domains and derive their name from the interaction with intracellular heterotrimeric G-proteins, Gαβγ. In response to agonist binding, the receptor becomes a guanine nucleotide exchange factor (GEF) of Gα, which causes an exchange of guanosine diphosphate (GDP) for guanosine triphosphate (GTP), and the dissociation of GPCR, Gα, and Gβγ subunits (Limbird, 2005). The GTP-associated Gα, as well as the Gβγ complex, activate various effectors that initiate intracellular signaling pathways. Even though Gα, Gβ, and Gγ each have multiple subtypes, the heterotrimer is most commonly classified by the Gα subunit into $G\alpha_{s/olf}$, $G\alpha_{i}$ (also referred to as $G\alpha_{i/o}$), $G\alpha_{q/11}$, and $G\alpha_{12/13}$ (Simon et al., 1991; Fields and Casey, 1997; Bridges and Lindsley, 2008). The effector for $G\alpha_{s}$, $G\alpha_{olf}$, and $G\alpha_{i}$ is adenylyl cyclase (AC), an enzyme family that generates the second messenger 3',5'-cyclic adenosine monophosphate (cAMP) from adenosine triphosphate (ATP). $G\alpha_{s}$ and $G\alpha_{olf}$ activate AC and elevate intracellular cAMP levels, whereas $G\alpha_{i}$ inhibits AC to prevent cAMP production. The primary effector for $G\alpha_{q}$ and $G\alpha_{11}$ is phospholipase C β (PLCβ),

an enzyme that converts phosphatidylinositol-4,5-bisphosphate (PIP_2) into the second messengers diacylglycerol (DAG) and inositol-1,4,5-trisphosphate (IP_3) (Figure 8).

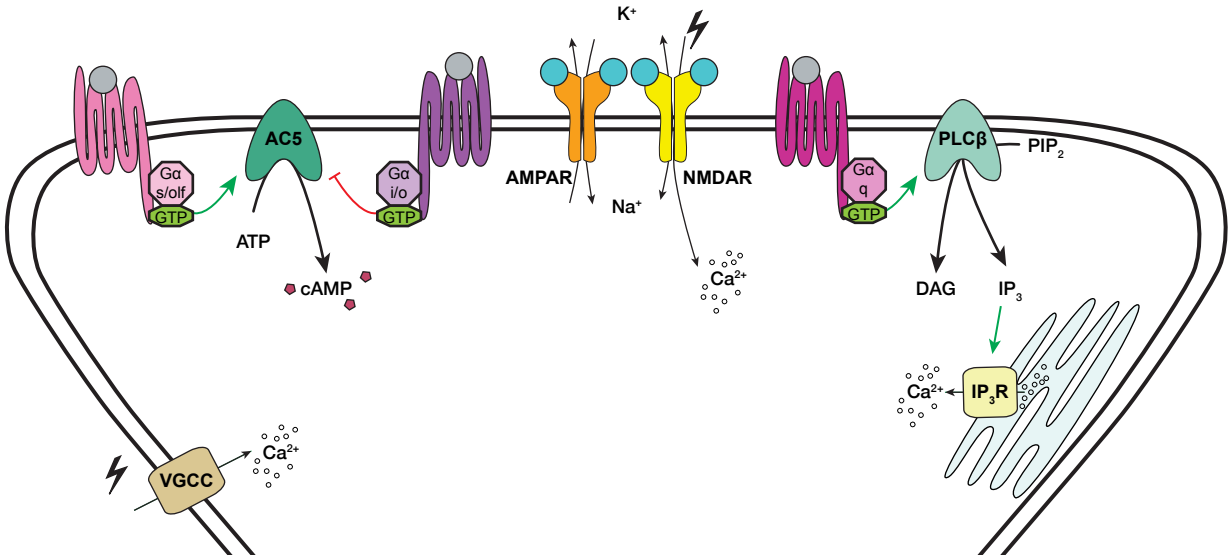

Figure 8. Schematic of major post-synaptic basal ganglia receptors and immediate effectors. $G\alpha_{s/olf}$ and $G\alpha_{i/o}$-coupled GPCRs oppositionally regulate AC5, which produces cAMP. $G\alpha_q$-coupled GPCRs activate PLCβ, which cleaves PIP_2 into DAG and IP_3. IP_3 triggers the release of Ca^{2+} from the ER by activation of IP_3Rs. AMPARs, when stimulated by glutamate, influx Na^+ and efflux K^+. NMDARs, in contrast, require both glutamate binding and voltage activation before becoming ion permeable, and also influx Ca^{2+}. Concurrently, neuron depolarization triggers the activation of VGCCs, increasing Ca^{2+} influx. AC5, adenylyl cyclase 5; PLCβ, phospholipase C β; VGCC, voltage gated Ca^{2+} channel. Adapted from Warren, 2017.

The D_1 class of DA receptors (D_1, D_5) and the adenosine 2A (A_{2A}) receptor couple to either $G\alpha_{olf}$ or $G\alpha_s$. D_1 receptors facilitate activity in dMSNs, which leads to disinhibition of the thalamus and facilitates movement. In PD, loss of DA stimulation of D_1 receptors impedes movement, whereas in dystonia, loss-of-function mutations in $G\alpha_{olf}$ cause repetitive twisting muscle contractions (Fuchs and Ozelius, 2013). A_{2A} receptors are concentrated in striatopallidal iMSNs, the first node of the indirect pathway, where they assemble as homodimers or heteromeric complexes with $G\alpha_{i/o}$-coupled DA D_2 receptors. These heteromeric complexes couple to $G\alpha_{q/11}$ rather than $G\alpha_{olf}$ and $G\alpha_{i/o}$ in the homomers (Morelli et al., 2007; Ferre et al., 2008). Because A_{2A} receptors antagonize the effect of D_2 receptors either through the formation of heteromers or through opposing actions on second messenger pathways, blockade of A_{2A} receptors has emerged as a potential approach for the treatment of PD (Schwarzschild et al., 2006).

$G\alpha_{i/o}$-coupled receptors are the most abundant group of GPCRs in the basal ganglia and include D_2-like DA receptors (D_2, D_3, D_4), metabotropic glutamate receptors (mGluRs), opioid receptors (δ, μ, κ), and muscarinic acetylcholine receptors (M2, M4) (Levey et al., 1991; Jiang and North, 1992; Mansour et al., 1995; Conn et al., 2005; Mátyás et al., 2006). Stimulation of $G\alpha_{i/o}$-coupled receptors decreases neuronal excitability. $G\alpha_{i/o}$-coupled receptors play an important role in the functional regulation of the basal ganglia. D_2-like DA receptors on striatopallidal neurons suppress activity in the indirect pathway and decrease the motor output of the basal ganglia. Inhibition of D_2-like receptors in the treatment of psychotic disorders can lead to unwanted motor side effects like tardive dyskinesia and other extrapyramidal symptoms (Divac et al., 2014). $G\alpha_{i/o}$-coupled receptors are also expressed in the direct pathway; for example, the M4 receptor is co-expressed with D_1 receptors in MSNs (and cholinergic interneurons), and dampens D_1 receptor-mediated increases in cAMP levels (Bernard et al., 1992; Sánchez-Lemus and Arias-Montaño, 2006). Feedback inhibition is generated through presynaptic autoreceptors. In addition to signaling through Gα, a large group of presynaptic $G\alpha_{i/o}$-coupled receptors inhibits vesicular release through Gβγ signaling (Wallmichrath and Szabo, 2002; Fisone et al., 2007). D_2 receptors, M2/4 receptors, and some mGluRs (ie, group II and group III receptors) act as autoreceptors at nigrostriatal and corticostriatal synapses. Collectively, $G\alpha_{i/o}$-coupled receptors are crucial for modulating afferent and efferent activities of the basal ganglia network.

$G\alpha_{q/11}$-coupled GPCRs activate PLCβ, which hydrolyzes the phosphatidylinositol PIP_2 into two different second messengers, IP_3 and DAG. Downstream, intracellular calcium (Ca^{2+}) levels are increased, and Ca^{2+}-sensitive effectors trigger a diverse array of signaling events. The primary $G\alpha_{q/11}$-coupled receptors in the striatum include mGlu1 (GRM1), mGlu5 (GRM5), and muscarinic receptors M1, M3, and M5. mGlu5 activity has been directly linked to endocannabinoid (eCB) signaling and the initiation of long-term depression (LTD), as well as to the potentiation of other receptors such as N-methyl-D-aspartate receptors (NMDARs), by amplifying signals associated

with increased Ca^{2+} influx (Harvey and Shahid, 2012). NMDAR-mediated signaling is also potentiated by the M1 receptor (Calabresi et al., 1998).

Ionotropic Receptors

Ligand-gated ion channels are transmembrane receptor complexes that conduct ion flow through channel pores in response to the binding of neurotransmitter. Unlike voltage-gated ion channels, these receptors are typically not sensitive to membrane potential ($\Delta\psi$). Although ionotropic receptors are commonly regarded as postsynaptic elements, they are also found in presynaptic membranes near release sites, where they play critical roles in regulating vesicle fusion (Engelman and MacDermott, 2004).

Ionotropic glutamate receptors (ie, NMDARs, alpha-amino-3-hydroxy-5-methyl-4-isoxazolepropionate receptors (AMPARs), and kainate receptors), and nicotinic acetylcholine receptors (nAChRs) are the primary cation-conducting ionotropic receptors in the basal ganglia (MacDermott et al., 1999). The nonspecific cation-conducting nAChRs and NMDARs channels pass monovalent and divalent cations along their electrochemical gradients (i.e., Na^+, K^+, and Ca^{2+}), while AMPARs and kainate receptors are RNA-edited to restrict permeability to monovalent cations (ie, Na^+ and K^+). Ionotropic glutamate receptors are heteromeric tetramers assembled in different combinations from a diversity of subunits. Receptor characteristics are determined by subunit compositions and molecular modifications. Specifically, AMPARs and kainate receptors undergo RNA editing to modulate Ca^{2+} permeability, as well as alternative splicing of RNA to modify receptor kinetics (Bernard et al., 1992; Paschen and Djuricic, 1994; Akbarian et al., 1995). NMDARs are partially voltage-dependent, as their activation is dependent on coincident glutamate stimulation and membrane depolarization to relieve a magnesium block within the channel (Figure 8). The complex molecular and functional regulation of ionotropic glutamate receptors enables integration of chemical, electrical, temporal, and developmental factors within the glutamatergic system (Kandel et al., 2000; Braidy et al., 2014).

Ion influx has three major roles—membrane depolarization, activation of Ca^{2+} channels, and activation of Ca^{2+}-sensitive second messengers. In response to ion flux through ionotropic receptors, voltage-gated ion channels open, action potentials are generated, and Ca^{2+} enters through L-type voltage-gated Ca^{2+} channels (VGCCs) (Kandel et al., 2000). Ca^{2+} entering through VGCCs or Ca^{2+}-permeable ionotropic receptors activates second messengers including calmodulin (CaM), Ca^{2+}/CaM-dependent protein kinases II and IV (CaMKII/IV), AC1 and AC8, and calcineurin (PP2B) (Xia and Storm, 2005).

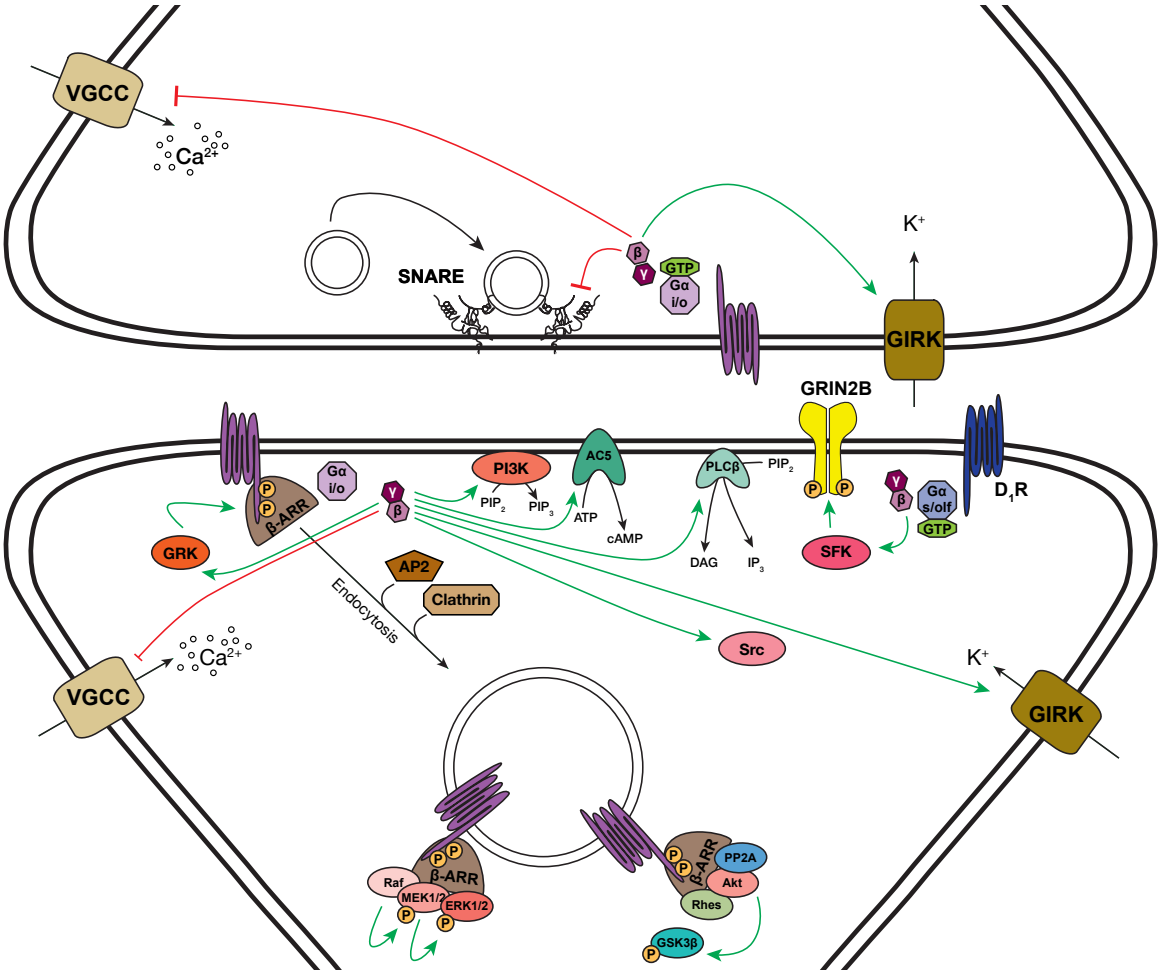

Figure 9. Schematic of Gβγ signaling.
Gβγ directly activates several effectors including PI3K, AC, PLCβ, Src, and SFK, potentiating a number of signaling cascades. Furthermore, multiple ion channels are regulated by Gβγ, including GIRKs, VGCCs, and NMDARs. At the presynaptic membrane, Gβγ can inhibit the binding of the SNARE complex and prevent vesicle fusion. Gβγ can recruit certain isoforms of GRK, which phosphorylate GPCRs and recruit β-arrestins. β-arrestins terminate GPCR signaling, and also facilitate receptor endocytosis. Moreover, β-arrestins can scaffold multiple components of signaling cascades and play an important role in signal transduction. Redrawn with permission from Warren, 2017.

1.3.3. Second Messenger Cascades Implicated in the Pathogenesis of PD and LID

Gβγ

Though GPCRs are frequently grouped on the basis of Gα class, Gβγ subunits can also activate signal transduction pathways independently (Smrcka, 2008) (Figure 9). A number of effectors bind directly to Gβγ, including the G-protein-activated inwardly rectifying K^+ channel (GIRKs), GPCR kinases (GRKs), N- and P/Q-type Ca^{2+} channels, PI3-kinases (PI3K), PLCβ1, Src, and ACs (Logothetis et al., 1987; Tang and Gilman, 1991; Camps et al., 1992; Pitcher et al., 1992; Stephens et al., 1994; Herlitze et al., 1996; Ikeda, 1996). Interestingly, Gβγ signaling by D_1 receptors potentiates NMDAR-mediated activation of the mitogen-activated protein kinase (MAPK) pathway. Gβγ activates a Src-family kinase (SFK), which phosphorylates the GRIN2B subunit of the NMDAR to increase its activity and mediate Ca^{2+} influx (Nishi et al., 2011).

Presynaptically, Gβγ subunits modulate neurotransmitter release. They can bind to presynaptic Ca^{2+} channels and reduce their sensitivity to membrane depolarization (Dolphin, 2003), or activate GIRK channels to further hyperpolarize the cell. Moreover, Gβγ subunits have a direct inhibitory effect on the transmitter release machinery by binding to proteins of the soluble N-ethylmaleimide-sensitive factor attachment protein receptor (SNARE) complex (Blackmer et al., 2005; Gerachshenko et al., 2005). In the basal ganglia, Gβγ modulates DA homeostasis by binding and inhibiting the DAT (Garcia-Olivares et al., 2013).

One of the most relevant targets for Gβγ in DA receptor signaling are GRKs. After an agonist binds to a GPCR, GRKs (Ser/Thr kinases) phosphorylate the receptor as part of the desensitization process. GRKs phosphorylate GPCRs at two residues to facilitate the high-affinity binding of an arrestin protein and prevent further coupling to G-proteins (Kohout and Lefkowitz, 2003). Of four known arrestins, two are restricted to the visual system, while the other two (β-arrestin 1 and 2) are expressed abundantly in the CNS, and both are found in dMSNs and iMSNs (Bychkov et al., 2012). Following arrestin binding, an internalization complex is formed with the

GPCR, β-arrestin, adaptor protein 2 (AP2), and clathrin, leading to receptor internalization through clathrin-mediated endocytosis (Beaulieu et al., 2007). The acidic environment of endocytosed vesicles facilitates the dissociation of the agonist from the receptor. Receptor internalization helps to control receptor numbers by shuttling internalized receptors to degradation, or recycling them back into the synapse (Marchese et al., 2008).

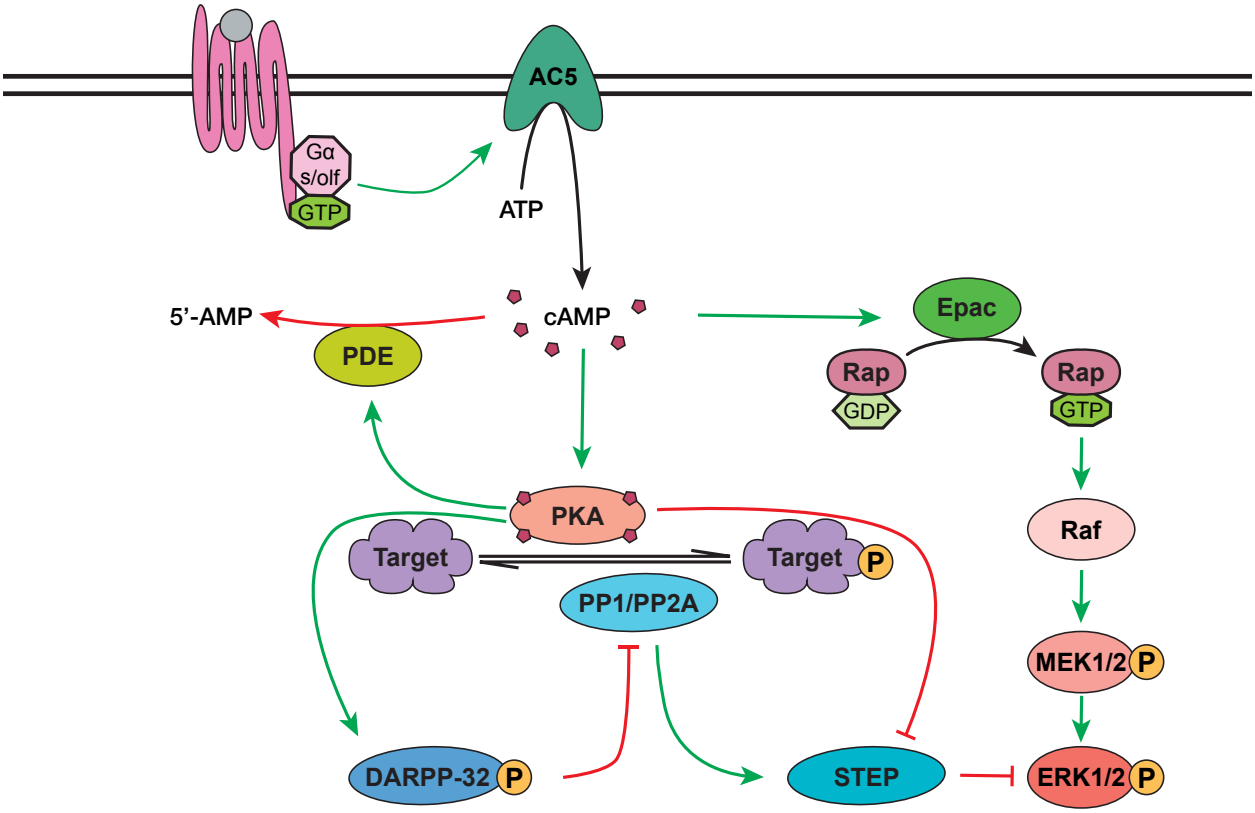

Figure 10. Schematic of $G\alpha_s$ and cAMP signaling.
PKA is one of the primary targets of cAMP, and it phosphorylates an array of intracellular targets. Phosphorylation is potentiated through the activation of DARPP-32, which inhibits phosphatase activity, though cAMP signaling is also terminated through the activation of PDE. cAMP additionally activates Epac, which can activate the MAPK cascade. This activation is also supported through PKA inhibition of STEP phosphatase. PDE, phosphodiesterase; DARPP-32, dopamine- and cAMP-regulated phosphoprotein; Epac, exchange protein activated by cAMP; STEP, striatal-enriched tyrosine phosphatase. Adapted from Warren, 2017.

β-arrestin signaling regulates kinase cascades and activates transcription factors. β-arrestin participates in scaffolding of MAPK pathway members, such as MAP3K (Raf), MAP2K (MEK), and extracellular signal-regulated kinase (ERK1/2), as well as Ask1/MAPKK4/JNK3 and Ask1/MAPKK3/p38 cascades, all of which can lead to changes in gene transcription (Lefkowitz

and Shenoy, 2005; DeWire et al., 2007). Interestingly, D_2 receptors utilize β-arrestin in a nontraditional cAMP-independent signaling pathway that involves Akt and PP2A (Beaulieu et al., 2007). Formation of the D_2 β-arrestin complex results in the dephosphorylation/inactivation of Akt by PP2A, and the subsequent dephosphorylation/activation of glycogen synthase kinase 3 (GSK3)-mediated signaling (Beaulieu et al., 2005). Of particular interest for the basal ganglia, the Ras homologue enriched in striatum (Rhes) has been shown to modulate the β-arrestin, PP2A, and Akt complex (Harrison et al., 2013). GSK3 is a regulator of many cellular functions, including cell architecture, motility, and survival (Jope and Johnson, 2004), as well as neurogenesis, synapse formation, and neurite outgrowth (Cole, 2012). Importantly, though DA stimulation of the D_2 receptor decreases the activation of protein kinase A (PKA) (see below), activation of this receptor may still induce DA-dependent adaptations in Gβγ and β-arrestin mediated signaling cascades.

$G\alpha_{s/i}$- and cAMP-linked cascades

$G\alpha_s$ and $G\alpha_i$-linked receptors compete to activate or inhibit AC, which produces cAMP. A major role of cAMP is to activate the serine/threonine (Ser/Thr) kinase PKA (Montminy, 1997), but also an exchange protein directly activated by cAMP (Epac), a GEF for small G-proteins Rap1 and Rap2 (Kawasaki et al., 1998) (Figure 10). cAMP signaling is terminated by the cessation of AC-mediated cAMP production and by phosphodiesterases (PDEs), which break down intracellular cAMP to 5'-AMP (Sassone-Corsi, 2012). Phosphorylation of PDE enzymes by PKA increases their catalytic activity. PKA transfers a phosphate from ATP onto the amino acids Ser or Thr within consensus amino acid sequences in substrate proteins (Ubersax and Ferrell, 2007). PKA signaling is facilitated and accelerated by scaffolding proteins known as "A kinase anchoring proteins" (AKAPs). AKAPs compartmentalize PKA and affiliated substrates and regulate the spatial and temporal organization of the cAMP-PKA pathway (Wong and Scott, 2004).

PKA plays a central role in the signaling cascades of the basal ganglia. In the postsynaptic area of dendrites, PKA phosphorylates the NMDAR subunit GRIN1 and facilitates NMDAR function (Dudman et al., 2003). In the nucleus, PKA activates the transcription factor cAMP response element binding protein (CREB), either directly (Montminy and Bilezikjian, 1987) or by initiating second messenger cascades at the synapse (Dudman et al., 2003). Phosphorylated CREB transactivates the DNA enhancer cAMP response element (CRE) and regulates many striatal genes. These include genes for the opioid peptides dynorphin (preprodynorphin – ppd) and enkephalin (preproenkephalin – ppe) (Konradi et al., 1993, 1995; Cole et al., 1995; Simpson and McGinty, 1995), the transcription factor cFos (Konradi et al., 1994; Konradi and Heckers, 1995) and others.

Rap1 and Rap2 are Ras-like proteins associated with cell adhesion and integrin signaling (Bos, 2003; Gloerich and Bos, 2010). While the precise mechanism of action is still controversial, it seems that Epac activity alone is insufficient to trigger Rap1 activation of Raf, and thus the MAPK pathway. In contrast, co-activation of Rap1 by Epac and PKA promotes the activation of Raf and MAPK signaling (Wang et al., 2006). Epac has been implicated in neuronal differentiation and growth, as well as synaptic plasticity and depression when linked to D_1 receptor activity (Beaulieu and Gainetdinov, 2011). Moreover, Epac signaling promotes vesicle release in neuroendocrine cells by inhibiting the action of K^+ ATP channels and interacting with RyRs to increase intracellular Ca^{2+} (Gloerich and Bos, 2010). Epac is thus a model for PKA-independent signaling of $G\alpha_{olf}$ and cAMP.

PKA can modulate the MAPK pathway as well, by disrupting inhibition of MAPK signaling. PKA phosphorylates and inactivates STEP (striatal-enriched tyrosine phosphatase), disinhibiting ERK1/2 phosphorylation, and indirectly prevents the activation of STEP via dopamine- and cAMP-regulated neuronal phosphoprotein (DARPP-32) (see below). This dual mechanism of STEP

suppression potentiates ERK1/2 activity, which further couples $G\alpha_S$-mediated signals to MAPK pathways.

PKA signaling is counteracted by the action of protein phosphatases, which dephosphorylate a number of PKA targets. They fall into three different groups based on their target residues —Ser/Thr (e.g., protein phosphatase 1 (PP1)), tyrosine (Tyr; e.g., STEP), and dual-specificity phosphatases (DUSPs) (Barford, 1996; Mansuy and Shenolikar, 2006; Roskoski, 2012). While all three classes of protein phosphatases play a role in dephosphorylating PKA targets in the basal ganglia, striatal phosphatases regulated by PKA have gained special attention. These include DARPP-32, regulator of CaM signaling (RCS), and ARPP16/19 (Walaas et al., 2011), which directly or indirectly control the activity of other protein phosphatases such as PP1, PP2B, and PP2A, respectively. DARPP-32, the best characterized of the PKA-regulated phosphatases in the striatum, has various phosphorylation sites that are connected to different signaling cascades. PKA phosphorylates Thr34, which facilitates inhibition of PP1, while phosphorylation of Thr75 by cyclin-dependent kinase 5 (CDK5) blocks PKA activity. mGlu5, a $G\alpha_{q/11}$-coupled metabotropic glutamate receptor co-expressed in MSNs with D_1 receptors, activates CDK5 to phosphorylate DARPP-32 (Conn et al., 2005). The balance of kinase and phosphatase activity in the basal ganglia is crucial for signal integration and transduction to the nucleus.

$G\alpha_q$- and Ca^{2+}-linked cascades

$G\alpha_{q/11}$ activates PLCβ, which converts PIP2 into DAG and IP_3. The most disease-relevant target of DAG and IP_3 is the PKC family of Ser/Thr kinases, and RasGRPs, a subfamily of GEFs. PKC is activated by DAG concurrent with IP_3-induced Ca^{2+} influx, and is involved in all aspects of neuronal function and malfunction - from neurotransmitter release and uptake, to receptor and ion channel function, to gene regulation, PKC modulates neuronal development, neuronal excitability, learning and memory, and neuronal death (Mellor and Parker, 1998). RasGRPs are

activated by DAG, and promote GDP/GTP exchange and activation of Ras GTPases. Ras GTPases activate the ERK/MAPK signal transduction cascade (Figure 11).

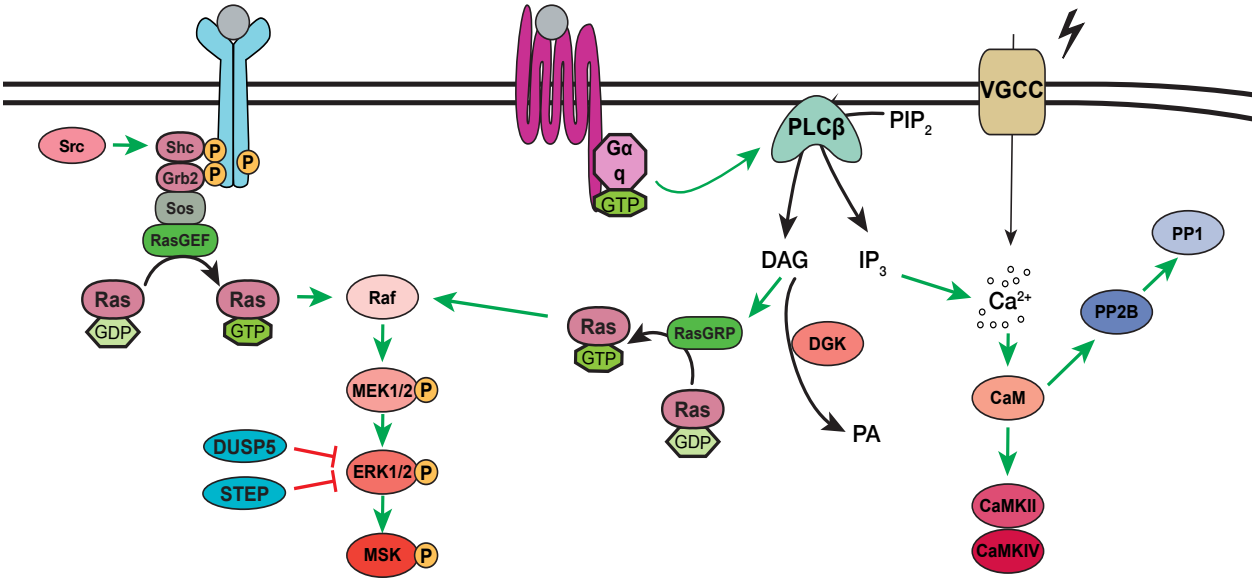

Figure 11. Schematic of $G\alpha_q$, Ca^{2+}, and RTK signaling.
$G\alpha_q$ stimulation-mediated activation of PLCβ releases both DAG and IP_3 as second messengers. IP_3 releases Ca^{2+} from intracellular stores, which combined with extracellular Ca^{2+} entry through VGCCs, activates CaM. CaM bidirectionally activates CaMKs, and Ca^{2+}-sensitive phosphatase PP2B. DAG activates RasGRPs, which can stimulate Ras, but is also cleaved by DGK as an entry for some lipid signaling. RTK activation also activates Ras, so both types of receptor stimulation can activate MAPK singaling, which is counteracted by phosphatase activity. CaM, calmodulin; CaMK, Ca^{2+} and CaM-kinase; DUSP, dual specificity phosphatase. Adapted from Warren, 2017.

DAG signaling is terminated by DAG kinase (DGK) (Mérida et al., 2008), which catalyzes phosphorylation of DAG to phosphatidic acid, and thus has a major role in deactivating DAG and its affiliated substrates. IP_3 mobilizes intracellular Ca^{2+} release through its interaction with IP_3 receptors (IP_3Rs). IP_3Rs are intracellular Ca^{2+} channels that are located primarily in the endoplasmic reticulum (ER) and are regulated by IP_3 and Ca^{2+} (Dawson, 1997).

PKC plays nearly as many roles as PKA in the basal ganglia. In projection neurons, PKC modulates voltage-gated ion channels and receptors, and through phosphorylation of Raf, activates the MAPK pathway, discussed below. PKC is also a key player in maintaining dopaminergic tone via regulation of DAT internalization at presynaptic membranes (Gabriel and Litchfield, 2013).

MAPK cascades regulate growth, proliferation, and cell migration, and pathological deregulations of these pathways are associated with different types of cancer. MAPK pathways are activated by receptor tyrosine kinases (RTKs), as well as by non-RTKs such as Src, or through transactivation of other pathways. An adaptor protein with a phosphotyrosine-binding domain and an SH2 domain (eg, Shc; Ginés et al., 2010) binds to phosphorylated residues of the tyrosine kinase. The SH2 domain of Shc links to the SH2 domain of Grb2 (growth factor receptor bound protein 2). Sos, a RasGEF, interacts with one of two SH3 domains on Grb2 and activates a Ras GTPase (Cullen and Lockyer, 2002), completing the chain from phosphorylated tyrosine kinase to MAPK signaling. GTP-bound Ras activates Raf, or a similar MAPKKK, while PKC activates Raf through phosphorylation (Kolch et al., 1993). Raf phosphorylates MEK1/2, a dual-specificity MAPKK, which phosphorylates ERK1/2 at Thr/Tyr residues.

MAPKs such as ERK1/2 and JNK can translocate to the nucleus where they phosphorylate and activate a plethora of downstream kinases and transcription factors such as CREB, SRF, c-Jun, c-Fos, and others (Vanhoutte et al., 1999; Turjanski et al., 2007). In some cases, phosphorylation of transcription factors increases transcriptional activity (ie, c-Jun, CREB), while in other cases phosphorylation stabilizes the protein and increases signal duration (ie, c-Fos at Ser374) (Wiegert and Bading, 2011). MAPK pathway regulation of transcription factor activities and histone modification alters the accessibility of DNA, recruits RNA polymerases, and alters the gene expression pattern in cells. Thus, MAPK signaling links receptor activation to nuclear activity and generates a distinct transcriptional profile that elicits cellular adaptations and influences behavioral outputs.

Among the kinases activated by ERK1/2 in the striatum is ribosomal S6 kinase (RSK) and mitogen and stress activated protein kinase (MSK) (Roskoski, 2012a), which phosphorylates transcription factors such as the serum response factor (SRF), NFκB, and c-Fos (at Ser362). RSK enzymes also regulate protein synthesis by phosphorylating ribosomal protein S6 itself and eukaryotic initiation factor 4B (eIF4B) (Roskoski, 2012a). MSK1 phosphorylates histone H3 at the

fosB promoter and increases the accumulation of ΔFosB (Feyder et al., 2014), a truncated splice variant of the fosB gene linked to the development of LID (Feyder et al., 2014) and addiction (Nestler, 2001). Interestingly, RSK/MSKs also phosphorylate/activate CREB at Ser133—the same residue phosphorylated by ERK1/2, PKA, CaMKII, and CaMKIV (Wiegert and Bading, 2011).

Various protein phosphatases counterregulate the MAPK pathway. MAPK phosphatases, a group of DUSPs that dephosphorylate Ser/Thr and Tyr residues, play a major role in the deactivation of MAPK. Among them, DUSP5 is specific for ERK1/2. The Ser/Thr phosphatases PP2A and PP2C are also active in MAPK pathways, while tyrosine residues can be dephosphorylated by STEP (Roskoski, 2012a, 2012b).

Ca^{2+} accumulation in the postsynaptic area initiates a cascade of events that can reach the nucleus and activate gene expression. Gene and protein expression patterns are modified to promote dendritic growth, improve synaptic strength, and shift neuronal homeostasis (Greer and Greenberg, 2008). An increase in cytosolic levels of Ca^{2+} activates kinases and phosphatases that affect the function and trafficking of various receptors and channels. At the presynaptic site, localized Ca^{2+} signals drive vesicle fusion at active zones to regulate neurotransmitter release (Schneggenburger and Neher, 2005). These vital roles of Ca^{2+}, together with the neurotoxicity of high Ca^{2+} concentrations (Choi, 1988), require neurons to expend considerable amounts of energy to rapidly restore low levels of cytosolic Ca^{2+}, against a gradient of extracellular Ca^{2+} levels 10^4 times greater than cytosolic Ca^{2+}. Ca^{2+} is therefore continuously pumped in an ATP-dependent process into the extracellular space or into internal Ca^{2+} storage sites like the ER or mitochondria (Verkhratsky and Petersen, 1998).

Ca^{2+} influx and propagation is tightly regulated in MSNs. The most robust Ca^{2+} influx comes from VGCCs, which open as the MSNs depolarize. Most isoforms of VGCCs are expressed in MSNs and are localized to distinct parts of the neuron. The Ca_{v2} family of channels, including P/Q-, N-, and R-type channels, has the highest level of expression, but the Ca_{v1} (L-type)

and Ca_{v3} (T-type) channels are also expressed and mediate important functional roles (Hurley and Dexter, 2012). L-type (mostly $Ca_{v1.3}$), R-type, and T-type channels are most prominent in MSN spines and shafts, and are crucial for dendritic signal integration, coincidence detection, and generation of Ca^{2+} waves (Higley and Sabatini, 2008). L-type Ca^{2+} channels play a particularly important role in gene expression and neuroplasticity in the striatum (Konradi et al., 1996, 2003; Rajadhyaksha et al., 1999), and are involved in the induction of eCB-mediated LTD in MSNs (Lovinger and Mathur, 2012).

Ca^{2+} release from intracellular stores is mediated by activation of IP_3Rs or ryanodine receptors (RyRs). Both receptor types are distributed throughout the ER and are sensors of Ca^{2+} levels. Increased cytosolic Ca^{2+} levels can potentiate Ca^{2+} release from IP_3Rs or RyRs and generate Ca^{2+} waves (Berridge, 1998).

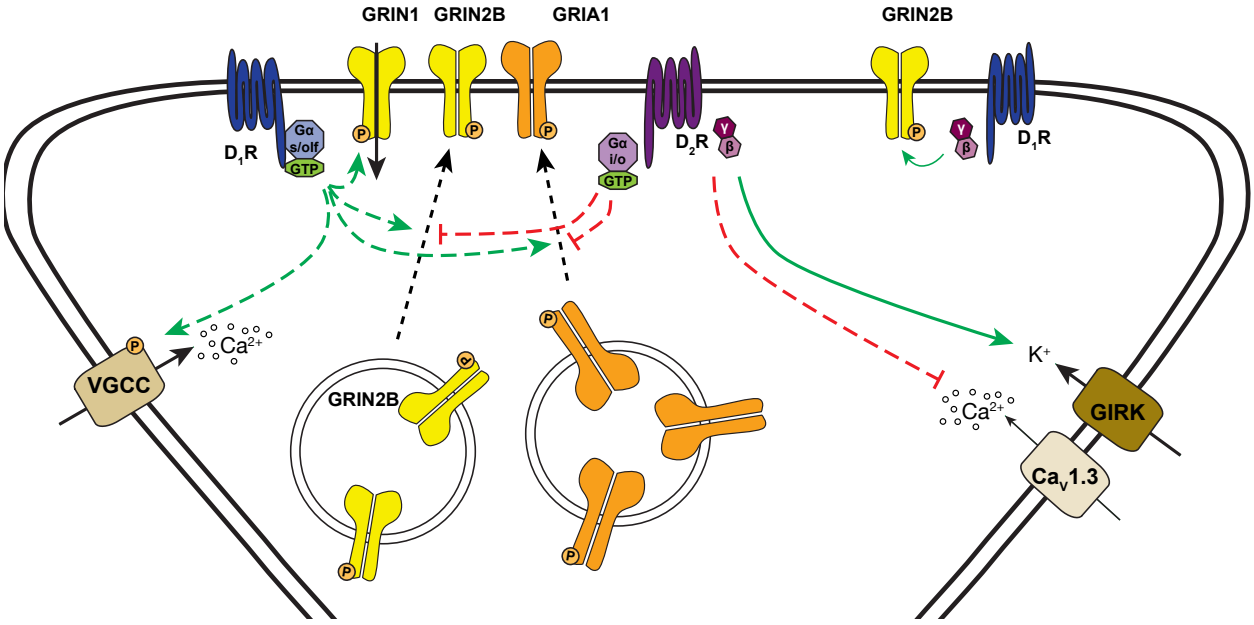

Figure 12. Simplified mechanisms of DAergic regulation of glutamatergic signaling.
D_1 activity potentiates glutamatergic signaling in a number of ways; by increasing conductance through GRIN1-containing NMDARs and ion channels such as VGCCs, and by increasing trafficking of both NMDARs and AMPARs to the synapse, likely through PKA-phosphorylation-dependent mechanisms. By inhibiting PKA activation, D_2 activity reduces receptor trafficking. D_2 βγ subunits additionally directly activate GIRK and indirectly inhibit $Ca_V1.3$ channels, reducing excitability. D_1 βγ subunits also promote phosphorylation and activation of GRIN2B-containing NMDARs.

The cytosolic rise in Ca^{2+} can activate a number of signal transduction pathways. CaM undergoes a conformational switch upon binding of Ca^{2+}, which leads to the activation of a number of effector proteins in the nucleus and the cytoplasm, including CaMKs, ACs, and PP2B. Members of the CaMK family are Ser/Thr kinases. CaMKII is among the most abundant proteins in the post synaptic density, where it plays a major role in modulating the activity of ion channels (Kennedy et al., 1983). CaMKII is thought to be the primary initiating signal in NMDAR-mediated long-term potentiation (LTP) and gene expression (Mayford, 2007; Swulius and Waxham, 2008). CaMKII is expressed at very high levels in the striatum, in MSNs, corticostriatal glutamatergic terminals, and dopaminergic terminals. CaMKIV is involved in the phosphorylation of a number of activity-dependent transcription factors such as CREB (Soderling, 1999).

Ca^{2+} influx is terminated by voltage- and Ca^{2+}- dependent inactivation of VGCCs. L-, N-, and R-type VGCCs undergo Ca^{2+}- and voltage- dependent inactivation (Evans et al., 2015). Molecules activated by Ca^{2+} signaling are deactivated by protein phosphatases like PP2B, which is enriched in the post synaptic density and the cell soma. PP2B is activated by binding of Ca^{2+}-bound CaM to the catalytic subunit together with concurrent binding of Ca^{2+} to the regulatory subunit. PP2B has many functions, including disinhibition of PP1, and the modulation of neurotransmitter release and receptor activity (Groth et al., 2003).

DAergic Regulation of Glutamatergic Activity

Mechanisms of pathway overlap or cross-talk are important considerations for the prediction of signal transduction outcomes. One of the most important examples of this overlap is the direct modulation of glutamatergic signaling through ionotropic receptors by DAergic stimulation, which is regulated differentially in dMSNs and iMSNs (Figure 12).

D_1 activation of PKA and downstream effectors can generally increase neuronal excitability by modulating ion flux through ligand-gated or voltage-gated Na^+, Ca^{2+}, and K^+ channels (Cepeda et al., 1993; Surmeier et al., 2007; Tritsch and Sabatini, 2012; Threlfell and

West, 2013). PKA facilitates NMDAR activity and gene expression by phosphorylating the GRIN1 subunit of NMDARs (Dudman et al., 2003), which has been shown to increase Ca^{2+} transients and current through the receptor (Murphy et al., 2014; Shen et al., 2017). AMPARs are activated by a different mechanism: The GRIA1 subunit is inserted into the postsynaptic membrane upon phosphorylation by PKA (Mangiavacchi and Wolf, 2004). D_1 stimulation can also increase surface expression of both AMPARs and NMDARs (Svenningsson et al., 2004; Shen et al., 2017). Activation of the cAMP pathway by D1- and other $G\alpha_s$-coupled receptors consequently potentiates excitatory neurotransmission (Cepeda and Levine, 1998; Konradi, 1998).

In contrast, D_2 activation in iMSNs reduces AMPAR currents (Cepeda et al., 1993), likely through dephosphorylation of GRIA1 which would, through the reverse mechanism observed in PKA activation, promote the trafficking of the receptor out of the synapse (Håkansson et al., 2006; Shen et al., 2017). D_2 activation also triggers the reduction in glutamate release from glutamatergic terminals, potentially though a presynaptic Gβγ-related mechanism (Bamford et al., 2004). Postsynaptically, Gβγ activation of PLCβ can mobilize sufficient Ca^{2+} to reduce activity of Cav1.3 channels through calcineurin (Hernandez-Lopez et al., 2000; Olson et al., 2005), and can reduce neuronal activity through the activation of GIRK channels (Greif et al., 1995).

As the activation of the D_1 and D_2 receptors induces contrasting signaling cascades, DA stimulation produces very different effects on glutamate signaling in dMSNs and iMSNs. Through the increase in the activity of multiple ion channels, D_1 stimulation increases dMSN responsiveness to prolonged glutamate release, while decreasing response to more uncoordinated signals, highlighting the role of DA in filtering signals from the cortex. In contrast, D_2 stimulation more generally reduces iMSN responsiveness to glutamate. This differential regulation highlights the essential role of DA in the striatum as well as the systems that are deregulated following its loss.

1.4. Molecular correlates of DA denervation and LID

As even the adult brain is a highly plastic and adaptable system, the DA denervation to the striatum that accompanies the onset of PD is accompanied by a vast array of molecular alterations in both the MSNs and their surrounding afferent presynaptic terminals. According to the classical model, DA denervation, by simultaneously decreasing stimulation of D_1 and D_2 receptors, hypoactivates dMSNs and hyperactivates iMSNs (Lanciego et al., 2012), reducing the net motor output of the thalamus. Reintroduction of DA into this system through L-DOPA treatment initially reverses some of these changes, and restores motor behavior. However, the persistent plasticity of the striatum induces further molecular alterations to the neurotransmitter mediated signaling pathways, which ultimately reverses the balance between the direct and indirect pathways. This reversal hyperactivates dMSNs, hypoactivates iMSNs, and produces a net overproduction of motor output from the thalamus, which presents as LID (Brotchie et al., 2005; Jenner, 2008) (see Figure 5). While a complete catalogue of the molecular, morphological, and electrophysiological alterations associated with both DA denervation and L-DOPA treatment is outside the scope of this chapter, the following sections will review the animal models used to study these systems, alterations in receptor expression and function, adaptations in signaling cascades, and changes in gene expression.

1.4.1. Animal models used to study DA depletion and LID

The depletion of DA in rat and primate models requires the targeted lesioning of the SNc. Though in PD, these neurons deteriorate gradually over the course of many years, toxicity-based DA denervation in animal models results in a more rapid onset. In rodents, 6-hydroxydopamine (6-OHDA), a potently neurotoxic analogue of DA, is typically stereotactically injected into the striatum, SNc, or median forebrain bundle, which contains the axon projections of the SNc (Tieu, 2011). 6-OHDA must be injected as it does not cross the blood-brain barrier. As it is also toxic to noradrenergic neurons, desipramine, a norepinephrine transporter (NET) inhibitor, is coinjected

to confer specificity to dopaminergic neurons (Ungerstedt, 1968; Kostrzewa and Jacobowitz, 1974). 6-OHDA is taken up through the DAT (Luthman et al., 1989), where it is then oxidized and produces reactive oxygen species (ROS) (Kumar et al., 1995) as well as inhibits mitochondrial respiratory chain (RC) activity (Glinka et al., 1997) and these concomitant effects cause cell death (Tieu, 2011). Typically, this lesioning is performed unilaterally, which both reduces mortality facilitates the *in* vivo determination of the completeness of the lesion. Application of a DA agonist following unilateral lesioning results in rotations, which correlate with the magnitude of the lesion (Przedborski et al., 1995; Tieu, 2011).

The other most frequently used compound to lesion the SNc is 1-methyl-4-phenyl-1,2,3,6-tetrahydropyridine (MPTP), a compound with a long history in PD research. The clinical relevance of MPTP was identified in 1983 (Langston et al., 1983) when, following its accidental synthesis in an attempt to produce MPPP (an analogue of meperidine), people who had injected it presented with parkinsonian symptoms. Subsequent studies determined that MAOB converts MPTP into MPP^+ (Heikkila et al., 1984), which is taken up through the DAT (Shen et al., 1986) and accumulated in dopaminergic neurons, where it inhibits mitochondrial function by interfering with Complex I activity (Ramsay et al., 1986). This inhibition causes nigral cell death, similarly to 6-OHDA (Langston, 2017). Interestingly, though this compound can be delivered systemically and still induce specific nigral cell death, MPTP is not a useful tool in rats, which due to differences in blood-brain barrier MAOB activity are largely resistant to the compound (Riachi et al., 1991).

In both models, LID is induced by treatment with L-DOPA, though approaches vary considerably in dose quantity and frequency, depending on the desired study outcomes. However, different criteria have been established for characterizing dyskinesia-like movements in both rodent and primate models. In rodents, L-DOPA treatment of unilateral lesioning eventually causes hyperkinetic movements in the contralateral forelimb, and involuntary movements of the axial and orofacial muscles. These are typically classified as abnormal involuntary movements (AIMs) and rating scales have been established to quantify symptom severity (Andersson et al.,

1999; Steece-Collier et al., 2003; Dekundy et al., 2007; Cenci and Ohlin, 2009). The primate model is an even better phenocopy of human LID, as the lesion is bilateral. Treatment with L-DOPA produces the characteristic choreiform and dystonic movements associated with LID in humans, that are essentially indistinguishable from the human presentation (Porras et al., 2012). Because of the clear translational application of both of these models, they have been used extensively to characterize the molecular alterations associated with the development of LID.

1.4.2. Receptors and Transporters

As dopaminergic input to the striatum is lost, one expected adaptation would be the upregulation of DA receptors. In many receptor systems, a withdrawal of a stimulus produces a sensitization response involving receptor upregulation, such as D_2 receptor binding has been shown to increase following amphetamine stimulation (Hume et al., 1992; Ginovart et al., 1999). However, no changes in D_1 or D_2 receptor density have been conclusively shown in PD (Cenci, 2017). In contrast, hyperactivation of the direct pathway is transduced through supersensitivity of the D_1 receptor, conferred though increased expression of its G protein, $G\alpha_{olf}$ (Corvol et al., 2004), and increased D_1-$G\alpha$ coupling (Hervé et al., 1993; Aubert et al., 2005) (Figure 13). Though this phenomenon has been less thoroughly documented, some studies have also reported that supersensitivity of the D_2 receptor contributes to the manifestation of motor fluctuations in response to L-DOPA (Gold et al., 2007). The relevance of DA receptor hyperactivation is further supported by studies demonstrating that overexpression of GRK proteins attenuates the development of LID (Ahmed et al., 2010, 2015), as GRK proteins initiate the termination of GPCR signaling and promote arrestin binding (Gurevich and Gurevich, 2006).

Conversely, the numbers and types of NMDA and AMPA receptors are altered during the induction of LID (Figure 13). The ratio of GRIN2A-containing to GRIN2B-containing receptors at the synapse increases, likely through a combination of an upregulation of GRIN2A subunits (Calon et al., 2002), and shuttling of GRIN2B-containing receptors to extra-synaptic sites (Huot

et al., 2013). Hyperactivation of NMDA receptors has also been directly implicated in LID as NMDA blockade improves motor symptoms (Metman et al., 1998; Chassain et al., 2003). Similarly, AMPA receptor trafficking and subunit expression is perturbed, as GRIA2/3-containing subunits are increased at the synapse. However, selective inhibition of AMPA receptor activity does not demonstrably improve LID symptoms (Huot et al., 2013). Increases in mGlu5 expression and binding have been reported in DA-denervated and in dyskinetic animals (Samadi et al., 2008; Ouattara et al., 2010), suggesting overactivity of this pathway in LID (Huot et al., 2013). Leveraging this difference has resulted in one of the more successful non-dopaminergic

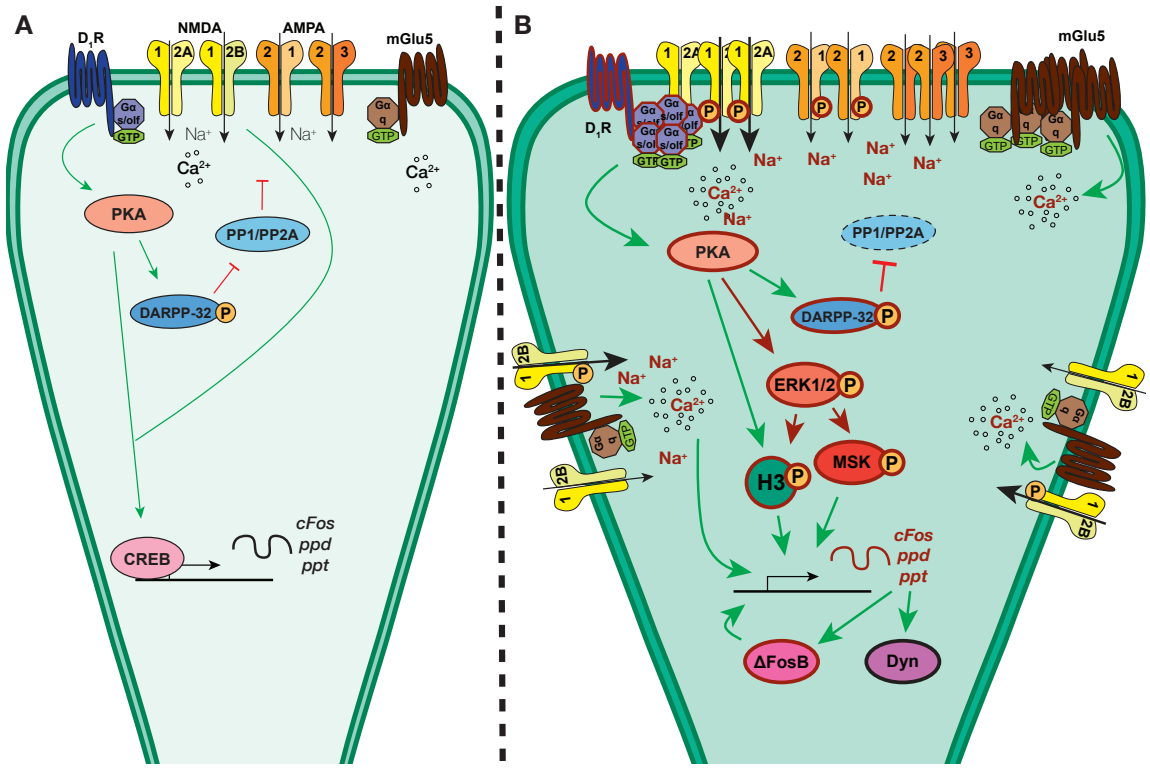

Figure 13. Pathological changes in D_1 signaling observed in LID.
(A) Simplified schematic of major dopaminergic and glutamatergic signaling pathways in dMSNs. D_1 stimulation activates PKA, which phosphorylates targets (see 1.3), and is counteracted by PP1/PP2B. Coactivation of D_1 and NMDARs stimulates IEGs. (B) Hypersensitization of the D_1 pathway increases activation of the canonical pathways (green arrows) and aberrant pathways (burgundy arrows). Intermediates with increased activity are outlined in burgundy. AMPA and NMDAR expression and phosphorylation are increased, and mGlu5 expression increases. PKA hyperactivation increases DARPP-32 activity, which restricts phosphatase activity. PKA also increases ERK1/2 activity, and together increase H3 and MSK phosphorylation. Combined with increased mGlu5 activity, IEG expression also increases, which leads to the sustained activation of ΔFosB and dynorphin. NMDA 1, 2A, 2B – GRIN1, GRIN2A/B subunits; AMPA 2, 1, 3 – GRIA2, GRIA1, GRIA3 subunits; H3, histone 3; MSK, mitogen and stress activated protein kinase; ppd, preprodynorphin; ppt, preprotachykinin. See text for more details.

approaches to modulating LID, i.e., mGlu5 negative allosteric modulators that reduce the activity of MSNs and ameliorate LID side effects (Rylander et al., 2010; Berg et al., 2011), though the beneficial effects of L-DOPA might also be reduced (Johnston et al., 2010).

Presynaptically, the loss of DA terminals also means a loss of both the DAT and DA autoreceptors (D_2Rs), which play an important role in the regulation of DA release in the intact striatum (Cenci, 2014). When DA denervation is complete, L-DOPA is taken up and converted to DA by other monoaminergic neurons, which also express AADC and VMAT2. Serotonergic neurons are reported to be the principle adoptive subtype for DA release (Lindgren et al., 2010; Navailles and Deurwaerdère, 2010) though other studies have demonstrated that the NET takes up more DA following denervation than the serotonin transporter (SERT) (Chotibut et al., 2012). Inhibition of serotonergic release through the agonism of 5-HT_{1A} and 5-HT_{1B} autoreceptors improves dyskinetic symptoms, indicating non-physiological DA release may significantly contribute to LID symptoms (Iderberg et al., 2015).

1.4.3. Supersensitization of D_1 signaling

Coincident with the changes in receptor population and activity, many alterations in second messenger cascades have been described in LID, mostly through the D_1 receptor and its associated signaling cascade (Cenci and Konradi, 2010; Feyder et al., 2011). In this pathway, alterations can be grouped into two categories: the hyperactivation of canonical D_1 signaling, and the aberrant activation of non-canonical cascades (Cenci and Konradi, 2010).

The hyperactivation of canonical D_1 signaling primarily occurs through an overactivation of PKA, and a subsequent increase in the phosphorylation of its targets (Cenci and Konradi, 2010) (Figure 13). DARPP-32 is one of the most characteristically hyperactivated members of the canonical D_1 pathway. Following DA denervation, D_1 stimulation dramatically increases its phosphorylation through PKA compared to intact controls (Nishi et al., 1997; Svenningsson et al., 2000). Chronic L-DOPA stimulation, followed by the development of dyskinesia, is paralleled with

a persistent DARPP-32 phosphorylation (Picconi et al., 2003). As this phosphorylation activates DARPP-32 inhibition of PP-1, this suppresses the dephosphorylation and deactivation of number of other signaling mediators (Fienberg et al., 1998; Santini et al., 2007). Similarly, DA denervation increases stimulation-induced phosphorylation of the GRIA1 subunit of the AMPA receptor, and this increase is also observed following the induction of LID (Oh et al., 2003; Santini et al., 2007). Increased phosphorylation of the GRIN1 and GRIN2A subunits of the NMDA receptor has also been observed following the emergence of LID symptoms, which may also be mediated through CaMKII (Dunah et al., 2000; Brotchie et al., 2005). CaMKII becomes hyperactive following striatal DA depletion, and its inhibition alleviates motor deficits in PD (Brown et al., 2005).

L-DOPA stimulation of the D_1 receptor following DA denervation non-canonically increases ERK1/2 phosphorylation, either acutely or following chronic dyskinesiogenic treatment (Gerfen et al., 1990; Santini et al., 2007; Cenci and Konradi, 2010). The degree of ERK1/2 phosphorylation in rodents is correlated with AIM scores (Cenci and Konradi, 2010). Importantly for the pathogenesis of LID, chronic L-DOPA administration also results in a sustained phospho-ERK1/2 elevation in animals expressing AIMs versus those without movement abnormalities (Valjent et al., 2000). One of the core LID signaling abnormalities then seems to arise from the inability to downregulate ERK1/2 activation, even though the mechanisms by which this leads to the production of dyskinesia are still unclear. However, ERK1/2 has a large number of downstream molecular targets, and can both acutely regulate molecular functions through mammalian target of rapamycin complex (mTORC) phosphorylation (Santini et al., 2009), as well as alter gene transcription for long term adaptations, particularly through the phosphorylation of histone kinase MSK1 (Santini et al., 2007; Cenci and Konradi, 2010). Additionally, acute inhibition of ERK phosphorylation with a MEK inhibitor reduces AIMs, once again highlighting the relevance of the activity of this kinase in LID (Lindgren et al., 2009).

One of the pathways to aberrant ERK activation may be through GEF proteins. RasGRP1 and RasGRP2 are expressed in striatal striosome and matrix compartments, respectively, and

are inversely regulated in LID in a rat model of PD (Crittenden et al., 2009). In the DA-depleted striatum, L-DOPA treatment upregulates RasGRP1 and activates the MAPK cascade (Yang and Kazanietz, 2003), and downregulates RasGRP2, which normally inhibits the ERK/MAPK cascade (Kawasaki et al., 1998). These dysregulations lead to increased ERK phosphorylation observed in a model of LID (Westin et al., 2007). RasGRF1 is involved in D1 and glutamate-mediated phosphorylation/activation of ERK1/2. Drugs that stimulate DA release increase RasGRF1 levels (Feig, 2011), while ERK1/2 phosphorylation is impaired in Ras-GRF1-deficient striatal cells (Fasano et al., 2009).

1.4.4. Transcriptional Deregulation in the Direct Pathway

As previously mentioned, increased ERK1/2 phosphorylation in LID induction is accompanied by increases in phosphorylated MSK1 and histone 3 (H3) (Santini et al., 2007), which connects D_1 pathway hyperactivation to changes in gene regulation (Figure 13). Phosphorylation of MSK1 and H3 are associated with chromatin remodeling during active transcription (Cenci and Konradi, 2010), and increased MSK1 phosphorylation also increases cFos expression (Brami-Cherrier et al., 2005). Interestingly, in the intact striatum, D_1 stimulation can induce the expression of immediate early genes (IEGs) through the PKA-mediated (and NMDAR-dependent) phosphorylation of CREB, which increases expression of cFos, ppd, and preprotachykinin (ppt). Following DA depletion, D_1 activation increases IEG expression through a PKA-ERK1/2 pathway that requires mGluR activity (Rajadhyaksha et al., 1998; Fieblinger et al., 2014; Keefe and Horner, 2017). Additionally, CRE/AP1 binding sites are transactivated by ΔFosB and JunD transcription factors instead of CREB (Andersson et al., 2001).

In both the DA denervated and dyskinetic states, D_1 stimulation produces a protracted induction in ΔFosB expression, which also directly drives the expression of ppd. Both ΔFosB and ppd remain hyper-elevated in response to L-DOPA for at least a year (Westin et al., 2001), and following discontinuation of chronic L-DOPA stimulation, these two proteins remain upregulated

for weeks (Andersson et al., 1999). The level of ΔFosB upregulation additionally positively correlates with the severity of dyskinesias (Andersson et al., 1999), and overexpression of ΔFosB in a DA denervated system induced dyskinetic behaviors independent of L-DOPA (Cao et al., 2010), strongly suggesting deregulation of transcriptional activity is another key component to dyskinesia pathogenesis (Cenci and Konradi, 2010; Huot et al., 2013).

1.5. Summary

The development of LID is molecularly characterized by maladaptive plasticity at the corticostriatal and nigrostriatal interface. Though nearly every neurotransmitter and receptor signaling pathway has been implicated (Huot et al., 2013), the majority of dyskinesiogenic changes are associated with a hypersensitization of the D_1 pathway in dMSNs. This sensitization is propagated through second messenger cascades and transcription factor regulation, initiating gene programs that alter the long-term plasticity of the striatum. However, though the molecular substrates of dyskinesia are increasingly identified, a lingering question about the pathogenesis of PD remains – what factors differentiate animals and patients that develop dyskinesia from those who do not?

An intriguing hypothesis emerges from a recurrent finding in L-DOPA treatment. It is increasingly accepted that one of the aspects of L-DOPA treatment that contributes to the development of LID is the non-physiological waves of high extracellular DA that oral L-DOPA dosage produces in the striatum. DA is typically released tonically from striatonigral afferents (in addition to stimulated bursting acitivity), so the peaks and valleys of oral L-DOPA appears to be detrimental in the long term (Cenci, 2014, 2017). This has long been theorized to be a contributing factor to the etiology LID, but proof of concept has recently been provided with the development of a jejeunal L-DOPA pump, which delivers a steady dose of L-DOPA and significantly reduces the incidence of LID (Oertel and Schulz, 2016). It is possible to extrapolate that the more

consistent supply of L-DOPA, DA, and DA stimulation are less energetically demanding than pulsatile surges, which would require constant recalibration and tuning of receptor responses and signaling cascades to maintain a consistent response. In this premise, a factor that may differentiate patients and animals more or less susceptible to dyskinesia would then be differences in bioenergetic capacity. Intriguingly, variabilities in mitochondrial function may underlie these differences.

2. Mitochondrial Form and Function

2.1. The mitochondrial genome and proteome

In contrast to the bean-shaped structures observed in some of the earliest images of mitochondria derived from electron microscopy, mitochondria are a large reticulated network of organelles distributed throughout the cell, in a constant state of fission and fusion (Chan, 2012). Other elements of the mitochondria initially visualized by electron microscopy have held up to subsequent scrutiny – they are double membraned, consisting of the OMM and inner mitochondrial membrane (IMM), and contain a complex membraneous system that extends into the mitochondrial matrix known as the cristae, which has recently been identified as distinct from the IMM. The different mitochondrial compartments and unique structures facilitate a number of different metabolic and biophysical roles (Pernas and Scorrano, 2015). For example, oxidative phosphorylation occurs across the cristae membrane, which allows the buildup of local proton circuits that generates the necessary energy to produce ATP, transport of most metabolites occurs across the OMM and IMM, and the TCA occurs amidst the enzymes of the mitochondrial matrix. Many of these regional functions will be elaborated in detail below.

2.1.1. mtDNA structure and replication

One unique aspect of mitochondria as intracellular organelles is their discrete genome, mitochondrial DNA (mtDNA), independent from the nuclear chromosomes (Schatz et al., 1964; Nass et al., 1965; Hutchison et al., 1974). Along with the proteins encoded by the mitochondrial genome, a large number of nuclear-encoded genes supply approximately 1000 proteins that comprise the 'mitochondrial proteome,' including additional subunits of the mitochondrial RC, mtDNA replication and transcription machinery, and transporters (Meisinger et al., 2008; Calvo and Mootha, 2010). Coordinating these two genomes to achieve mitochondrial function poses a particular challenge for the cell to maintain energy metabolism.

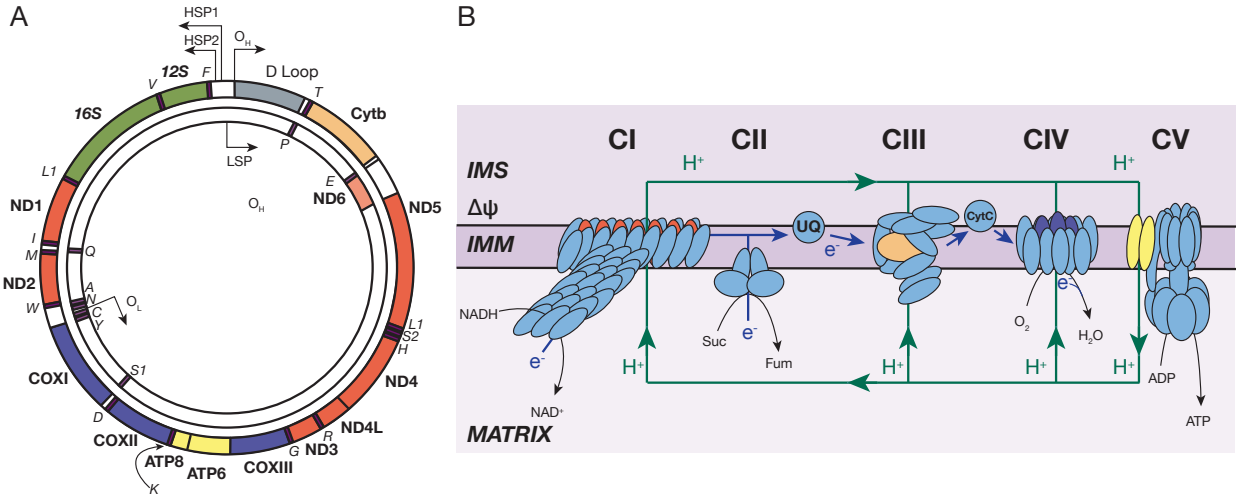

Figure 14. mtDNA encodes respiratory chain subunits.
(A) The mtDNA plasmid encodes 13 RC proteins (bold), 2 rRNAs (bold italic), and 22 tRNAs (italic). (B) Location of the mtDNA-encoded protein subunits in complexes with the nuclear-encoded subunits of the RC. The mtDNA subunits are highly hydrophobic, and are found exclusively within the mitochondrial inner membrane. Activity of the RC transports electrons from NADH and/or succinate across the complexes to O_2, forming H_2O, which facilitates the pumping of H^+ and the creation of a proton circuit, which ultimately powers generation of ATP through ATP synthase. HSP, heavy strand promoter; LSP, light strand promoter; O_H, origin of heavy strand replication; O_L, origin of light strand replication; CI-V, RC complexes; IMS, intermembrane space; IMM, inner mitochondrial membrane. (A) Redrawn with permission from Schon et al., 2012, (B) adapted from Schon et al., 2012.

Though their internalization was evolutionarily ancient, mitochondria retain a fraction of their original prokaryotic genome. The vast majority of the mitochondrial proteome is encoded by the nuclear genome, likely due to the gradual drift of some genes from the mitochondria to the nucleus (Stewart and Larsson, 2014), but a small number of essential genes have been retained

within mtDNA plasmid, accompanied by requisite tRNA and rRNA translation machinery (Anderson et al., 1981; Wallace et al., 2013). In total, 37 genes are encoded by the 16.6kb mtDNA plasmid, including 2 rRNas, 22 tRNAs, and 13 protein coding genes, on “light” and “heavy” strands, termed because of the differential weight conferred by their nucleotide composition (Clayton, 2000). The vast majority of the coding genes, most of the mRNAs and tRNAs, and both rRNAs, are found on the heavy strand, with one protein-coding gene (ND6) and 8 tRNAs on the light strand. All of these protein-coding genes code for subunits of complexes in the RC (Schon et al., 2012) (Figure 14). Four of the five ‘canonical’ complexes are represented, with seven of the thirteen protein encoding genes belonging to complex I. Though most of the mtDNA genes correspond to different complexes, they are united by their hydrophobicity, which may explain their retention in the mtDNA genome (Johnston and Williams, 2016). Transcription and translation within the mitochondrial matrix allows their direct insertion into the IMM, circumventing the complex import mechanism through the translocation of the outer and inner membrane (TOM/TIM) complexes (see below). Instead, these proteins are inserted into the membrane through the function of the oxidase assembly translocase (Oxa1l), which additionally coordinates the insertion of nuclear-encoded RC subunits (Richter-Dennerlein et al., 2015).

The minimal mtDNA ‘replisome’ consists of four major proteins: the mtDNA helicase (Twinkle), a single-stranded DNA binding protein (mtSSB), and the mtDNA polymerase, POLγ, which is composed of a catalytic subunit (POLG) and two accessory subunits (POLG2) (Stumpf and Copeland, 2011) (Figure 15A). The heavy strand and the light strand have two different origins of replication – for the heavy strand, O_H, and the light strand, O_L. Broadly, mtDNA replication proceeds by Twinkle separating the two strands of mtDNA, while the POLγ holoenzyme (POLG combined with a POLG2 dimer) synthesizes the nascent strands. Initiation of this replication, when it begins at the heavy strand origin, creates a characteristic D-loop structure as the helicase unwinds the two strands and synthesis begins, forming a three-strand region (Clayton, 1982; Fish et al., 2004). Interestingly, the D-loop region is mostly non-coding, but

contains two hypervariable regions. Polymorphisms in these regions can be used for mtDNA haplogroup identification (Levin et al., 1999), though variations in this region may also be pathogenic (Fliss et al., 2000).

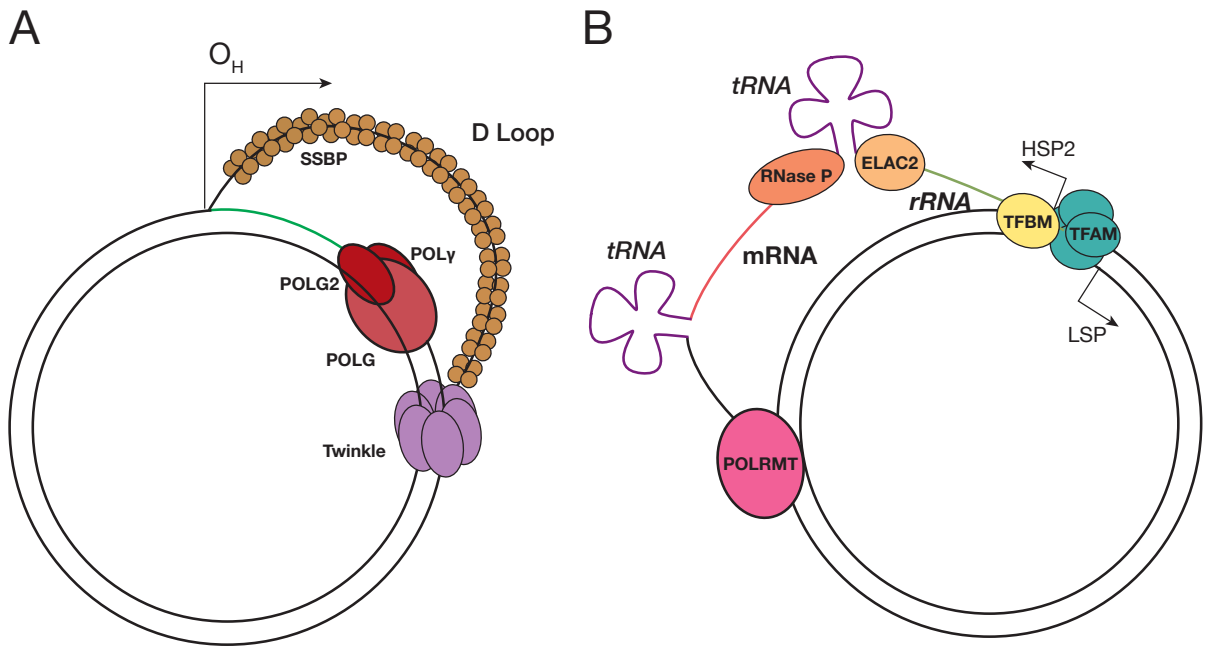

Figure 15. mtDNA replication and transcription.
(A) Core mtDNA replisome. Beginning at the O_H, Twinkle unwinds the mtDNA strands, Ssbp binds the non-replicating strand, and the POLγ holoenzyme begins replication. This initiation creates the triple-stranded D loop. (B) mtRNA transcription is initiated with the binding of TFAM between the HSP and LSP, along with TFB1M or TFB2M. POLRMT begins polycistronically transcribing mtDNA, and tRNAs begin folding into cloverleaf structures. To separate these molecules, RNase P and Elac2 cleaves the nascent molecules at 5' and 3' ends respectively. *In vivo*, replication and transcription are likely coupled. POLγ, the mtDNA polymerase holoenzyme; POLG, the p140 subunit of POLγ; POLG2, the p55 accessory subunit of POLγ; SSBP, single strand binding protein; TFAM, mitochondrial transcription factor A; TFBM, mitochondrial transcription factor B; POLRMT, mitochondrial RNA polymerase. Adapted from Hudson and Chinnery, 2006, and Mercer, 2011.

Following the synthesis of the D-loop, two primary competing hypotheses describe the remainder of the mechanism of replication. The best-supported current theory suggests mtDNA replication proceeds through a strand-displacement process. In this model, following the initial unwinding of the mtDNA, one strand is synthesized while mtSSB binds the other strand, and synthesis on the second only begins when the replisome reaches the light strand origin of replication (Clayton, 2003; Gustafsson et al., 2016). In contrast, the opposing model proposes

strand-coupled replication, where both strands are replicated more or less simultaneously (Yang et al., 2002; Bowmaker et al., 2003).

The mtDNA replication process is primarily perturbed through mtDNA damage. A number of mechanisms and involved proteins that correct for different types of damage, but these are much less complex than the mechanisms involved in the nucleus, even though some nuclear repair proteins have mitochondrial activity as well. Briefly, only two types of repair have been extensively characterized in mammalian mitochondria. The most common form is single-nucleotide base excision repair, which can in large part be performed the 3'-5' exonuclease function of POLγ (Copeland, 2010). Interestingly, the recently discovered MGME1 protein has the complementary 5'-3' exonuclease activity, and though its function has not been comprehensively defined, it is thought to cleave the ssDNA formed through the D loop (Kornblum et al., 2013). The other major mechanism, long patch base excision repair, does involve activity of nuclear endonucleases FEN-1 and DNA2 (Liu et al., 2008; Szczesny et al., 2008). Mismatch repair has also been observed in yeast mitochondria, but the mammalian homologues of the involved genes are still being discovered. Importantly, nucleotide excision repair, the mechanism required for correcting mutations induced by UV exposure or alkylation damage, is not repaired in mtDNA (Copeland and Longley, 2014). In addition, mutated or damaged mtDNA is eliminated through mitophagy (see section 2.4).

In contrast to the majority of its prokaryotic ancestors, multiple copies of mtDNA are contained within mitochondria. Estimates of copy number vary considerably between cell types, but range between 2-10 copies per mitochondrion, and 10^3-10^4 per cell (Scarpulla, 2008). Though mtDNA does not condense around histones into chromosomes like nuclear DNA, mtDNA is packaged into nucleoids in the mitochondrial matrix. In addition to mtDNA molecules, these nucleoids also contain a number of proteins, particularly those involved with mtDNA replication and transcription, though chaperones, proteases, and ribosomal proteins have also been identified (Bogenhagen, 2012). Considering the variability in mtDNA copy number, it is clear that

there must be pathways involved in regulating this copy number. mtDNA copy numbers can be controlled via regulation of POLγ, addition to the myriad other functions of POLγ. DNMT1 methylates POLG on exon 2, and high levels of this methylation correlate with lower levels of mtDNA copy number. Interestingly, this relationship persists both in stem cells and in terminally differentiated cells (Kelly et al., 2012; Lee et al., 2015). Differential degrees of POLG methylation may account for the large differences in mtDNA copy number across tissues.

2.1.2. mtRNA and related proteins

mtDNA replication and transcription are tightly coupled (Lee and Clayton, 1998; Bonawitz et al., 2006). The replication promoters (heavy strand promoter (HSP) 1 and 2, and light strand promoter (LSP)), are located almost adjacent to the O_H, though the transcription complex is oriented in the opposite direction from the replisome (Figure 15B). Two proteins have dominating roles in mtDNA transcription – the mitochondrial RNA polymerase, POLRMT, and mitochondrial transcription factor A, TFAM (Yakubovskaya et al., 2014). TFAM has several roles in addition to that of stimulating mtDNA transcription. First, its function in transcription regulates mtDNA replication, as transcripts from the LSP are used as primers for POLγ in heavy strand replication. TFAM can also bind non-specifically to mtDNA, is a primary component of mtDNA nucleoids, and regulates polymerase accessibility and replication through a histone-like function (Lezza, 2012). Two additional transcription factors, TFB1M and TFB2M, also play roles in stimulating transcription initiation, and while both are homologously related to rRNA methyltransferases they likely also regulating mt-rRNA. Moreover, most studies have concluded that POLRMT, TFAM, and TFB2M act as the core transcription machinery (Gaspari et al., 2004; Falkenberg et al., 2007).

Transcription of mtDNA is stimulated by binding of TFAM tetramers at upstream sites of the LSP and HSP, which may promote bidirectional transcription (Gaspari et al., 2004). This facilitates the binding of POLRMT, and begins transcription at one of the three promoter regions. Though HSP1 and HSP2 are in proximity (Figure 14A), initiation at HSP1 results in the exclusive

transcription of the 12S and 16S rRNAs (Montoya et al., 1982; Martin et al., 2005). In contrast, initiation at either HSP2 or LSP results in the full transcription of the heavy and light strand, respectively. Atypically to nuclear DNA, both strands of mtDNA are transcribed polycistronically, requiring subsequent processing to release distinct mtDNA-encoded protein-coding mRNAs (mtRNAs). The dominant model of this process suggests that the mtDNA-encoded tRNAs, which on the heavy strand of mtDNA lie between each mtRNA, form clover leaf structures following transcription that recruit cleavage enzymes. Most evidence suggests that RNase P performs the necessary 5' endonucleolytic cleavage (Tullo et al., 2008), while ELAC2 performs the 3' cleavage (Rorbach and Minczuk, 2012; Bruni et al., 2017). mtRNAs processing is variable across individual mtRNAs, cell types, and organisms. In particular, these transcripts are not capped at the 5' end, and are differentially 3' poly-adenylated (Temperley et al., 2010; Rorbach and Minczuk, 2012). This differential may account to some degree for the range of mtRNA concentrations (for example, mtCo2 is usually substantially more abundant than ND5), despite the polycistronic transcription (Mercer et al., 2011), though mtRNA levels do not correlate with the degree of polyadenylation. mtRNA turnover is also extensively regulated, but only a fraction of the relevant factors has been identified. A putative mtRNA "degradosome" has been identified as a complex of SUV3, a surveillance helicase, and PNPase, a mitochondrial 3'-5' exonuclease RNase (Wang et al., 2009), and knockdown of either of these genes results in the accumulation of mtRNA intermediates (Wang et al., 2010). Full degradation of mtRNA, however, requires the activity of REXO2, a 3'-5' exonuclease necessary for the breakdown of oligonucleotides under 5 nucleotides, in order to free nucleotides for new synthesis (Bruni et al., 2013).

2.1.3. Mitochondrial proteostasis and the UPR^{mt}

The processes regulating mtRNA translation are even less definitively described (reviewed in detail in Christian and Spremulli, 2012, and Richter-Dennerlein et al., 2015), and there are extensive species differences. In mammals, the 12S rRNA and 16S rRNA correspond

to the small ribosomal subunit (mtSSU, 28S) and large ribosomal subunit (mtLSU, 39S), and form the mitochondrial ribosome complex (55S) to translate mt-mRNAs (Greber and Ban, 2016) (Figure 16). This ribosome is similar to E. coli, though considerably more protein-dense than most prokaryotic ribosomes. Accordingly, mtSSU has about 29 mitochondrial ribosomal proteins, and mtLSU has about 48, with bacterial homologs of only about half of these proteins. Two translation initiation factors and three elongation factors have been identified (Christian and Spremulli, 2012). Perhaps most relevant for the ultimate function of mitochondrially-encoded genes is the interaction of nascent proteins with Oxa1l, a 5 transmembrane-spanning domain protein that forms a large heteroligomeric complex, crosses the IMM and facilitates the insertion of these mitochondrial proteins into the inner membrane (Stiburek et al., 2007; Haque et al., 2010). These mitochondrially-encoded subunits form a small proportion of the proteins of the complexes of the RC, and as a result Oxa1l, along with complex-specific assembly factors, must coordinate the import, insertion, and stoichiometry of both nuclear and mitochondrially-derived proteins (Fernández-Vizarra et al., 2009; Richter-Dennerlein et al., 2016). An area of ongoing investigation is the mechanisms by which the nucleus and mitochondria communicate to achieve proteostasis.

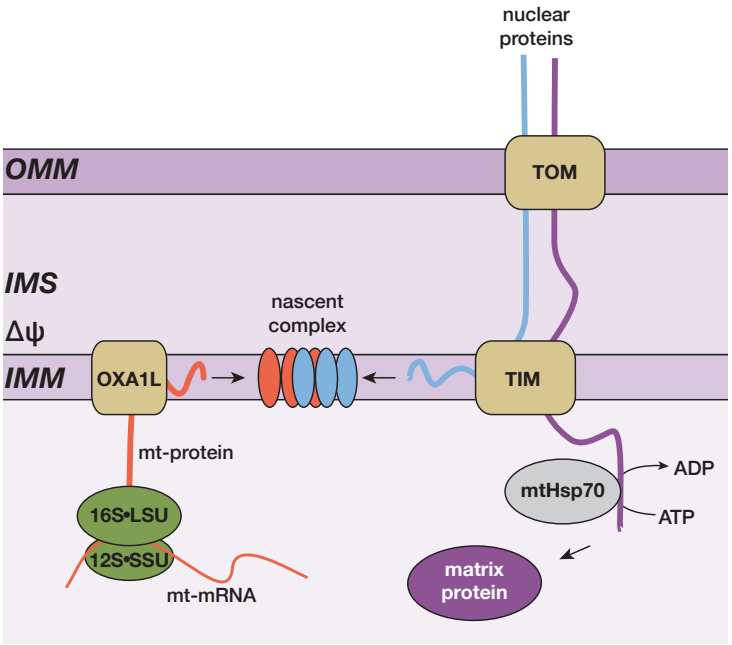

Figure 16. Simplified schematic of mitochondrial protein import. mtDNA-encoded proteins are transcribed, as described above, and translated by the 55S ribosome, comprised of the 12S rRNA-containing SSU, and 16S rRNA-containing LSU. These are inserted into the membrane through OXA1L, where they are complexed with nuclear-encoded RC subunits. Nuclear-encoded proteins pass through the TOM and TIM complexes, and are then inserted into the membrane. In contrast, matrix-targeted proteins are ratcheted through both complexes with the activity of mtHsp70. LSU, large ribosomal subunit; SSU, small ribosomal subunit; TOM/TIM, outer/inner membrane translocase. Adapted from Richter-Dennerlein et al., 2016.

Interestingly, a recent study demonstrated that one such mechanism of regulation may occur through mitochondrial ribosomal translational plasticity – translating proteins only in concert with an influx of nuclear encoded proteins (Richter-Dennerlein et al., 2016).

This influx of nuclear-encoded proteins occurs through complex import mechanisms; across both the OMM and IMM for matrix proteins, or crossing a subset of these boundaries for inner membrane space (IMS) or integral membrane proteins. Briefly, mitochondrially-targeted polypeptides contain a mitochondrial targeting presequence (MTS) that directs them to the TOM complex, which channels the nascent protein then through the TIM complex. In general, nuclear-encoded subunits of the RC may be released directly from the TIM complex into the inner membrane, but some may be fully imported into the matrix for additional folding. Importantly, though this process is driven in part by the $\Delta\psi$, which electronegatively encourages the accumulation of the positively charged MTS, full translocation into the matrix is ATP-dependent. mtHsp70, a protein chaperone, binds the preprotein, and acts as an import motor by using the available energy from ATP hydrolysis to complete translocation. This ATP and $\Delta\psi$ dependence for protein import indicates mitochondrial respiration is required for mitochondrial protein maintenance (Schmidt et al., 2010; Wiedemann and Pfanner, 2017). This relationship can link mitochondrial dysfunction to cell-wide responses, as disruptions to the mitochondrial protein import system can trigger the mitochondrial unfolded stress response (UPR^{mt}) or mitophagy (Haynes and Ron, 2010; Pellegrino et al., 2013).

In order to maintain proteostasis within the mitochondria, a specific protein quality control and degradation pathway operates to maintain the balance of nuclear and mitochondrial protein stoichiometry, and to eliminate misfolded or damaged proteins. The complex machinery of this system involves close to 50 members (Quirós et al., 2015), some of which have important roles in other systems. In particular, the four ATP-dependent proteases, the ATP-independent serine protease OMI/HTRA2, and the presenilins-associated rhomboid-like protein PARL, play important roles in clearing protein damage and in mitophagy. Two of the ATP-dependent proteases, mAAA

and iAAA, integral IMM proteins that face the matrix or IMS respectively, are important for degrading non-functioning subunits of the RC (Gerdes et al., 2012; Stiburek et al., 2012). A subunit of the iAAA protease, YME1L1, also cleaves optic atrophy 1 (OPA1), a protein involved in regulating mitochondrial fusion, discussed below (MacVicar and Langer, 2016). LONP is possibly the best-known mitochondrial matrix protease, and it is responsible for degrading oxidatively damaged proteins as well as mediating the turnover of several RC units (Bezawork-Geleta et al., 2015 . Through the lens of mtDNA homeostasis, LONP also plays a role in regulating mtDNA copy number through its degradation of Tfam (Lu et al., 2013; Matsushima et al., 2010) . CLPP, which also forms the CLPXP complex, also proteolytically degrades misfolded or damaged proteins, though its function has been identified more through its role in the UPR^{mt}, as one of the proteins involved in the activation of this cascade (Haynes et al., 2007). Finally, OMI/HTRA2 and PARL have been extensively studied in the context of neurodegeneration, in part because of their respective associations with familial PD gene protein phosphatase and tensin homolog (PTEN)-induced kinase (PINK1). Differential activation of OMI/HTRA2 can activate both autophagy (Li et al., 2010) and apoptosis (Cilenti et al., 2004), and is directly phosphorylated by PINK1 (Clausen et al., 2011). In contrast, PARL is the protease responsible for cleaving and degrading PINK1, preventing its accumulation and recruitment of parkin, an E3 ubiquitin ligase that constitutes a key part of the mitophagy pathway (Jin and Youle, 2013; Thomas et al., 2014). The two proteases together may have a coordinated function in the induction or suppression of apoptosis (Cipolat et al., 2006; Chao et al., 2008; Quirós et al., 2015).

The UPR^{mt} is a highly active area of mitochondrial research. In mammalian systems, the heat shock unfolded protein response and ER-stress unfolded protein response (UPR^{ER}) have previously been described. The heat shock UPR is characterized by interactions between the HSF1 transcription factor chaperones Hsp70 and Hsp90 (Pellegrino et al., 2013), and the ubiquitin-proteasome system. In contrast, the UPR^{ER} is characterized by bZip-protein mediated induction of ER-directed protein folding and degradation, alongside the pancreatic enriched ER

kinase (PERK) and eukaryotic initiation factor 2 (eIF2) mediated reduction of protein translation (Harding et al., 1999; Pellegrino et al., 2013). There pathways overlap partially with the UPR^{mt}, as its induction also increases expression of molecular chaperones (Hsp60, Hsp10, mtDNAJ), proteases (CLPP, YME1L1), and transcription factors modulating their expression (CHOP, C/EBPβ) (Zhao et al., 2002; Aldridge et al., 2007; Haynes and Ron, 2010; Quirós et al., 2016). Interestingly, this pathway is activated in several types of mitochondrial dysfunction, including interruption of mitochondrial fusion (Song et al., 2015) and mutations in Twinkle (Khan et al., 2014; Quirós et al., 2016).

2.1.4. A summary of mitochondrial transporters: The SLC25A family and related transporters

The metabolite transporters are an important component of the mitochondrial proteome. They are expressed on the IMM and shuttle a diverse array of substrates into and out of the mitochondrial matrix. A high density of the voltage dependent anion channel (VDAC), a β-barrel porin on the OMM, allows metabolites up to 5kD to diffuse across the outer membrane and into the IMS, though VDAC permeability is altered through changes in mitochondrial function (Colombini, 2012; Shoshan-Barmatz and Mizrachi, 2012). All of these forms of transport are highly dependent on the mitochondrial Δψ and pH gradient, which can be leveraged in different ways. Most common are either electroneutral or electrogenic transporters of metabolites, using symport or antiport mechanisms, though some ions can be antiported or uniported using the chemical gradient (Kunji, 2004).

The majority of these transporters fall under the SLC25A family of solute carriers, which despite their variety of substrates share a number of characteristic features. They are typically single polypeptides rather than oligomers, about 30-40kD in size, and share characteristic amino acid consensus sequences – PX[D/E]XX[R/K] on the matrix side, and [Y/F][D/E]XX[K/R] on the cytoplasmic side (Robinson et al., 2008). Genomically, 53 members of this family with 24

subfamilies have been identified, importing and exporting the necessary substrates for

Human gene name	Protein name	Predominant substrates	Coupling ions	Brain expression?	Link to disease
SLC25A1	**CIC (citrate carrier)**	**Citrate, isocitrate, malate, PEP**	**citrate-H+/malate**	**Y**	
SLC25A2	**ORC2 (ornithine carrier 2)**	**Ornithine, citrulline, lysine, arginine, histidine**	**ornithine/citrulline + H+; ornithine/H+**	**Y**	
SLC25A3	**PHC (phosphate carrier)**	**Phosphate**	**phosphate + H+; phosphate/OH−**	**isoform B**	**Mitochondrial phosphate carrier deficiency**
SLC25A4	**ANT1 (adenine nucleotide translocase-1)**	**ADP, ATP**	**ADP/ATP**	**Y**	**AAC1 deficiency, autosomal dominant progressive external ophthalmoplegia (adPEO)**
SLC25A5	ANT2 (adenine nucleotide translocase-2)	ADP, ATP	ADP/ATP	Y	
SLC25A6	ANT3 (adenine nucleotide translocase-3)	ADP, ATP	ADP/ATP	Y	
SLC25A7	**UCP1 (uncoupling protein 1)**	**H+**			**(obesity)**
SLC25A8	UCP2 (uncoupling protein 2)	H+			obesity, type 2 diabetes, congenital hyperinsulinism
SLC25A9	UCP3 (uncoupling protein 3)	H+			(obesity, type II diabetes)
SLC25A10	**DIC (dicarboxylate carrier)**	**Malate, phosphate, succinate, sulphate, thiosulphate**	**malate/phosphate**	**Y**	
SLC25A11	**OGC (oxoglutarate carrier)**	**α-ketoglutarate, malate**	**α-ketoglutarate/malate**	**Y**	
SLC25A12	**AGC1 (aspartate/glutamate carrier 1)**	**Aspartate, glutamate**	**aspartate/glutamate + H+**	**Y**	**AGC1 deficiency, (autism)**
SLC25A13	AGC2 (aspartate/glutamate carrier 2)	Aspartate, glutamate	aspartate/glutamate + H+		Citrullinemia type II (CTLN2), neonatal intrahepatic cholestasis (NICCD)
SLC25A14	UCP5 (uncoupling protein 5)	Orphan		Y	
SLC25A15	ORC1 (ornithine carrier 1)	Ornithine, citrulline, lysine, arginine	ornithine/citrulline + H+; ornithine/H+	Y	Hyperornithinemia-hyperammonemia-homocitrullinuria (HHH) syndrome
SLC25A16	GDC (Graves' disease carrier)	Orphan		Y	
SLC25A17		CoA, FAD, NAD+, AMP, ADP, PAP, dPCoA, FMN	CoA/PAP, CoA/dPCoA, CoA/AMP, FAD/FMN, NAD+/AMP	Y	
SLC25A18	GC2 (glutamate carrier 2)	Glutamate	glutamate + H+; glutamate/OH−	Y	
SLC25A19	**DNC (deoxynucleotide carrier)**	**Thiamine pyrophosphate (ThPP), thiamine monophosphate (ThMP), (deoxy)nucleotides ((d)NTPs)**	**ThPP/ThMP, ThPP/(d)NTPs**	**Y**	**Congenital Amish microcephaly (MCPHA), neuropathy with bilateral striatal necrosis**
SLC25A20	**CAC (carnitine/acylcarnitine carrier)**	**Carnitine, acylcarnitine**	**carnitine/acylcarnitine**	**Y**	**Carnitine acylcarnitine carrier deficiency**
SLC25A21	**ODC (oxoadipate carrier)**	**Oxoadipate, oxoglutarate**	**oxoadipate/oxoglutarate**	**Y**	
SLC25A22	GC1 (glutamate carrier 1)	Glutamate	glutamate + H+; glutamate/OH−	Y	Early epileptic encephalopathy
SLC25A23	APC2	ATP-Mg2+, ATP, ADP, AMP and Pi	ATP-Mg/Pi	Y	
SLC25A24	APC1	ATP-Mg2+, ATP, ADP, AMP and Pi	ATP-Mg/Pi		
SLC25A26	**SAMC**	**S-adenosyl-methionine (SAM), S-adenosyl-homocysteine (SAH)**	**SAM/SAH**	**Y**	
SLC25A28	Mitoferrin 2 (Mfrn2)	Fe2+		Y	
SLC25A29	ORNT3	Ornithine, acylcarnitine		Y	
SLC25A31	AAC4, ANT4 (adenine nucleotide carrier 4)	ADP, ATP	ADP/ATP		(spermatogenesis)
SLC25A32	MFT	Folate			
SLC25A33	**PNC1 (pyrimidine nucleotide carrier 1)**	**UTP**			
SLC25A36	PNC2 (pyrimidine nucleotide carrier 2)	Pyrimidine nucleotides			
SLC25A37	Mitoferrin 1 (Mfrn1)	Fe2+		Y	
SLC25A38		Glycine?			Sideroblastic anemia
SLC25A41	APC4	ATP-Mg/Pi		Y	
SLC25A42		CoA, ADP, ATP, adenosine 3',5'-diphosphate, dPCoA		Y	

Table 1. Mitochondrial metabolite carriers.
The SLC25A family of transporters, substrates, and links to disease. Adapted with permission from Palmieri, 2013.

metabolism through the TCA cycle and oxidative phosphorylation. The identified transporters can be roughly grouped into amino acid, nucleotide, carboxylates, keto acids, and 'other' substrates (Palmieri, 2004, 2013). Two of the well-defined transporters are both particularly important for mitochondrial function – the adenine nucleotide transporter (ANT1, SLC25A4) and the phosphate carrier (PiC, SLC25A3).

Characterization of ANT1, which catalyzes the exchange of ADP for ATP into and out of the mitochondrial matrix, respectively, was facilitated by the discovery of two specific toxins. Bongkrekate binds the matrix-facing side of the transporter, blocking the side that binds ATP, while carboxyatractylate binds the side at the inner membrane space, blocking ADP. Interestingly, the two toxins cannot bind simultaneously, indicating ATP and ADP are alternately exchanged rather than antiported. The ANT only exchanges free ATP and free ADP (i.e. ATP^{4-} and ADP^{3-}), but not their Mg-bound counterparts, indicating this transport is electrogenic (Halestrap and Brenner, 2003; Pebay-Peyroula et al., 2003). In contrast, PiC is likely an H^+:$H_2PO_4^-$ symporter, instrumental in electroneutrally bringing in phosphates for ATP synthesis. With the exception of a few residues in its salt bridges that confer substrate specificity, PiC is highly similar to the ANT (Runswick et al., 1987; Cerson and Kunji, 2012; Nicholls and Ferguson, 2013). All of the carriers however play important roles in mitochondrial function, and additional factors are schematized in Figure 17 and Table 1.

In addition to the SLC25A family, two other transporters are uniquely important for mitochondrial function. First, the mitochondrial pyruvate carrier (MPC), which was only very recently identified in mammalian systems (Bricker et al., 2012; Herzig et al., 2012). As the connection between glycolytic metabolism and the initiation of the TCA, the transport of pyruvate into mitochondria had long been theorized, but the distinct transporter formed from a heterocomplex of MPC1 and MPC2 proteins was unexpected. Its function is similarly dependent on the mitochondrial $\Delta\psi$, as pyruvate is symported with H^+ (Papa et al., 1971; Bender and Martinou, 2016). Another very important and yet only recently identified transporter is the

mitochondrial Ca^{2+} uniporter (MCU) (Baughman et al., 2011; Stefani et al., 2011). Though the MCU protein in itself is the Ca^{2+} channel, another transmembrane protein, the essential MCU regulator (EMRE), is required for Ca^{2+} transport (Sancak et al., 2013). Additionally, two EF hand Ca^{2+} binding proteins, mitochondrial calcium uptake 1 and 2 (MICU1/MICU2), work in combination to mediate flux through the channel, though their precise function is ambiguous (Kamer and Mootha, 2015a, 2015b).

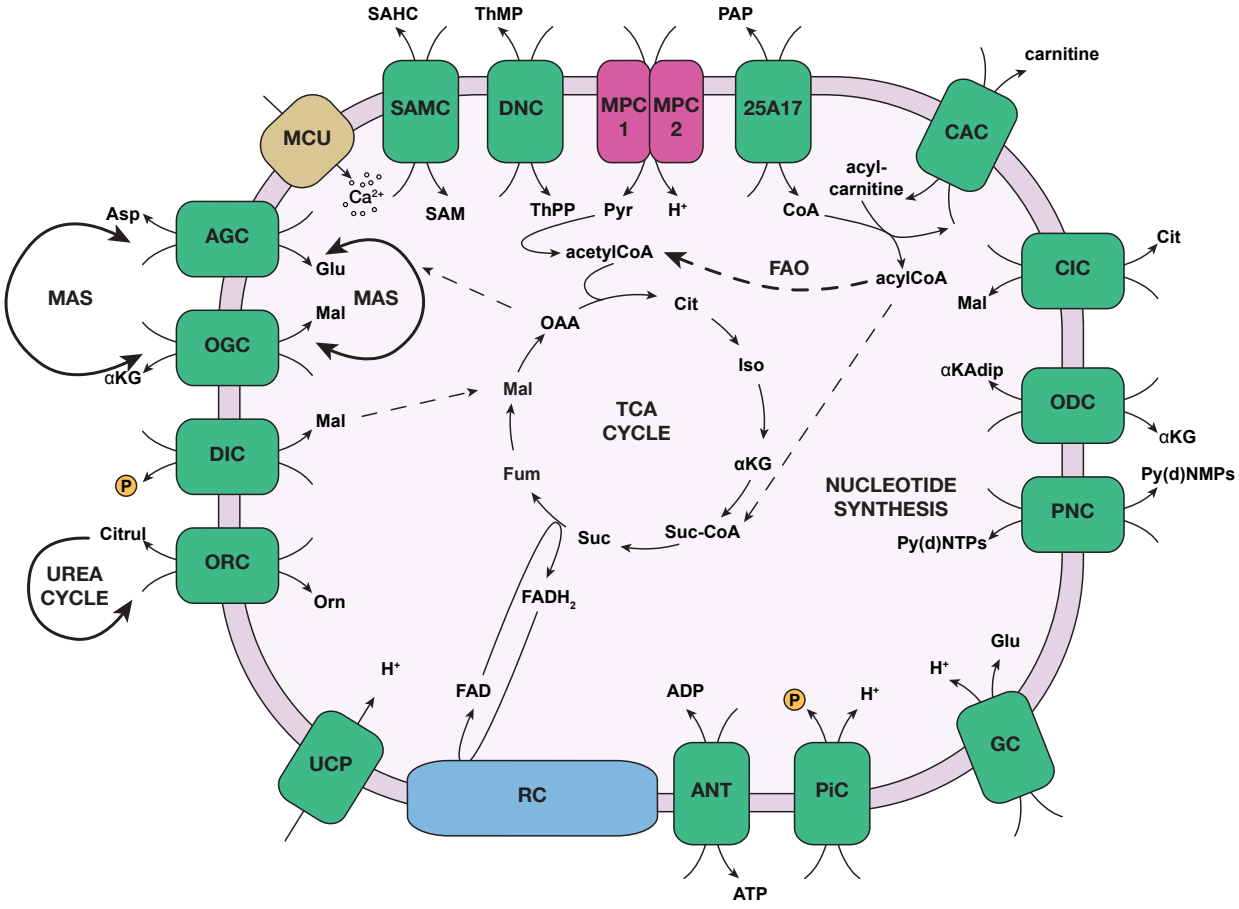

Figure 17. Major mitochondrial metabolite carriers.
The SLC25A family of transporters (and the MCU and MPC) regulate the influx and efflux of mitochondrial metabolites. Above, an overview of the essential transporters and their interactions with the TCA and other metabolic pathways, including the urea cycle, malate-aspartate shuttle (MAS), fatty acid oxidation (FAO), and nucleotide synthesis. Several transporters and pathways have been excluded for clarity. See Table 1 for transporter abbreviations. Redrawn with permission from Palmieri, 2014

Even in this brief overview of a subset of the numerous functions of mitochondria, it is evident that it is a vastly complex, highly regulated, and multifunctional organelle. It is a cell within a cell – with its own distinct genome, transcription and translation machinery, and characteristic

and distinct set of transporters. These functions are further complicated by the coordination of its activities with those of the engulfing cell. All of this complexity is necessary to essentially serve that cell through its best-known bioenergetic function – the generation of ATP.

2.2. Glucose catabolism and bioenergetics

The 'energy currency' of all organisms is ATP, which is required for almost all cellular processes. In the brain in particular (Erecińska and Silver, 1989), production of ATP is essential for maintenance of the Δψ following action potentials (Nicholls and Budd, 2000; Nicholls and Ward, 2000), release and reuptake of synaptic vesicles (Sudhof, 2004; Pathak et al., 2015) and neurotransmitters (Magistretti, 1999), and transport of various intracellular cargos across a highly polarized cell morphology (Schwarz, 2013). To generate ATP, the brain primarily catabolizes glucose (Gerard and Schachter, 1932; Gautron and Layé, 2005; Duarte and Gruetter, 2012), but there remains a substantial debate about the relevant biochemical pathways for this process between the two major cell types of the brain – neurons and glia. The following sections will give an overview of this process, from glycolysis to oxidative phosphorylation, and discuss some of the different models of neuronal and glial metabolism.

2.2.1. Glycolysis and the Pentose-Phosphate Pathway

In most cell types in the brain, glucose is taken up by the glucose transporter (GLUT1 and GLUT3 isoforms are present in neurons and astrocytes (Vannucci, 1994)). Glucose is then phosphorylated by hexokinase into glucose 6-phosphate (G6P), and from there its metabolic pathway can diverge (Figure 18).

In one branch of this pathway, glucose undergoes glycolysis by converting G6P into fructose 6-phosphate (F6P) by phosphoglucose isomerase. Following the standard glycolytic pathway (Figure 18), one molecule of glucose is thus converted into two molecules of pyruvate, which can be transported into the mitochondria by the pyruvate carrier for further oxidation.

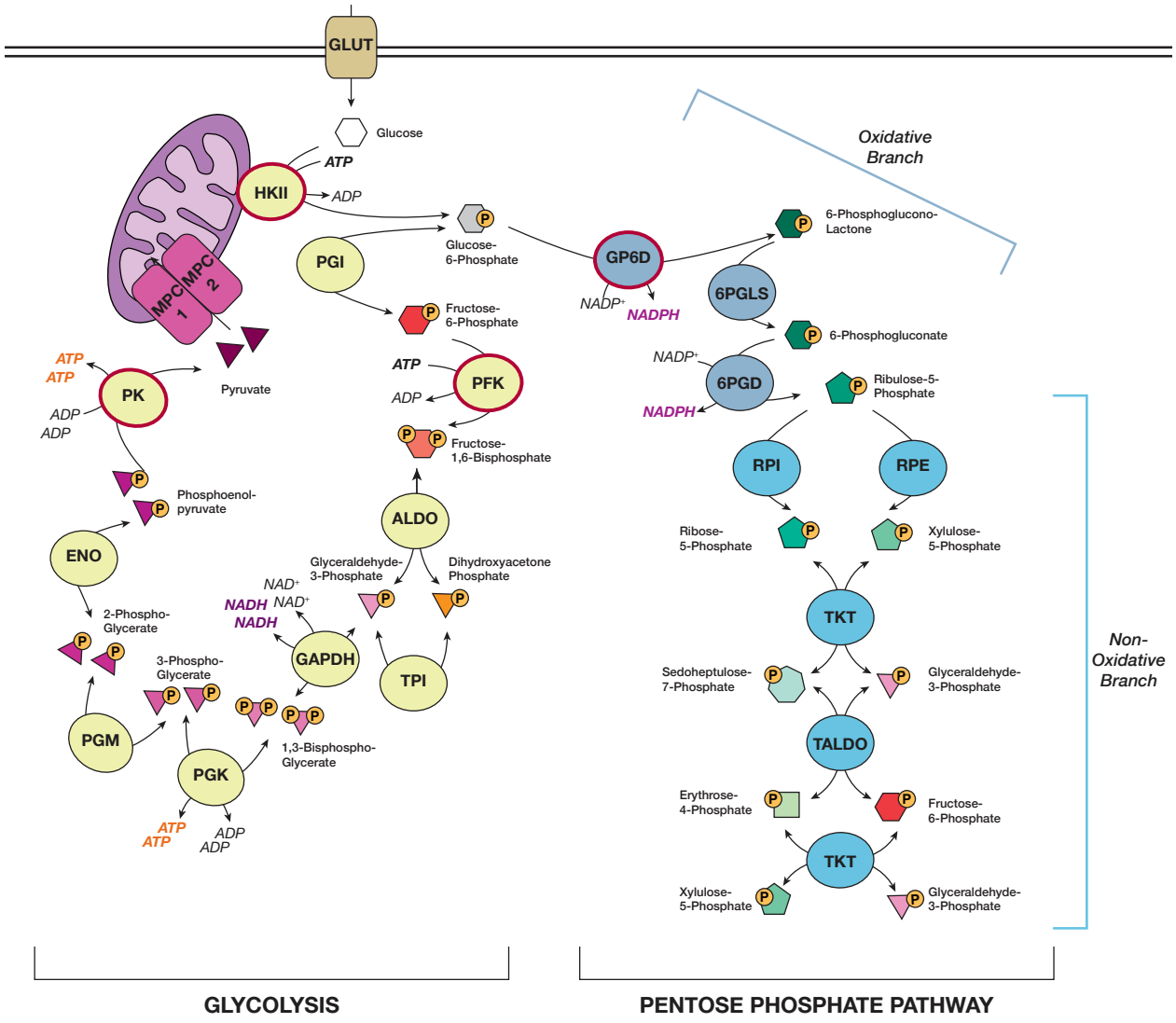

Figure 18. Glycolytic and Pentose Phosphate Pathways for glucose oxidation.
Glucose is taken up into the cell through GLUT, where it is phosphorylated into G6P by HKII. It can then be routed into the glycolytic pathway, where one molecule of glucose yields two pyruvate, two ATP, and two NADH. In contrast, metabolism through the pentose phosphate pathway yields ribulose-5-phosphate, yielding two NADPH, and can be subsequently interconverted into substrates that can supply the glycolytic cascade. Metabolite shape reflects number of carbons. Enzymes outlined in red reflect key regulatory sites; see text for details. GLUT, glucose transporter; HKII, hexokinase II; PGI, phosphoglucose isomerase; PFK, phosphofructokinase; ALDO, aldolase; TPI, triosephosphate isomerase; GAPDH, glyceraldehyde phosphate dehydrogenase; PGK, phosphoglycerate kinase; PGM, phosphoglycerate mutase; ENO, enolase; PK, pyruvate kinase; G6PD, glucose-6-phosphate dehydrogenase; 6PGLS, 6-phosphogluconolactonase; 6PGD, 6-phosphogluconate dehydrogenase; RPI, ribulose-5-phospate isomerase; RPE, ribulose-5-phosphate 3-epimerase; TKT, transketolase; TALDO, transaldolase.

Glycolysis generates a net of two molecules of ATP, which under some conditions can be a sufficient ATP output to bypass mitochondrial respiration, and 2 molecules of nicotinamide

adenine dinucleotide (NADH), which are used as reducing equivalents for the mitochondrial RC (Boiteux and Hess, 1981; Nelson and Cox, 2004).

Though many of the enzymes involved in glycolytic metabolism can be transcriptionally regulated to meet metabolic needs of the cell, the pathway has three major regulatory steps with rate limiting enzymes. First, hexokinase, the enzyme mediating the first step of the glycolytic pathway (Mathupala et al., 1997), is inhibited by excess production of G6P (Crane and Sols, 1954). Hexokinase II, localized on the OMM of mitochondria, directly receives exported ATP to phosphorylate glucose, and it mediates the opening of the mitochondrial permeability transition pore (mPTP) and the initiation of the apoptotic cascade (Mathupala et al., 2006). Second, phosphofructokinase (PFK), which catalyzes the conversion of F6P to fructose 1,6-bisphosphate, is a vital step in the cascade both for its irreversibility of reaction and its abundance of allosteric modulators. PFK is stimulated by the binding of AMP, whose concentration increases as the balance shifts from energy production to energy consumption (i.e., use of ATP generates AMP). This is an important step in which the cell can integrate signals about nutrient status (Passonneau and Lowry, 1964; Hofmann, 1976; Tornheim and Lowenstein, 1976). The final rate-limiting enzyme of glycolysis is pyruvate kinase, which converts phosphoenolpyruvate to pyruvate. In some tissues, pyruvate kinase is regulated by phosphorylation (Holness and Sugden, 2003; Muñoz and Ponce, 2003), in order to inhibit its function when the reverse pathway is in operation – i.e., pyruvate carboxylase, which catalyzes an important anapleurotic reaction to generate new TCA intermediates through oxaloacetate (OAA).

Under certain metabolic conditions, G6P converted into 6-phosphoglucono-δ-lactone, by G6P-dehydrogenase (G6PD) and routed to the pentose phosphate pathway (PPP) (Wamelink et al., 2008; Baquer et al., 1988). This step is irreversible step rate-limiting. The PPP has two phases – oxidative and non-oxidative. The primary goal of the oxidative phase is the generation of nicotinamide adenine dinucleotide phosphate (NADPH), as well as the generation of ribose 5-phosphate, which is important for nucleotide synthesis pathways. However, the non-oxidative

phase interconverts various five-carbon sugars, including F6P and glyceraldehyde 3-phosphate, both of which may re-enter the glycolytic pathway. Additionally, G6P itself can be resynthesized for additional production of NADPH. The only definitively characterized regulatory step of this pathway is inhibition or stimulation of G6PD, by excess NADPH or NADP+, respectively, as this initial step generates NADPH. The other NADPH-generating enzyme of this pathway, 6-phosphogluconate dehydrogenase (6PGD), may be similarly regulated (Jiang et al., 2014). Under some conditions, particularly in cancer, G6PD may also be regulated by the activity of p53 (Jiang et al., 2014), PTEN (Hong et al., 2013), and AMP kinase (AMPK) (Kohan et al., 2009; Stanton, 2012). These enzymes typically inhibit the function of G6PD, which may be part of a regulatory mechanism coordinating the activity of glycolysis and the PPP.

Pyruvate is another pathway nexus for further glucose catabolism. Pyruvate may be oxidized in the TCA cycle, but it has other metabolic fates under different intracellular conditions. For example, in hypoxic scenarios, further pyruvate oxidation (which requires mitochondrial activity – especially considering pyruvate must be imported through the MPC which requires mitochondrial polarization) can be shunted toward the conversion of pyruvate into lactate by lactate dehydrogenase (Firth et al., 1995; Kim et al., 2006). This mechanism also regenerates NAD+, which can then be fed back into the glycolytic pathway for further production of ATP.

Noteworthy in Neurons and Glia:

Glycolytic mechanisms have been identified as one of the key differences in neuronal and glial metabolism. However, the precise segregation (or lack thereof) of pathways remains controversial, to the point where it is still unclear if neurons even use glucose or lactate as a primary carbohydrate substrate, or to which pathway it is shunted (Dienel, 2011; Pellerin and Magistretti, 2011). One such body of work, falling loosely under the Astrocyte-Neuron Lactate Shuttle (ANLS) hypothesis (Pellerin and Magistretti, 2011), suggests that glia that use glucose predominantly for glycolysis, with lactate as its primary metabolic fate. Glia-synthesized lactate is

shuttled to neurons, which can convert lactate back into pyruvate to feed the TCA cycle and perform oxidative metabolism (Figure 7). Interestingly, the neuronal substrate preference for glucose or lactate may be activity dependent, as some studies have indicated glucose is more readily consumed during periods of neuronal firing (Bak et al., 2006, 2009).

Glucose in neurons may be predominantly shunted through the PPP (Bolaños et al., 2008; Bolaños and Almeida, 2010). This pathway has been postulated to be particularly important for neurons, as NADPH is required for the reduction of glutathione, an important countermeasure to oxidative stress. Additional support for this theory comes from an interesting cell-type dependent difference in PFK regulation. PFK can be stimulated by fructose 2,6-bisphosphate, which dramatically impacts the degree of glycolytic flux. In order to produce this metabolite, F6P is phosphorylated by an isoform of PFK(2) – PFKFB3 (Goren et al., 2000; Kessler et al., 2008). In glia, this enzyme is abundant, permitting the increase of glycolytic flux. Though PFKFB3 is also expressed and translated in neurons, it is constitutively degraded by the anaphase promoting complex and adaptor protein (APC/C-Cdh1), which eliminates the neuronal capacity to upregulate glycolytic activity. Interestingly, overexpression of PFKFB3 or inhibition of APC/C-Cdh1 in neurons, ultimately increases neuronal death, suggesting that increased glycolytic activity may be toxic for neurons (Herrero-Mendez et al., 2009). This toxicity may be partially attributable to the shunting of glucose from the PPP to glycolysis, which would result in the insufficient production of NADPH, leaving neurons more vulnerable to ROS toxicity (Bolaños et al., 2010; Bolaños, 2016).

Glycogen synthesis is another function restricted in to astrocytes which express glycogen synthase (McKenna et al., 2012). The steady state concentration of glycogen in the brain is less than 10% of that in the liver (Brown, 2004), but a considerable flux through the glycogen shunt, indicates that glycogen may play an important role in regulating the metabolic coupling between neurons and astrocytes during periods of activity, more than serving as a site of glucose storage. Both glycogen synthesis and degradation pathways are inversely regulated by intracellular and

extracellular signaling mechanisms responding to energy supply. Intracellularly, accumulation of AMP, indicating depletion of ATP supplies, stimulates glycogen phosphorylase (GP) to generate glucose from glycogen. G6P accumulation activates glycogen synthase, to promote glycogen formation. However, both enzymes are modulated by PKA phosphorylation, which indirectly activates GP, and inhibits glycogen synthase, for the net result of glucose mobilization. Additionally, recent studies have suggested that glycogen is essential for neurotransmission (Gibbs et al., 2006; Suzuki et al., 2011) and glutamate uptake (which requires integration with the TCA cycle, discussed below) (Hertz, 2004, 2010; Schousboe et al., 2010). Glycogen is thus an additional integration point for intracellular signaling, and illustrates the activity dependence of many of these metabolic pathways.

2.2.2. The Tricarboxylic Acid (TCA) Cycle

Pyruvate is imported into the mitochondria through the MPC1/MPC2 heterocomplex (Bender and Martinou, 2016). In an overview of the TCA, pyruvate dehydrogenase (PDH) removes a carbon from pyruvate to generate acetyl-CoA (additionally reducing one NAD+ to form NADH). Acetyl-CoA is added to an existing 4-carbon OAA by citrate synthase to form 6-carbon citrate. Subsequent steps of the cycle (see Figure 19) oxidize the newly formed citrate, coupled to the reduction of three NAD+. The NADH generated is fed into Complex I of the RC. Eventually, with the release of the additional carbons as CO_2, OAA is regenerated for another turn of the cycle (Nelson and Cox, 2004). The major regulatory step of the TCA cycle is the PDH- (or PDH complex-) (Patel and Korotchkina, 2006) mediated breakdown of pyruvate into acetyl-CoA. Its activity is regulated through phosphorylation by PDH kinases and dehydrogenases, but these enzymes are themselves primarily allosterically modulated by their respective substrates, similarly to many other enzymes of the TCA cycle (specifically, citrate synthase (Weitzman and Dunmore, 1969), isocitrate dehydrogenase (ICDH) (Reitman and Yan, 2010), and α-ketoglutarate dehydrogenase (αKGDH) (Bunik and Fernie, 2009)). ADP also activates these enzymes while

ATP inhibits them, sensitizing this pathway to the metabolic status of the cell. Similarly, as procession through the cycle generates NADH, increases in the NADH/NAD+ ratio reduce the activity of these enzymes. Finally, Ca^{2+} also potently activates dehydrogenases (PDH (Denton et al., 1972), ICDH (Denton et al., 1978), αKGDH (McCormack and Denton, 1979)), increasing TCA activity and eventually, ATP supply. This further integrates TCA activity to mitochondrial and

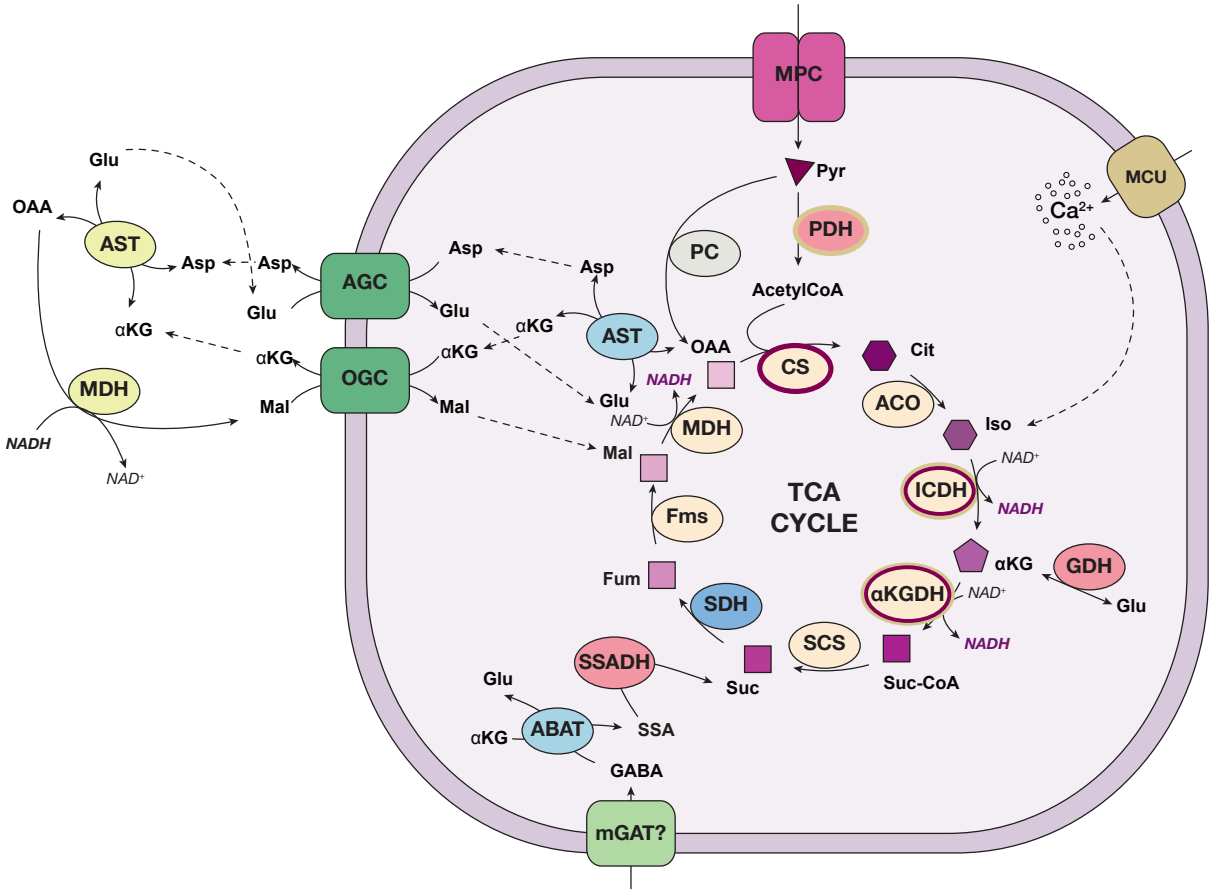

Figure 19. The TCA cycle and its regulation.
Pyruvate enters the mitochondria through the MPC to continue oxidation. It is converted to acetyl-CoA by PDH, and acetyl-CoA is combined with existing OAA to form citrate. One turn of the cycle generates three NADH, and re-forms OAA. Anapleurotic reactions regenerate TCA intermediates. Metabolite shape reflects number of carbons. Enzymes outlined in red are allosterically regulated, those outlined in tan are regulated by Ca^{2+}. Neurotransmitters glutamate and GABA can be integrated as α-KG and succinate, respectively, while the malate-aspartate shuttle both supplies malate and transfers cytosolic NADH electrons to the mitochondria. PC can create new molecules of OAA, but this enzyme is only expressed in glia. MPC, mitochondrial pyruvate carrier; PDH, pyruvate dehydrogenase; PC, pyruvate carboxylase; CS, citrate synthase; ACO, aconitase; ICDH, isocitrate dehydrogenase; αKGDH, α-ketoglutarate dehydrogenase; SCS, succinyl-CoA synthetase; SDH, succinate dehydrogenase (Complex II); Fms, fumarase; MDH, malate dehydrogenase; AST, aspartate transaminase; AGC, aspartate-glutamate carrier; OGC, αKG carrier; ABAT, aminobutyrate transaminase; SSADH, succinyl semialdehyde dehydrogenase.

intracellular function, as mitochondrial Ca^{2+} uptake is increased during periods of increases in cytosolic Ca^{2+}, which typically occurs during periods of high activity (Griffiths and Rutter, 2009).

The TCA cycle is ambipleurotic, as external metabolites may be fed into the cycle to replenish it (catapleurosis) or TCA intermediates may be shunted into separate biosynthetic pathways. Generally, most of the catapleurotic reactions result in the synthesis of new amino acids, purines, pyrimidines, or fatty acids. Anapleurotic reactions are more limited, though some amino acids can regenerate intermediates – in particular, aspartate can be transaminated with αKG to form OAA and glutamate, glutamate and pyruvate can be transaminated to form αKG and alanine, and glutamate can be converted directly to αKG by glutamate dehydrogenase. Succinyl-CoA can also be regenerated from fatty acid oxidation (or GABA, see below). OAA can be generated directly from pyruvate and CO2 by pyruvate carboxylase (Owen et al., 2002).

An important cycle adjacent to the TCA, involving many of its intermediates, is the malate aspartate shuttle (MAS), which transports the NADH produced in glycolysis to the mitochondria, circumventing the impermeability of mitochondria to NADH (McKenna et al., 2006; Llorente-Folch et al., 2013). In this shuttle, two exchanges occur: malate for αKG through SLC25A11 (the malate-αKG exchanger), and glutamate for aspartate through SLC25A12 (AGC1, or Aralar1), which occurs across the IMM. Malate and glutamate are imported into the matrix, while αKG and aspartate are exported into the IMS. In the IMS, aspartate and αKG are transaminated to form glutamate and OAA by aspartate transaminase (AST). OAA is converted into malate by malate dehydrogenase (MDH), which transfers an electron from NADH to malate. In the matrix, MDH catalyzes the reverse reaction, regenerating OAA and NADH, transporting the NADH from the cytosol into the matrix. OAA and glutamate are then transaminated into aspartate and αKG, completing the shuttle. Though the main purpose of this shuttle is the transport of NADH, it is also important for the neurotransmitter cycle (Lund et al., 2009).

Noteworthy in Neurons and Glia:

At least three of the metabolic intermediates have particular roles in neuronal and glial function. First, αKG is interconverted with glutamate, through the actions of either transaminases or glutamate dehydrogenase (Schousboe et al., 2013). This is the entry point for glutamine into the oxidative metabolic pathway, as glutamine is converted into glutamate, followed by αKG, as one of the anapleurotic pathways for the TCA cycle. The reverse reaction, converting αKG into glutamate, is an important part of the neurotransmitter synthesis cycle – allowing for *de novo* glutamate synthesis from glucose oxidation in the absence of glutamine uptake (Hertz, 2013; Schousboe et al., 2013). These metabolic mechanisms are highly segregated between neurons and glia. Only glia are capable of synthesizing glutamine from glutamate, due to the restricted expression of GS in the brain (McKenna et al., 2012). Glia are a vital component of the neurotransmitter cycle for glutamatergic neurons, as they are the primary uptake mechanism for neuronally-released glutamate, through EAAT1 and EAAT2 (Anderson and Swanson, 2000). This glutamate can thus be converted into αKG and metabolized through the TCA (Bak et al., 2006), or directly converted into glutamine by GS. Glia release glutamine onto neurons which convert it into glutamate with the selective expression of PAG (Kvamme et al., 2001). In neurons, this glutamate can also be incorporated into the TCA cycle, though most is likely repackaged into vesicles for release (Westergaard et al., 1995; Rothman et al., 1999; McKenna et al., 2012) The mechanisms dictating the segregation of these metabolites into the metabolic versus neurotransmitter pools remain somewhat ambiguous, but it is clear that both mechanisms operate in both neurons and glia, highlighting the importance of mitochondrial function and metabolic stability even for neurotransmitter cycle operation.

This cycle becomes more complex when considering GABAergic neurons. GABA can be directly converted from glutamate by GAD, and released as a neurotransmitter. GABAergic neurons have a higher fidelity uptake mechanism than glutamatergic neurons through the GABA transporter (GAT), which regulates more immediate neurotransmitter recycling (Savtchenko et

al., 2015). However, some GABA that diffuses away from the synaptic cleft may also be taken up by glia. No evidence has been found for the direct conversion of GABA back into glutamate; instead, GABA is converted into succinyl semialdehyde, followed by succinate, where it can be incorporated into the TCA cycle. Subsequent turns of the cycle can then facilitate the conversion of this intermediate into αKG, and the glutamine/glutamate cycle with GABAergic neurons can then operate similarly to that in the interaction between glutamatergic neurons and glia (Bak et al., 2006; Hertz, 2013).

Finally, OAA is another metabolite that differentiates neuronal from glial metabolism. An important anapleurotic mechanism for adding new carbon intermediates into the TCA cycle is the carboxylation of 3-carbon pyruvate to 4-carbon OAA, mediated by pyruvate carboxylase. This can ensure the continued production of NADH, even if αKG is removed from the cycle to produce glutamate. However, pyruvate carboxylase is only expressed in glia – perhaps once again highlighting the importance of the metabolic 'support' glia provide to neurons *in vivo* (McKenna et al., 2012).

2.2.3. Oxidative Phosphorylation and the Respiratory Chain

The RC is a circuit, coupling the pumping of protons and shuttling of electrons to the consumption of O_2, generation of H_2O, and synthesizing of ATP from ADP. The mitochondrial RC is a series of five transmembrane protein complexes spanning the IMM that transfer protons from the mitochondrial matrix into the IMS and use the resulting energy gradient to generate ATP. The canonical complexes consist of NADH-ubiquinone oxidoreductase (Complex I), succinate dehydrogenase (Complex II), ubiquinone-cytochrome c oxidoreductase bc_1 complex (Complex III), cytochrome c oxidase (Complex IV), and ATP synthase (Complex V). However, as the names imply, two additional essential components of the chain are ubiquinone and cytochrome c, which are mobile within the IMM and transfer electrons between complexes (DiMauro and Schon, 2003; Nicholls, 2013). In the classic model, electrons flow sequentially across the different complexes,

from complex I to ubiquinone to complex III to cytochrome c to complex IV to oxygen, accompanied by proton pumping in complexes I, III, and IV. These pumped protons are eventually funneled through ATP synthase, providing sufficient energy to generate ATP.

Complex I is composed of a hydrophilic and hydrophobic domain, which perform two different functions (Efremov et al., 2010; Zickermann et al., 2015). Oxidized flavin mononucleotide (FMN), bound in the hydrophilic domain, strips electrons off of NADH, transfers them through a series of iron-sulfur (FeS) centers, and then passes them to ubiquinone. The transfer of two electrons is accompanied by the pumping of four protons in the hydrophobic domain, which is coupled to the redox state of the complex. Similarly, oxidized flavin adenine dinucleotide (FAD), bound within complex II, strips electrons from succinate, and transfers these electrons to ubiquinone. However, complex II does not pump protons (Cecchini, 2003; Sun et al., 2005). Reduced ubiquinone is then oxidized by complex III, through a complex three-part mechanism involving sequential electron transfer to the two cytochrome b heme groups within the complex, which is also coupled to the translocation of four protons, and in some cases the generation of ROS (Świerczek et al., 2010; Bleier and Dröse, 2013). These electrons are eventually passed to cytochrome C, which is subsequently oxidized by complex IV, which passes electrons across its respective redox centers to oxygen, while additionally pumping 2 protons (Kaila et al., 2010; Yoshikawa et al., 2011). In total, for every two electrons removed from NADH and transferred to $½O_2$, 10 protons are transferred from the matrix into the IMS, and an additional two are used in the production of H_2O (Nicholls, 2013). Finally, though a number of physiological conditions can affect this stoichiometry, particularly the proton motive force across the membrane, the structure of ATP synthase allows 3 ATP molecules to be produced with the translocation of 8 protons back into the matrix (Boyer, 1997; Okuno et al., 2011; Adachi et al., 2012; Nicholls, 2013).

Despite the presentation of this classical model of the RC, multiple other proteins, such as dihydroorotate dehydrogenase (Schaefer et al., 2010), and *sn*-glycerol-3-phosphate dehydrogenase (Mráček et al., 2013) feed electrons onto ubiquinone as well, additionally fueling

the RC. Furthermore, recent evidence demonstrates the regular assembly of RC components into supercomplexes, which suggests electron conductance is unlikely to be linear (Lenaz and Genova, 2010; Cogliati et al., 2013; Lapuente-Brun et al., 2013).

The establishment of this proton circuit is sustained by an electrochemical gradient which provides proton motive force. This gradient is composed both of the mitochondrial $\Delta\psi$, and the ΔpH across the IMM. Consequently, events that disrupt either aspect of the gradient (e.g. obstruction of ion channels, the opening of the mPTP) compromise the operation of the RC, which impacts the production of ATP. However, both aspects of the gradient are also impacted by the proton circuit, so disruptions in RC function (e.g. inhibition of any of the complexes) can depolarize mitochondria, which may affect its other functions including metabolite transport (Brand and Nicholls, 2011; Nicholls, 2013).

Even in cases of intact/functional respiration and proton circuit conductance, metabolic perturbations can result in changes in respiration rate typically measured through the rate of oxygen consumption. An early generation of experiments examining respiration rates of isolated mitochondria classified five respiratory states, classified by the rate of oxygen consumption and availability of substrates (Chance and Williams, 1955), and newer studies have expanded these definitions (Brand and Nicholls, 2011; Nicholls, 2013). In the absence of substrate (e.g. succinate, malate) or ADP, with or without free phosphate, mitochondria do not consume O_2, which is considered state 1 respiration. State 2 respiration is calculated in the presence of an electron-donating substrate, which allows the buildup of a proton gradient in the IMS. In this case, detected O_2 consumption is a measure of the leak current, i.e. O_2 that is converted into H_2O as a consequence of spontaneous proton transit across the IMM. In the presence of ADP and a substrate, mitochondrial respiration is at its most rapid (while still tethered to ATP synthesis). In some cases, two types of state 3 respiration are classified – state 3_{ADP}, i.e. maximal respiration achievable while tethered to ATP synthesis, and state 3_u, i.e. the maximal respiration that can be achieved in the presence of an uncoupler – signifying the uncoupling of respiration from ATP

production. Typically, uncouplers are ionophores, which render the IMM fully permeable to protons. In this state, O_2 consumption is only rate-limited by the oxidation and proton-pumping rates of the mitochondrial complexes. State 4 is achieved when available ADP is converted to ATP. This slows the rate of O_2 consumption, as high availability of ATP decreases the energetic favorability of ATP synthase rotation, and thus reduces proton flow through this complex. This state is comparable to state 2, and is also achievable by the addition of oligomycin, which inhibits the activity of ATP synthase, and consequently residual O_2 consumption is also attributable to proton leak. State 5 is anoxia, which is usually a background measurement for experimental artifacts. The classification of these different respiratory states clearly illustrates the different drivers of respiratory rate: ADP/ATP availability, substrate availability, and proton pumping capacity. In most physiological contexts, mitochondria operate between state 3 and state 4, and cells can modulate availability of substrate or ADP depending on conditions such as nutrient starvation. However, comparing O_2 consumption during state 3 respiration following application of exogenous compounds or stressors may be useful for evaluating the mitochondrial toxicity of various compounds (Brand and Nicholls, 2011; Nicholls, 2013).

Noteworthy in Neurons and Glia:

While there are no known differences in the makeup of the RC between neurons and glia, differences in their rate of respiration have been reported, though these reports are contradictory. As previously mentioned, a high rate of glia glycolysis is frequently reported (Itoh et al., 2003; Bittner et al., 2010), even if the degree or pathway in which neurons metabolize glucose is disputed (Jolivet et al., 2010; Mangia et al., 2011). Many studies report then that neurons more exclusively rely on mitochondrial activity for ATP production, and have a higher rate of respiration than glia (Itoh et al., 2003; Boumezbeur et al., 2010; Bouzier-Sore and Pellerin, 2013). However, a high respiratory rate has been reported in glia as well (Hertz et al., 2007). This controversy is compounded by conflicting observations of the expression of AGC1, a component of the malate-

aspartate shuttle essential for lactate-independent regeneration of NAD+ for continued glycolysis. Reports demonstrating low glia expression of AGC1 purport low mitochondria respiration, and vice versa (Contreras, 2015). The differences between these two cell types are most likely highly activity and brain region dependent, and fully differentiating the metabolic burdens between different types of neurons and glia will likely require many additional years of study.

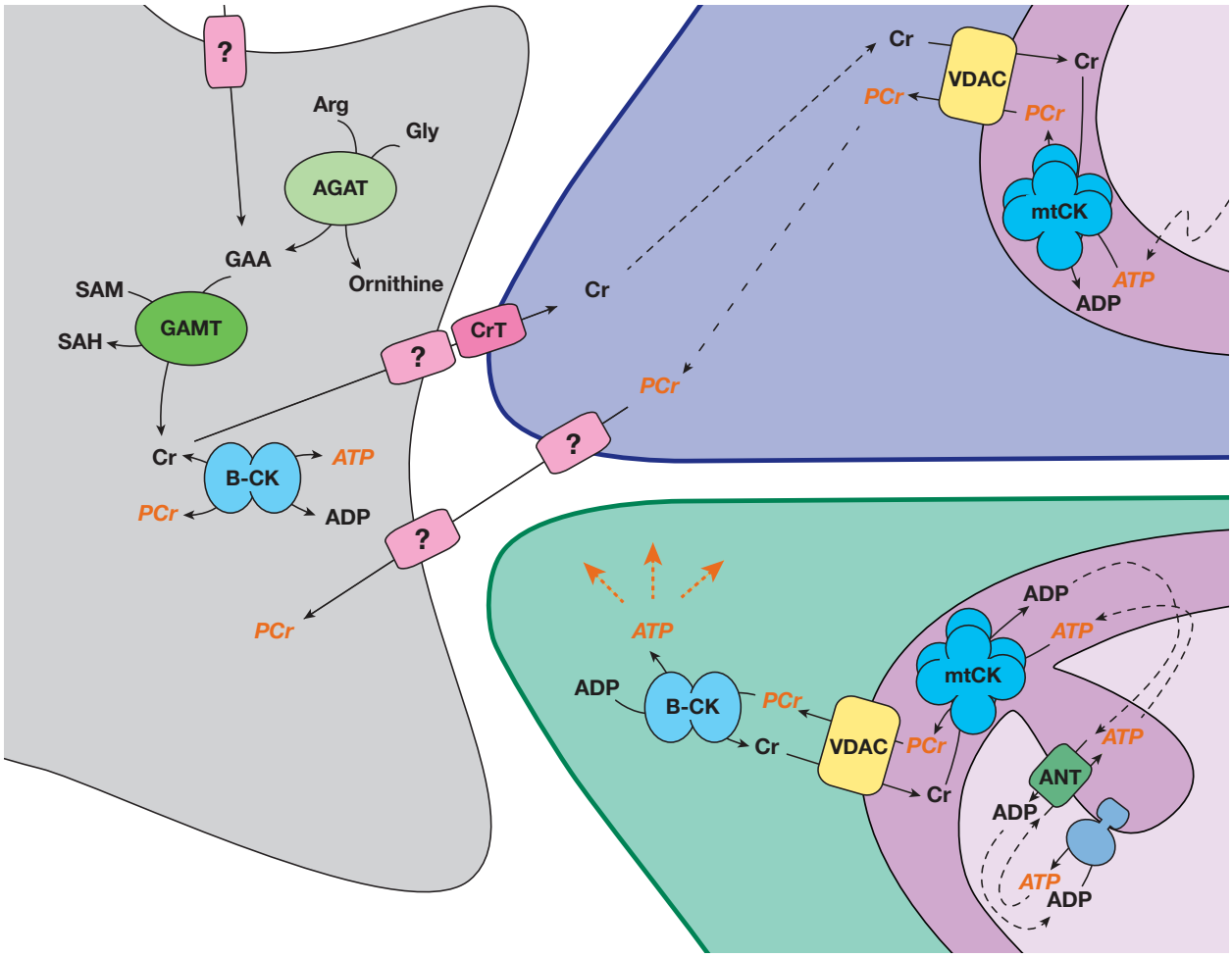

Figure 20. Creatine/Phosphocreatine Shuttle.
Cr is predominantly synthesized locally in the brain from arginine and glycine. Neurons can take up creatine through the CrT, though the other transporters required for Cr transfer between neurons and glia have not been identified. In most cell types (and MSNs), the Cr-PCr shuttle operates through two enzymes. ATP synthesized in the mitochondrial matrix is exported through the ANT into the IMS. There, mtCK transfers a phosphate from ATP to Cr, to generate PCr. Both PCr and Cr can be exchanged through the OMM via the VDAC. In the cytosol, B-CK regenerates ATP from PCr, where it can be used throughout the cell. However, B-CK and mtCK are typically segregated to astrocytes and neurons, respectively, indicating a more complex shuttle pathway between these cell types. AGAT, arginine:glycine amidinotransferase; GAMT, guanidinoacetate methyltransferase; CrT, creatine transporter; B-CK, brain cytosolic creatine kinase; mtCK, mitochondrial creatine kinase.

2.2.4. Phosphate Handling and the Creatine/Phosphocreatine Shuttle

As a result of the activity of the RC, ATP is synthesized in the mitochondrial matrix. ATP is rapidly exported from the matrix through the ANT and for ADP to maintain the necessary concentration gradient for efficient ATP synthase activity. However, ATP is a large and highly polar molecule, and in highly differentiated and polarized cell types, distribution of ATP to the necessary sites of use by simple diffusion is inefficient. One physiological solution to this problem is the creatine-phosphocreatine (Cr-PCr) shuttle, which utilizes a pair of dual-function kinase/phosphatases to transport the terminal phosphate of ATP to its destination (Wallimann and Hemmer, 1994).

Cr is a small molecule, synthesized in a two-step process through the activity of arginine:glycine amidinotransferase (AGAT) and guanidinoacetate N-methyltransferase (GAMT). AGAT combines glycine and arginine to produce guanidinoacetate (GAA) (and ornithine) while GAMT converts GAA to creatine, with the transfer of a methyl group from S-adenosylmethionine. Cr can also be acquired through the diet, but the specific creatine transporter, CrT (SLC68A), limits its uptake in certain tissues (Braissant et al., 2010; Brosnan et al., 2011; Tachikawa and Hosoya, 2011).

Mitochondrial creatine kinase (mtCK) is an octomeric protein situated in the IMS, typically in complex with the ANT and VDAC (Datler et al., 2014). This structural configuration facilitates the translocation of freshly-synthesized ATP out of the matrix, into the IMS, where mtCK directly phosphorylates Cr, generating PCr and ADP. ADP is then translocated back through the ANT, while phosphocreatine is then exported from the mitochondria. PCr is moved throughout the cytosol to sites of use, where cytosolic creatine kinase (in the brain, B-CK) dephosphorylates it to re-form ATP and Cr (Schlattner et al., 2006; Wallimann et al., 2011). In the cytosol, B-CK can also generate PCr from glycolytically synthesized ATP (Schlattner et al., 2016). Interestingly, some studies suggest that in addition to the improved diffusion capacity of PCr when compared to ATP, multiple copies of the creatine kinases may operate in concert to form a ‘phosphate wire.’ In this

model, a chain of creatine kinases with coupled Cr-PCr reactions forms, connecting the mitochondria to sites of ATP consumption, which indicate that when the 'first' ATP in the mitochondria is converted to PCr, this chain of reactions immediately results in an ATP being re-generated at the site of consumption. This process would greatly accelerate the energy availability of mitochondrially-produced ATP (Dzeja and Terzic, 2003).

Noteworthy in Neurons and Glia:

The Cr-PCr shuttle is instrumental for brain function, highlighted by the disorders that accompany dysfunction in the gene products of the system. Mutations in SLC6A8, or either synthetic enzyme (AGAT and GAMT) result in cerebral creatine deficiency syndromes (CCDS). Though the severity of the syndrome varies with the gene mutation, CCDS is unified by mental retardation, developmental delay, seizures, and in some cases movement disorders and muscle weakness (Salomons et al., 2001; Hahn et al., 2002; Schulze et al., 2003; Edvardson et al., 2010).

In contrast to other tissues, the Cr-PCr shuttle is reportedly segregated by cell type in the brain. Despite abundant systemic production of Cr through the coordinated actions of the liver and kidneys, little of this Cr crosses the blood-brain barrier (Braissant et al., 2010; Braissant, 2012). Instead, especially in the adult animal, Cr is predominantly synthesized locally, as GAMT and AGAT are expressed in both neurons and astrocytes. Though the distribution of the synthetic pathway across the cell types remains ambiguous, it is clear that only neurons (and to a lesser degree, oligodendrocytes) express the CrT (Lowe et al., 2015). This would suggest a pathway in which glia synthesize the majority of brain Cr, and then export it to neurons. Curiously, the phosphotransfer system is reportedly segregated in the brain, as multiple studies have shown B-CK is preferentially expressed in glia, while mtCK is preferentially expressed in neurons (Tachikawa et al., 2004; Lowe et al., 2013). Interestingly, MSNs were one of the only cell types with high expression of both enzymes (Lowe et al., 2013).

In summary, the seemingly canonical biochemical pathways involved in the production of ATP from glucose become extensively complex when considering the metabolic coupling between neurons and astrocytes, as well as metabolic demands that are continuously in flux as neurons receive stimuli, depolarize, and fire. As these pathways interact heavily with those involved in neurotransmitter synthesis and reuptake, future studies investigating the ways glycolytic and mitochondrial perturbations affect neurotransmission may be warranted.

2.3. Mitochondrial Dynamics

In order to ensure the allocation of ATP across the cell, mitochondria must be distributed to sites of energetic demand. The mitochondrial network is thus regulated and organized by four major mechanisms – fission, fusion, trafficking, and biogenesis-mitophagy, all of which work in concert to maintain mitochondrial quantity and location. The underlying cellular 'rationale' behind various instances of fission and fusion is still contested (for example, to what degree mitochondrial fusion promotes content mixing to ensure intracellular mitochondrial homogeneity, versus simply metabolite exchange (Chan, 2012; Pernas and Scorrano, 2015)), but recent advances have illustrated some essential points. First, mitochondrial fusion – producing larger, elongated mitochondria, seems to promote mitochondrial respiration (Westermann, 2012). In the absence of a fermentable substrate (i.e. glucose), mitochondria will typically undergo fusion to increase oxidative respiration (Sauvanet et al., 2010). Secondly, mitochondrial fission – producing small, fragmented mitochondria, is a response to a large number of cellular stressors (i.e. Ca^{2+} overload, respiratory uncouplers), and seems to be essential for the segregation of damaged mitochondria for mitophagy for the preservation of healthy and functional mitochondria (Frank et al., 2012; Youle and van der Bliek, 2012). Finally, tipping the balance in either direction between fission or fusion can be detrimental for the cell. Hyperfusion can be a protective response under certain types of stressors (Gomes et al., 2011; Rambold et al., 2011), but reduction in fission also reduces

the ability of the cell to distribute mitochondria to sites of need, and also reduces mitochondria quality control by blocking mitophagy (Twig et al., 2008). More directly, increased mitochondrial fission decreases respiratory capacity, and is typically a direct precursor to cytochrome c release and apoptosis (Breckenridge et al., 2003). Maintenance of the balance between the both fusion and fission is essential for cellular health, further underscored by the disorders that emerge from its disruption.

2.3.1. Fission

Mitochondrial fission is predominantly regulated by Dynamin-related protein 1 (Drp1), a large GTPase which is itself regulated through several signaling mechanisms (see below). Drp1 is a cytosolic protein, but when activated assembles into multimeric ring structures that constrict around dividing mitochondria, much in the same way dynamin itself facilitates the constriction and budding off of endocytic vesicles (Bleazard et al., 1999; Ingerman et al., 2005; Mears et al., 2010). The precise mechanisms underlying the recruitment of Drp1 are still somewhat ambiguous, but an increasing number of studies have indicated that the action of the fission receptors (discussed below), and the ER, which has been shown to create initial constriction points for Drp1, are required (Friedman et al., 2011; Rowland and Voeltz, 2012). Importantly, Drp1 plays a critical role in brain development, as knockout mice are embryonic lethal, while brain-specific knockouts exhibit cerebellar hypoplasia and enlarged mitochondria (Ishihara et al., 2009; Wakabayashi et al., 2009).

Drp1 may undergo a large number of post-translational modifications, the best understood of which are its phosphorylation at two different residues, S616 and S637, which stimulates and inhibits its activity, respectively. S616 is primarily phosphorylated by Cdk1, as part of mitosis (Taguchi et al., 2007). Appropriate segregation of mitochondria into the two daughter cells is essential to cell proliferation, and this mechanism seems to coordinate mitochondrial fission with cell division. In contrast, S637 is phosphorylated by PKA and dephosphorylated by calcineurin,

indicating that stimulation of $G\alpha_s$-coupled GPCRs could evoke a pro-fusion response by inhibiting fission (Chang and Blackstone, 2007; Cribbs and Strack, 2007). The best-documented example of this phenomenon is through cold-evoked norepinephrine release (Gao and Houtkooper, 2014).

Four different fission receptors have been identified – mitochondrial fission protein 1 (Fis1), mitochondrial fission factor (Mff), and mitochondrial dynamics proteins 49 and 51 (MiD49/MiD51), all of which are transmembrane proteins integrated into the OMM and seem to participate in Drp1-mediated fission. Fis1 was first identified as the primary fission receptor, as its knockout produces elongated mitochondria (suggesting a reduction in fission), but subsequent studies have shown that Fis1 knockout does not reduce recruitment of Drp1 to the mitochondria. Mff has instead subsequently emerged as the primary fission receptor, as it is required for the recruitment of Drp1. MiD49 and MiD51 similarly appear to interact with Drp1, though their roles have not been fully elucidated. MiD49 and MiD51 are however unique to the mitochondrial membrane, whereas Fis1 and Mff can both be found in lysosomes (Elgass et al., 2013; Palmer et al., 2013; Pernas and Scorrano, 2015).

2.3.2. Fusion

Fusion of the OMM is mediated by two homologous transmembrane GTPases – mitofusins 1 and 2 (Mfn1 and Mfn2) (Chen et al., 2003). Compared to other proteins which mediate membrane fusion (members of the SNARE complex, for example), these proteins are quite large, and have multiple functional domains that suggest they may be regulated through a variety of mechanisms (Pernas and Scorrano, 2015). Though there appears to be some functional redundancy between these two proteins, knockout of one or the other isoform produces little effect (Chen et al., 2005). Mfn1 and 2 are not identical, for example, Mfn1 has an eight-fold higher GTPase activity than Mfn2 (Ishihara et al., 2004). Additionally, the two genes show some tissue-specific differences in expression – for example, the Purkinje cells of the cerebellum degenerate in the absence of Mfn2 (Chen et al., 2007), whereas no effect is observed with Mfn1 knockouts.

Mutations in Mfn2 are also linked to forms of Charcot Marie Tooth disease (CMT2A), though these defects perturb mitochondrial transport as well as fusion (Cartoni and Martinou, 2009). Both proteins can form forming homo or heterooligomers to mediate fusion, but importantly, both of the fusing mitochondria must contain a mitofusin protein (Koshiba et al., 2004).

In contrast, fusion of the IMM is orchestrated by a single, complexly regulated GTPase, Opa1 (Cipolat et al., 2004). Opa1 has eight different mRNA splice variants, and two different regulatory cleavage sites. In healthy mitochondria, Opa1 is present in both uncleaved (long Opa1/lOpa1) and cleaved (short Opa1/sOPa1) forms – the long form is transmembrane, while the short version is soluble (Anand et al., 2014). Yme1L is the protease that cleaves Opa1 into its short form under standard conditions (Song et al., 2007). Additionally, under these standard conditions, both long and short forms are required for membrane fusion. However, under certain types of stress, long Opa1 can be sufficient for fusion (Tondera et al., 2009). Opa1 only needs to be present on one of the two fusing mitochondria for fusion to proceed. When mitochondria are depolarized, however – under conditions of respiratory insufficiency, for example – Opa1 is cleaved by Oma1, which is activated by depolarization (Ehses et al., 2009). This cleavage inhibits fusion activity, and consequently promotes fission. Opa1 is also important for cristae structure and remodeling, and may be a mechanism of regulating RC efficiency and metabolite flux by modulating their shape (Frezza et al., 2006; Varanita et al., 2015).

2.3.3. Transport and trafficking

Similar to many other types of endosomal trafficking, mitochondria are transported around the cell on microtubules, utilizing kinesin and dynein motors. This process has been characterized extensively in axons, which rely on active retrograde and anterograde mitochondrial transport (Hollenbeck and Saxton, 2005). The KIF5 family of kinesins mediates most anterograde transport (Wang and Schwarz, 2009), while a dynein and dynactin complex regulates retrograde activity (Schiavo et al., 2013). Some of the specific adaptor proteins between mitochondria and the

kinesins have been identified. Miro1 and 2 are integral membrane GTPases spanning the OMM (Fransson et al., 2006; Devine et al., 2016). These proteins associate with TRAK1 and 2 (also identified as Milton in drosophila), which are adaptor proteins for the KIF5 family. In Drosophila, Milton is more specific for mitochondria and kinesin (Stowers et al., 2002; Wang and Schwarz, 2009), but TRAK proteins can traffic other endosomes and interact with dyneins (Koutsopoulos et al., 2010; van Spronsen et al., 2013). Miro is a particularly interesting adaptor protein, as it possesses Ca^{2+}-binding EF hand motifs (Rice and Gelfand, 2006). When these motifs are engaged, i.e. in cases of high cytosolic Ca^{2+}, Miro dissociates from Milton, which interrupts mitochondrial motility and causes 'halting' (MacAskill et al., 2009). Additionally, high local glucose concentrations may also induce halting, as Milton may be modified with O-linked N-acetylglucosamine (O-GlcNAc) (Pekkurnaz et al., 2014). Both of these mechanisms provide methods by which mitochondria may be localized to locations of increased metabolic demand and locally increase ATP production, either through increased TCA flux in response to Ca^{2+}, or increased oxidative phosphorylation in response to glucose. Maintenance of mitochondrial trafficking is particularly important for highly polarized cells such as neurons, which need to sustain ATP production at the highly energetically demanding vesicle release site of the synapse (Pathak et al., 2015).

2.3.4. Biogenesis and Mitophagy

The final 'mechanism' mediating mitochondria dynamics are the opposing forces of mitochondrial biogenesis and mitophagy. Generation of new mitochondria is driven primarily by the peroxisome proliferator-activated receptor gamma coactivator family of proteins (PGCs), highly transcriptionally regulated transcription factors which serve as integration points for a variety of signaling pathways (Scarpulla, 2011). However, PGC-1α is more typically considered the 'master regulator' of mitochondrial biogenesis. Like Drp1, cold exposure (and other stimuli) triggers PGC-1α activation through the cAMP signaling cascade, to stimulate thermogenesis and

biogenesis (Cowell and Blake, 2007; Scarpulla, 2008). Its expression is also tightly linked to glucose metabolism through AMPK, which activates it through phosphorylation. AMPK is itself activated by increases in the AMP/ATP ratio, which rises during states of high ATP consumption (Hardie, 2014). PGC-1a induces the expression of Nrf1 and Nrf2, transcriptional regulators of a wide array of genes associated with mitochondrial function (Lin et al., 2005). Nrf1 activates the transcription of TFAM and TFB1/2M, mtDNA transcription factors, along with nearly 700 other genes associated with mitochondrial biogenesis and metabolism. Nrf2 regulates a partially-overlapping cohort of genes (Scarpulla, 2008), in addition to a transcriptional program that protects against oxidative stress (Zhang, 2006). Neuronal activation can additionally stimulate Nrf2 activity in astrocytes (Habas et al., 2013), demonstrating another avenue for neuronal activity-dependent regulation of mitochondrial function as well as the metabolic coupling between neurons and glia.

Conversely, mitophagy (mitochondria + autophagy) is the selective degradation of dysfunctional mitochondria. This process is initiated through the inhibition of fusion of functional mitochondria with dysfunctional ones – depolarized mitochondria are fusion-inhibited, due at least in part to the cleavage of Opa1 by the potential-sensitive Oma1 (Pernas and Scorrano, 2015; Song et al., 2015). However, this process is mostly under the jurisdiction of the PD-associated enzymes PINK1 and parkin (Youle and Narendra, 2010), though the most conclusive work highlighting their importance was performed in cell lines instead of neuronal cultures (Grenier et al., 2013). In the absence of alternative mechanisms, the PINK1 and parkin pathway is at least one relevant mechanism for mitophagy. PINK1 is constitutively imported through the TOM/TIM complexes, where while mitochondria are normally polarized, it is then degraded (primarily by the PARL protease). However, depolarized mitochondria no longer import PINK1 into the matrix, resulting in its accumulation on the mitochondrial surface. As it accumulates, PINK1 phosphorylates and recruits Parkin, the E3 ubiquitin ligase, as well as pre-existing mitochondrial protein ubiquitins, which promotes further Parkin activity in a feed-forward cycle (Kane et al.,

2014). This activation leads to the recruitment of autophagy adaptor proteins, including OPTN, NDP52, and p62 (Matsuda, 2016) (though importantly, new intermediates in this process are regularly being identified (Heo et al., 2015)), which together polymerize and activate the formation of autophagosomes with LC3 (Pankiv et al., 2007). In this way, mitophagy acts as a quality control pathway to eliminate dysfunctional mitochondria, while biogenesis ensures mitochondria are not depleted through this process.

3. Contributions of Mitochondrial Dysfunction to Neurodegeneration

3.1. Disorders of mtDNA – convergence and divergence

Mitochondrial dysfunction has been implicated in the pathogenesis of diseases in an extremely wide range of organ systems and functions (Wallace, 1999). A vast spectrum of disorders has been grouped into this category – from “classical” mitochondrial diseases, resulting from primary mutations in mtDNA or in genes responsible for mtDNA maintenance (Taylor and Turnbull, 2005; Wallace, 2010), to more the more complex disorders of aging, including cancer, metabolic diseases and neurodegenerative disorders (Lin and Beal, 2006; Moiseeva et al., 2009; Reeve et al., 2016).

Two unique aspects of mitochondrial biology make definitive characterization of mtDNA disorders difficult – mtDNA heteroplasmy and post-mitotic mtDNA replication. mtDNA is transmitted almost exclusively maternally (Hutchison et al., 1974; Giles et al., 1980; Case and Wallace, 1981; Patel, 2017), which can aid in the clinical diagnosis of mitochondrial disorders. However, even in the maternal oocyte, multiple copies of mtDNA are present (Marchington et al., 1997; Chinnery et al., 2000). Heteroplasmy occurs in the offspring when not all of the copies of mtDNA within the oocyte are genetically identical – which can become clinically relevant when some mtDNA copies carry disease-causing mutations. In the event of one of these mutations, the expansion of mtDNA occurring during embryogenesis can cause the asymmetric distribution, and

even enrichment, of the mutant mtDNA into different tissues (Wallace and Chalkia, 2013). Though the mechanisms that regulate this process are still being investigated (Mishra and Chan, 2014), this asymmetry explains in part the wide range of phenotypes that can be associated with the same mtDNA mutation. Similarly, mtDNA is also consistently replicated over the course of an organism's life, even in post-mitotic tissues such as neurons and myocytes (John, 2014). As a result, the ratio of mutant mtDNA may shift over time, or mtDNA may accumulate new mutations that subsequently compromise function.

3.1.1. Common clinical features

For these reasons, even 'classical' mitochondrial diseases present with a wide range of symptoms. However, a core set of clinical features have emerged, which are associated with dysfunctions in tissues most dependent on oxidative phosphorylation (Chinnery and Schon, 2003). The systems most typically affected are neurological, cardiac, gastrointestinal, respiratory, and ophthalmological, and symptoms fall under a number of different 'syndromes.' Leber's Hereditary Optic Neuropathy (LHON), mitochondrial encephalopathy, lactic acidosis, and stroke-like episodes (MELAS), and myoclonic epilepsy with ragged red fibers (MERRF), are most commonly associated with direct mtDNA mutations, and the acronyms for these disorders give a broad summary of their associated symptoms (Taylor and Turnbull, 2005; Alston et al., 2017). In contrast, mutations in genes associated with mtDNA homeostasis are more frequently associated with symptom clusters that fall under Alper's Syndrome (characterized by seizures, spasticity, and liver disease) (Saneto et al., 2013), chronic progressive external ophthalmoplegia (CPEO, characterized by gradual loss of control of the muscles around the eye) (Pfeffer et al., 2011), and the more general "mtDNA depletion syndrome" (MDS, which itself has several different subtypes differentially affecting the aforementioned organ systems) (Suomalainen and Isohanni, 2010). These syndromes are differentiated from each other mostly by severity, age of onset, or the particular cluster of symptoms and affected systems. These two types of mutations present

clinically with considerable overlap, and determination of the causative mutation may require either genotyping or an examination of the pattern of inheritance.

3.1.2. Representative mtDNA point mutations and their specific disorders

Disease-causing mutations have been identified in every protein-coding gene in mtDNA, and some more well-characterized mutations have been found in mitochondrial tRNAs as well. A comprehensive list of these mutations can be found in the MitoMap database (www.mitomap.org), but a few examples of the better-known mutations causing the syndromes and disorders mentioned above, with particular emphasis on neurological disorders, will be detailed below.

Over 30 mtDNA mutations are associated with the presentation of LHON (Y-W-Man et al., 2002), though 3 of these mutations comprise 95% of cases (Perez et al., 2009). These three mutations are mtND4^{G11778A}, mtND1^{G3460A}, and mtND6^{T14484C}, presenting a clear example of mitochondrial disease genotype convergence, where mutations in three distinct mtDNA genes present with the same syndrome. Interestingly, though the primary symptomology of this disorder is a loss of central vision, LHON is also a neurodegenerative disorder, involving progressive loss of retinal ganglion cells. In some cases, additional neurological dysfunctions have been reported, including parkinsonism and dystonia.

Similarly, a number of mutations have been identified as pathogenic for MELAS, but many of these overlap with other syndromes. However, the tRNA$^{Leu(UUR)\ A3243G}$ (Goto et al., 1990; Davidson et al., 2009) mutation is found in 80-90% of MELAS patients, although it occasionally overlaps with other disorders. As this mutation affects a tRNA, responsible for translating all of the mitochondrially encoded genes, all mitochondrial RC complexes should be affected by this disorder. However, clinical presentation varies, and complexes I and IV are most frequently affected. As its name suggests, the cardinal manifestation of MELAS is a combination of clinical stroke, seizures, lactic acidosis, ragged-red fibers, exercise intolerance, and onset of symptoms before age 40, but other associated features include dementia, myoclonus, and optic atrophy.

Informatively, the type of stroke associated with this disorder has been described as 'metabolic stroke,' as risk of stroke increases during coincidence with other disease states when energetic demands are highest, and the dysfunctional mitochondria fail to meet this demand (Hirano and Pavlakis, 1994). This energetic deficiency likely underlies the majority of MELAS symptoms (El-Hattab et al., 2015).

In contrast, a mutation in a different tRNA, $tRNA^{Lys\ A8344G}$, is pathogenic for MERRF, causing similar deficiencies in mitochondrial protein synthesis, and is observed in over 80% of MERRF cases (Larsson et al., 1992). Myoclonus and epilepsy are typically the first symptoms of this disorder, but ataxia, weakness, and dementia follow (Hirano and DiMauro, 1996). Additionally, the presence of ragged red fibers, initially considered to be one of the definitive hallmarks of mitochondrial disease, is observed in muscle biopsies. The term refers to the Gömöri Trichome staining of muscle fibers, in which abnormally proliferated mitochondria (a characteristic response to energetically deficient mtDNA) stain red, among blue-staining normal muscle fibers (Bourgeois and Tarnopolsky, 2004).

In addition to inherited mutations, mtDNA can also accumulate mutations from oxidative damage or replication errors (Copeland and Longley, 2014). Oxidative damage to mtDNA typically manifests in the form of G:C to T:A transversions (Beckman and Ames, 1999). These result from the formation of 8-oxodG adducts, which cause guanine residues to bond to adenine in the place of cytosine (Moriya, 1993). Two systems combat the accumulation of these residues – OGG1, which removes the adducts (Bohr et al., 2002), and 8-oxoGTPases, which eliminates their precursors (Kang et al., 1995). While the accumulation of these adducts is frequently reported as a marker of oxidative stress (Valavanidis et al., 2009), their increased prevalence in the OGG1 knockout mouse does not adversely affect viability (Stuart et al., 2005). Additionally, the frequency of these mutations does not increase with age, suggesting that oxidative damage is not a primary source of age-related mtDNA mutation accumulation (Kennedy et al., 2013). In contrast, a second class of mtDNA mutations, arising from nucleotide misinsertion, are the most common type of

mtDNA mutation, and do increase up to five-fold with age (Larsson, 2010; DeBalsi et al., 2017). These mutations arise from POLγ, and will be discussed in more detail below.

3.1.3. Mendelian sources of mitochondrial disorders – mtDNA deletions and depletions

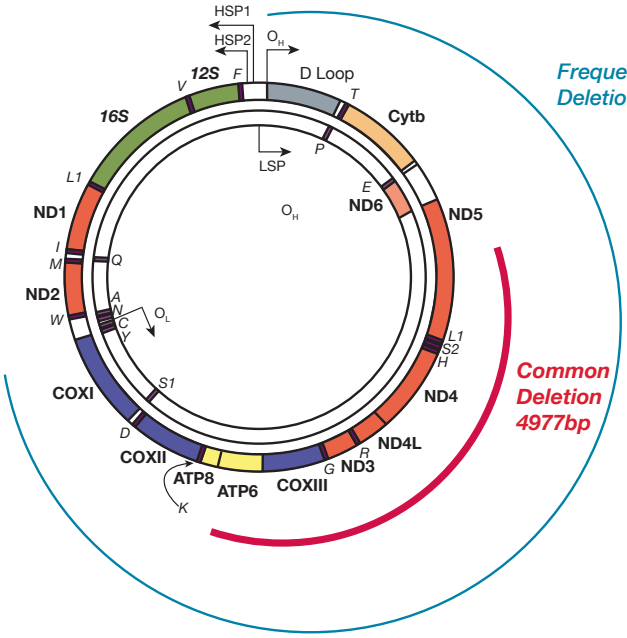

Figure 21. mtDNA common deletion. In humans, a 4,977bp region between ND5 and ATP8, which falls between two 13bp repeat regions, is frequently deleted, compromising mitochondrial function (red arc). However, mtDNA deletions are frequently found in the entire region between the O_H and O_L, likely as a result of the order of Polγ-mediated strand-displaced replication (blue arc). Adapted from Schon 2012, see Figure 17.

While mutations in mtDNA are maternally inherited, a number of Mendelian-inherited genes encoded by the nucleus are also associated with "mitochondrial disease" phenotypes. These genes fall into four major categories of pathophysiological consequences: mtDNA deletions and depletion, RC subunit and accessory protein defects, synthesis and metabolism defects, and dynamics defects (Angelini et al., 2009). mtDNA depletion symptoms typically emerge when quantities fall below 30% of wildtype (Rötig and Poulton, 2009). In contrast, deletions are characterized by the loss of a large segment of mtDNA. Deletions are frequently seen in a particular mtDNA region which is known as the 'common deletion,' a 4977bp deletion from ATP8 to Cytb (in humans, though a similar range is frequently deleted in rodents and other species) (Figure 21) (Schon et al., 1989; Samuels et al., 2004). The most commonly mutated genes causing mtDNA deletions and depletions will be discussed below.

Defects of the mtDNA Replisome

The gene most regularly tied to both mtDNA deletions and depletion is POLγ. POLγ, the only known mitochondrial DNA polymerase out of 17 known eukaryotic DNA polymerases, is a remarkably high-fidelity enzyme, making only one base substitution every 500,000 bases (Young and Copeland, 2016). Its high fidelity is supported by its 3'-5' exonuclease domain, which improves strand proofreading. Interestingly, association of the POLG2 accessory subunits somewhat decrease replication fidelity, but greatly increase its speed by improving DNA binding affinity. Nonetheless, this mutation rate is sufficient to be the primary cause of the accumulation of mtDNA mutations (Larsson, 2010). This mutation accumulation is more frequent in mtDNA in contrast to nuclear DNA, despite its high fidelity, because mtDNA is continuously replicated even in post-mitotic tissues, which can cause reductions in function over the course of an organism's lifespan.

Mutations in POLG present phenotypically with a number of mitochondrial diseases. Best-known are Alpers syndrome, which typically presents with seizures, movement disorders, and liver disease, and CPEO (Copeland, 2010). However, over 200 mutations in POLG have been identified that cause a range of neuromuscular disorders, though as with all mitochondrial disorders, the clinical presentation of these mutations varies enormously. Interestingly, these disease-causing mutations are not constrained to one function of POLγ, but instead can affect its enzymatic activity, its fidelity, or assembly with either its accessory subunits or additional replication machinery (Copeland and Longley, 2014). Experimentally-induced mutations in POLγ have been equally informative about the pathogenic capacity of mtDNA mutation accumulation. The exonuclease function of POLγ has been exploited for the generation of the mutator mouse (Kujoth, 2005). By removing the functionality of the exonuclease domain, POLγ produces a much greater number of mtDNA mutations. Homozygous mice display a progeroid phenotype, suggesting a strong relationship between the aging and the accumulation of mtDNA mutations.

Mutations in the mtDNA helicase, Twinkle, also leads to the accumulation of mtDNA deletions (Spelbrink et al., 2001). Interestingly, most of the identified mutations in this gene cause CPEO (though other symptoms frequently co-occur), somewhat in contrast to the wide range of mutations and phenotypes observed with POLγ mutations. However, this may be related to the restriction in functional deficits identified in Twinkle – a study examining 20 different mutants demonstrated that all of these retained helicase activity, and none profoundly altered its activity beyond changes to DNA binding or reaction kinetics (Longley et al., 2010).

Defects of Nucleotide Handling

Mutations in three other genes have been reported to cause mtDNA deletions or depletions – SLC25A4 (ANT1), thymidine phosphorylase (TP), thymidine kinase (TK2) and deoxyguanosine kinase (DGUOK), all of which are associated with dysfunctional nucleotide handling.

Several mutations in ANT1, the ATP/ADP translocator have been identified and produce phenotypes falling into two broad categories – recessive mutations, which cause an early-presenting cardio/myopathy disorder (also classified as an isoform of mtDNA depletion syndrome - MTDPS12), or missense mutations causing a form of CPEO (Thompson et al., 2016). Though the crucial function of this enzyme is clear, it is somewhat surprising that mutations are pathogenic, as several isoforms of ANT are encoded in the humans and could compensate for one another. However, ANT1 has been identified as the key isoform in highly energetic tissues – skeletal muscle, heart, and brain (Stepien et al., 1992).

Thymidine phosphorylase catalyzes the interconversion of thymidine (or deoxyuracil) into thymine or uracil, and is part of the salvage pathway from nucleotide catabolism. Mutations in this enzyme result in accumulated thymidine and deoxyuracil, but also a unique mitochondrial pathology known as mitochondrial neurogastrointestinal encephalopathy (MNGIE – alternately MTDPS1), a predominantly intestinal dysmotility disorder that eventually progresses to symptoms

associated with other mitochondrial diseases, including ophthalmoplegia, neuropathy, and weakness (Hirano et al., 1994; Nishino et al., 1999; et al., 2011).

In a related pathway, TK2 is the mitochondrial isoform of an enzyme that phosphorylates thymidine to make thymidine monophosphate, for re-incorporation into DNA, and is thus also part of the nucleotide salvage pathway (Saada et al., 2001). Similarly, DGUOK performs the same function to produce deoxyguanosine monophosphate (Mandel et al., 2001), which is also incorporated into newly synthesized mtDNA. Mutations in either of these genes also result in mtDNA depletion, producing MTDPS2 and MTDPS3, respectively. These syndromes have considerable overlap with MTDPS1, as both have depleted mtDNA in affected tissues, but MTDPS2 more frequently presents with hypotonia and muscle weakness, while MTDPS3 causes liver dysfunction and encephalopathy.

3.1.4. Mitochondrial disorders of both genomes or neither (LS and KSS)

Many forms of mtDNA-related disorders can be traced back to either mtDNA mutations or mutations in genes regulating mtDNA maintenance, as discussed above. However, two interesting examples of exceptions to this rule are Kearns-Sayre Syndrome (KSS), which currently has no known related gene deficiency, and Leigh Syndrome (LS) which can develop from mutations in either mtDNA or multiple nuclear genes.

KSS was one of the first “mitochondrial diseases” identified, and its canonical sign is the accumulation of mtDNA deletions throughout the body (Zeviani et al., 1998). The symptoms of KSS overlap with CPEO, but usually also include pigmentary retinopathy and additional cardiac and neurological abnormalities (Wittich et al., 2014). The mechanism producing mtDNA deletions without any obvious gene mutation is still unknown, but some studies have suggested it may emerge from sporadic defects in replication causing double strand breaks (Shoffner et al., 1989; Bharti et al., 2014).

Pathogenic mutations in mtDNA and nuclear genes can both produce mitochondrial deficits leading to LS, also known as subacute necrotizing encephalopathy, a primarily neurological mitochondrial disorder that frequently presents with hypotonia, movement disorders like chorea, and deterioration of the basal ganglia and brainstem (Baertling et al., 2014). Similarly to other mitochondrial disorders, and MELAS in particular, the onset of LS typically coincides with another illness, which likely presents a sufficient metabolic stressor. Approximately 20% of LS cases arise from mtDNA mutations (Makino et al., 2000), but half of these cases have the mtATP6$^{T8993G/C}$ mutation, which compromises the function of ATP synthase, and additionally can cause a less severe version of LS as such as neuropathy, ataxia, and retinitis pigmentosa (NARP) (Fryer et al., 1994; Rojo et al., 2006). The other 80% of cases are caused by mutations in nuclear genes (Lake et al., 2015). This includes direct mutations in nuclear-encoded RC subunits, which most frequently causes Complex I or IV deficiencies, as well as mutations in complex assembly factors, such as SURF1 and LRPPRC, both of which are involved in Complex IV assembly.

The genotype and phenotype interactions in “mitochondrial diseases” present an interesting example of convergence and divergence considerably more complex than most genetic disorders originating in the nucleus. It is tempting to combine all of these types of disorders into a single category, but specific mutations have hallmark features. One of the more interesting aspects is how perturbations in mtDNA quantity or maintenance frequently affect neurological function. Though it is well-established that mitochondrial function is important for neurons and the brain, it is nonetheless useful to observe how changes in mtDNA quantity can cause encephalopathy, dystonia, ataxia, and chorea. While these disease syndromes arise from primary mutations, further study into the consequences of acquired mutations or changes in mtDNA copy number in specific organ systems may prove informative.

3.2. Disorders of mitochondrial signaling

In addition to the essential metabolic function of generating energy, mitochondria are also complex hubs of a number of signaling pathways. Communication between the nucleus and mitochondria, which occurs in both anterograde and retrograde directions, is instrumental for regulating metabolic rate, but also for the induction of necessary gene transcription programs (Cagin et al., 2015; Chandel, 2015). One of these mechanisms, the UPR^{mt}, was discussed previously (see section 2.1) (Haynes and Ron, 2010), but this section will cover mitochondrial signaling through the use of second messengers, also discussed in a broader context for the basal ganglia in section 1.2. Two of the essential second messengers of the mitochondria are Ca^{2+} and ROS, and their physiological and pathophysiological functions will be discussed below.

3.2.1. Calcium

Mitochondria buffer cytosolic Ca^{2+} in a manner analogous to the ER. Across the inner membrane, Ca^{2+} is taken up electrogenically through the MCU. In contrast, efflux occurs through either the H^+/Ca^{2+} exchanger (Letm1) (Tsai et al., 2014), or the Na^+/Ca^{2+} exchanger (NCLX) (Bernardi et al., 1999), which is effectively coupled to the Na^+/H^+ exchanger (mNHE1) (Jouaville et al., 1998; Nicholls, 2005). These mechanisms are dependent on the presence of the mitochondrial $\Delta\psi$, and the RC-generated proton gradient. Ca^{2+} efflux can also occur in bulk through the opening of the mPTP, an event which typically proceeds the apoptotic cascade and can occur during excitotoxic events like ischemia-reperfusion (Hansson et al., 2003) or NMDA overactivation (Alano et al., 2002).

Free mitochondrial matrix Ca^{2+} concentration ranges from about 0.5-2μM, and mitochondria begin taking up cytosolic Ca^{2+} when it exceeds 0.5μM. In neurons, basal cytosolic Ca^{2+} is approximately 0.1μM, so free matrix Ca^{2+} remains low (Thayer and Miller, 1990; Pivovarova et al., 2004). However, upon stimulation, L-type voltage gated Ca^{2+} channels open, flooding the cytosol with Ca^{2+}. In these cases, mitochondria can modulate the Ca^{2+} signal, either

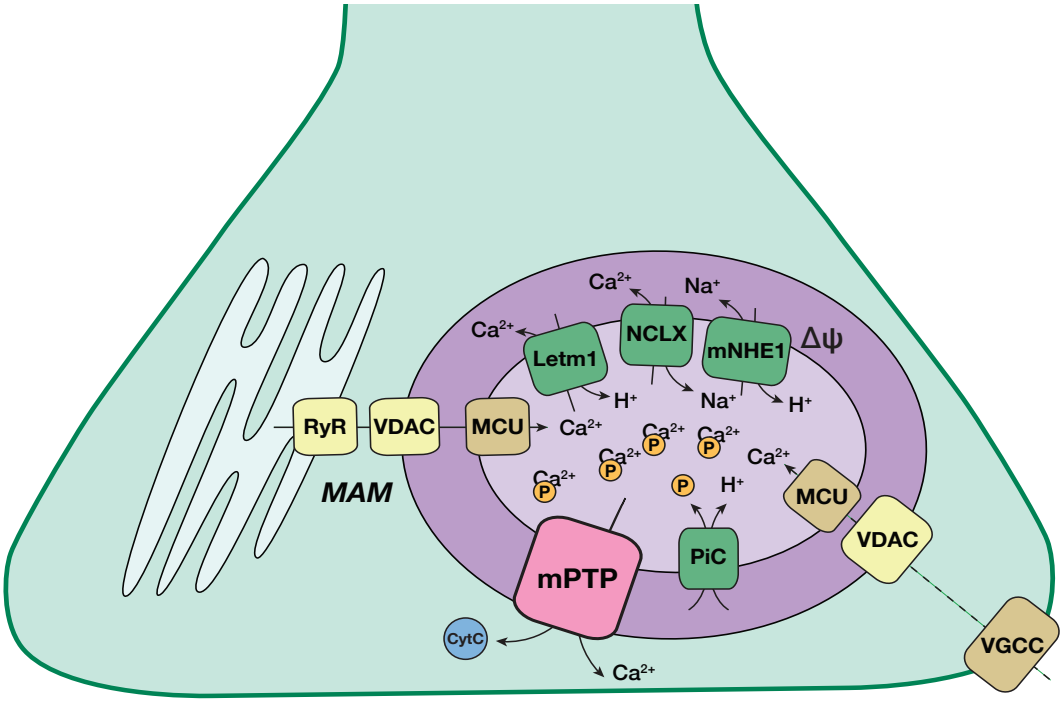

Figure 22. Mitochondrial calcium influx and efflux.
Ca^{2+} enters the mitochondria through the MCU, a Ca^{2+} sensing protein complex. The MCU can take up cytosolic Ca^{2+} that enters through the activation of VGCCs, but are frequently aligned with VDAC and RyR/IP_3Rs to couple ER and mitochondrial Ca^{2+}. Once within the matrix, Ca^{2+} is buffered by complexing with phosphate, which is imported through the PiC. Ca^{2+} efflux is regulated by three antiporters: Letm1, a Ca^{2+}/proton exchanger, NCLX, a sodium/Ca^{2+} exchanger, and mNHE1, a sodium/proton exchanger. Both influx and efflux mechanisms are highly dependent on Δψ. Finally, the opening of the mPTP allows the unregulated release of Ca^{2+}, which contributes to the induction of apoptosis. RyR, ryanodine receptor; VDAC, voltage dependent anion channel; MCU, mitochondrial Ca^{2+} uniporter; VGCC, voltage gated Ca^{2+} channel; mPTP, mitochondrial permeability transition pore; CytC, cytochrome C; PiC, phosphate carrier. permeability transition pore; CytC, cytochrome C; PiC, phosphate carrier.

by acting as a sink and rapidly clearing the cytosol (Budd and Nicholls, 1996), or by extending the elevation of cytosolic Ca^{2+} with efflux (David et al., 2003). Importantly, mitochondria are able to take up large amounts of Ca^{2+} because once imported, Ca^{2+} forms Ca^{2+}-phosphate complexes. The PiC is highly active, and imported phosphate rapidly complexes with Ca^{2+}, limiting the accumulation of free matrix Ca^{2+} which may trigger the opening of the mPTP. In contrast to the low micromolar concentrations of free matrix Ca^{2+}, total matrix Ca^{2+} (including Ca^{2+}-phosphate complexes) may approach 1M (Nicholls, 2013). These complexes are highly pH dependent, and acidification of the matrix (caused by a protonophore, or increased flux through the RC) causes rapid dissociation of these complexes and liberation of free matrix Ca^{2+} (Nicholls, 2005).

Largely through the use of compounds that specifically inhibit mitochondrial Ca^{2+} uptake (i.e., ruthinieum red, which inhibits the MCU), a number of studies demonstrated that mitochondria take up Ca^{2+} during neuronal stimulation (Friel and Tsien, 1989; Babcock et al., 1997), and even interact with Ca^{2+} released from IP_3-mediated signaling (Simpson and Russell, 1996). In addition to buffering the cytosol, one of the major functions of this activity is the increase in metabolic activity to accommodate the increased energetic burden of electrical stimulation. Three of the dehydrogenase enzymes of the TCA are Ca^{2+} sensitive (Figure 19), and increase their rate of activity in response to increased Ca^{2+}, up to about 3μM free matrix Ca^{2+} (McCormack and Denton, 1990; Jouaville et al., 1999; Pitter et al., 2002; Szabadkai et al., 2006). This increase in activity generally correlates with increased ATP production, though no direct regulation of ATP synthase by Ca^{2+} has been observed (Griffiths and Rutter, 2009).

Mitochondria have long been known to be positioned near IP_3Rs and RyRs, the Ca^{2+}-releasing channels of the ER (Jouaville et al., 1998; Szabadkai and Rizzuto, 2004), and crosstalk between these two organelles has been demonstrated as an important part of intracellular Ca^{2+} regulation. However, only recently have some of the protein complexes mediating these interactions been identified. Contact sites between the ER and mitochondria are referred to as mitochondria-associated ER membranes (MAMs), while the protein complex mediating this interface is the ER-mitochondrial encounter structure (ERMES) (Marchi et al., 2014). MAMs have been identified across cell types and species, but the proteins associated with ERMES have only been conclusively identified in yeast, and only approximately identified in proteomic screens in mammals (Poston et al., 2013). These interactions are reported to have a number of functions, including the regulation of mitochondrial fission (Friedman et al., 2011), but they are also clearly involved in the exchange of Ca^{2+}. This appears to occur mostly through the positioning and interaction of the IP_3R and VDAC on the OMM (Csordás et al., 2010; Golenar et al., 2010; Naon, 2014), which also facilitates the influx of Ca^{2+} through the MCU. Despite their recent discovery, deregulations in these contacts have already been associated with Alzheimer's Disease (de Brito

and Scorrano, 2010; Area-Gomez et al., 2012; Schon and Area-Gomez, 2012; Burté et al., 2015), where increases in MAM proteins have been demonstrated to be upregulated in post mortem samples (Hedskog et al., 2013).

As previously discussed, mitochondrial Ca^{2+} uptake and efflux are dependent on the maintenance of Δψ. As a result, disruption of Δψ, through mtDNA depletion or respiratory insufficiency, increases cytosolic Ca^{2+} and perturbs signaling pathways, predominantly through the increase in expression of Ca^{2+} handling genes (Biswas et al., 1999; Amuthan et al., 2001). Increases in cytosolic Ca^{2+} arising from mitochondrial dysfunction increases PP2B activity, induces the expression of NFAT and NFκB, and increases PKC, CAMKIV, JNK, and MAPK (Rizzuto et al., 1993; Babcock et al., 1997; Ichas et al., 1997; Butow and Avadhani, 2004). In a seminal study, depolarization of the mitochondria through the use of carbonyl cyanide-4-phenylhydrazone (FCCP) was also shown to increase ERK phosphorylation (Luo et al., 1997). Interestingly however, the interactions between the overactivation of these Ca^{2+} handling pathways as a result of reduced mitochondrial Ca^{2+} buffering, and the activation of these similar pathways through the agonism of Ca^{2+}-related GPCRs or voltage gated Ca^{2+} channels remains somewhat underexplored.

Dysfunctional mitochondrial Ca^{2+} handling has been linked to neurodegenerative disorders, including ALS, PD, HD, and AD (Bezprozvanny, 2009; Gibson et al., 2010; Pivovarova and Andrews, 2010; Duchen, 2012), particularly as a major mechanism for apoptosis or necrosis of neurons. However, despite the preponderance of evidence linking destabilization of intracellular Ca^{2+} in these disorders, in most cases the proposed mechanism involves the overloading of mitochondrial matrix Ca^{2+} and subsequent opening of the mPTP (Duchen, 2012). The relevance of this mechanism in these cases remains controversial, as the strongest evidence for mPTP has been observed in models of glutamate induced excitotoxicity (Nicholls, 2009) (though a more complex model of Ca2+ deregulation is relevant for PD, see section 3.3.2). In this case, hyperactivation of NMDARs causes Ca^{2+} influx, dramatically increasing cytosolic Ca^{2+}. This drives

mitochondrial matrix Ca^{2+} increase, which either directly overloads them depending on the magnitude of stimulus, or causes a phenomenon of delayed Ca^{2+} deregulation (DCD) in adjacent neurons (within the stroke penumbra, for example), as Ca^{2+} loaded into the mitochondria during the stimulus is then subsequently released (Choi, 1985; Tymianski et al., 1993; Nicholls, 2009; Duchen, 2012). Hyperactivation of NMDARs dramatically increases cytosolic Na+, which the Na^{+}/K^{+} ATPase must then pump back out to repolarize the cell. This increased metabolic burden may also sensitize the mitochondria to disruptions in Ca^{2+} handling (Henneberry, 1989; Soane et al., 2007). A subtler relationship between mitochondrial Ca^{2+} and neuronal dysfunction has also been implicated in the Ca^{2+} regulation of mitochondrial dynamics. Most of the GTPases mediating mitochondrial fission and fusion are Ca2+ sensitive, implying that these processes are likely dependent on both intramitochondrial and cytosolic Ca^{2+} (Ishihara et al., 2012; Mishra, 2016). Miro, one of the two major proteins involved in mitochondrial trafficking, contains two EF Ca^{2+} binding domains, and is highly Ca^{2+} dependent. High Ca^{2+} concentrations stop Miro on its microtubule tracks, presumably as another mechanism to respond to increased metabolic demand (Tang, 2015; Devine et al., 2016). However, pathological increases in Ca^{2+} deregulate this process and may disturb mitochondrial quality control, in ways that have been shown to contribute to degeneration in models of ALS and HD (Orr et al., 2008; Misko et al., 2010).

3.2.2. Reactive Oxygen Species

Mitochondrial production of ROS is one of the best-known mechanisms of endogenous cell damage. Intramitochondrial ROS species are $O_2^{\bullet-}$ (superoxide), and H_2O_2. These species cause oxidizing damage by stripping electrons off of any proximal biomolecule, disrupting the redox balance. ROS has been posited as the cause for a wide range of disorders, including aging itself through the mitochondrial free radical theory of aging (MFRTA) (Harman, 1972, 1981). MFRTA speculates that throughout the lifetime of an organism, ROS production from the mitochondria gradually damages mtDNA and the surrounding lipids of the mitochondrial

membranes through lipid peroxidation, or proteins through cysteine oxidation (Schieber and Chandel, 2014). However, this theory is losing prominence as age-related mtDNA mutations are infrequently caused by oxidant damage (Larsson, 2010), and there is generally a low correlation between ROS production and aging (Stuart et al., 2014). Focus is instead shifting toward ROS as signaling molecules, though ROS dysregulation can still play a role in neurodegenerative disorders.

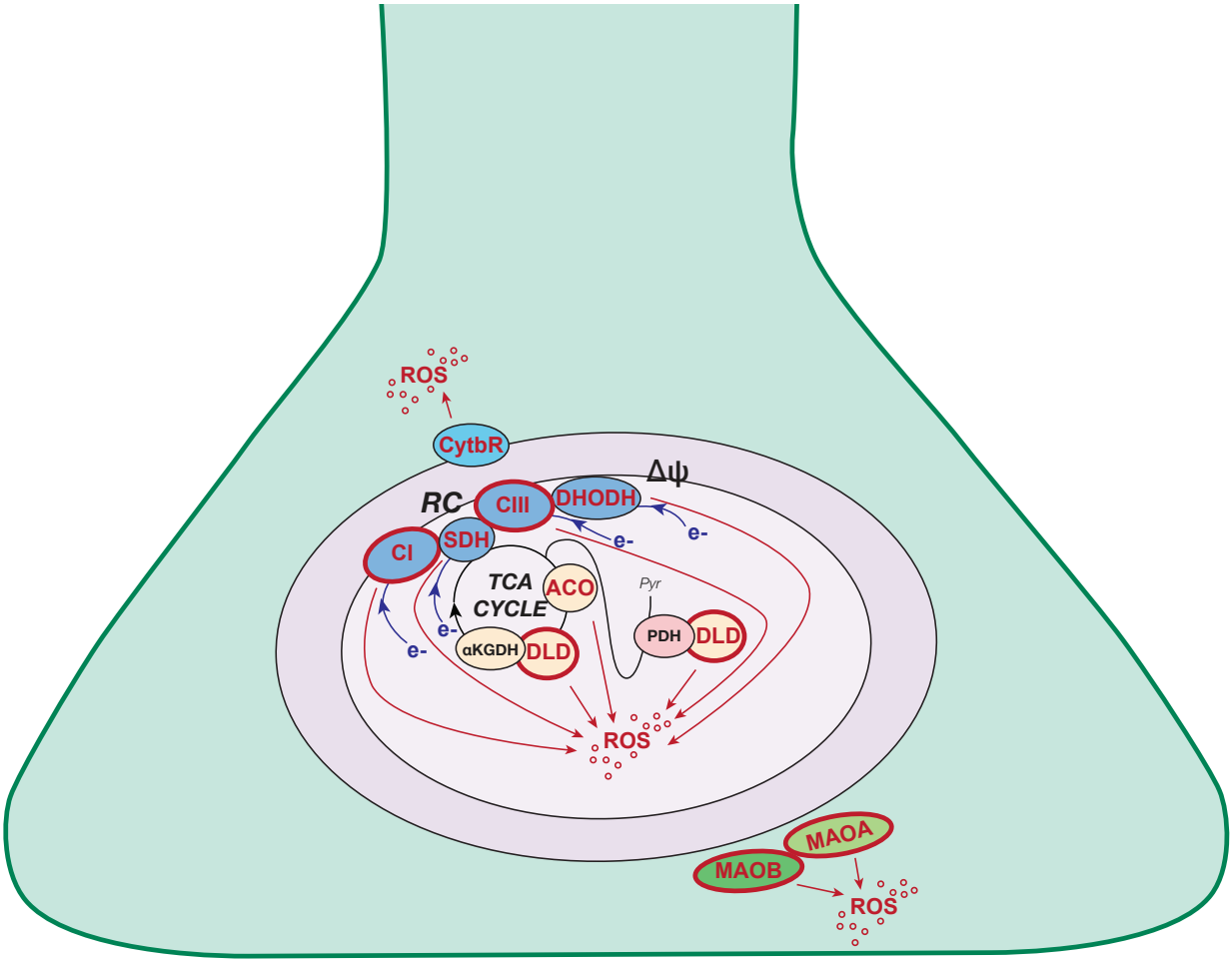

Figure 23. Sites of mitochondrial ROS production.
Multiple enzymes, particularly within the RC and TCA cycle, contribute to the production of mitochondrial ROS (red labeled). Those that are more physiologically relevant for ROS production in the brain are additionally outlined in red. CytbR, cytochrome b5 reductase; CI/CIII, complex I/III; SDH, succinate dehydrogenase; DHODH, dihydroorotate dehydrogenase; ACO, aconitase; DLD, dihydrolipoamide dehydrogenase; MAO, monoamine oxidase. Adapted from Andreyev, 2005.

Nine sites of mitochondrial ROS production have been identified, though their physiological relevance in many cases is still under scrutiny (Andreyev et al., 2005) (Figure 23).

These include RC Complex I, Complex II, and Complex III, MAOA/MAOB, cytochrome b5 reductase (an OMM protein that oxidizes NADPH), glycerol-3-phosphate dehydrogenase (mGPDH), aconitase (which catalyzes the conversion in the TCA from citrate to isocitrate), dihydrolipoamide dehydrogenase (DLD) – which is involved in the dehydrogenation of pyruvate, αKG, and glycine cleavage, and dihydroorotate dehydrogenase (in the IMS and important for pyrimidine synthesis). Finally, $p66^{shc}$ has been identified as another source of mitochondrial ROS (Giorgio et al., 2005; Pinton et al., 2007; Gertz and Steegborn, 2010; Galimov et al., 2014). $p66^{shc}$ is normally a cytosolic protein, but following stress stimuli, it translocates to the mitochondria and generates ROS. However, the mechanism by which this protein generates ROS is still unclear and warrants further investigation (Andreyev et al., 2015).

The most important areas of ROS production in the brain are CI of the RC (from Complex I (Kushnareva et al., 2002; Pryde and Hirst, 2011; Treberg et al., 2011) and CIII of the RC (Quinlan et al., 2011)), MAO (Hauptmann et al., 1996; Maurel et al., 2002; Kumar et al., 2003), and DLD (Starkov et al., 2004). Though these three produce ROS under physiological conditions, the specific mechanisms of production are controversial (Panov et al., 2007; Nicholls, 2013; Andreyev et al., 2015). In the RC complexes, $O_2^{\bullet-}$ production is thought to occur as electrons from the transport chain are instead transferred to the readily available O_2, and are likely major sources of matrix ROS. MAOA and MAOB are proteins of the OMM that oxidatively deaminate monoaminergic neurotransmitters (Johnston, 1968; Knoll and Magyar, 1972; Bach et al., 1988; Grimsby et al., 1991). MAOA degrades DA, norepinephrine, and serotonin, while MAOB degrades DA. This metabolism in the brain can generate high quantities of ROS (Hauptmann et al., 1996), which has been linked to both aging (Maurel et al., 2002), and PD (Kumar et al., 2003). Finally, DLD has been identified as a major producer of both superoxide and H_2O_2 in brain mitochondria, particularly in its participation in the conversion of αKG to succinate in the TCA, tethering ROS production to non-RC metabolic flux (Starkov et al., 2004; Adam-Vizi and Tretter, 2013; Starkov, 2013).

The systems that remove ROS are as complex and multifactorial as those that generate them (Figure 24). They are grouped into three major categories: proteins that don't require reducing equivalents - superoxide dismutases (SOD1/Cu,Zn-SOD and SOD2/MnSOD) and catalase, glutathione (GSH)-dependent proteins, including glutathione reductase (GR), glutathione-S-transferase (GST), and glutathione peroxidases (GPx), and thioredoxins (Trx) and peroxiredoxins (Prx) as the final group (Andreyev et al., 2005, 2015). The latter two groups are dependent on NADPH, produced largely through the PPP. Within the matrix, NADPH reduction requires the activity of either ICDH (NADP-linked) (Jo et al., 2001), MDH (NADP-linked) (Brdiczka and Pette, 1971), or nicotinamide nucleotide transhydrogenase (NNT) (Rydström, 2006; Lopert and Patel, 2014). The interrelationship between these enzymes is schematized in Figure 24. The SODs are the only enzymes in this group that converts the initial ROS species, $O_2^{\bullet-}$, into H_2O_2 (Gardner et al., 1995). Though SOD1 reportedly localizes to the IMS, while SOD2 is found in the matrix, SOD2 appears to be more important for mitochondrial ROS scavenging (Fukui and Zhu, 2010) and its activity is especially high in the brain (Remmen et al., 1999). Interestingly, recent kinetic analyses have suggested that the Trx/Prx system metabolize the bulk of produced ROS in brain mitochondria (Rydström, 2006; Lopert and Patel, 2014). The relevance of this system in the brain has been further supported in the context of neurodegeneration, as Prx3 has been reported to be reduced in AD and PD post mortem (Ruszkiewicz and Albrecht, 2015).

Any discussion of ROS needs to include oxidative stress as a result of the imbalance between ROS production and ROS scavenging. This imbalance can initiate a feedforward cycle, as initial oxidative damage to the mitochondria can cause the generation of additional ROS (Andreyev et al., 2005). While a comprehensive overview of this literature is outside the scope of this chapter, this imbalance has been implicated in nearly every aging-related disease (Cui et al., 2011), including cardiovascular disease (Navab et al., 2011), diabetes (Giacco and Brownlee, 2010), and neurodegeneration (Lin and Beal, 2006). Neurons and the brain are thought to be particularly vulnerable to oxidative stress for a multitude of reasons (Friedman, 2011), where the

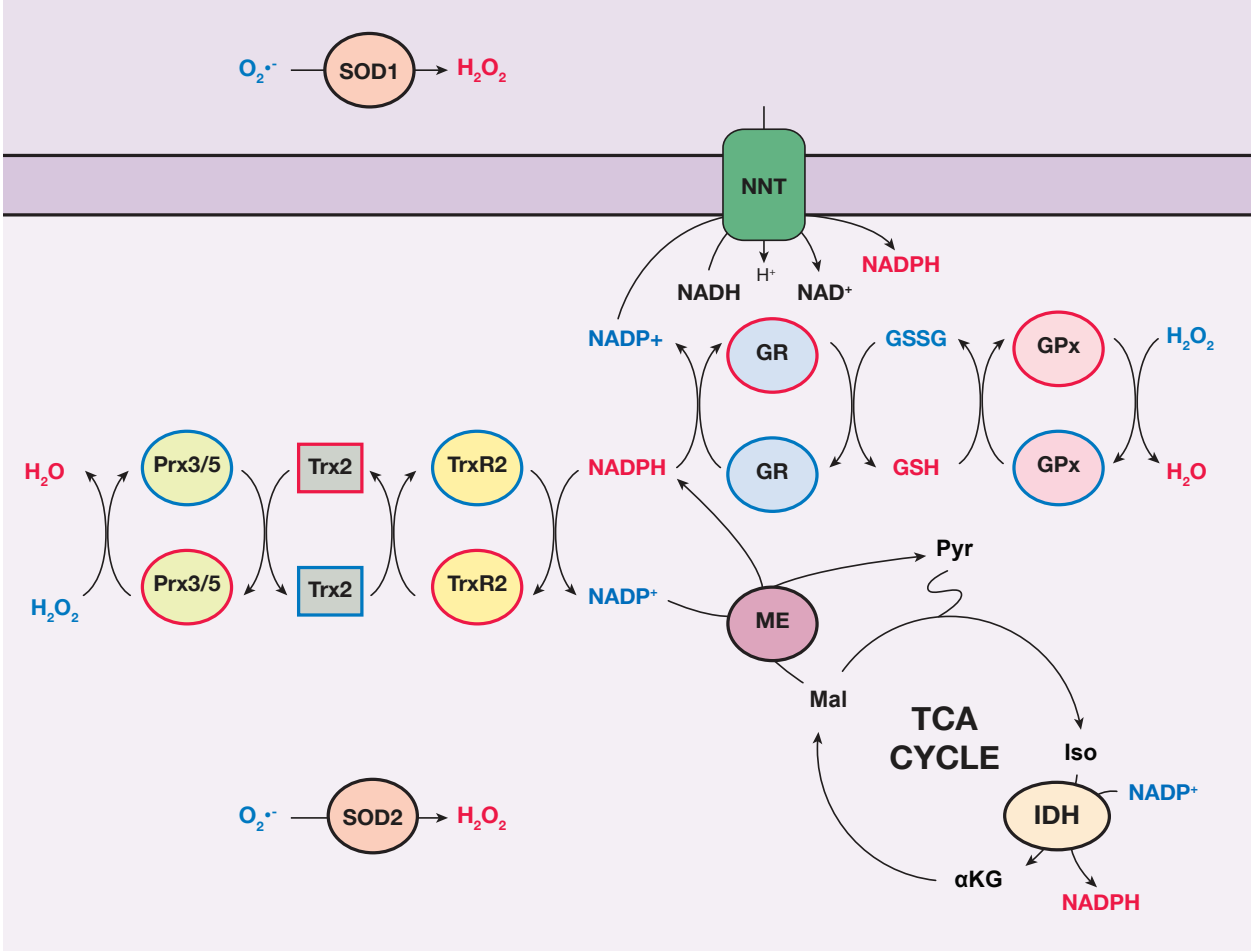

Figure 24. Mitochondrial ROS scavenging enzymes.
Superoxide, produced from any of the ROS sources in Figure 23, is first detoxified into H_2O_2 by cytosolic/IMM SOD1, or matrix SOD2. Subsequently, H_2O_2 is further reduced to H2O by either the GSH or Trx/Prx system. In the GSH branch, GPx reduces H_2O_2, and then returns to its reduced state by oxidizing GSH. GSSG is returned to GSH by GR, which itself must oxidize NADPH to reduce itself. Similarly, Prx3 or Prx5 reduce H_2O_2, which then require Trx2, which requires TrxR2, which requires NADPH to return to reduced states. Red and blue outlines reflect enzyme reduced and oxidized states, respectively. NADPH is intramitochondrially regenerated through NNT, ME, and IDH. SOD, superoxide dismutase; NNT, NAD(P) transhydrogenase; GPx, glutathione peroxidase; GR, glutathione reductase; Prx, peroxiredoxin; Trx, thioredoxin; TrxR, thioredoxin reductase; ME, malic enzyme/malate dehydrogenase; IDH, isocitrate dehydrogenase.

combination of high O2 consumption and high concentration of unsaturated membrane lipids (PUFAs) which are vulnerable to peroxidation make neurons intrinsically vulnerable. In this vein, elevated peroxidated lipids have been found in the plasma of AD patients (Baldeiras et al., 2008), HD patients (Klepac et al., 2007), and in the brains of PD patients (Dexter et al., 1989; Manoharan et al., 2016). These markers point to increased oxidative stress in these disease states, though the causality of oxidative stress in the etiology of these disorders is still contested.

ROS functioning as signaling molecules, rather than non-specific byproducts producing cellular stress, is gaining increased appreciation, though this characterization is in its infancy (Hamanaka and Chandel, 2010; Sena and Chandel, 2012; Holmström and Finkel, 2014; Shadel and Horvath, 2015). In pathways that overlap with canonical intracellular signaling, ROS have oxidize cysteine-cysteine interactions within proteins (Janssen-Heininger et al., 2008; Hamanaka and Chandel, 2010). This disruption inhibits several classes of phosphatase, including PTPs, PTEN, and MAPK phosphatases (Meng et al., 2002; Leslie et al., 2003; Kwon et al., 2004), which may prolong activation of these typically-regulated pathways. Similarly, through the oxidation of methionine, CaMKII is also activated by ROS (Erickson et al., 2008), and ROS stimulates the activity of guanylate cyclase (Dröge, 2002). Collectively, these perturbations in signaling may provide a mechanism for the use of ROS as a second messenger between neurons and glia (Atkins and Sweatt, 1999), and in their interference with the induction of LTP (Hu et al., 2006).

Mitochondria are highly complex signaling organelles, and use many other biomolecules to interact with the nucleus and cytosolic environment, including NAD(P)H, AMP, and metabolites. However, the examples of Ca^{2+} and ROS present avenues for these communication mechanisms, as well as the toxicity that arises when these systems are perturbed.

3.3. Mitochondrial Dysfunction in PD and LID

Though mitochondrial dysfunction has been linked to most neurodegenerative disorders as well as aging itself, PD has the most persuasive and elaborate link to mitochondria. Genetic, environmental, and physiological factors in the disorder have all pointed toward perturbations of mitochondrial function, even though complete definition of a causative mechanism has been elusive in all but the most definitive genetic examples. Despite general acceptance of this connection, fewer associations have been made with the development of LID. This may be attributable in part to the different primary brain regions and pathology associated with PD and

LID – PD involves the degeneration of the SNc, while LID involves maladaptive plasticity in the neurons of the striatum. A preponderance of evidence suggests a unique vulnerability of the SNc (which will be discussed in this section), but the striatum is not immune to pathological perturbations in mitochondrial activity. Several classical mitochondrial disorders cause basal ganglia deterioration and striatal calcification, and HD uniquely causes striatal deterioration despite systemic expression of mutant huntingtin. Further studies are thus warranted to explore the impact of mitochondrial dysfunction in LID, especially at the intersection of known mitochondrial pathologies in PD and known signaling maladaptations in LID.

3.3.1. The Genetics of PD and LID

Mutations in the protein-coding regions of six different genes have been directly associated with autosomal dominant and autosomal recessive forms of PD, and explain about 3-5% of sporadic cases and 30% of familial cases (Klein and Westenberger, 2012). These genes include α-synuclein (PARK1, SNCA), Parkin (PARK2), PINK1 (PARK6), DJ-1 (PARK7), LRRK2 (PARK8), and ATP13A2 (PARK9). Nearly all of these genes relate to mitochondrial function, which will be discussed below.

α-synuclein is the gene most commonly associated with familial PD, as it causes autosomal dominant PD and forms the major component of Lewy Bodies, the protein inclusions that form the hallmark of post-mortem diagnosis of the disorder (Spillantini et al., 1997). Though the question of the neurotoxicity or neuroprotection of these inclusions remains unclear (Quilty et al., 2006; Sidhu et al., 2004), the ability of mutant forms of α-synuclein, which oligomerize and form aggregates, to cause disease, is well-established (Polymeropoulos et al., 1997; Conway et al., 1998). Additionally, this aggregate formation links the pathophysiology of PD to that of AD, wherein aggregates of amyloid β form, pointing to a potential shared mechanism of neurodegeneration (Marsh and Blurton-Jones, 2012). The most common mutation in α-synuclein is the A53T missense mutation (Klein and Schlossmacher, 2006). Though the physiological role

of α-synuclein is still unknown, a number of studies have demonstrated that aggregations of the mutant form interact with mitochondria, causing oxidative stress (Parihar et al., 2008), inhibition of complex I (Chinta et al., 2010), and increased release of cytochrome c (Smith et al., 2005).

The roles of PINK1 and parkin, in contrast, have been robustly established in cell culture models (Narendra et al., 2008, 2010). Though the model continues to be refined, both proteins are implicated in the mitophagy pathway. PINK1, is constitutively imported into the mitochondria through the TOM/TIM complex, where in healthy mitochondria it is cleaved by PARL and released for degradation into the cytosol. However, protein import is dependent on mitochondrial polarization, so when unhealthy mitochondria depolarize (as a result of respiratory deficits, for example), PINK1 import is inhibited and it accumulates on the surface of the mitochondria. This accumulation recruits Parkin, an E3 ubiquitin ligase, which ubiquitinates multiple OMM proteins (Chan and Chan, 2011; Sarraf et al., 2013), targeting them for autophagic degradation (Youle and Narendra, 2010; Pickrell and Youle, 2015). Hundreds of mutations have been identified in Parkin, including both missense SNPs and large deletions, but most affect the ubiquitin like domain and linker structures. In contrast, only about 60 missense or nonsense mutations have been identified in PINK1. Both are associated with autosomal recessive forms of PD (Matsumine et al., 1997; Valente et al., 2001; Klein and Westenberger, 2012).

Leucine-rich repeat kinase 2 (LRRK2) is the most common cause of autosomal dominant forms of PD (Zimprich et al., 2004), and like α-synuclein, its physiological function is unknown. From its protein structure, it may act as a kinase, GTPase, and scaffold, though the more than 50 mutations appear to either increase kinase function or decrease GTPase activity (Nuytemans et al., 2010; Exner et al., 2012). A fraction of LRRK2 endogenously localizes to the OMM (Biskup et al., 2006), but pathological mutations have been reported to induce mitochondrial damage and aggregation (Ramonet et al., 2011), reducing mitochondrial fission through interactions with Drp1 (Wang et al., 2012), and inducing mtDNA damage (Sanders et al., 2014).

DJ-1 causes a rare form of autosomal recessive PD (Abou-Sleiman et al., 2003; Bonifati et al., 2003), though approximately 10 pathogenic mutations have been identified (Klein and Westenberger, 2012). DJ-1 appears to function as a redox sensor, as its cysteine residues are oxidized by ROS (Mitsumoto and Nakagawa, 2001). Though this mechanism is unclear, DJ-1 confers protection against oxidative stress, demonstrated by the increased susceptibility to ROS in knockout or mutant models (Canet-Avilés et al., 2004; Meulener et al., 2005; Dodson and Guo, 2007).

As these mutations account for only a small fraction of sporadic PD cases and a modest percentage of heritable cases (Keller et al., 2012), a number of GWAS analyses have been performed to attempt to identify further risk alleles. A recent meta-analysis of these GWAS studies identified 28 allelic variants at 24 gene loci (Nalls et al., 2014). Of these, two have well-established contributions to PD risk. SNP variations in the enhancer region of α-synuclein are significantly associated with a greater risk of PD (Nalls et al., 2014), but only a very recent study demonstrated that these polymorphisms increase α-synuclein expression (Soldner et al., 2016). The locus for glucocerebrosidase (GBA) was also validated, supporting a large existing body of literature indicating a relationship between mutations in this gene and an increased risk of PD (Goker-Alpan et al., 2003; Sidransky and Lopez, 2012). Homozygous mutations in GBA cause Gaucher's Syndrome, a lysosomal storage disorder, but heterozygous carrier mutations are found in approximately 10 percent of PD cases (Klein and Westenberger, 2012; Sidransky and Lopez, 2012). A recent meta-analysis has also been applied to examine the effect of different environmental factors in PD etiology, though due to a huge heterogeneity in the study populations, only constipation was identified as a risk factor, while physical activity was protective (Bellou et al., 2017). Both of these factors however may be related to the pathogenesis of PD – constipation may be a prodromal symptom of gut dopaminergic neuron degeneration, and patients with developing movement disorders may have reduced physical activity.

In contrast to PD, no large-scale GWAS studies have been performed in LID identifying particular risk loci for LID. As previously discussed, the most commonly attributed factors in LID risk include extent of SNc denervation, younger age of onset, and duration of treatment (Hauser et al., 2006; Jankovic, 2008). Nonetheless, as even animal models have demonstrated differential responses to L-DOPA following lesioning (Valastro et al., 2007; Hurley et al., 2014), it remains clear that additional molecular factors and predispositions are at play. A number of studies have attempted to identify risk genes or SNPs associated with LID, largely based on putative roles in the dopaminergic system. Special attention has been paid, for example, to the DAT (SLC6A3) (Fuke et al., 2001; Kaiser et al., 2003; et al., 2014), D_2R (DRD2) (Oliveri et al., 2000; Rieck et al., 2012), D_3R (DRD3) (Lee et al., 2011; Comi et al., 2017), and DA metabolism through COMT and MAOB (Białecka et al., 2004; Bialecka et al., 2008). Of these studies, one of the only SNPs verified to decrease latency to LID (i.e., increase risk of developing LID) is the rs6280 25G>A SNP in DRD3, which was confirmed in two ethnically distinct populations (Lee et al., 2011; Comi et al., 2017). Particularly when contrasted with PD itself, this field is still in its infancy, and more large-scale analyses may be informative to help disambiguate between PD patients at higher risk for dyskinesia.

3.3.2. The Contribution of Mitochondrial Dysfunction to Nigral Degeneration in Idiopathic PD

One of the enduring questions of PD is the specificity of neuronal degeneration – why do the DAergic neurons of the SNc preferentially degenerate in contrast to other neurons? The development of Lewy bodies, the hallmark post-mortem feature of PD, is not constrained to the SNc. Lewy bodies proliferate through a range of deep brain nuclei, in neurons of different neurotransmitter types, including the serotonergic raphe nucleus, the noradrenergic locus coeruleus, the cholinergic nucleus basalis of Meynert, the histaminergic tuberomammillary nucleus, and even the dopaminergic retrorubral field (Braak et al., 2002; Jellinger, 2012; Zampese

et al., 2017). In early stages of PD, Lewy bodies are also frequently found in neurons of the olfactory bulb, myenteric and submucosal plexuses, and the dorsal motor nucleus of the vagus, which innervates the enteric nuclei (Wakabayashi et al., 1989; Braak et al., 2006; Olanow and Brundin, 2013). This wide distribution of Lewy bodies suggests that α-synuclein may propagate across neuron types analogously to prions, and the ability of mutant or overexpressed α-synuclein to cross neuron barriers has been demonstrated in multiple mouse models (Luk et al., 2012; Masuda-Suzukake et al., 2013). Interestingly, these studies showed contradictory relationships between the appearance of Lewy bodies and motor deficits, and in combination with the presence of Lewy bodies in largely unaffected brain regions, highlights the tenuous connection between the appearance of Lewy bodies and neuronal death. DA and its metabolites have also been proposed to be neurotoxic (Bisaglia et al., 2014), but there is a noted lack of degeneration in other dopaminergic brain regions (Hirsch et al., 1988), and L-DOPA treatment, which increases DA concentration, does not accelerate disease progression (Oertel and Schulz, 2016). Consequently, two of the hallmark features of the SNc in PD do not appear to significantly contribute to SNc neurodegeneration.

Recent focus has shifted to the architecture of SNc neurons to explain their unique vulnerability. SNc dopaminergic neurons have an especially large and densely branched axonal arbor (Matsuda et al., 2009), with nigrostriatal axon projections comprising up to 6% of striatal volume. In the rat brain, each SNc dopaminergic neuron is projected to make somewhere between 100-200,000 synapses, though in the human this may be closer to 1-2 million (Bolam and Pissadaki, 2012). This number is approximately two orders of magnitude higher than the other neuron types of the basal ganglia, and differentiated from the other dopaminergic neurons of the ventral tegmental area (VTA), which are projected to have one order of magnitude fewer synapses (Bolam and Pissadaki, 2012). This densely branched network presents two large burdens on the function of these neurons – first, the large number of release sites requires a large amount of cellular energy to maintain vesicle packing, release, and reuptake (Wellstead and

Cloutier, 2011), as well as action potential propagation (Pissadaki and Bolam, 2013). Secondly, synaptic homeostasis of this large number of sites requires continuous trafficking (anterograde and retrograde) of metabolites, proteins, and organelles, which is physically constrained by the single axon supplying the entire arbor and may be preferentially affected by disruptions in the function of α-synuclein or LRRK2 (Hunn et al., 2015).

SNc dopaminergic neurons are also electrically unique, exhibiting both tonic pacemaker activity as well as burst firing. Pacemaker firing is mediated largely through L-type Ca^{2+} channels, and SNc neurons have a uniquely high expression of $Ca_V1.3$ channels (Chan et al., 2007). These channels open at a comparatively hyperpolarized $\Delta\psi$ (Puopolo et al., 2007; Guzman et al., 2009), indicating a high metabolic burden of continuous Ca^{2+} influx. Phasic burst firing is highly regulated in the SNc neurons, mediated by K_{ATP} channels (Schiemann et al., 2012), Ca^{2+}-activated SK3 K^+ channels (Stocker, 2004), and NMDAR activation (Deister et al., 2009). Maintenance of the activity of these channels is imperative for SNc neuronal function, as reduction in firing precedes neuron degeneration (Roselli and Caroni, 2015). These combined firing mechanisms increase the cytosolic Ca^{2+} concentration, which is poorly buffered in SNc neurons (Foehring et al., 2009).

Together, the unique architectural and electrophysiological properties of the DAergic neurons of the SNc are highly energetically demanding. Though DA-mediated oxidative stress and the accumulation of α-synuclein aggregates likely contribute to neuronal dysfunction, increasing evidence suggests that SNc vulnerability is a disorder of energy metabolism and compromised mitochondria (Wellstead and Cloutier, 2011; Zampese et al., 2017). Supported by the association of familial and environmental causes of PD with mitochondrial dysfunction, these recently-described characteristics of SNc neurons have helped refine the hypothesis of the mitochondrial contribution to the etiology of PD.

3.3.3. Mitochondrial Dysfunction in LID

The role of mitochondrial dysfunction in the etiology of LID has been less comprehensively explored. As previously discussed, numerous alterations in the signaling pathways and structure of MSNs during both DA denervation and LID induction have been characterized (section 1.4). While these studies have identified a number of molecular changes that seem to contribute to the development of LID, it remains unclear what factors differentiate dyskinetic and non-dyskinetic PD patients, or animals that develop AIMs in response to L-DOPA from those that do not.

Several studies have attempted to address this discrepancy using transcriptomic and proteomic analyses of rat and non-human primate models of LID. In these models, dopaminergic nigral neurons are ablated through the use of 6-OHDA or MPTP, L-DOPA is given, and then animals are separated into groups depending on their response. A transcriptomic analysis of a rat model (Konradi et al., 2004) identified increases in genes relating to Ca^{2+} signaling and homeostasis, glutamatergic activity, MSN activity, as well as an increased expression of the D_1 receptor and ppt, supporting hypotheses about signaling deregulation and hyperactivation of the D_1 pathway. However, this study also documented deregulations in gene programs involved in energy production. For example, two of the gene families upregulated in Ca^{2+} homeostasis, the sarco/endoplasmic reticulum Ca^{2+}-ATPase (SERCA) and plasma membrane Ca^{2+} ATPase (PMCA) Ca^{2+} pumps, are also ATPases. This suggests possible excess intracellular Ca^{2+}, as well as increased cellular ATP consumption. Combined with increased expression of the Na^{+}/K^{+}-ATPase, which other studies have demonstrated consumes a large percentage of neuronal mitochondrial ATP, this pointed to large increases in energy demand in the rats presenting with LID. Further, this study (Konradi et al., 2004) identified significant reductions in the expression of two enzymes in the PCr shuttle – GAMT and mtCK, suggesting disruption of ATP distribution. Though these mechanisms have not been fully elucidated, the CK system may be particularly important for the function of the MSNs of the striatum. A recent study (Schlattner et al., 2016) demonstrated that MSNs had high expression of both mtCK and BCK, in contrast to other brain

regions where these enzymes are segregated between astrocytes and neurons (see section 2.2.4).

A follow-up study used a proteomic screen on the same rat model of LID to further probe these changes (Valastro et al., 2007). This study used 2D protein gels followed by LC/MS/MS quantification to identify differentially expressed proteins, and following this two-step screening process, five proteins were found. Among these was GAMT, which was expressed in dyskinetic animals at about 80% the level of non-dyskinetic animals. Interestingly, γ-enolase (occasionally referred to as neuron-specific enolase, though its expression has been observed in astrocytes (Deloulme et al., 1997; Vizin and Kos, 2015)), which catalyzes the penultimate step in glycolysis, was increased, suggesting an increase in glycolytic flux. Together, these two protein alterations further support perturbations in energy metabolism in dyskinetic animals, which were supported by the broader range of proteins identified through the initial 2D gel process. In this first step, 67 proteins were identified, including B-CK, which was downregulated. In this wider protein cluster, additional changes in proteins regulating synaptic plasticity, oxidative stress, and protein degradation were observed, supporting the trend observed in the transcriptomic screen.

A recent proteomic study using an MPTP-based model of LID in marmosets (Hurley et al., 2014), grouped animals into high and low dyskinesia responses to L-DOPA. This study also observed perturbations in energy metabolism in the high dyskinesia group through increased expression of five different proteins. Lactate dehydrogenase (which catalyzes the conversion of pyruvate to lactate) was the most dramatically increased protein in the entire screen, but the study also reported increases in malate dehydrogenase, dimethyladenosine transferase, and MnSOD. However, the authors of this study largely dismissed these observations as being related to dyskinesia pathogenesis, suggesting they were likely attributable to the increased energetic requirements of the dyskinetic movements themselves.

Gene expression analysis of PD patients has also implicated mitochondrial dysfunction as a significant factor differentiating dyskinetic and non-dyskinetic groups. In a study comparing the

post-mortem putamen of control subjects, dyskinetic PD and non-dyskinetic PD patients, mtDNA quantity and integrity was significantly different between dyskinetic PD patients and the other two groups (Naydenov et al., 2010). In this study, mtDNA copy number in the putamen was reduced by about 50% in the dyskinetic PD group, while no changes were observed in the cerebellum, an area largely unaffected by PD. Additionally, an increased number of mtDNA deletions were specifically observed in the dyskinetic PD group. Further transcriptomic analysis of this patient population (Naydenov et al., 2010) revealed reductions in the expression of nuclear-encoded mitochondrial RC subunits, significantly affecting Complex I, III, IV, and V. In these cases, significant reductions were frequently observed in non-dyskinetic PD patients as well, but the magnitude of reduction in dyskinetic PD patients relative to controls was greater. Additionally, this analysis identified increases in the expression of genes in the ion channel, signal transduction, and apoptosis families in the dyskinetic PD group, further supporting earlier findings in animal models.

Though MSNs are highly dissimilar to SNc neurons, there may be some overlap in the phenomena preceding dysfunction/degeneration. For example, while pacemaking activity, involving heightened/continued influx and efflux of Ca^{2+}, produces an increased mitochondrial burden to re-establish $\Delta\psi$, non-physiologic waves of DA resulting from L-DOPA may also create a large energetic burden due to the continual upregulation and downregulation of signaling cascades and ion channel trafficking. The continued supersensitization of the direct pathway and dMSNs over the progression of LID likely also increases energetic demand in the striatum. Understanding the contribution of mitochondrial function and dysfunction to LID may help characterize factors that make PD patients more vulnerable to developing LID.

RIGHTS AND PERMISSIONS

Some of the material in this chapter has been previously published, and has been reproduced here with permission.

Figure 2: Appears as Figure 1 in:

> *Jankovic J (2005) Motor fluctuations and dyskinesias in Parkinson's disease: Clinical manifestations. Mov Disord 20 Suppl 11:S11–6.*

Publisher: John Wiley and Sons; License Number: 4127711278809

Figure 4 and 5: Appears as Figure 2 in:

> *Jenner P (2008) Molecular mechanisms of L-DOPA-induced dyskinesia. Nat Rev Neurosci 9:665–677.*

Publisher: Nature Publishing Group; License Number: 4127720324081

Figure 9: Appears as Figure 8 in:

> *Warren EB, Sillivan SE, Konradi C (2017) Receptors and Second Messengers in the Basal Ganglia. In: Handbook of Basal Ganglia Structure and Function, 2nd ed. (Steiner H, Tseng KY, eds), pp 555–581 Handbook of Behavioral Neuroscience. Academic Press.*

Publisher: Academic Press, Elsevier; License Number: 4282540136143

Figure 14A and 21: Appears as Figure 1 in:

> *Schon E, DiMauro S, Hirano M (2012) Human mitochondrial DNA: roles of inherited and somatic mutations. Nat Rev Genet 13:878–890.*

Publisher: Nature Publishing Group; License Number: 4127781491739

Figure 17 and Table 1: Appears as Figure 1 and Table 1 in:

> *Palmieri F (2013) The mitochondrial transporter family SLC25: Identification, properties and physiopathology. Mol Aspects Med 34:465–484.*

Publisher: Elsevier; License Number: 4130381454595

Some of the text in **Chapter 1.3, Molecular physiology of the SNc and Striatum**, appears in:

> *Warren EB, Sillivan SE, Konradi C (2017) Receptors and Second Messengers in the Basal Ganglia. In: Handbook of Basal Ganglia Structure and Function, 2nd ed. (Steiner H, Tseng KY, eds), pp 555–581 Handbook of Behavioral Neuroscience. Academic Press.*

Publisher: Academic Press, Elsevier; License Number: 4282540136143

CHAPTER II

MATERIALS AND METHODS

1. Primary murine striatal cultures

All animal experiments were conducted under institutional guidelines and were approved by the Institutional Animal Care and Use Committee of Vanderbilt University.

1.1. Mouse Experiments

Breeding pairs of C57/B6 mice (Jackson Labs, Bar Harbor, ME) were housed in the Vanderbilt Animal Facilities. P0 C57/B6 mouse pups were collected for these experiments. Pups were decapitated, brain isolated, midbrain structures discarded, and median ganglionic eminences (MGEs), the striatal precursor, were removed for striatal neuron-enriched cocultures (NECos). Dissected tissue was glass-pipette homogenized and suspended in plating media. NECos were seeded using .5 dissected striata/mL media. Mouse preparations were plated assuming a fixed 'number-of-striata' to 'number-of-plate' density. Cells were plated into tissue culture plates previously coated with consecutive solutions of 0.5% PEI and 2.5% FBS.

Mouse NECo cultures were grown in 3:1 DMEM:F12 supplemented with 1 x B27, penicillin (100 U/ml)/streptomycin (100 µg/ml), 2.5 mM pyruvate, and 42mM glucose. Cultures were harvested 7 days after plating.

1.2. Rat Experiments

Striata (for neuronal cultures and NECos or cortices (for glial cultures) were dissected from E18 Sprague-Dawley rat fetuses (Charles River Laboratories, Raleigh, NC), as described previously (Rajadhyaksha et al., 1999) with minor modifications. Pregnant rat dams were anaesthetized with a lethal dose of pentobarbital, 130mg/kg, and the uterus and pups removed. Fetal pups were decapitated, brain isolated, midbrain structures discarded, and MGEs were

removed for either NECo or neuronal cultures. Subsequently, the dura was removed from the remaining cortices, along with non-cortical structures (e.g. the hippocampus), and cortices were segregated for glial cultures.

After mechanical dissociation in HBSS/5mM HEPES, preparations were monitored for viability and cell number by diluting a small number of cell suspension with 4% Trypan Blue (Fisher). Cells were plated into tissue culture plates previously coated with consecutive solutions of 0.5% PEI and 2.5% FBS. NECos and neuronal cultures were grown in 3:1 DMEM:F12 supplemented with 1 x B27, penicillin (100 U/ml)/streptomycin (100 µg/ml), 2.5 mM pyruvate, and 2.5 mM glucose, which approximates physiological CNS glucose concentrations (Silver and Erecińska, 1994; Kleman et al., 2008), glucose concentration was measured daily, using an ABTS-HRP (both, Sigma) colorimetric assay, and maintained at 2.5 mM, and cell viability was carefully monitored. Representative traces of media glucose concentrations for each culture condition (when initial glucose was 2.5mM) are shown in Supplemental Figure 1 (Chapter V).

1.2.1. Cell-type specific seeding conditions

NECos were seeded at $1.3*10^5$ cells/cm^2, and at $3.8*10^5$ cells/cm^2 for Seahorse experiments, unless otherwise indicated. Neurons were seeded at $1.6*10^5$ cells/cm^2 and at $4.7*10^5$ cells/cm^2 for Seahorse experiments. To inhibit glial growth in neuronal cultures, 5 µM cytosine arabinoside (AraC) was added on DIV2 for 24 hours. Experiments with NECos and neurons concluded on DIV7.

Glia media contained 10% FBS instead of B27 to promote glia proliferation. Cells were plated at $1.3*10^5$ cells/cm^2 and grown to confluence (DIV6-10). Media was replaced every two days. Once confluent, glia were re-seeded at $3.25*10^4$ cells/cm^2 and at $9.4*10^4$ cells/cm^2 for Seahorse experiments. Glia were assayed 5 days after re-seeding, unless otherwise indicated. Ethidium bromide (EtBr) (1% solution, 10 mg/mL) was added to cultures as indicated in each

experiment. All cell culture materials were purchased from Thermo Fisher Scientific (Waltham, MA). Cr for neuronal supplementation was purchased from Sigma-Aldrich (St. Louis, MO).

Glial fibrillary acidic protein (GFAP) (1:750, Abcam, Cambridge, MA) immunostaining showed that glia cultures were >90% astrocytic, and β3-tubulin (1:1000, Cell Signaling Techology (CST), Cambridge, MA) immunostaining confirmed that neuronal cultures were >95% pure. NECos were approximately 75% neuronal and 25% glial in rat cultures, and approximately 67% neuronal and 33% glial in mouse cultures. A minimum of two dissections was performed for each experiment, unless otherwise noted.

2. Mammalian cell culture

Neuroblastoma 2a (N2a) cells (courtesy of the Eugenia Gurevich Lab, Vanderbilt University) or STHdh$^{Q7/Q7}$ cells (courtesy of the Aaron Bowman Lab, Vanderbilt University Medical Center) were seeded at 1*10^5/mL, and passaged at 80% confluence. Cells were grown in DMEM with 4mM glutamine, 10% FBS, penicillin (100 U/ml)/streptomycin (100 µg/ml), and 25mM glucose (or galactose, as indicated). N2a cells were grown at 37˚C, STHdh$^{Q7/Q7}$ cells were grown at 33˚C, due to a temperature-sensitive large-T antigen that was used to generate the line (Trettel et al., 2000).

3. Polg shRNA

Clone name	Sequence
POLG1	CCGGCGGACCTTATAATGATGTGAACTCGAGTTCACATCATTATAAGGTCCGTTTTTG
POLG2	CCGGTCTCAGGAGAGAGGTACAAAGCTCGAGCTTTGTACCTCTCTCCTGAGATTTTTG
POLG3	CCGGGTTGTCCAGGGAGAGTTTATACTCGAGTATAAACTCTCCCTGGACAACTTTTTG
POLG4	CCGGCCATGTCTGATACACCACGTACTCGAGTACGTGGTGTATCAGACATGGTTTTTG

Table 2. Anti-POLG shRNA sequences.
Sequences of four shRNA constructs against POLG; subsequently inserted into lentiviruses. Constructs designed and synthesized through the MISSION system.

N2as cells or STHdh$^{Q7/Q7}$ cells were infected with lentiviruses carrying shRNAs directed against Polg, or carrying a non-mammalian targeted (NMT) shRNA, plasmid-backbone matched,

(MISSION system, Sigma) for 24 hours, and then media was changed. Cell lines were incubated with 1.6μg/mL puromycin to eliminate uninfected cells. Resistant cells were assumed to be stably transfected.

4. Determination of mtDNA and mtRNA levels

DNA was extracted using the DNeasy kit (Qiagen, Valencia, CA). qPCR analysis was carried out with 20 ng of DNA with SYBR green I for detection of product. For culture experiments, three mitochondrial DNA (mtDNA) primer pairs were used for mtDNA analysis, and three nuclear DNA (nDNA) primer pairs for reference genes; for human experiments, six mitochondrial primer pairs and two reference genes were used, as previously described (Naydenov et al., 2010). As no difference was observed in the levels or pattern of the mtDNA primer pair products, they were combined for the analysis and normalized to the nDNA primer pair products as described (Hellemans et al., 2007).

RNA was extracted from human tissue samples with the RNeasy kit (Qiagen) after rotor-stator homogenization. Complementary DNA (cDNA) synthesis was carried out with 150 ng total RNA using the SuperScript IV cDNA synthesis kit and random hexamers (Thermo Fisher Scientific). Rat samples were harvested in RNeasy lysis buffer and extracted according to protocol. 150 ng of total RNA was used in the iScript cDNA synthesis kit (Bio-Rad, Hercules, CA). The KAPA SYBR FAST master mix (KAPA Biosystems, Wilmington, MA) was used for the PCR reaction.

All qPCR reactions were performed using a Strategene MX3000 or MX3005p (Agilent, Santa Clara, CA), and a meltcurve analysis from 55°C to 90°C was performed after the last PCR cycle. Standard curves with four 1:4 serial dilutions were run for each primer pair to determine its efficiency. The highest and lowest dilutions of the standard curve plus a non- template control and a no reverse transcriptase control were examined on a 3% agarose gel to verify product size and primer specificity. A minimum of two reference genes was used for normalization of RNA

measurements. These genes were selected as stable references following BestKeeper analysis (Pfaffl et al., 2004). Efficiency-corrected log2 fold changes were calculated as described (Hellemans et al., 2007).

Mouse Primers:	Sequence
mtCo1 F	CCCACCTCTAGCCGGAAATC
mtCo1 R	GGCTGGGGGTTTCATGTTGA
mtCytb F	TGCATACGCCATTCTACGCT
mtCytb R	TACTGGTTGGCCCCCAATTC
mtND1 F	GGCCCATTCGCGTTATTCTT
mtND1 R	AGCGTGGATAAGATGCTCGG
mtND2 F	ATAAAACTAGGCCTCGCCCC
mtND2 R	AGTCCTCCTCATGCCCCTAT
nDNA F	ACCTGCTACAGTTTCCCTGC
nDNA R	TTCCTAGTCCGGTGTTTGCC
Polg F	CTGACCTAATCCCTTTGGGGG
Polg R	CTTGTGCTTTCCCTGCTTGG
cFos F	GGCTTTCCCCAAACTTCGAC
cFos R	GATCTGCGCAAAAGTCCTGT
Egr1 F	ACAACCCTATGAGCACCTGA
Egr1 R	GAGGTCGGAGGATTGGTCAT
Arc F	CTGAGTCCTCACACCCAGC
Arc R	TTGGAACCCATGTAGGCAGC
Actb F	CCTGTGCTGCTCACCGAGGC
Actb R	GCACAGTGTGGGTGACCCCG
Dnm1l F	GCCTCAGATCGTCGTAGTGG
Dnm1l R	GAGTTTTTCCATGTGGCAGGG
Fis1 F	AGGGTTACAGTGTTGCGTGT
Fis1 R	CCAGGCACCAGGCATATTCA
Opa1 F	GAAGTTTCTGAGGCCCTTCTCT
Opa1 R	GCGCTCCAAGATCCTCTGAT
Mfn1 F	CCTCCTCTCCGCCTTTAACT
Mfn1 R	GCACAAAGTGCTTCAGTGGA
Mfn2 F	TATCCACTTCCCTCCTCCCG
Mfn2 R	GAGATCTTCACAGGGTAGGCA

Rat	Sequence
mtCo1 F	AGGAGCAGTATTCGCCATCA
mtCo1 R	CGACGAGGTATCCCTGCTAA
mtCytb F	CGCCCCATCTAACATCTCAT
mtCytb R	GTCCCACATGGAGGAATAGG
mtND1 F	CCTCACCCCCTTATCAACCT
mtND1 R	GGAGCCGCTTATTAGGAGGA
mtATP6 F	CACACCAAAAGGACGAACCTGA
mtATP6 R	CTGCTCATAGGGGGATGGCT
Tuba1a F	ACCAAGCGTACCATCCAGTT
Tuba1a R	CCACGTACCAGTGCACAAAG
Crh F	GCTAACTTTTTCCGCGTGTT
Crh R	GGTGGAAGGTGAGATCCAGA
Pdyn F	GCAGGAAGCCCCCATAGC
Pdyn R	CGCAAATACCCCAAGAGGAG
mtCK F	GAATGAGGAGGACCACACACG
mtCK R	CAGTGCCCAGGTTAGATGGAC
B-CK F	AACAGCCACAACACGCAGAA
B-CK R	TCGTAACTCTCCTCGTCGCC
Canx F	TGACCCCTCCGGTAAACCCT
Canx R	CCTCCCATTCTCCGTCCATATCC
18S F	TGGCTCAGCGTGTGCCTACC
18S R	TAGTAGCGACGGGCGGTGTG
cFos F	CGGCAGAAGGGGCAAAGTAGA
cFos R	ATCTTGCAGGCAGGTCGGTG
Egr1 F	GAGCGAACAACCCTACGAGCA
Egr1 R	AGGCCACTGACTAGGCTGAAAAG
Dnm1l F	AGAATATTCAAGACAGCGTCCCAAAG
Dnm1l R	CGCTGTGCCATGTCCTCGGATTC
Fis1 F	TTTGAATACGCCTGGTGCCT
Fis1 R	CTGTAACAGTCCCCGCACAT
Mff F	AACTGTCCATTCTGGCGAACA
Mff R	AACCTCTGGCGCTGAAAACA
Opa1 F	TCCTCCTTCACAGCCTCCTT
Opa1 R	CGAGAACATCTACCTCCCAGC
Mfn1 F	GATAAAGTCCTCCCCAGCGG
Mfn1 R	GGGCCAAAATACGTGCACAA

Mfn2 F	GGACTTTCACCCATCCCCAG
Mfn2 R	GATTCCGCACAGACACAGGA
Actb F	TACCCCATTGAACACGGCAT
Actb R	GCATACAGGGACAACACAGC

Human Primers:	Sequence
mtCK F	ACATCAAACTGCCCCTGCTA
mtCK R	ATCAAAGACACCGCCTGTAG
B-CK F	CGGTATCTGGCACAATGACA
B-CK R	ATGGGCAGGTGAGGATGTAG
Canx F	ACTTGTGTTGATGTCTCGGGC
Canx R	CGTTTTGGGGTTTTTGTGTCGG
Itm2b F	CATTGTTATGCCACCCAGAA
Itm2b R	GCAGTTTGTAAGTTTCCTTGTCA

Table 3. Primer Sequences.
Mouse, rat, and human primer sequences for all qPCR experiments.

5. Western Blots and ICW

12 well tissue culture plates (Corning, Corning, NY) were used for all Western Blot experiments. 100µL of Laemmli buffer per well was used to harvest each sample. Samples were warmed to 70˚C before SDS-PAGE separation on 10-20% Tris-Glycine gels (Thermo Fisher Scientific, Waltham, MA), and blotting onto polyvinylidenedifluoride (PVDF) membrane (Perkin-Elmer, Waltham, MA) was conducted using XCell II blot modules (Thermo). Primary antibodies used were used 1:1000 dilutions included phospho-p44/42, p44/42, Acetyl-Histone H4 (Lys8), Acetyl-Histone H3 (Lys9), Histone H3 (Lys14), Histone H3 (Lys18), Histone H3 (Lys27), Histone H3 (CST). β-Actin and β-Tubulin were used as controls at 1:5000. HRP-conjugated secondary antibodies (CST) were used at 1:5000, and blots were exposed to a luminescence reagent (Thermo) and imaged using a Kodak Image Station 440 CL. 680 or 800-fluorophore-conjugated secondary antibodies (LI-COR, Lincoln, NE) were used at 1:10000, and imaged using an Odyssey CLx imager (LI-COR).

96-well black walled, clear bottom plates (Corning) were used for in-cell western (ICW) experiments. Plates were prepared according to CST protocol. Phospho-p44/42 (1:200), p44/42 (1:400) (CST), and β-tubulin (1:1000) (Sigma) were used as primary antibodies, 680 or 800-fluorophore-conjugated secondary antibodies (LI-COR) were used at 1:10000, and imaged using an Odyssey CLx imager (LI-COR).

6. Mitochondrial Morphology Experiments

Following 7 days of culture in a 96 well plate, rat NECo cultures were treated with 150nM Mitotracker Red CMX-ROS (Thermo) for 15 minutes, then fixed with 10% formalin. Cultures were stained with GFAP (1:750, Abcam, Cambridge, MA), β3-tubulin (1:1000, CST, Cambridge, MA), and DAPI (1:2000, Thermo). Images were taken using an EVOS FL microscope, with two pictures per well. From each image, every identifiable glia was outlined and cropped for distinct analysis in FIJI (FIJI Is Just Image J, (Schindelin et al., 2012)). For each glia, mitochondrial segmentation was performed using Squassh (Rizk et al., 2014), which calculated object area, length, and coordinates. Nuclear coordinates were further calculated in FIJI and were used to calculate mitochondrial distance from the nucleus.

7. Seahorse Experiments

The Seahorse XF^{e}96 bioanalyzer was used to conduct all experiments (Agilent). One hour before the start of the assay, media was replaced with XF Base Media (Agilent) supplemented with 2.5 mM glucose, 2 mM glutamine, and 1 mM pyruvate. The MitoStress Test program was used for the recordings of three mix and measure cycles following each drug addition. 1 μM of oligomycin, FCCP, rotenone and antimycin were determined to be the most effective concentration for all cell types. Following the experiments, cells were fixed with 10% formalin and Hoechst (1:2000, Thermo) stained for cell counting. Cells were counted using the MetaXpress imager (Molecular Devices, Sunnyvale, CA) with automated software. Each OCR measurement was normalized to cell number.

8. NADH Experiments

Relative NADH was quantified using an MTS assay (Cell Titer 96 Aqueous One Solution Cell Proliferation Assay, Promega, Madison, WI), which measures the transfer of electrons to a tetrazolium compound. The MTS assay data were comparable to data from a NAD^+/NADH Assay (NADH-Glo, Promega), (Supplemental Figure 3, Chapter V). Assays were incubated for an average of 2 hours. After the assay was completed, cells were fixed, Hoechst stained, and counted as described above.

9. ADP/ATP Experiments

Total ATP quantities were determined using a luminescence-based viability assay (Cell Titre Glo, Promega) Relative ADP and ATP quantities were determined with an ADP/ATP assay (Biochain, Newark, CA) and data normalized to average cell number per treatment per experiment.

10. ^{1}H NMR

Samples were prepared as described (Tyagi et al., 1996) with minor modifications. Cultures were grown in 100 mm plates, rinsed 3 times with ice-cold saline, and harvested in 4 mL MeOH at -80˚C. Samples were homogenized with an ultrasonicator, and 4 mL ice cold chloroform and 4 mL ice cold H2O were added. The samples were vortexed for 30 seconds and centrifuged for 1 hour at 3600 rpm and 4˚C. The supernatant was transferred to a new tube with a small amount Chelex-100 and Fluka pH indicator (Sigma-Aldrich), vortexed for 30 seconds, and centrifuged for 15 minutes at 3600 rpm and 4˚C. The supernatant was vacuufuged and reconstituted in 200 µL 5 mM $Na_{(2)}H_{(2)}PO_4$ (Sigma-Aldrich) in D_2O (99.9%, Cambridge Isotope Labs, Andover, MA) containing 0.25 mM sodium trimethylsilyl propionate-d_4 (TMSP, 98%, Cambridge Isotope Labs), pH corrected, and transferred to a 3 mm NMR tube (Bruker BioSpin, Rheinstetten, Germany).

^{1}H NMR spectra were recorded using a Bruker AVANCE III 600 MHz spectrometer equipped with a 5 mm CPQCI cryoprobe (Bruker), at 298K. A water signal presaturation sequence (zgpr) was used, with the following acquisition parameters: 256 scans, 64k data points, 14 ppm spectral width, 4s acquisition time, 6s relaxation delay. An independent inversion-relaxation T1 experiment was performed using Cr, PCr, ATP, ADP, and TMSP standards to calculate an appropriate relaxation delay. For PCr, we calculated a T1 relaxation of 1.3s at the 3.0 ppm peak. For Cr, T1 was 1.9s at the 3.0 ppm peak. ATP and ADP overlap in the ^{1}H spectrum, and the T1 at their 8.54 ppm peak was 316ms. 6s was determined to be a sufficient relaxation delay. The relaxation time of TMSP was 3.27s. Because the difference in amplitude between a 20s and 6s relaxation was 6%, this was applied as a scaling factor to concentration calculations.

Spectra were processed using Topspin software (v3.5, Bruker) with automatic apodization and line broadening (0.3Hz), and manual reference, phase, and baseline correction. Peaks were identified and assigned using Chenomix (v8.2) and cross-referenced against the Human Metabolomic Database (hmdb.ca). Peak fitting and deconvolution were performed using ACD/SpecManager (v12, Advanced Chemistry Development, Toronto, Canada). Concentrations were calculated using peak areas by reference to TMSP. Cell number was extrapolated from seeding density and aggregated cell counting data from similar experiments. Final metabolite concentrations are expressed as nmol/10^{7} cells.

11. Post mortem samples

Human putamen samples were collected at the Harvard Brain Tissue Resource Center at McLean Hospital, Harvard Medical School, Belmont, MA (HBTRC; http://www.brainbank.mclean.org), as previously described (Naydenov et al., 2010). Analysis was carried out in the putamen of 12 control individuals, 10 individuals with PD and LID, and 10 individuals with PD without LID, all of whom were male.

All medical records were carefully examined for any symptoms attributable to LID, under observation of all HIPAA and IRB guidelines. Medical records were scanned for clinical symptoms such as 'dyskinesia', 'chorea', 'wearing off', 'on-off periods' and prescription of Comtan (entacapone) or Tasmar (tolcapone), and recorded together with information on medications, signs of PD, L-DOPA prescription records, neuropathological findings, signs of dementia and cause of death. From the prescription records the total amount of L-DOPA administered over the entire treatment period divided by the prescription years is given as L- DOPA exposure per year. Exclusion criteria included incomplete medical records, exposure to environmental toxins and use of respiratory devices before death. Investigators were blinded to the diagnosis (Naydenov et al., 2010).

Diagnosis	n	Age	PMI	Years diagnosed	Fresh brain weight (g)	Treatment duration (y)	Average levodopa per year (g)	SN-pigmentation (pallor)(1)	SN-cell loss(2)
control	12	74.7±3.6	16.6±4.4		1304.6±138.6				
dys	10	76.5±7.5	12.2±6.9	11.8±4.6	1300.6±59.8	7.9±5.3	174.7±74.8	3.3±0.7	2.7±0.3
nondys	10	75.5±2.3	16.1±5.9	8.0±3.1	1370.8±178.4	5.1±2.8	169.1±72	2.8±0.7	2.5±0.8

(1) Scale from 0-4
(2) Scale from 0-3
All samples male

Dys, Dyskinetic PD patients
Nondys, Nondyskinetic PD patients

Table 4. Patient Demographics.
Demographics of human patient samples used for RNA analysis. Dys, PD-diagnosed patients with LID; nondys, PD-diagnosed patients without LID. Patient groups were matched for age, PMI, treatment duration, and average L-DOPA.

12. Statistical Analysis

All statistical analyses were conducted in R (cran.r-project.org). Relevant tests used are mentioned in text. A difference in mean was considered statistically significant when $p < 0.05$.

CHAPTER III

ESTABLISHING AND EVALUATING MTDNA REDUCTION

1. Abstract

The appreciation for mitochondrial dysfunction in neurodegenerative disorders continues to grow. While the role of many biophysiological deficits has been characterized, the contribution of differences in mtDNA to neuronal dysfunction has been underexplored. Here, we assessed different approaches to model reduced mtDNA in the striatum. We attempted to knock down *Polg* expression using stable shRNA expression, but observed that the achieved degree of mtDNA depletion was unstable. In contrast, we observed that EtBr treatment of primary striatal cultures may be one of the most efficient and reproducible methods of modeling mtDNA reduction in neurons. We also confirm previous observations that in cell lines, mitochondrial toxin susceptibility is highly media substrate dependent. Finally, we noted that mtDNA reduction in primary striatal cultures has functional impacts through reducing ADP and increasing available reducing equivalents such as NADH, which may be a sign of a metabolic shift toward glycolysis. Together, we characterize several aspects of mtDNA quantity reduction in multiple culture systems.

2. Introduction

Mitochondria play an important role in the function of highly energetic tissues such as the brain, heart, and skeletal muscle, providing a reliable quantity of ATP for rapid consumption (Wallace, 2005). Consequently, factors that impair mitochondrial function (i.e. aging (Wallace, 2005; Hur et al., 2010; Surmeier et al., 2010), gene mutations (Taanman, 1999; Tzoulis et al., 2014; Paramasivam et al., 2016), and exposure to environmental toxins (Tanner, 1989; Di Monte, 2003; Cicchetti et al., 2009)) similarly impair the function of many of these organ systems, leading to a pleiotropic set of neuromuscular dysfunctions that are implicated in a number of different

diseases (Wallace, 1992, 1999). Developing and understanding new methodologies for studying mitochondrial function is vital piece of continuing to disentangle the pathogenesis of these disorders (Brand and Nicholls, 2011).

One particularly complex aspect of studying mitochondrial function is that mitochondria possess a unique genome, or mtDNA, distinct from the nucleus, which is contained in a high copy number within the mitochondria (Taanman, 1999). While mitochondrial function is heavily dependent on import of proteins encoded by genes in the nucleus (Rehling et al., 2001; Truscott et al., 2003; Neupert and Herrmann, 2007), the small number of mitochondrially-encoded genes form essential components of the mitochondrial RC. Loss of function in any of the protein-coding genes, or in the genes encoding tRNAs which translate these proteins, can cause disease (Taylor and Turnbull, 2005). Similarly to the nuclear genome, mtDNA function can be impaired both by inherited mutations (Schon et al., 2012) and the accumulation of somatic mutations (Wallace, 2005, 2010). Unprotected by the nuclear envelope, mtDNA is more susceptible to damage, which can arise from environmental toxins, exposure to radiation, and reactive products of metabolism. In particular, as mtDNA plasmids are positioned next to the mitochondrial RC, one of the most potent sources of ROS, mtDNA is also more likely to encounter damaging influences (Shokolenko et al., 2009; Cline, 2012). The mtDNA polymerase, POLγ, is also more error-prone and has a lower proofreading capacity than nuclear polymerases, and is the primary source of accumulated errors in mtDNA (Copeland, 2010).

Though defects in mitochondrial function are implicated in nearly every age-related disease, they have been particularly well-connected to PD, through the identification of gene mutations in autosomal dominant forms of PD that have mitochondria-related functions (Davie, 2008), and through the association of exposure to mitochondrial toxins with the development of parkinsonian symptoms (Tanner, 1989; Di Monte, 2003; Reeve et al., 2016). However, one of the side effects that emerges from pharmacotherapy of PD, LID, has previously been shown in our lab to have a relationship to mitochondrial function. We determined that PD patients with LID had

significantly less mtDNA in the putamen than PD patients who had not yet developed LID (Naydenov et al., 2010). This led to the hypothesis that mtDNA quantity may be a factor that differentiated these two groups of patients, and may potentiate the development of LID during L-DOPA treatment. mtDNA depletion has been associated with a number of different diseases (Montier et al., 2009), but the relationships between degree of copy number variation and impaired function are highly variable across tissues. Recently, reduced mtDNA copy number in peripheral tissues has been identified as a biomarker of PD (Pyle et al., 2016), and mtDNA is depleted in the SNc of PD patients (Dölle et al., 2016). Consequently, we determined that establishing a model of reduced mtDNA in the putamen (or striatum in rodents), and different methods of evaluating some of the functional consequences of reduced mtDNA would be imperative for exploring the effects of reduced mtDNA in the striatum.

The present study sought to evaluate a few different methodologies for studying mitochondrial biology, through the lens of changes in mtDNA quantity. First, we evaluated different approaches to reducing mtDNA, both in cell lines and in primary neuronal cultures, with genetic and chemical methods. Second, we confirmed the importance of media carbohydrate selection when studying mitochondrial inhibition in propagating cell lines. Finally, we used two whole-cell measures, ATP and reducing equivalent-based viability, to examine their suitability for identifying mtDNA-quantity based cellular dysfunctions. In this way, we identified important aspects of experimental procedure for studying mitochondrial function in both neurons and cell lines.

3. Results

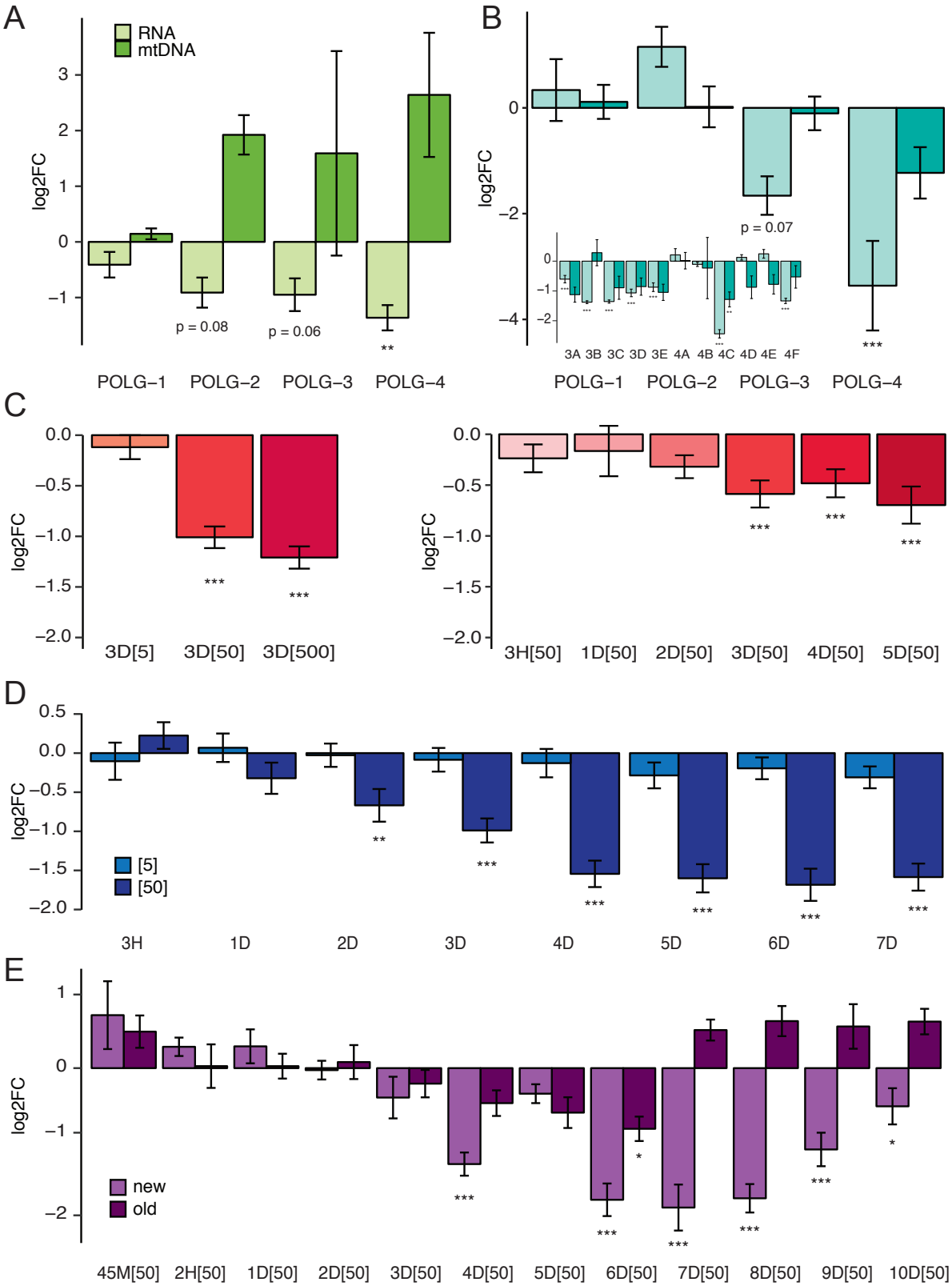
A
RNA
mtDNA
log2FC
p = 0.08
p = 0.06
**
POLG–1
POLG–2
POLG–3
POLG–4
B
log2FC
p = 0.07
***
3A 3B 3C 3D 3E 4A 4B 4C 4D 4E 4F
POLG–1
POLG–2
POLG–3
POLG–4
C
log2FC
***
***
3D[5]
3D[50]
3D[500]
***
***
***
3H[50]
1D[50]
2D[50]
3D[50]
4D[50]
5D[50]
D
log2FC
[5]
[50]
**
***
***
***
***
***
3H
1D
2D
3D
4D
5D
6D
7D
E
log2FC
new
old
***
*
***
***
***
*
45M[50]
2H[50]
1D[50]
2D[50]
3D[50]
4D[50]
5D[50]
6D[50]
7D[50]
8D[50]
9D[50]
10D[50]

Figure 25. Efficacies of different approaches to mtDNA reduction.
2D[5] = 5ng/ml EtBr for 2 days, 4D[50] = 50ng/ml EtBr for 4 days, as indicated for different dose and time points. (A) Four different lentiviruses carrying shRNAs directed against polymerase gamma (POLG) were applied to ST*Hdh*$^{Q7/Q7}$ cells. Log2-fold change of POLG mRNA and mtDNA quantity, relative to respective controls, are presented. (B) Log2-fold change of POLG mRNA and mtDNA quantity, relative to respective controls, following lentiviral treatment of N2a cells. (Inset) POLG and mtDNA expression following monoclonal expansion of previously-infected N2as, using shRNA vector 3 and 4. (C) Log2-fold change of mtDNA in mouse primary striatal NECos in response to different doses of EtBr (Left) or different duration of EtBr application (Right). (D) Log2-fold change of mtDNA in rat primary striatal NECos in response to both different doses of EtBr and different durations in application. (E) Log2-fold change of mtDNA in rat primary glial cultures in response to different durations in application. Both 'new' glia isolated from the initial dissection and 'old' glia plated for this experiment following three passages are shown. *** = $p < 0.001$; ** = $p < 0.01$; * = $p < 0.05$, relative to controls, (A-C) following Tukey's HSD post-hoc test, (D-E), following Dunnett's post-hoc test. Error bars reflect delta-method propagated +/- SEM.

3.1. *Polg* knockdown does not stably reduce mtDNA quantity in transformed cell lines

In order to examine the effects of mtDNA reduction in the striatum, we evaluated several different approaches. First, as transformed cell lines greatly minimize animal suffering, and the ST*Hdh* line has been well characterized for studying striatal dysfunction in models of HD (Trettel et al., 2000), we chose to transfect ST*Hdh*$^{Q7/Q7}$ cells with lentiviruses carrying shRNAs (POLG1-4) directed against *Polg*, the catalytic subunit of the POLγ holoenzyme (Figure 25A). Though the different shRNAs reduced the mRNA expression of *Polg* ($n = 4$, $F = 6.159$, $p < 0.001$), in none of these cases did the reduction of *Polg* reduce mtDNA quantity ($n = 2$, $F=2.47$, n.s.). In order to determine if this was a cell-line specific effect, we additionally infected the N2a cell line (Olmsted et al., 1970) with the same 4 shRNAs (Figure 25B). Here, only two of the clones were initially successful at reducing *Polg* expression (control $n = 6$, treated $n = 8$, $F = 12.84$, $p < 0.0001$), and none reduced mtDNA. We attempted to apply additional selection pressure to the clones with a significant degree of knockdown, and isolated single cells from both POLG-3 and POLG-4 infected cell lines. Following this process, we observed that the majority of these secondary cell lines had significantly reduced *Polg* mRNA (control $n = 12$, treated $n = 3$, $F = 3.367$, $p < 0.01$), but only one of these had significantly reduced mtDNA copy number (control $n = 12$, treated $n = 3$, $F = 2.551$, $p = 0.02$). We concluded that stable expression of an shRNA against POLG does not consistently reduce mtDNA in cell lines.

3.2. Ethidium bromide dose- and time- dependently reduces mtDNA quantity in both mouse and rat primary striatal culture

As our attempt to reduce mtDNA through genetic manipulation was unsuccessful, we turned to a chemical approach, a model that has a higher fidelity to the *in vivo* physiology of the striatum – EtBr treatment of primary striatal cultures. We first tested this approach in mouse NECos (Figure 25C), and observed a dose (three dissections, total n = 12, $F = 73.53$, $p < 0.0001$) and time (three dissections, total control n = 31, treated n ranges 4-19, $KW = 22.465$, $p < 0.001$) dependent relationship between magnitude of EtBr exposure and degree of mtDNA reduction. We observed a similar effect in rat primary striatal NECos (two dissections, control n=16, treated n = 5, $F = 9.969$, $p < 0.0001$) (Figure 25D). Additionally, we evaluated the efficacy of this approach in primary glia, and compared freshly isolated glia to glia that had been allowed to propagate through three passages (Figure 25E). In this culture type, EtBr reduction of mtDNA was less consistent, especially in 'old' glia, which were only significantly reduced at one time point (one dissection, control n = 24, treated n = 4, $F = 5.128$, $p < 0.0001$). 'New' glia were more vulnerable to mtDNA reduction than NECos, though this relationship was not as consistently time-dependent as NECos (control n = 24, treated n = 4, $F = 19$, $p < 0.0001$).

3.3. Substrate dependence on cell line vulnerability to mitochondrial toxins

We next evaluated the effect of cell media carbohydrate substrate on the relative toxicity of the mitochondrial toxin, rotenone, by determining its IC50 under different conditions. First, we observed that ST*Hdh*$^{Q7/Q7}$s cultured in 25mM glucose (Figure 26), rotenone had an IC50 >500nM, while in 25mM galactose, the IC50 for rotenone was 12.7+/-0.07nM (n = 8 per concentration). We next examined if a reduction in *Polg* expression would impact vulnerability to rotenone, by comparing shRNA infected cells to their non-mammalian target (NMT)-infected controls, and cultured under both glucose and galactose conditions. Though we observed the same galactose-

dependent toxicity for rotenone, the IC50 was not significantly different between control and POLG knockdown (3.3+/-10.8nM, and 5.1+/-49.3nM, respectively, n = 2 per concentration).

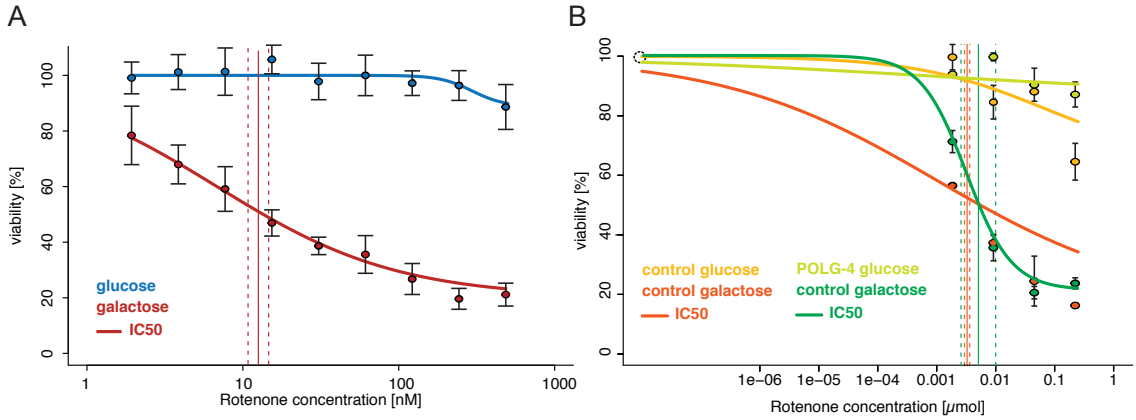

Figure 26. Substrate-dependency of mitochondrial inhibition in cell lines.
(A) IC50 curves for ST*Hdh*$^{Q7/Q7}$ cells, grown in either glucose or galactose media, exposed to varying concentrations of rotenone for 24h. (B) IC50 curves for lentivirus-infected N2a cells. 'Controls' are infected with an shRNA directed against a non-mammalian target (NMT) while 'POLG-4' are infected with an shRNA directed against POLG. Both were grown in either glucose or galactose media and exposed to varying concentrations of rotenone for 24h. Solid vertical lines reflect the calculated IC50, while dashed lines reflect the SD.

3.4. The ATP/ADP ratio is a more sensitive indicator of mtDNA reduction than total cell ATP

In order to begin evaluating physiologic ramifications of mtDNA reduction in our culture model, we next sought to measure changes in ATP as a metric of changes in bioenergetic availability. In our mouse cultures (Figure 27A), we evaluated different EtBr concentrations (one dissection, n = 3, F = 8.474, p < 0.01), and exposure durations (one dissection, control n = 8, treated n = 4, F = 3.669, p = 0.02). We only observed a correlation between ATP and EtBr dose, in that only the highest concentration of EtBr reduced ATP. In rat cultures (Figure 27B), we observed a pattern of ATP reduction in response to EtBr dose and duration that much more closely mirrored mtDNA quantity (one dissection, control n = 23, treated n = 6, F = 21.95, p < 0.0001). We subsequently probed the ATP/ADP ratio in our rat cultures (Figure 27C), and observed a time (but not dose) dependent increase in the ATP/ADP ratio following EtBr treatment.

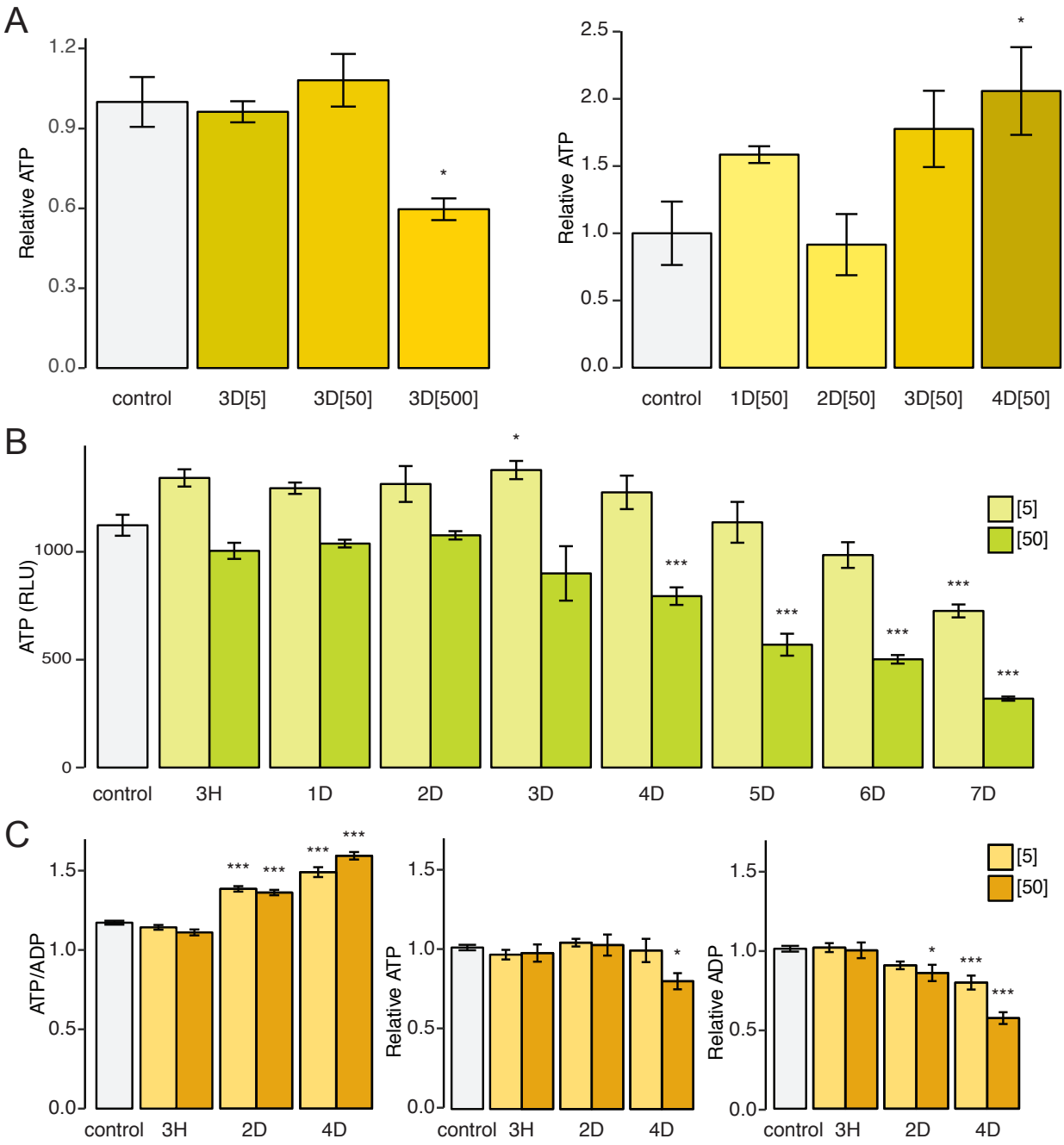

Figure 27. The ATP/ADP ratio is impacted more readily than total ATP by EtBr.
(A) Relative ATP from primary striatal mouse NECos, following different doses (Left) and durations (Right) of EtBr treatment. (B) Relative ATP from primary striatal rat NECos, following different doses and durations of EtBr treatment. (C) ATP/ADP ratio (Left), relative ATP (Center) and relative ADP (Right) from primary striatal rat NECos, following indicated doses and durations of EtBr treatment. *** = $p < 0.001$; ** = $p < 0.01$; * = $p < 0.05$, relative to controls, (A,C) following Tukey's HSD post-hoc test, (B), following Dunnett's post-hoc. Error bars reflect +/- SEM.

Relative ATP and ADP concentrations revealed that the increase in the ATP/ADP ratio was primarily attributable to a reduction in ADP, and that the degree of ADP reduction corresponded

better to both dose and time of EtBr exposure.

3.5. Reducing equivalent-dependent viability assays show different trends in cell lines and primary neurons

Reducing equivalent-dependent viability assays, including the MTS assay, typically reflect changes in viability in cell lines, following the application of a toxin or other cell stressor, by detecting changes in intracellular metabolism (Riss et al., 2016). Despite the lack of mtDNA reduction in the anti-*Polg* shRNA-infected ST*Hdh*$^{Q7/Q7}$ cell lines, we assessed changes in these clones to determine if reduction in *Polg* expression may yet affect cell function. Indeed, we observed that two of the four shRNA clones had significantly reduced MTS absorbance following *Polg* knockdown (n = 16, F = 5.775, p < 0.000114) (Figure 28A). Conversely, in our rat cultures, we observed a dose- and time-dependent effect of EtBr exposure and mtDNA reduction which instead significantly increased MTS absorbance at several time points (Figure 28B) (one dissection, control n = 8, treated n = 5, F = 10.8, p < 0.0001).

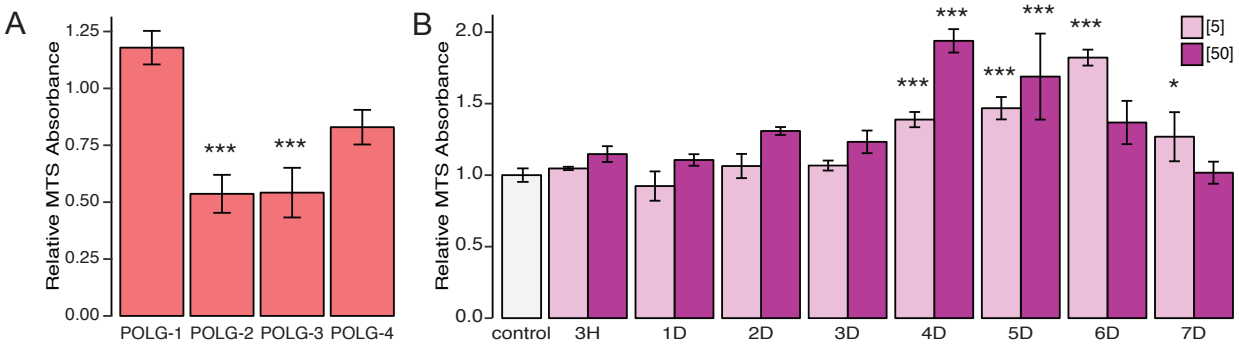

Figure 28. The two sides of reducing equivalent-based viability assays.
(A) Relative MTS absorbance in ST*Hdh*$^{Q7/Q7}$ cells following infection with lentiviruses carrying shRNA directed against *Polg*. (B) Relative MTS absorbance in rat primary striatal NECos following indicated doses and durations of EtBr treatment. *** = p < 0.001; ** = p < 0.01; * = p < 0.05, relative to controls, (A) following Tukey's HSD post-hoc test, (B), following Dunnett's post-hoc. Error bars reflect +/- SEM. Tukey's HSD post-hoc test, (B), following Dunnett's post-hoc. Error bars reflect +/- SEM.

4. Discussion

Though mitochondrial dysfunction comes in many forms, variations in mtDNA copy number in the context of neurodegenerative disease is poorly understood. We previously identified mtDNA quantity as one of the factors differentiating dyskinetic PD patients from nondyskinetic PD patients. We have hypothesized that this difference may underlie a bioenergetic deficit in the putamen of PD patients that consequently predisposes these patients to developing LID following L-DOPA treatment. The present study evaluates different models of mtDNA reduction in the putamen, as well as the utility of different physiological metrics for assessing the degree of cellular dysfunction induced by mtDNA reduction.

4.1. POLG knockdown does not effectively reduce mtDNA in cell lines

POLG is the only known mtDNA polymerase. Genetic disorders with mutations in POLG, such as CPEO and Alper's syndrome, typically present with both a reduction in mtDNA quantity and an increase in mtDNA mutations (Copeland, 2010). We hypothesized that knockdown of this gene would reduce the quantity of mtDNA by impairing its replication. We were thus surprised to observe that despite achieving successful knockdown of *Polg* mRNA in both ST*Hdh*$^{Q7/Q7}$ and N2a cell lines with some of the shRNA clones, we did not detect a reduction in mtDNA quantity in almost all examined cases. However, there are a few likely reasons for this phenomenon, all of which point to why this model is likely unsuitable for studying the effects of reduced mtDNA. First, it is possible that *Polg* is expressed at a sufficiently high copy number that even in cases where significant reduction in *Polg* expression was achieved, this was not sufficient to impair the function of the polymerase, leaving mtDNA quantity unchanged. Secondly, without clonal selection, it is likely that cells from the initial infected pool with a lower degree of *Polg* knockdown outgrew cells with a more severe knockdown over several cell divisions, making any phenotypic consequence of this knockdown difficult to detect. This phenomenon is somewhat corrected through the

monoclonal expansion of infected cell lines, which leads to a homogenous degree of knockdown. Indeed, our preliminary experiment evaluating this phenomenon shows an improved degree of correlation between *Polg* knockdown and mtDNA reduction in the monoclonally expanded N2as. However, even under these conditions, the achieved degree of *Polg* knockdown did not achieve a significant reduction in mtDNA in nearly every case.

The lack of success with these experiments does not conclusively demonstrate the futility of genetic manipulations in reducing mtDNA. Interestingly, in a primary retinal ganglion cell model of glaucoma, *Polg* knockdown effectively reduced mtDNA and increased mtDNA mutations (Zhang et al., 2016). Transgenic animal models have been very successful in modeling reduced mtDNA. In particular, the Tfam heterozygous mouse typically presents with an approximately 50% reduction in mtDNA quantity (Silva and Larsson, 2002). Subsequent studies aiming to examine the effects of mtDNA reduction in the striatum, particularly on the progression of LID, may be successful with striatum-specific knockdown of Tfam.

4.2. Circumventing the Warburg effect is essential to studying mitochondrial toxicity

In the present study, we demonstrated that the IC50 of a mitochondrial toxin, the Complex I inhibitor rotenone, is extremely dependent on the available carbohydrate substrate. This effect has been previously observed in two related phenomena, the Warburg and Crabtree effects (Diaz-Ruiz et al., 2011), which describe 'aerobic glycolysis,' initially described in cancer (though its presentation in different types of cancers is controversial (Zheng, 2012)). When supplied with an excess of glucose in the media, cell lines can generate sufficient ATP through glycolysis, and mitochondrial function may not be required for cell viability or propagation. As we observed, cell lines in culture readily undergo this metabolic shift in glucose media, making defects in mitochondria activity difficult to detect. Substituting galactose eliminates the net ATP produced during glycolysis, forcing carbohydrate oxidation through oxidative phosphorylation, or the uptake

of glutamine into the TCA cycle, a step which also requires mitochondrial activity (Rossignol et al., 2004; Marroquin et al., 2007).

Importantly, this phenomenon is primarily a concern when examining cell lines, though it has interesting implications for the metabolic coupling undergone by neurons and glia (Magistretti, 2006). Similar to cell lines, glia can undergo aerobic glycolysis, while neurons are incapable of upregulating glycolysis and rely on mitochondrial function for the eventual generation of ATP (Bolaños et al., 2010). This difference may point to a difference in susceptibility to mitochondrial insult between the two cell types.

4.3. EtBr exposure consistently reduces mtDNA quantity

As a positively charged cation with delocalized pi orbitals, EtBr is rapidly and selectively accumulated into mitochondria, where it intercalates with mtDNA and inhibits its replication (Leibowitz, 1971; Desjardins et al., 1985). This unique selectivity of EtBr has been exploited in a variety of model systems to reduce mtDNA (Armand et al., 2004; Kai et al., 2006; Yu et al., 2007), but to our knowledge this is one of the first studies to examine its utility in murine primary striatal neuron and glia NECos. EtBr effectively dose- and time-dependently reduces mtDNA quantity in both mouse and rat systems, though interestingly, the fold change reduction in mtDNA induced by EtBr appeared to be more stable in the rat system. Primary glial cultures appear to be more resistant to EtBr-induced mtDNA reduction than combined neuron and glia NECos, particularly ‘older’ glia that have been passaged multiple times. This differential in mtDNA quantity stability may warrant further study.

4.4. Changes in the ATP/ADP ratio may reflect subtle mitochondrial dysfunction, while decreases in total ATP likely reflects changes in viability

Two different experiments examining the effects of EtBr treatment (dose vs duration) in mouse cultures demonstrated a reduction in ATP with a high dose of EtBr, but an increase in ATP with a long dose of EtBr. This would suggest that in mouse cultures, mtDNA quantity is more or less independent from ATP quantity. In contrast, rat cultures exposed to different doses and durations of EtBr demonstrate a more consistent relationship to ATP quantity. This discrepancy however is likely irrelevant to future studies investigating the physiological consequences of mtDNA reduction, as this decrease in ATP is likely a precursor to cell death (Eguchi et al., 1997). The variability across these cultures is likely attributable to different percentages of glia in the treatment groups, especially in the mouse cultures. As our previous experiments illustrated that glia are less susceptible to mtDNA reduction by EtBr than neurons, an increased percentage of glia in the mouse NECos may protect against ATP reduction. Additionally, the severe reduction of ATP in the longest EtBr exposure times suggests that the reduction in mtDNA quantity achieved at these times may be a lower limit for these neurons to sustain viability.

In contrast, the ATP/ADP ratio begins to significantly shift at lower doses and shorter exposures than those required to detect significant reductions in mtDNA. At these lower doses, it is likely that the adenine nucleotide pool is sufficiently large to allow the conversion of ADP into ATP to fill cellular needs, selectively reducing ADP. However, further studies are needed to comprehensively probe this mechanism.

4.5. Viability assays may reflect subtle metabolic perturbations

The interpretation of reducing equivalent-dependent viability assays, such as the MTT or MTS assay, is based on the assumption that cell metabolism generates reducing equivalents, such as NADH and $FADH_2$, and a greater number of cells will generate a greater amount of NADH

(Riss et al., 2016). This standard interpretation explains the results of this assay in our anti-*Polg* shRNA-infected STHdh$^{Q7/Q7}$s. Though the reduction in *Polg* was insufficient to reduce mtDNA, it seems to have impacted some aspect of cellular metabolism, most likely through retarding replication. Importantly, this assay was performed in galactose, so even small inhibitions of mitochondrial function may readily translate to deficits in cell replication or glycolytic synthesis of NADH.

Interestingly, the situation is neatly reversed in neuron and glia cultures. Here, when mitochondrial activity is inhibited by the reduction in mtDNA from EtBr, this reduces the consumption of NADH by the ETC, causing its accumulation. This accumulation is compounded by the likely upregulation of glycolysis by glia to compensate for deficient ATP production, producing additional NADH. Thus, reducing equivalent-dependent viability assays may also be used as markers of reductive stress/indicators of reducing equivalent accumulation following mitochondrial inhibition.

5. Conclusion

Though the importance of mitochondrial function has been highlighted in the pathogenesis of neurodegenerative disorders numerous times, the contribution of mtDNA quantity remains to be fully elucidated. We have established a straightforward model for examining the physiologic effects of reduced mtDNA quantity in primary neurons, through the application of EtBr. Our dose and time titration should provide a useful starting point for different degrees of mtDNA reduction in future experiments. Additionally, we confirmed that the ATP/ADP ratio is a useful tool for identifying bioenergetic deficits before viability is compromised, and highlighted an alternative use for reducing equivalent-dependent viability assays in demonstrating accumulation of reducing equivalents.

CHAPTER IV

DYSKINESIOMIMETIC SIGNALING ALTERATIONS IN THE MTDNA-DEPLETED STRIATUM

1. Abstract

The induction of LID is associated with hallmark molecular alterations in the striatum, particularly in D_1-expressing medium spiny neurons. These include increased DA-mediated phosphorylation of ERK1/2, increased expression of IEGs, and other mediators of D_1 pathway hyperactivity. As mitochondrial dysfunction has been proposed to play a large role in the pathophysiology of PD, we previously probed the possibility of mitochondrial dysfunction in LID, and observed a reduction in mitochondrial DNA (mtDNA) in human dyskinetic PD patients. Here, we examined the possibility that reduced mtDNA might contribute to the development of D_1 hypersensitivity. These results were largely contradictory, but we observed that in some cases, mtDNA reduction increases basal ERK1/2 phosphorylation and basal histone acetylation, both of which may predispose the striatum to the maladaptive plasticity that accompanies the onset of dyskinesia. We further examined the relationship between mtDNA quantity and mitochondrial fission and fusion, and found that mtDNA reduction may promote mitochondrial fusion, though further studies are warranted.

2. Introduction

PD is a debilitating and progressive movement disorder that causes bradykinesia, tremor, limb rigidity, and postural instability (Jankovic, 2008). It is the second most common neurodegenerative disorder, affecting more than half a million people in the United States alone (Kowal et al., 2013). Bradykinesia, tremor, and rigidity are primarily caused by the degeneration of dopaminergic neurons in the SNc, a midbrain nucleus of the basal ganglia (Fahn, 2003; Davie, 2008; Magrinelli et al., 2016). SNc neurons supply tonic and phasic DA to the striatum, which aids

in filtering glutamatergic inputs from the cerebral cortex that forms the first step of the basal ganglia motor circuit (Lanciego et al., 2012; Gerfen and Bolam, 2017). The major projection neurons of the striatum, MSN, fall into two subtypes determined by their discrete expression of DA receptors, projection sites, and roles in modulating the motor circuit (Smith et al., 1998; Calabresi et al., 2014; Vicente et al., 2016) . dMSNs are striatonigral, and exclusively express D_1Rs. D_1Rs are Gαs/olf-coupled GPCRs, and are consequently stimulated by DA. In contrast, iMSNs are striatopallidal, and exclusively express D_2Rs. These are $G\alpha_{i/o}$-coupled GPCRs, and are inhibited by DA (Gurevich and Gurevich, 2010) . The loss of dopaminergic input thus favors the activity of the indirect pathway, which suppresses movement and presents as bradykinesia (Jenner, 2008). Pharmacotherapy for PD predominantly consists of dopamimetic agents or dopaminergic replacement (Clarke, 2004; Chen and Swope, 2007; Oertel and Schulz, 2016) . The most commonly used of these compounds is the DA precursor, L-DOPA. L-DOPA supplementation initially alleviates parkinsonian motor deficits through its replacement of DA, which restores regulation of the direct and indirect pathways. However, over time L-DOPA causes its own characteristic set of side effects that are broadly classified as a hyperproduction of choreiform movements, known as LID. Overproduction of movement is a result of another shift in the balance between the direct and indirect pathways; as DA reintroduction to the striatum becomes pathological, the direct pathway is hyperactivated while the indirect pathway is suppressed, favoring the production of movement uncoupled from cortical control (Jenner, 2008; Ghiglieri et al., 2012; Iravani et al., 2012; Bastide et al., 2015) .

Despite decades of research, the etiology of LID remains elusive. The development of animal models has however facilitated the identification of several molecular correlates of LID. In particular, these studies have determined that the primary contribution to the phenomenology of LID is the hypersensitization of the D_1 signaling pathway (Aubert et al., 2005; Berthet and Bezard, 2009; Guigoni and Bezard, 2009; Feyder et al., 2011). Comparing dyskinetic and nondyskinetic animals, no consistent changes in the levels of the D_1 receptor occur (Turjanski et al., 1997;

Hurley et al., 2001; Guigoni et al., 2005). In contrast, expression of $G\alpha_{olf}$ (Corvol et al., 2004; Penit-Soria et al., 1997) and coupling between D_1R and this G protein increases (Hervé et al., 1993; Guigoni et al., 2005), promoting activation of its downstream signaling molecules such as DARPP32 and PKA (Picconi et al., 2003; Aubert et al., 2005; Cenci, 2007), which even along its canonical signaling pathway promotes the increase in expression of IEGs such as cFos, Egr1, and Arc (Robertson et al., 1989; Gerfen et al., 1990; Keefe and Gerfen, 1996; Konradi et al., 1996; Berke et al., 1998; Gerfen, 2000). This pathway also promotes the transcription of neuropeptides such as ppd and ppt in dMSNs (Keefe and Horner, 2017). The induction of LID is also associated with dopaminergic activation of non-canonical signaling pathways, such as the MAPK pathway through the activation of ERK1/2, which also promotes histone phosphorylation and changes in histone acetylation state (Santini et al., 2009; Cenci and Konradi, 2010; Feyder et al., 2011; Fieblinger et al., 2014). These modifications can further alter gene transcription programs, and may be responsible for deregulating the expression of structural genes that regulate synaptic homeostasis, which are also substantially affected by LID (Stephens et al., 2005; Zaja-Milatovic et al., 2005; Moratalla et al., 2017).

Through clinical studies, several risk factors for LID have been identified. Patients with a younger age of PD onset, and those given a higher dose of L-DOPA, are at a greater risk of developing LID, suggesting disease severity and degree of neurodegeneration may play a role in LID susceptibility (Rascol et al., 2006; Fabbrini et al., 2007; Olanow et al., 2013), even in mouse models (Shan et al., 2015). Patients given a continuous supply of L-DOPA through a jejunal pump are less likely to develop LID, suggesting the plasma (and by extension, CSF) concentration fluctuation inherent in oral L-DOPA dosage may also magnify the pathogenicity of the drug (Zesiewicz et al., 2007; Oertel and Schulz, 2016). However, these factors do not entirely explain the discrepancy between PD patients that rapidly develop LID and those that develop it more gradually; i.e., though 90% of PD patients treated with L-DOPA will develop LID within 10 years, approximately 50% have developed it in 4-6 years (Ahlskog and Muenter,

2001). In a previous study, our lab attempted to identify additional risk factors by comparing post-mortem putamen samples from dyskinetic and non-dyskinetic PD patients (Naydenov et al., 2010). This study discovered that dyskinetic PD patients had a reduction in mtDNA copy number in the putamen, relative to control and non-dyskinetic PD patients, while no abnormalities were observed in the cerebellum, a brain region unaffected by LID. We subsequently hypothesized that this difference in mtDNA copy number could precede the development of PD and LID, and as a result may act as a risk factor for the development of LID in response to L-DOPA.

The present study used a previously-established model of mtDNA depletion (see Ch III and V); treatment of mouse and rat primary striatal neuron-enriched cocultures (NECos) with EtBr. As the doses and exposure times were previously validated, two days and four days of exposure at 50ng/mL (2D[50] and 4D[50]) were used as doses that significantly reduce mtDNA, and two days or four days of exposure at 5ng/mL (2D[5], 4D[5]) were doses that accounted for EtBr exposure without mtDNA reduction (though mtRNA synthesis may have been impaired, see Ch V). Finally, in a small subset of experiments, acute EtBr exposure (three hours – 3H[5/50]) was used to attempt to identify any non-mtDNA related EtBr responses. In this study, we attempted to determine if mtDNA reduction independently reproduced any of the molecular signaling maladaptations observed in animal models of LID. We concentrated on aberrant signaling responses to DA; i.e., phosphorylation of ERK, prepropeptide expression, induction of IEGs, and histone acetylation. We additionally examined alterations in mitochondrial dynamics through differential regulation of mitochondrial fission and fusion genes, and changes in mitochondrial morphology.

3. Results

3.1. mtDNA reduction may increase basal ERK1/2 phosphorylation

We examined both ERK1/2 phosphorylation at baseline and following stimulation with 50μM DA for 15 minutes (Figure 29A). Initially, we observed both a significant increase in ERK1/2 phosphorylation at baseline, and a hyperphosphorylation in response to DA (Figure 29A, set A; n

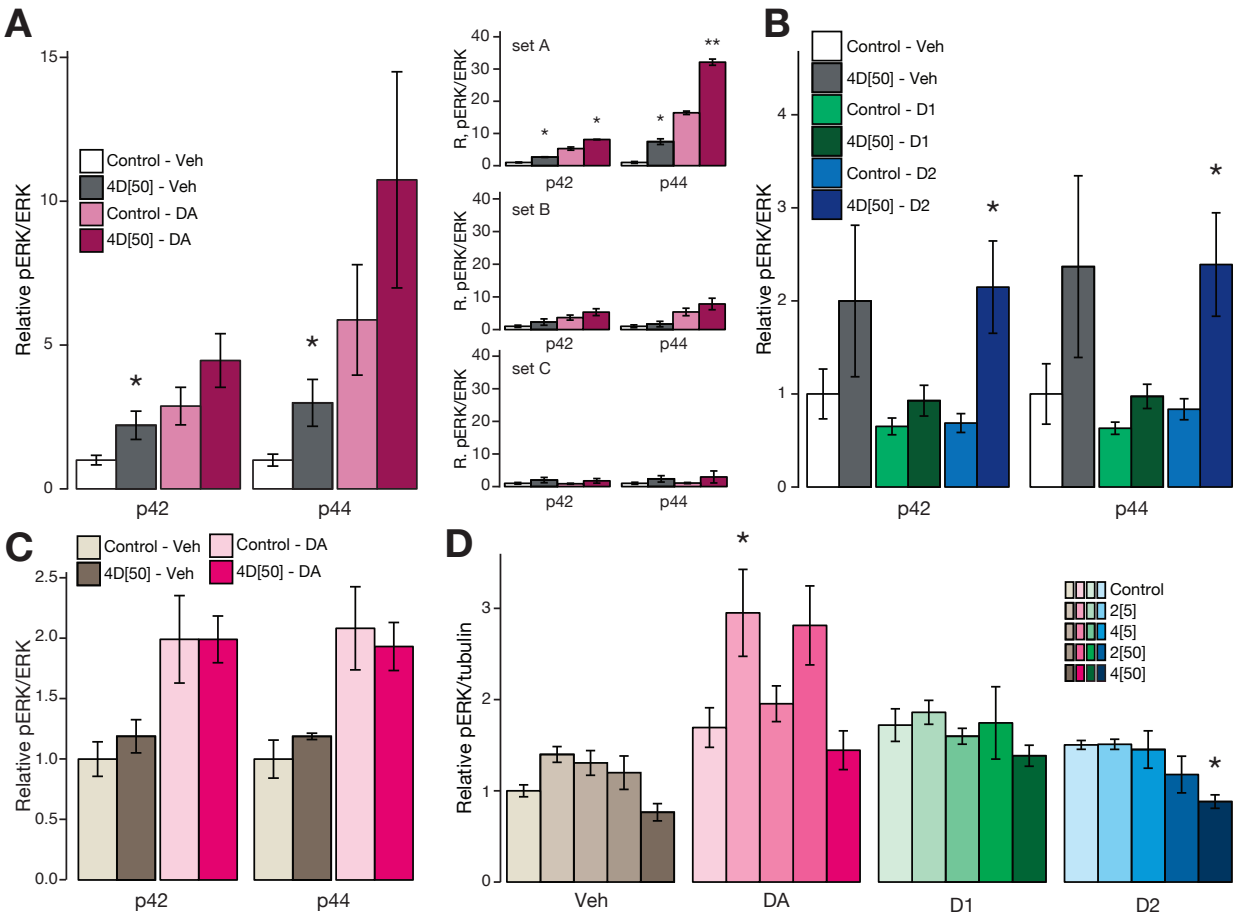

Figure 29. The relationship between mtDNA reduction and ERK1/2 phosphorylation.
(A) Basal and DA stimulation-mediated ERK phosphorylation in mouse primary striatal NECos, quantified from western blots. Left, aggregated ERK phosphorylation in response to EtBr and DA. 3 dissections, n = 10. Right, segregated results from the three dissections. Set B/C, n = 4. ** = $p < 0.01$, * = $p < 0.05$, following Student's t-test within each treatment paradigm. (B) D_1 and D_2 stimulation of control and EtBr-treated mouse primary striatal NECos. Single dissection, n = 4. * = $p < 0.05$, following Student's t-test within each stimulation paradigm. (C) Basal and DA stimulation-mediated ERK phosphorylation in control and EtBr-treated rat primary striatal NECos, quantified from western blots. Single dissection, n = 3. (D) Basal and DA/D_1/D_2 stimulation-mediated ERK phosphorylation in rat primary striatal NECos, quantified from in-cell westerns. * = $p < 0.05$, following Dunnett's post-hoc test within each stimulation paradigm.

= 2), but subsequent experiments did not validate these results (Figure 29A, set B and C; n = 4). However, a compilation of these results demonstrates a significant increase in basal ERK1/2 phosphorylation following EtBr treatment (Figure 1A, left; n = 10 from 3 dissections). To attempt to probe the DA receptor subtype specificity of this effect, we stimulated mouse NECos with either 50μM of a D_1 agonist (Chloro-APB), or 50μM of a D_2 agonist (PPHT) for 15 minutes prior to harvest (Figure 29B, single dissection, n = 4). Though D_2-mediated ERK1/2 phosphorylation was significantly greater in EtBr-treated cultures compared to controls, this activation was not significantly elevated relative to basal ERK1/2 phosphorylation. To pursue these findings, we performed the same initial experiment in rat NECos, and observed no significant difference in ERK1/2 phosphorylation with either vehicle or DA treatment between control and EtBr-treated cultures (Figure 29C, single dissection, n = 3). We also attempted an approach which allowed the simultaneous evaluation of multiple EtBr treatment groups (in-cell westerns), but once again did not reproduce our earlier finding that EtBr treatment elevated basal ERK1/2 phosphorylation (Figure 29D, (Veh), 4 dissections, n = 12). We observed a modest increase in ERK1/2 phosphorylation following DA treatment of the 2D[5] group ($F = 4.179$, $p = 0.009$) (Figure 29D, (DA), 2 dissections, n = 6), and a modest decrease in ERK1/2 phosphorylation following D_2 treatment of the 4D[50] group ($F = 4.693$, $p = 0.01$) (Figure 29D, (D_1/D_2), 1 dissection, n = 4).

3.2. mtDNA reduction does not consistently affect the expression or induction of neuropeptides nor immediate early genes by dopaminergic agents

Another consistent hallmark of dyskinesia development is the prolonged overexpression of ppd, so we next assessed the gene expression of striatal neuropeptides ppd, ppe, and ppt. We stimulated mouse NECos with DA, or D_1 or D_2 agonists (50μM), for either 18 hours or 45 minutes (Figure 30). No agonist significantly changed expression of any pro-peptide after 45 minutes of stimulation, in either control or EtBr-treated groups. However, 18 hours of D_2 agonism reduced

expression of ppd only in control cultures (F = 2.573, p = 0.047). In contrast, 18 hours of exposure to each agonist reduced expression of ppe (F = 12.22, p < 0.001) (ppd/ppe(veh), 4 dissections, n = 24; ppd/ppe(DA/D_1/D_2), 1 dissection, n = 3), and the same exposure to DA reduced ppt expression in EtBr-treated cultures (F=8.97, p = 0.007) (Figure 30) (tac1(veh), 3 dissections, n = 18; tac1(DA), 1 dissection, n = 3).

We next evaluated the effect of EtBr treatment on the expression and induction of IEGs cfos, egr1 (zif628), and arc. We first measured basal expression of these genes in mouse NECos between control and EtBr-treated groups (Figure 31A, cfos(veh), 9 dissections, n = 39; egr/arc(veh), 7 dissections, n = 27), and detected no significant differences. As DA stimulation (45 minutes, 50μM) did robustly stimulate the expression of cfos and egr1, we chose to only compare the magnitude of induction between control and EtBr treatment. Interestingly, we did

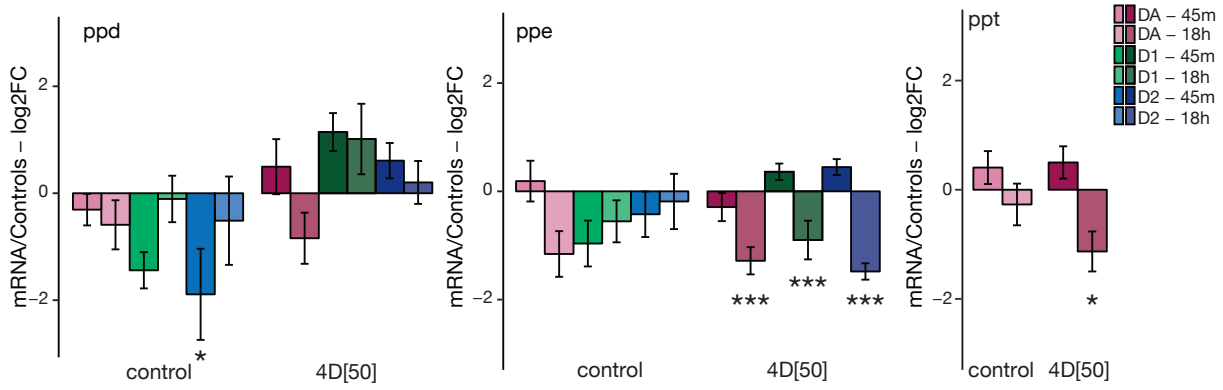

Figure 30. Reduced mtDNA decreases preproenkephalin expression following prolonged DAR-mediated stimulation.
Log2-fold change in mouse primary striatal NECos neuropeptide gene expression following DA, D_1, or D_2 stimulation 45 minutes or 18 hours prior to harvest, relative to unstimulated cultures. *** = p < 0.001, * = p < 0.05, following Dunnett's post-hoc test. Error bars reflect delta-method propagated +/- SEM. Ppd, preprodynorphin, ppe, preproenkephalin, ppt, preprotachykinin.

observe a significant increase in the DA-mediated induction of cfos and egr1 expression following

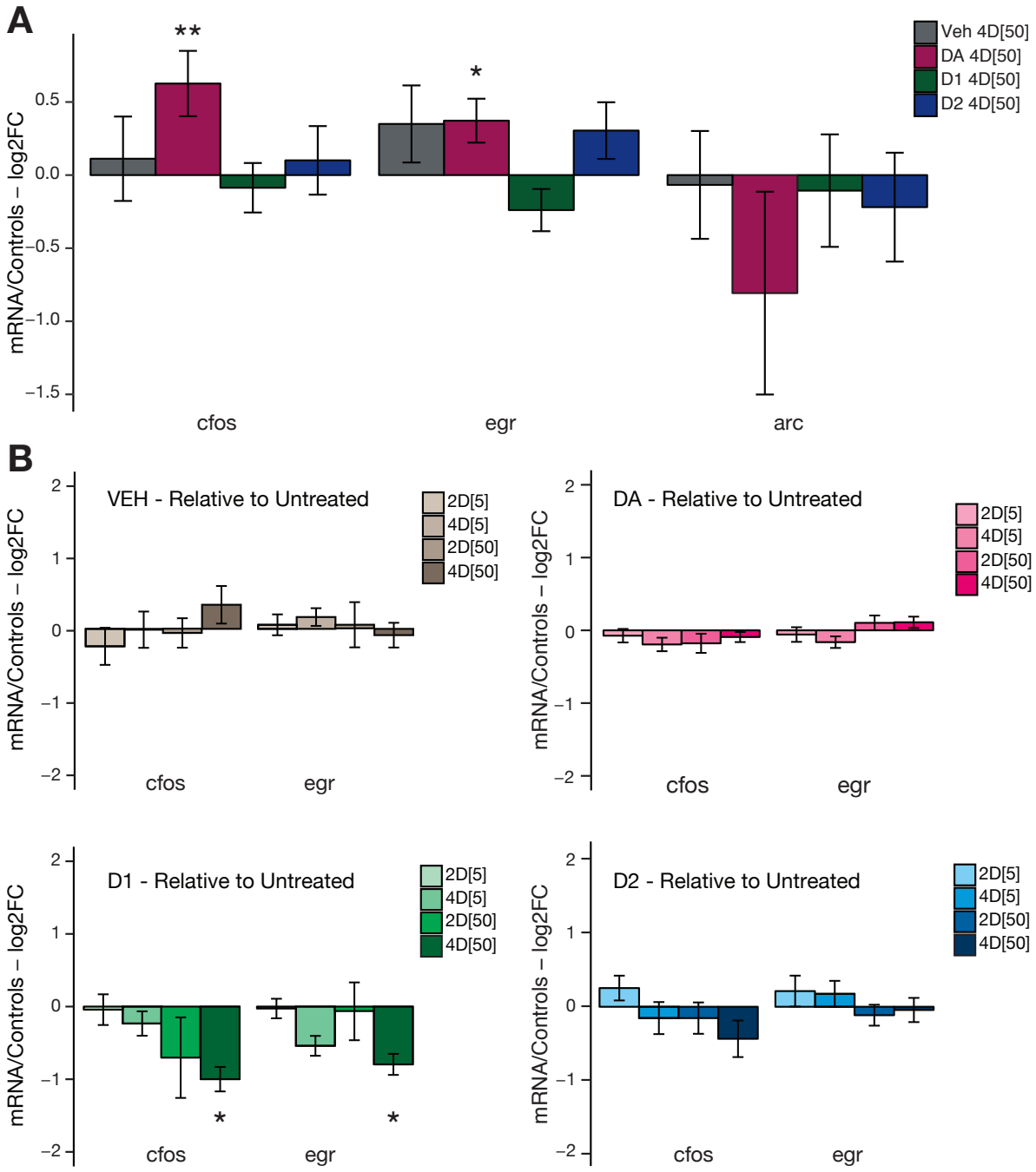

Figure 31. Impact of mtDNA reduction on DAR-mediated IEG expression.
2D[5] = 2 days 5ng/mL EtBr exposure, 4D[50] = 4 days 50ng/mL EtBr exposure. (A) Mouse primary striatal NECos were stimulated with 50μM DA, Chloro-APB (D_1), or PPHT (D_2) 45 minutes before harvest. Log2 fold change in expression of cfos, egr (zif628), and arc, comparing control and EtBr-treated conditions within each stimulation paradigm. * = $p < 0.05$, ** = $p < 0.01$, following Student's t-test between each paired group. (B) Rat primary striatal NECos stimulated under the same parameters. Log2 fold change for each EtBr treatment group relative to equivalently treated control. * = $p < 0.05$, following Dunnett's post-hoc test. Error bars reflect delta-method propagated +/- SEM.

EtBr treatment (Figure 31A, cfos(DA), 4 dissections, n = 12; egr/arc(DA), 3 dissections, n = 9), and no change in response to either D_1 or D_2 agonists (45 minutes, 50μM) (Figure 31A, cfos(D_1/D_2), 3 dissections, n = 11; egr/arc(D_1/D_2), 2 dissections; n = 8). In contrast, we observed no significant differences in either basal or DA-stimulated expression of cfos or egr in rat co-coultures (Figure 31B, (veh) 4 dissections, n(control) = 32, n(EtBr-treated) = 16; cfos/egr(DA), 2 dissections, n(control) = 12, n(EtBr-treated) = 8). Interestingly, D_1-mediated induction of both cfos and egr1 was suppressed in 4D[50] treated cultures (cfos, F=3.332, p = 0.031; egr, F=4.147, p = 0.01), though there was no change in D_2 induction (Figure 31B, 1 dissection, n(control) = 8, n(EtBr-treated) = 4).

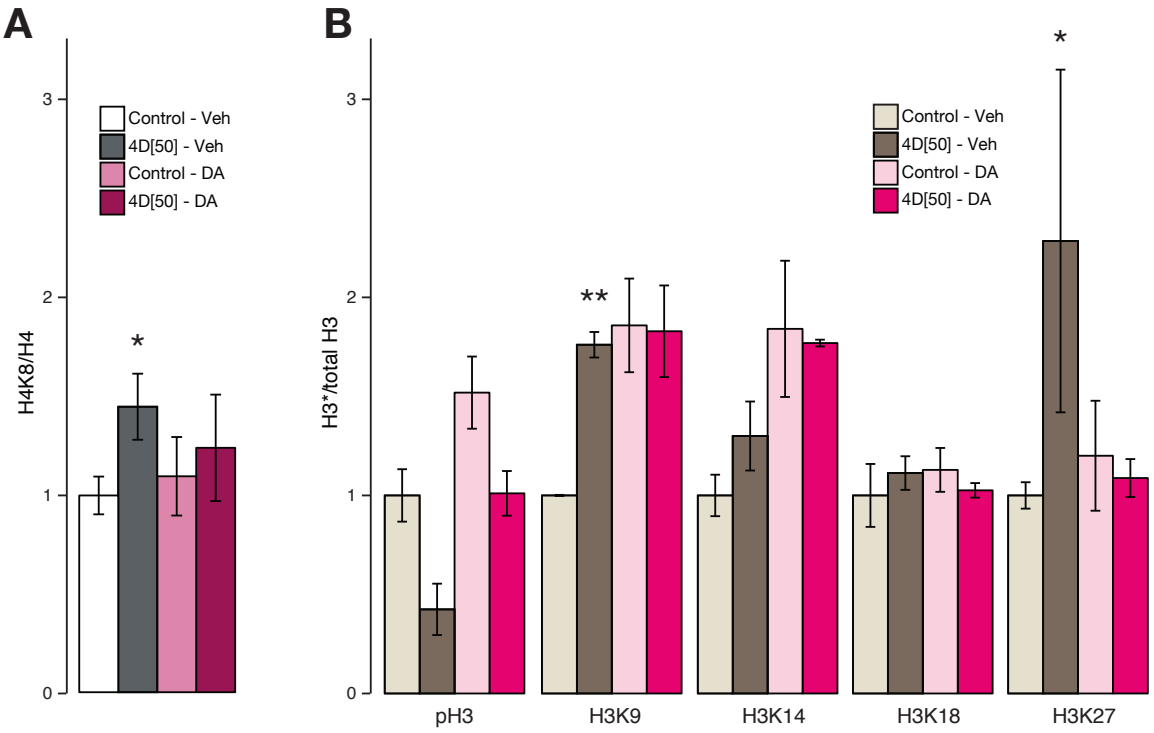

Figure 32. Alterations in Histone 3 and 4 modifications in response to EtBr and/or DA.
(A) Basal and DA-stimulated H4K8 acetylation, in control and EtBr-treated mouse primary striatal cultures, quantified by western blot. * = p < 0.05, following Student's t-test between stimulation paradigms. (B) Basal and DA-stimulated H3 phosphorylation or acetylations, in control and EtBr-treated rat primary striatal cultures, quantified by western blot. ** = p < 0.01, * = p < 0.05, following Student's t-test between stimulation paradigms. Error bars reflect +/-SEM.

3.3. mtDNA reduction perturbs basal histone modifications, but not modifications in response to DA

We next examined alterations in histone modifications, as these have been previously reported in animal models of LID and may be important mediators of some of the large changes in gene expression. First, we quantified histone H4 acetylation at the K8 residue at baseline and following DA stimulation (15 minutes, 50μM) in control and EtBr stimulated mouse NECos (Figure 32A, 3 dissections, (veh) n = 12, (DA) n = 9). H4K8 was significantly increased in EtBr-treated cultures, but there was no significant difference between the two groups following DA stimulation. We also used rat NECos to quantify different histone H3 modifications (4 different acetylation sites and one phosphorylation site) under the same EtBr and DA stimulation conditions (Figure 32B, single dissection, n = 3). Interestingly, we observed a significant increase in basal acetylation at H3K9 and H3K27, but again did not observe any changes between these two groups following DA stimulation.

3.4. mtDNA reduction may promote mitochondrial fusion

Alterations in mitochondrial dynamics have been tied to many neurodegenerative disorders, though no direct link has yet been established for LID. We thus attempted to use our culture systems to first investigate alterations in the expression of mitochondrial fission and fusion genes, following EtBr-treatment induced reduction in mtDNA. In mouse NECos, we observed significant reductions in the expression of both measured fission genes (Dnm1l and Fis1), and an increase in the expression of Opa1, a mediator of mitochondrial inner membrane fusion (Figure 33A, Dnm1l/Opa1/Mfn1, 4 dissections, n = 23; Fis1, Mfn2, 2 dissections, n = 11). However, in rat NECos, the same 4D[50] EtBr treatment increased Dnm1l expression and Opa1 expression, with no significant effect on any other measured gene (Figure 33B, two dissections, n(control) = 10, n(EtBr-treated) = 6).

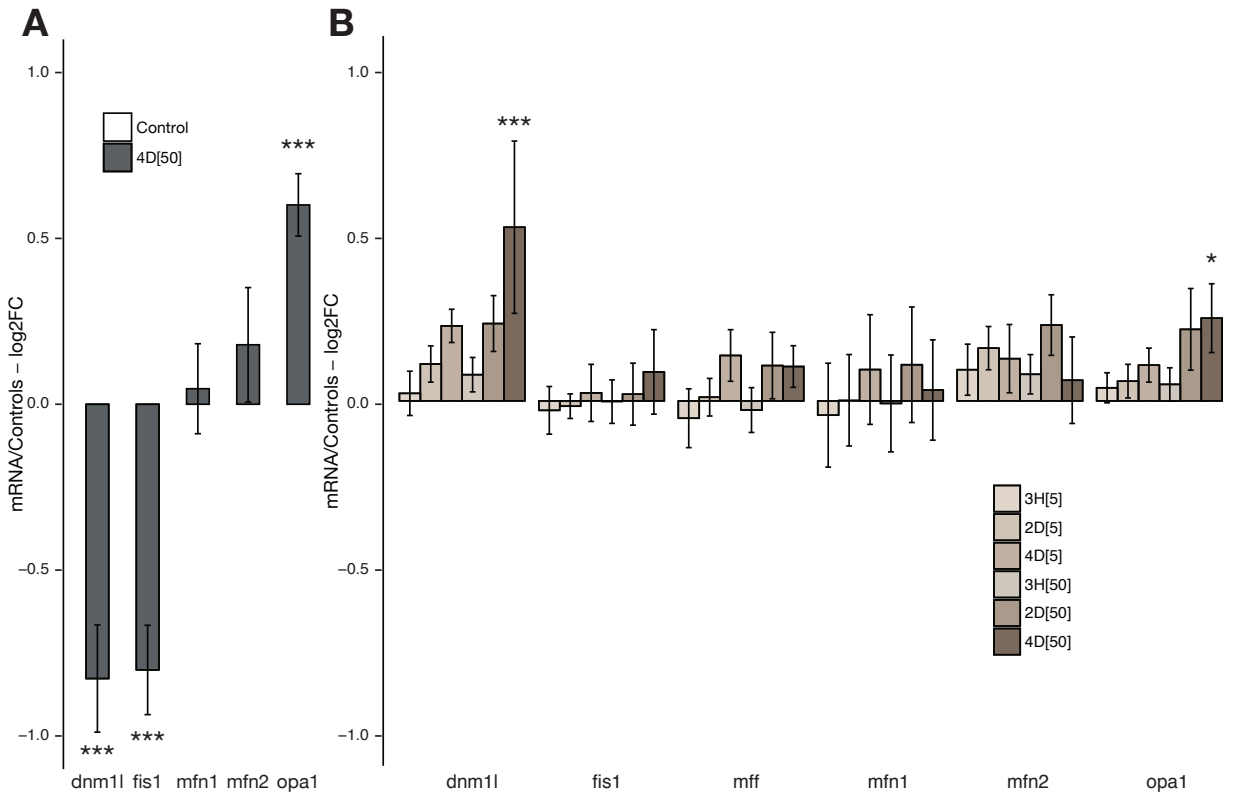

Figure 33. mtDNA reduction increases Opa1 expression.
(A) Log2 fold change in mitochondrial fission and fusion gene expression in control and EtBr-treated mouse primary striatal cultures. *** = $p < 0.001$, following Student's t-test. (B) Log2 fold change in mitochondrial fission and fusion gene expression in control and EtBr-treated rat primary striatal cultures. *** = $p < 0.001$, * = $p < 0.05$, following Dunnett's post-hoc test. Error bars reflect delta-method propagated +/- SEM.

As these gene expression changes point to potential alterations in mitochondrial morphology following EtBr treatment, we next quantified mitochondrial area, length, and distance from nucleus in glia identified in ICC images of rat NECos. Glia were selected due to their combination of visibly discrete mitochondria at a magnification where their entire cell body was visible. Neuronal mitochondria were excluded for an inability to meet these criteria. Figure 34A shows a representative glia used for this analysis, but see Materials and Methods for a detailed description of ICC and selection procedures.

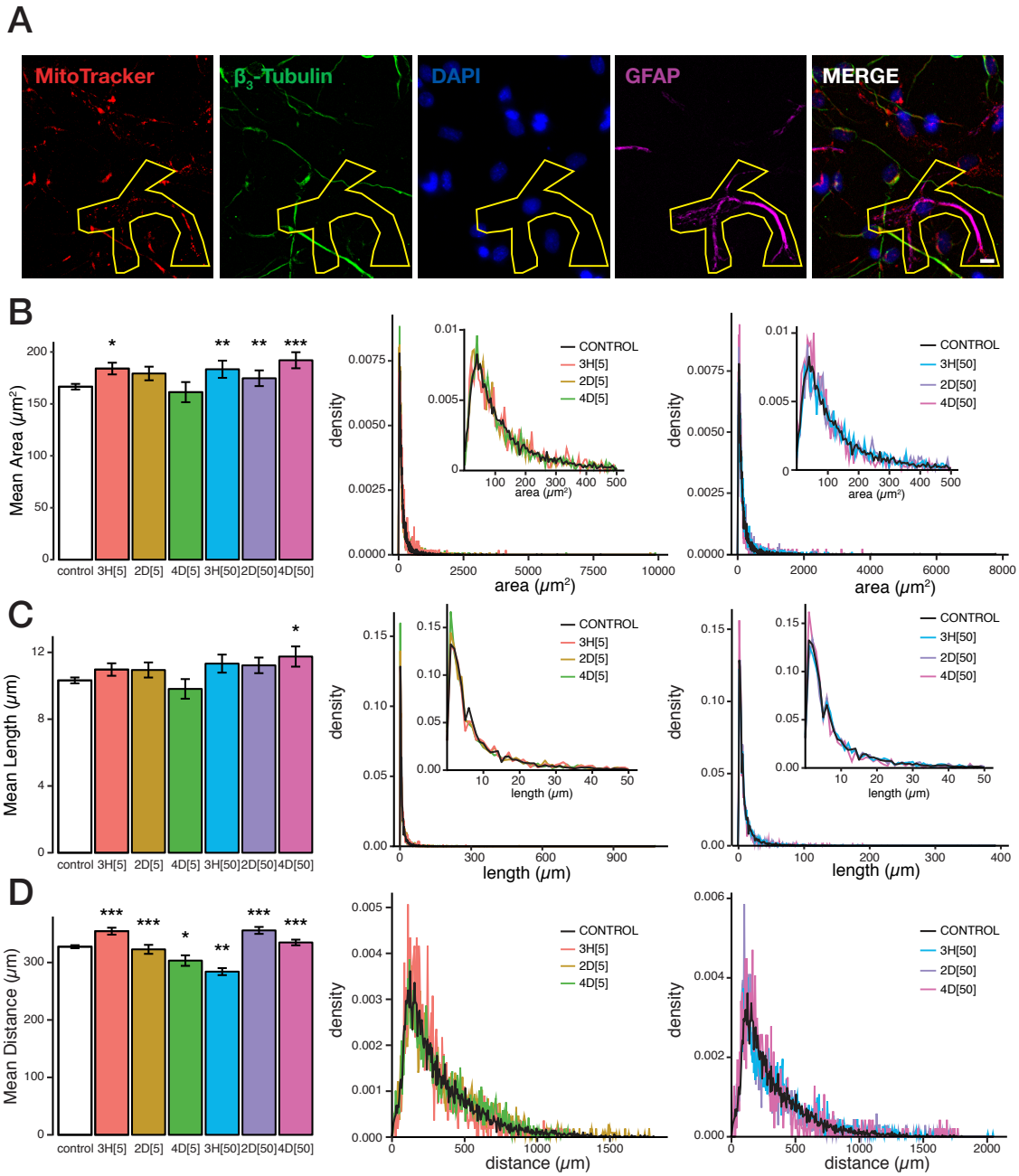

Figure 34. mtDNA reduction increases glial mitochondrial size and distance from nucleus. Control and EtBr-treated glia were identified from ICC images of rat primary striatal NECos, and their respective mitochondria were quantified. (A) Representative glia selected for image analysis (yellow outline). (B) Calculated mitochondrial area in control and EtBr-treated groups. Left, mean mitochondrial area. Right, frequency distribution of all calculated mitochondrial areas, with 5μm^2 bin width. [5] and [50] doses separated for visual clarity. Insets, magnification of data points from 0-500μm^2. (C) Calculated mitochondrial length in control and EtBr-treated groups. Left, mean mitochondrial length. Right, frequency distribution of all calculated mitochondrial lengths, with 1μm bin width. [5] and [50] doses separated for visual clarity. Insets, magnification of data points from 0-50μm. (D) Calculated mitochondrial distance from nucleus. Left, mean mitochondrial distance. Right, frequency distribution of all calculated mitochondrial distances from nucleus, with 5μm bin width. [5] and [50] doses separated for visual clarity. (B-D), single dissection. Mitochondria quantified from minimum of 12 images per treatment condition. *** = $p < 0.001$, ** = $p < 0.01$, * = $p < 0.05$, relative to control following Dunn's post-hoc test.

We observed an increase in the mean mitochondrial area in multiple EtBr treatment conditions, including both doses of acute EtBr treatment (3H[5] and 3H[50]) (KW chi = 46.068, $p < 0.001$) (Figure 34B, left), but also following 2D[50] and 4D[50] treatment. Interestingly, by plotting the frequency of mitochondrial are in all conditions, (Figure 34B, right) we observed an increase in the frequency of small mitochondria in the 4D[50] condition. We also observed an increase in mean mitochondrial length following 4D[50] EtBr exposure (KW chi = 31.55, $p < 0.001$) (Figure 34C, left), though curiously saw increases in the frequency of shorter mitochondria in both 4D[5] and 4D[50] doses (Figure 34C, right). Finally, mean mitochondrial distance from the nucleus was significantly altered in every EtBr treatment group (KW chi = 95.5, $p < 0.001$), though no consistent relationship between EtBr dose and this distance was observed (Figure 34D).

4. Discussion

Though the majority of PD cases are idiopathic, a number of risk factors for the development of PD have been identified, including genetic polymorphisms (Klein and Westenberger, 2012; Nalls et al., 2014), environmental factors (Tanner, 1989), and aging (Eeden et al., 2003). In contrast, relatively few risk factors for developing LID have been identified, though a large number of molecular and morphological correlates for the disorder has been characterized (Cenci and Konradi, 2010). As we previously determined that mtDNA quantity is significantly lower in dyskinetic PD patients relative to non-dyskinetic PD patients (Naydenov et al., 2010), we have hypothesized that this reduced copy number may contribute to the pathogenesis of LID and act as a risk factor. In the present study, we determined that mtDNA reduction through EtBr treatment induces some changes in DAergic signaling pathways, but additional studies will be needed to clarify some of these results. We also demonstrated that reduced mtDNA copy number may affect mitochondrial dynamics. Similarly, further studies will be needed to evaluate the contributions of these perturbations to the pathogenesis of LID.

4.1. mtDNA reduction has a mixed impact on DAR signaling in primary striatal cultures

As previously discussed, DA-mediated phosphorylation of ERK1/2 is one of the most canonical molecular hallmarks of the induction of LID. The induction of this phosphorylation is considered part of an aberrant signaling pathway, because in the intact striatum, DA receptor stimulation does not strongly induce ERK1/2 phosphorylation (Cenci, 2017). ERK1/2 is the nexus for a large number of signaling pathways, and the pathway connecting DA receptor stimulation and ERK1/2 phosphorylation has not been fully elucidated. However, this connection likely occurs through PKA activation of a MAP3K such as Raf, and may be facilitated by the hyperactivation of DARPP32, which disinhibits multiple effectors (Santini et al., 2007, 2009). Interestingly, our experiments in mouse cultures indicated EtBr treatment elevated basal ERK1/2 phosphorylation. Though we did not pursue the molecular mediators of this elevation in this study, a number of pathways may contribute to this elevation – in particular, if EtBr treatment compromises nutrient status by increasing the AMP/ATP ratio, mtDNA reduction may activate AMPK activity (Hardie et al., 2012). Some evidence suggests AMPK activation increases ERK phosphorylation (Hattori et al., 2006), providing one potential mechanism to link these two phenomena. This basal hyperphosphorylation may also explain the increase in DA-induced ERK phosphorylation we observed in a subset of our mouse experiments, but further studies may be needed to explain this discrepancy. Though we did observe an induction of ERK1/2 phosphorylation in response to DA in all of our mouse cultures, the magnitude of this induction was dramatically different between experiments. We were unable to determine the source of this disparity, though a contributing factor may include differential ratios of neurons and glia between dissections.

In an attempt to validate the increased basal ERK1/2 phosphorylation, we performed the same experiment using rat NECos. Though DA stimulation induced ERK1/2 phosphorylation, EtBr treatment did not have an effect in either the basal or DA-stimulated condition. The absence of a significant relationship was consistent between western blot and in-cell western experiments, though curiously the 2D[5] (and 2D[50], though non-significantly) EtBr doses did increase DA-

mediated ERK1/2 phosphorylation. While this suggests the possibility of mtDNA-independent effects of EtBr on DAR signaling, additional experiments may be needed to probe the reproducibility of these findings. Finally, the inverse relationship between D_2 stimulation of EtBr-treated mouse cultures (which elevated ERK1/2 phosphorylation) and rat cultures (which reduced ERK1/2 phosphorylation) could be re-examined. Once again, this may be partially attributable to different populations of glia (which have been shown to robustly express D_2 receptors), or to different receptor density between species.

This study also gave preliminary indications that EtBr treatment and mtDNA reduction may impact histone H3 and H4 acetylation. Histone acetylation is a major mechanism for modulating active gene transcription, as increased acetylation promotes chromatin relaxation, which gives transcription machinery access to the genome. Acetylation is regulated by two major classes of enzymes – histone acetyl transferases (HATs or KATs), which increase acetylation, and histone deacetylases (HDACs), which counteract their activity (Turner, 2000). Relevantly for LID, a principle HAT is CREB binding protein (CBP), which is potently activated through D_1-mediated activation of CREB (Chrivia et al., 1993). HDACs are a diverse group of proteins, including sirtuins, and the different members of this family are regulated by multiple mechanisms, including phosphorylation by PKA and CaMKs (Sengupta and Seto, 2004). The net acetylation of any residue in response to DA stimulation is thus difficult to predict *a priori*, and in this present study we attempted identify both which residues may be acetylated in response to DA, and if EtBr treatment affected either basal acetylation or DA-stimulated acetylation.

We first demonstrated that EtBr treatment significantly elevates H4K8 in mouse cultures, which may indicate an increase in the number of active gene transcription sites (Wang et al., 2008). Curiously, though acetylation at this residue is at least partially regulated by CBP (and p300) activity (Vernarecci et al., 2010; Gajer et al., 2015), we did not observe DA-dependent increases in acetylation at this residue. Total H4 deacetylation has been reported following the induction of LID (Nicholas et al., 2008), so it is unclear if this finding contributes to this process.

We next quantified acetylation at multiple H3 residues, including H3K9, H3K14, H3K18, and H3K27. Of these, we observed DA-dependent increases in acetylation at H3K9 and H3K14 in both control and EtBr-treated cultures. Acetylation at both of these residues are indicative of active gene transcription (Kouzarides, 2007; Karmodiya et al., 2012), and are likely linked to DA receptor stimulation through activation of CREB and CBP/p300. Though we observed no significant differences in DA-mediated acetylation following treatment with EtBr, EtBr treatment did significantly increase basal H3K9 and H3K27 acetylation. Interestingly, elevated acetylation at both of these residues promotes neuron differentiation (Ye et al., 2016), and alterations at these sites may be more important for the primary neuronal culture model. Synaptic remodeling is a key component of the pathophysiology of LID (Moratalla et al., 2017), and it is possible that deregulation of expression of these gene families may contribute to this mechanism. Total H3 acetylation is bidirectionally regulated in different animal models of LID, suggesting further research into specific residue modifications may be required (Nicholas et al., 2008). Finally, though these relationships did not achieve statistical significance in the present study, we did observe deficient H3 Ser10 phosphorylation in response to EtBr, both at baseline and in response to DA. This phosphorylation also facilitates gene transcription, similarly to acetylation. Our findings contrast with the observation that H3 phosphorylation is increased in animal models of LID, likely through an ERK1/2-dependent mechanism (Santini et al., 2012). As we also observed an inconsistent elevation in ERK1/2 phosphorylation, it is likely that further experiments may be necessary to solidify these findings.

We also examined the DA- and DA-agonist-dependent induction of both neuropeptide and IEGs, and though these systems were not dramatically affected by EtBr treatment, some inferences may be made to help guide future experiments. First, though none of these treatments reached statistical significance, DA or DA agonists predominantly increased ppd expression in EtBr-treated mouse cultures, while these treatments decreased ppd expression in control cultures. As ppd expression is substantially increased in response to DA in LID (Westin et al.,

2001), this difference may be a possible mechanism by which decreased mtDNA exacerbates dyskinesiogenic plasticity. Also in mouse cultures, EtBr treatment elevated cfos and egr in response to DA. These transcription factors are activated by the same Ca^{2+}-sensitive signaling pathway as ppd and may even regulate ppd expression (Sheng et al., 1990; Douglass et al., 1994; Konradi et al., 1996). Ca^{2+} may be the mechanism through which EtBr treatment and mtDNA reduction increase gene expression. A major function of mitochondria is the activity-dependent sequestration and buffering of Ca^{2+} (Nicholls, 2005), and it is possible that mtDNA reduction may compromise this activity, which would raise cytosolic Ca^{2+}. Elevated cytosolic Ca^{2+} could be a primary mechanism through which reduced mtDNA increases the activation of several DA-dependent pathways, though further studies would be beneficial to address it.

These experiments suggest that EtBr treatment may perturb DA signaling, but the poor reproducibility of the majority of these experiments and inconsistencies in results across species make it difficult to draw conclusions about these interactions. Broadly, the results of these experiments do seem to suggest that EtBr treatment and mtDNA reduction may perturb the basal activity of multiple DA signaling targets, such as ERK1/2 phosphorylation and histone acetylation. However, these findings may need to be repeated, as this study did not comprehensively evaluate the contributions of media components to basal signaling (i.e., glucose concentration, B27 addition – see Materials and Methods), and it may be fruitful to attempt these studies in pure neuronal cultures to isolate the variable contributions of glia across cultures. In order to examine alterations in response to DA, it may also be useful for future studies to evaluate the duration of some of these signaling responses. Many previous studies have demonstrated that a key component of pathological ERK1/2 phosphorylation and ppd expression is the persistence of their activation in response to stimulation (Santini et al., 2008). These types of analyses, in combination with the analysis of essential signaling intermediates such as Ca^{2+}, may prove essential to disambiguating our previous results.

4.2. Reduced mtDNA may promote mitochondrial fusion

While mitochondrial DNA encodes critical subunits of the RC, a family of nuclear genes mediates mitochondrial fusion and fission. Mitochondrial inner membrane fusion is orchestrated by Opa1, and outer membrane fusion is coordinated by Mfn1 and 2; all of which are small GTPases. In contrast, mitochondrial fission is predominantly performed by the GTPase Dnm1l/Drp1, which is recruited to the mitochondrial outer membrane by receptors such as Fis1 and Mff (Chan, 2012; Pernas and Scorrano, 2015). As mutations in these fusion genes are linked with distinct neurodegenerative disorders, perturbations in mitochondrial dynamics have been increasingly investigated as a component of the pathogenesis of neurodegenerative and neurological disorders. Interestingly, multiple studies have demonstrated that interference with mitochondrial fusion or fission reduces mtDNA copy number (Ono et al., 2001; Parone et al., 2008; Chen et al., 2010), but evidence for a reciprocal relationship is sparse. This study attempted to determine if EtBr-induced reduction of mtDNA could induce alterations in mitochondrial morphology. In our mouse experiments, we observed both a downregulation of Dnm1l and Fis1 and an upregulation of Opa1, which in concert suggest a pro-fusion response. An increase in mitochondrial fusion has been previously reported as a response to stress stimuli, as increasing fusion may increase respiratory efficiency. However, we observed an upregulation in both Opa1 and Dnm1l in our rat cultures in response to EtBr, suggesting instead the activation of gene programs responsible for both fission and fusion, and obscuring the type of response activated by mtDNA reduction.

To attempt to resolve this discrepancy, we used fixed-cell images of rat striatal NECos to quantify mitochondrial area, length, and distance from the nucleus, though we were only able to perform this analysis in glia. In response to the highest dose of EtBr, both mitochondrial area and length were significantly increased. However, we observed a significant increase in mitochondrial area in response to multiple EtBr exposure conditions, so it is unclear if this effect is a response to EtBr. Potentially, the combination of increased mitochondrial area and length may support our

gene-expression driven hypothesis that reduced mtDNA promotes fusion, but the effect size is modest, and additional studies will be required to support this conclusion. We also observed significant differences in mitochondrial distance from nucleus in every EtBr treatment group, with no correlation to dose or exposure time. This may suggest this metric is not particularly useful, especially considering distance was calculated without respect to the geometry of the glia. We had hypothesized that an increase in mitochondrial fusion may impair the efficient distribution of mitochondria to the more distal portions of the cell, which may deregulate ATP availability at sites of high demand like ion channels and vesicle release. However, it may be more useful in future studies to measure mitochondrial distribution using live cell imaging, which would facilitate the measurement of mitochondria along an axon and eliminate the necessity of imaging an entire neuronal cell body. This would also address the possibility that mtDNA reduction could affect mitochondrial trafficking kinetics.

5. Conclusion

The pathophysiology that underlies the development of LID is complex, especially as studies begin to consider not merely the hypersensitization of the D_1 signaling cascade, but also the pathways and intracellular perturbations that may promote this sensitization. Mitochondrial dysfunction may promote this hypersensitization in a number of way; from depolarization which may increase cytosolic Ca^{2+}, to impaired segregation and trafficking which may impair the distribution of energetic resources. The present study examined the impact of mtDNA reduction on several markers of LID signaling alterations, and observed some increases in ERK1/2 phosphorylation, IEG expression, and histone acetylation. Though these findings were not sufficiently reproducible to be conclusive, this work may provide directions for subsequent studies to continue investigating the contribution of mtDNA quantity to LID pathogenesis.

CHAPTER V

MTDNA DEPLETION DECREASES MITOCHONDRIAL CREATINE KINASE: IMPLICATIONS FOR L-DOPA INDUCED DYSKINESA

N.B.: Portions of this chapter (including text and figures) have been published in:

Warren EB, Aicher AE, Fessel JP, Konradi C (2017) Mitochondrial DNA depletion by ethidium bromide decreases neuronal mitochondrial creatine kinase: Implications for striatal energy metabolism. PLoS ONE 12(12): e0190456.

1. Abstract

LID is a debilitating treatment side effect in PD. Our lab previously found significantly lower levels of mtDNA in the post-mortem dorsal striatum (putamen) of individuals with LID. Given the disproportionately high energy demand of neurons, low mtDNA levels could cause disturbances in energy metabolism and prompt neuronal instability of the dyskinetic putamen. To understand the connection between mtDNA levels and bioenergy metabolism in the brain, we decreased mtDNA with EtBr in pure striatal neurons, pure glia, or NECos. The decrease in mtDNA reduced oxygen consumption in neurons and glia demonstrated a link between mtDNA levels and mitochondrial respiration. Interestingly, neurons and glia employed different adaptive mechanisms to meet their bioenergetic requirements. While glial cells increased their glycolytic activity, neurons responded by decreasing PCr levels. Concomitantly, mtCK was downregulated in neurons but not in glia. A downregulation of mtCK was also observed in the putamen of dyskinetic PD patients, indicating a similar adaptive mechanism. The data suggest that decreased mtDNA may impart a vulnerability for LID in PD patients by destabilizing the energy homeostasis of striatal neurons. Importantly, decreased Cr phosphorylation may serve as a potential biomarker for LID susceptibility.

2. Introduction

L-DOPA therapy of PD can lead to deleterious side effects known as LID (Rascol et al., 2000). Although both the stage of PD at the initiation of L-DOPA therapy and the dose of L-DOPA are risk factors for LID (Bastide et al., 2015), a considerable range in the liability to develop LID is observed (Ahlskog and Muenter, 2001; Fabbrini et al., 2007). In a previous attempt to identify etiological factors that may confer vulnerability for LID, we found that PD patients with LID had a 50% reduction of mtDNA in the dorsal striatum, or putamen compared to matched non-dyskinetic PD patients and healthy controls (Naydenov et al., 2010). The brain depends on energy availability more than any other organ (Du et al., 2008), and obstructions in oxidative metabolism in the striatum can lead to movement disorders (Janavs and Aminoff, 1998). However, a connection between mitochondrial abnormalities, bioenergetic metabolism and LID has not been made yet, and the relationship between mtDNA levels and bioenergetic health in the striatum is currently unknown. We were therefore interested to develop an experimental model in which we can study the bioenergetic consequences of mtDNA loss in striatal neurons and glia, as a step toward understanding how to interpret mtDNA loss in LID.

mtDNA, the discrete (non-nuclear) mitochondrial genome, encodes 37 genes, 13 of which are protein-coding (Figure 35A) (Wallace, 1999). These proteins are important components of the mitochondrial RC, which transfers electrons from NADH and $FADH_2$ to O_2, and establishes a proton gradient across the inner mitochondrial membrane to generate ATP (Nicholls and Budd, 2000). Maintenance of the mitochondrial genome is essential for the expression and function of the RC, evidenced by the multitude of mitochondrial diseases arising from mtDNA mutations (Taylor and Turnbull, 2005; Wallace, 2010). Consequently, the reduced levels of mtDNA in the putamen of dyskinetic PD patients may render them bioenergetically compromised and vulnerable to developing LID. A better understanding of the effects of mtDNA reduction on energy homeostasis in the striatum can help to build a bridge between the post-mortem observations and treatment approaches to LID.

Destabilization of energy homeostasis induces a variety of intracellular responses, many of which are cell-type specific. Some cell types can circumvent mitochondrial respiration and produce ATP via increased metabolic flux through glycolysis (Marrif and Juurlink, 1999; Volobоueva et al., 2007; von Kleist-Retzow et al., 2007; Wu and Wei, 2012). In the brain, for example, glia can upregulate glycolysis due to the differential expression of several key metabolic enzymes in neurons and glia (Fernandez-Fernandez et al., 2012; Bouzier-Sore and Pellerin, 2013). ATP balance and distribution in the brain can also be maintained through the Cr-PCr shuttle, which is active in high-energy tissues (Wallimann and Hemmer, 1994). mtCK transfers phosphates from newly generated ATP to Cr, to make PCr. PCr is trafficked through the cytosol and converted back into Cr by the cytosolic CK (in the brain, B-CK), to regenerate ATP. Not surprisingly, a significant fraction of B-CK is co-localized with ATPases such as ion pumps, which depend on ATP to maintain $\Delta\psi$ and neuronal network function (Andres et al., 2008). Perturbations in both glycolytic flux and in the Cr-PCr shuttle have been reported in many diseases related to mitochondrial dysfunction, from cancers to neurodegenerative disorders.

In the present study, we developed a model in rat primary cultures using EtBr to reduce mtDNA levels and to study the metabolic consequences. It has long been established that low concentrations of EtBr selectively reduce mtDNA without affecting nuclear DNA (Leibowitz, 1971), in a rapid and reproducible manner (Kai et al., 2006). To disambiguate the consequences of mtDNA loss in different cell types, we examined neuronal, glial, and NECos. Our goal was to gain insight into the bioenergetic repercussions of decreased mtDNA levels on striatal neurons and glia, for a better understanding of how low mtDNA levels might contribute to cellular malfunction in LID.

3. Results

3.1. EtBr dose- and time-dependently reduces mtDNA and mtRNA in rat primary cultures.

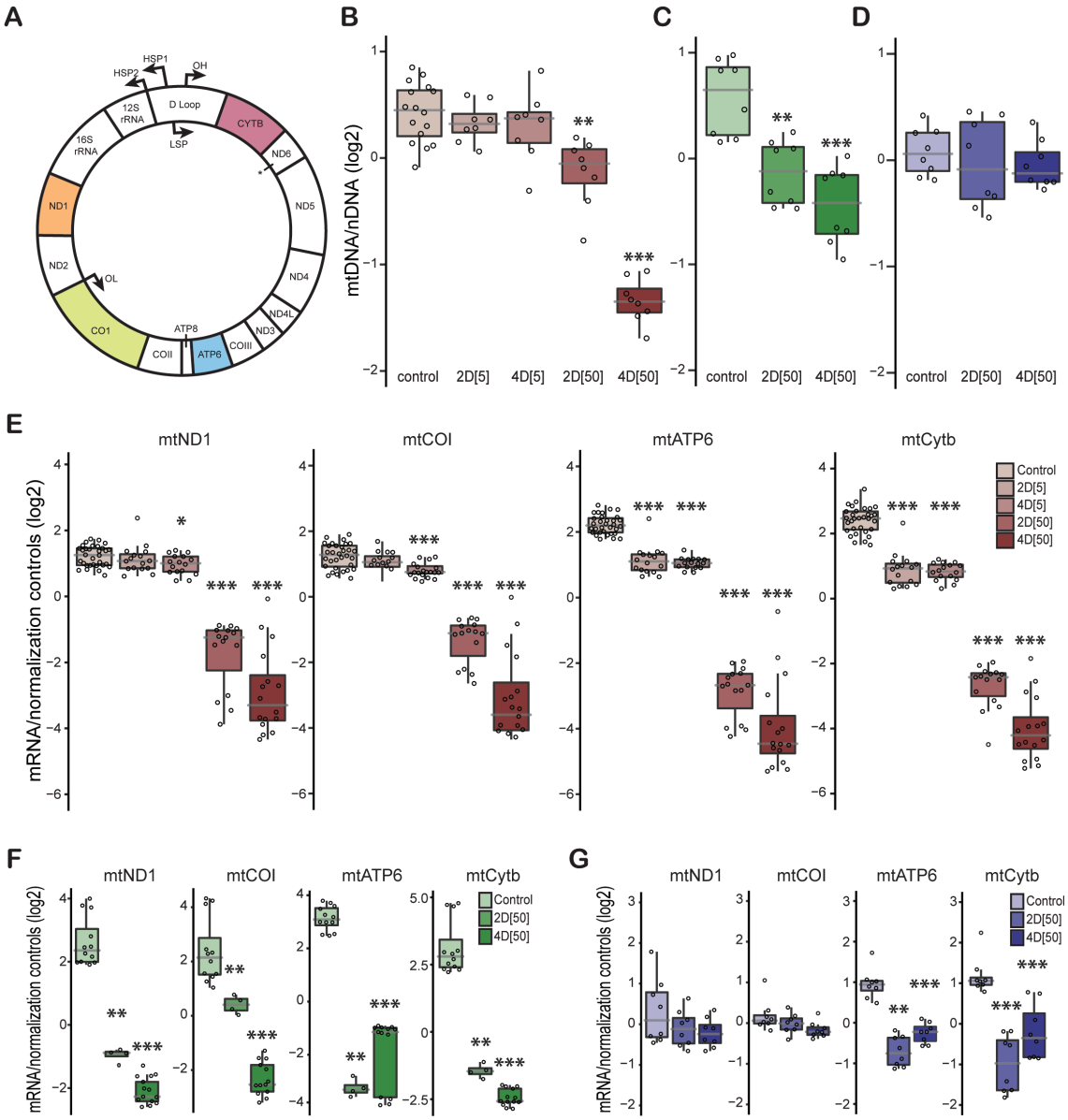

Figure 35. Exposure to EtBr dose- and time-dependently decreases mtDNA and mtRNA.
(A) The mitochondrial genome, with genes used for mRNA (mtRNA) analyses in color. OH, OL – origin of heavy or light chain replication; HSP1/2, LSP – heavy or light chain promoter; * - the ND6 gene is the only protein-coding gene on the light chain. Adapted from Schon, et al., 2012. (B-D) mtDNA quantity in response to EtBr treatment, normalized to nDNA, in neuron-enriched cocultures (B), pure neuronal cultures (C), and glia (D). (E-G) mtRNA expression in response to EtBr treatment, normalized to reference genes, in neuron-enriched cocultures, (E), pure neuronal cultures (F), and glia (G). Each point represents an independent sample, though the same samples were used across mtRNAs. 2D[5] = 5ng/ml EtBr for 2 days, 4D[5] = 5ng/ml EtBr for 4 days, 2D[50] = 50ng/ml EtBr for 2 days, 4D[50] = 50ng/ml EtBr for 4 days. *** = $p < 0.001$; ** = $p < 0.01$; * = $p < 0.05$, relative to controls following Wilcoxon's post-hoc test.

Optimal EtBr doses and exposure durations were determined in NECos. Treatment with 50 ng/ml EtBr two or four days before harvest (2D[50] and 4D[50], respectively) significantly reduced the relative quantity of mtDNA compared to controls (Figure 35B). In contrast, 5 ng/ml EtBr applied for two or four days (2D[5], 4D[5]) did not reduce mtDNA (Kruskal Wallis chi (KW) = 28.97, $p < 0.0001$). A similar response was observed in neuronal cultures (KW = 18.57, $p < 0.0001$), (Figure 35C), but not in glial cultures (Figure 35D).

EtBr intercalation also inhibited mtRNA transcription. Four protein-coding mtRNAs (mtNd1, mtCoI, mtAtp6, mtCytb – see Figure 35A) were robustly downregulated after EtBr treatment of NECos and neurons (Figure 35E, 35F), (NECo: mtNd1 – KW = 65.66, $p < 0.0001$; mtCoI – KW = 69.62, $p < 0.0001$; mtAtp6 – KW = 82.533, $p < 0.0001$; mtCytb – KW = 83.87, $p < 0.0001$), (Neuron: mtNd1 – KW = 23.44, $p < 0.0001$; mtCoI – KW = 23.44, $p < 0.0001$; mtAtp6 – KW = 20.85, $p < 0.0001$; mtCytb – KW = 23.44, $p < 0.0001$), with varying magnitude. Although glial mtDNA was not significantly reduced by EtBr, multiple mtRNAs were downregulated (Figure 35G), (mtNd1 – ns; mtCoI – ns; mtAtp6 – KW = 52.17, $p < 0.0001$; mtCytb –KW = 52.17, $p < 0.0001$), suggesting that this dose of EtBr does affect glial mitochondria. It has previously been observed that exposure of cells to EtBr promotes supercoiling and reduces access of pancreatic DNAse to mtDNA (Leibowitz, 1971). Such an occlusion will also affect RNA transcription and explains the difference in vulnerability between mtDNA and mtRNA. This notion is further supported in NECos, as 5 ng EtBr did not significantly affect mtDNA, but did significantly reduce the expression of some mtRNAs. To verify that glia mtDNA is not insensitive to EtBr, we treated glial cultures with 500 ng/mL EtBr over 4 days and observed a large downregulation in mtDNA and mtRNA (Supplemental Figure 2). However, in order to directly compare the three culture conditions, we used the 2D[50] and 4D[50] doses for all subsequent experiments, with particular emphasis on 4D[50].

3.2. mtDNA and mtRNA reduction decrease mitochondrial oxygen consumption

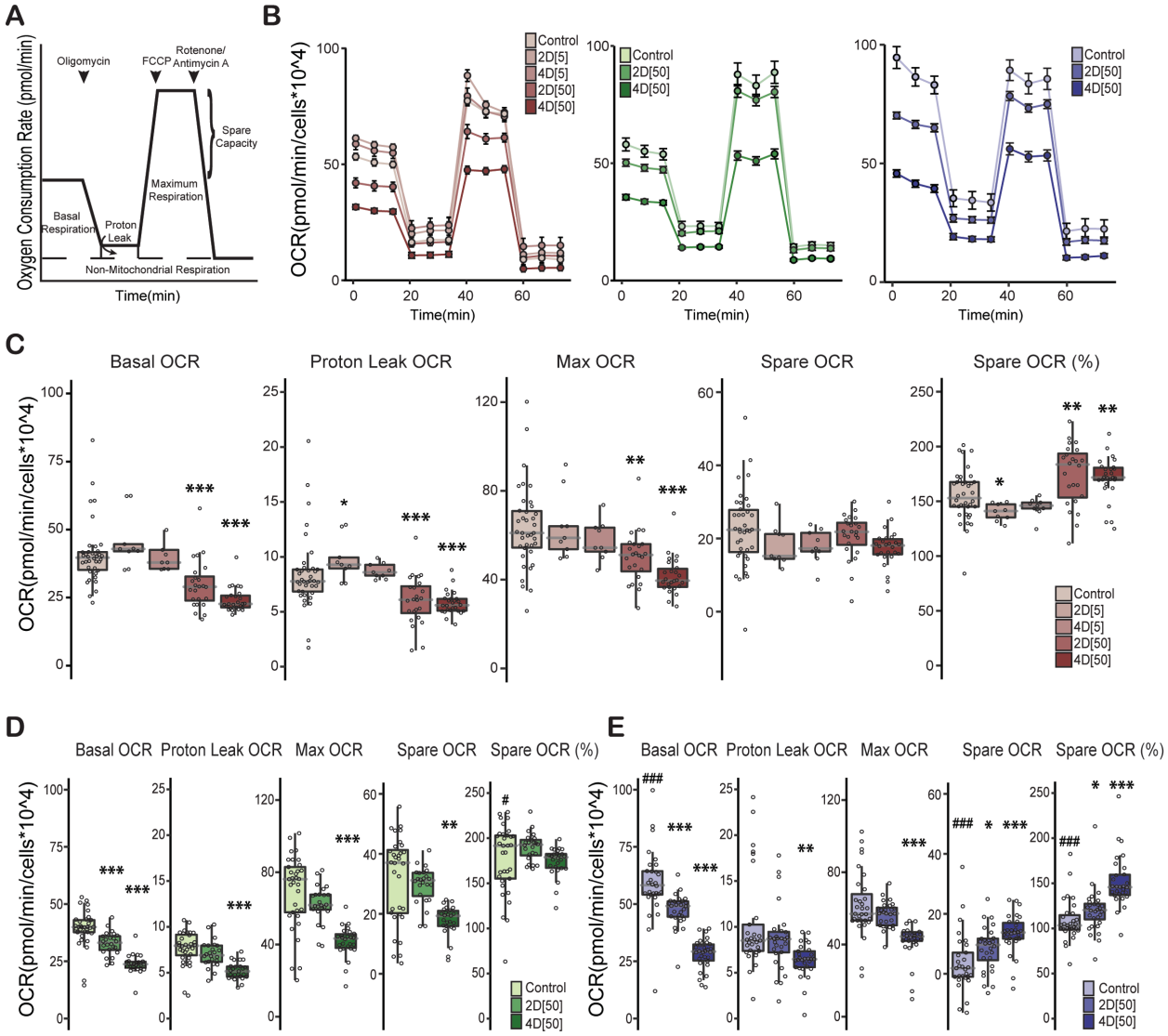

Figure 36. EtBr treatment reduces oxygen consumption and increases mitochondrial spare capacity in glia.

(A) Diagram of the procedure and measurements of the Seahorse assay. The sequential addition of mitochondrial toxins permits the measurement of different respiratory states. After recording basal respiration, oligomycin is added to block complex V and to eliminate ATP production-linked oxygen consumption. Addition of FCCP allows the free flux of protons through the mitochondrial inner membrane and maximum oxygen consumption. Rotenone and antimycin A inhibit complex I and III, and prevent proton pumping. Non-mitochondrial residual oxygen consumption is subtracted from all measurements. (B) Effect of EtBr on oxygen consumption rate (OCR) of NECos (left), neurons (middle), and glia (right). Error bars reflect +/-SEM. (C-E) Effect of EtBr on basal OCR, max OCR, leak OCR, spare OCR, and spare OCR as a percent of basal respiration in NECos (C), neurons (D) and glia (E). Each point represents an independent sample, though the same samples were used across measurements. *** = $p < 0.001$; ** = $p < 0.01$; * = $p < 0.05$, relative to in-group controls after Wilcoxon's post-hoc. ### = $p < 0.001$, relative to cell type controls following Tukey's HSD post-hoc.

To examine the functional consequences of mtDNA and mtRNA reduction, we measured oxygen consumption rate (OCR) in the Seahorse extracellular flux analyzer (Figure 36A). In NECo, neuron, and glia preparations, a reduction in OCR was observed in all mitochondria-linked stages (Figure 36B). In NECos, EtBr significantly reduced basal, maximum, and leak OCR, and increased spare OCR as a percent of baseline (Figure 36C), (basal – KW = 58.65, $p < 0.0001$, leak – KW = 45.66, $p < 0.0001$, max – KW = 39.35, $p < 0.0001$, spare percent – KW = 28.42, $p < 0.0001$). We observed a similar trend in neuron and glia cultures in response to EtBr (Figure 36D, 36E), (Neuron: basal – KW = 57.93, $p < 0.0001$, leak – KW = 42.93, $p < 0.0001$, max – KW = 45.15, $p < 0.0001$, spare – KW = 32.08, $p < 0.0001$, spare percent – KW = 28.42, $p < 0.0001$) (Glia: basal – KW = 73.89, $p < 0.0001$, leak – KW = 29.42, $p < 0.0001$, max – KW = 53.67, $p < 0.0001$, spare – KW = 24.38, $p < 0.0001$, spare percent – KW = 38.57, $p < 0.0001$). A comparison of untreated NECo, neuron, and glial cultures provided further insight. While the maximum OCR of all cultures was similar, the most dramatic difference was between the basal OCR of glia and neurons ($F = 7.87$, $p < 0.0001$). Glial basal OCR was not different from its maximum OCR, indicating a lack of spare capacity, whereas neuronal basal OCR was 60% of maximum (Figure 36D, 36E), (spare – $F = 23.33$, $p < 0.0001$; spare percent – $F = 19.05$, $p < 0.0001$). Glia cultures also diverged in their response to EtBr, which reduced basal OCR in glia much more than in NECos or neurons, and introduced a spare capacity into glial mitochondrial respiration (Figure 36E).

3.3. Glia, but not neurons, can respond to mitochondrial impairment by increasing glycolytic flux

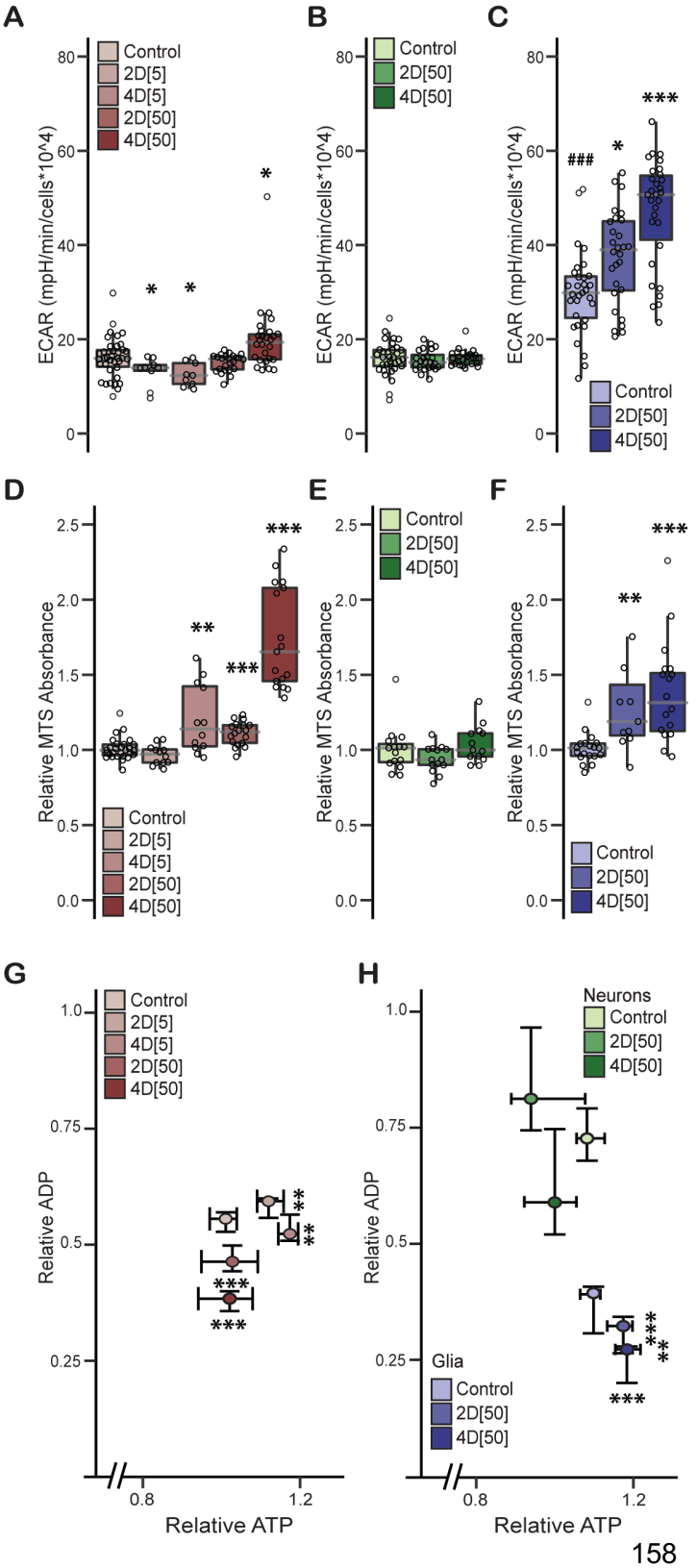

Figure 37. Impaired mitochondrial respiration increases glial, but not neuronal, rate of glycolysis.
(A-C) Effect of EtBr on basal extracellular acidification rate (ECAR) of NECos (A), neurons (B), and glia (C). (D-F) Relative quantity of electron donors (i.e. NAD(P)H, FADH2) in NECos (D), neurons (E), and glia (F), measured by MTS absorbance and normalized to cell number. Each point represents an independent sample. (G-H) Relative ADP plotted against relative ATP, in NECos (G), neurons (green; H), and glia (blue; H). *** = $p < 0.001$; ** = $p < 0.01$; * = $p < 0.05$, relative to in-group controls after Wilcoxon's post-hoc. ### = $p < 0.001$, relative to cell type controls following Tukey's HSD post-hoc. Error bars reflect interquartile range.

The reintroduction of a mitochondrial 'spare capacity' in glia may be partially explained by the change observed in basal extracellular acidification rate (ECAR), recorded simultaneously with OCR. Following EtBr treatment, glial basal ECAR increased by nearly 60% (Figure 37C), ($KW=23.08$, $p<0.0001$), suggesting a shift from oxidative phosphorylation to glycolysis for ATP production. Similarly, NECo ECAR, following EtBr treatment at 4D[50], increased by 18% (Figure 37A) ($KW = 106.9$, $p < 0.0001$). In contrast, EtBr treatment of neurons did not change basal ECAR (Figure 37B). ECAR of untreated glia was also over 90% greater than the ECAR of untreated neurons (compare Figure 37B to 37C), and 86% greater than the ECAR of untreated NECos (compare Figure 37A to 37C) ($F = 35.31$, $p < 0.0001$), suggesting that the rate of glial glucose catabolism exceeds that of neurons.

An increase in glycolytic activity together with a reduction in RC activity should lead to the accumulation of NADH. In NECo cultures, decreased mtDNA was accompanied by increased absorbance in an electron donor-dependent assay (Figure 37D), ($KW = 55.18$, $p < 0.0001$). This was also observed in glial cultures (Figure 37F) ($KW = 39.35$, $p < 0.0001$) but not in neuronal cultures (Figure 37E). Likewise, EtBr treatment of NECos and glia increased NADH without changing NAD+ levels in a specific NAD+/NADH assay (Supplemental Figure 3).

Decreased mitochondrial function also perturbed the ADP-ATP balance of NECos, (Figure 37G), (ATP – $KW = 18.11$, $p < 0.0001$; ADP – $KW = 45.35$, $p < 0.0001$) and glia (Figure 37H), (ATP – $KW = 21.18$, $p < 0.0001$; ADP – $KW = 17.38$, $p < 0.0001$). EtBr reduced ADP with little effect on ATP, and significantly changed the ADP/ATP ratio. In contrast, the reduction in neurons was not significant and did not affect the ratio (Figure 37H).

3.4. Neurons, but not glia, respond to mitochondrial impairment with a disruption in the phosphocreatine-creatine shuttle

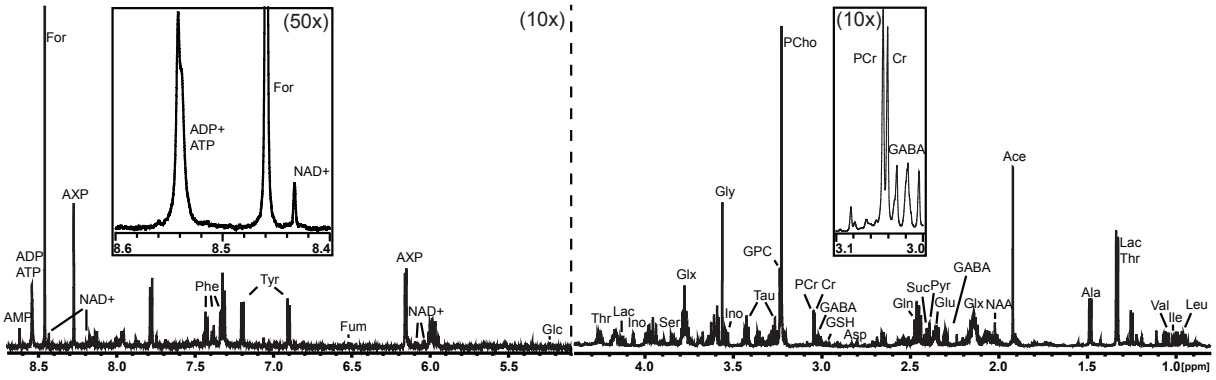

Figure 38. Representative NECo ^{1}H NMR spectra at 600MHz from control NECo cultures from 0.8-4.5 ppm and from 5.0-8.8 ppm.
5.0-8.8 ppm section is magnified 10x relative to 0.8-4.5 ppm section. Leu – leucine; Ile – isoleucine; Val – valine; Lac – lactate; Thr – threonine; Ala – alanine; Ace – acetate; NAA – N-acetyl aspartate; Glx – glutamine/glutamate; GABA- gamma-amino butyrate; Glu – glutamate; Pyr – pyruvate; Suc– succinate; Gln – glutamine; Asp – aspartate; Cr – creatine; PCr – phosphocreatine; PCho – phosphocholine; GPC – glycerophosphocholine; Tau – taurine; Gly – glycine; Ser - serine; Ino – myoinositol; Glc – glucose; Fum – fumarate; Phe – phenylalanine; Tyr – tyrosine; AXP – combined adenine nucleotides; For – formate. Acetate and formate peaks are contaminants from sample preparation. Insets – Metabolites quantified for this study. Right, PCr and Cr peaks, 10x magnified. Left, ADP+ATP peak, 50x magnified.

While our data showed that glia increased glycolytic activity in response to decreased mitochondrial respiration, neurons did not have that capacity. Previous studies in other neurological disorders have linked mitochondrial dysfunction to perturbations in CK gene expression (MacDonald et al., 2006; Clay et al., 2011) and PCr utilization (Zhang et al., 2010; Yuksel et al., 2015). CK isoforms and the CrT are differently expressed in neurons and glia (Tachikawa et al., 2004; Lowe et al., 2013, 2015), which could allow for cell-type specific mechanisms of regulating the Cr-PCr shuttle. We were therefore interested in quantifying Cr and PCr with ^{1}H-NMR. Figure 38 shows a representative ^{1}H-NMR spectrum from NECo cultures. We identified 30 different metabolites with a targeted metabolomic approach in NECo extracts, and quantified Cr, PCr, and the combined ADP+ATP peak in NECo, neuronal, and glial cultures. Decreased mtDNA significantly decreased the amount of PCr increased the amount of Cr, and decreased the PCr/Cr ratio in NECo cultures (n = 16), (Figure 39A). Neurons similarly had a

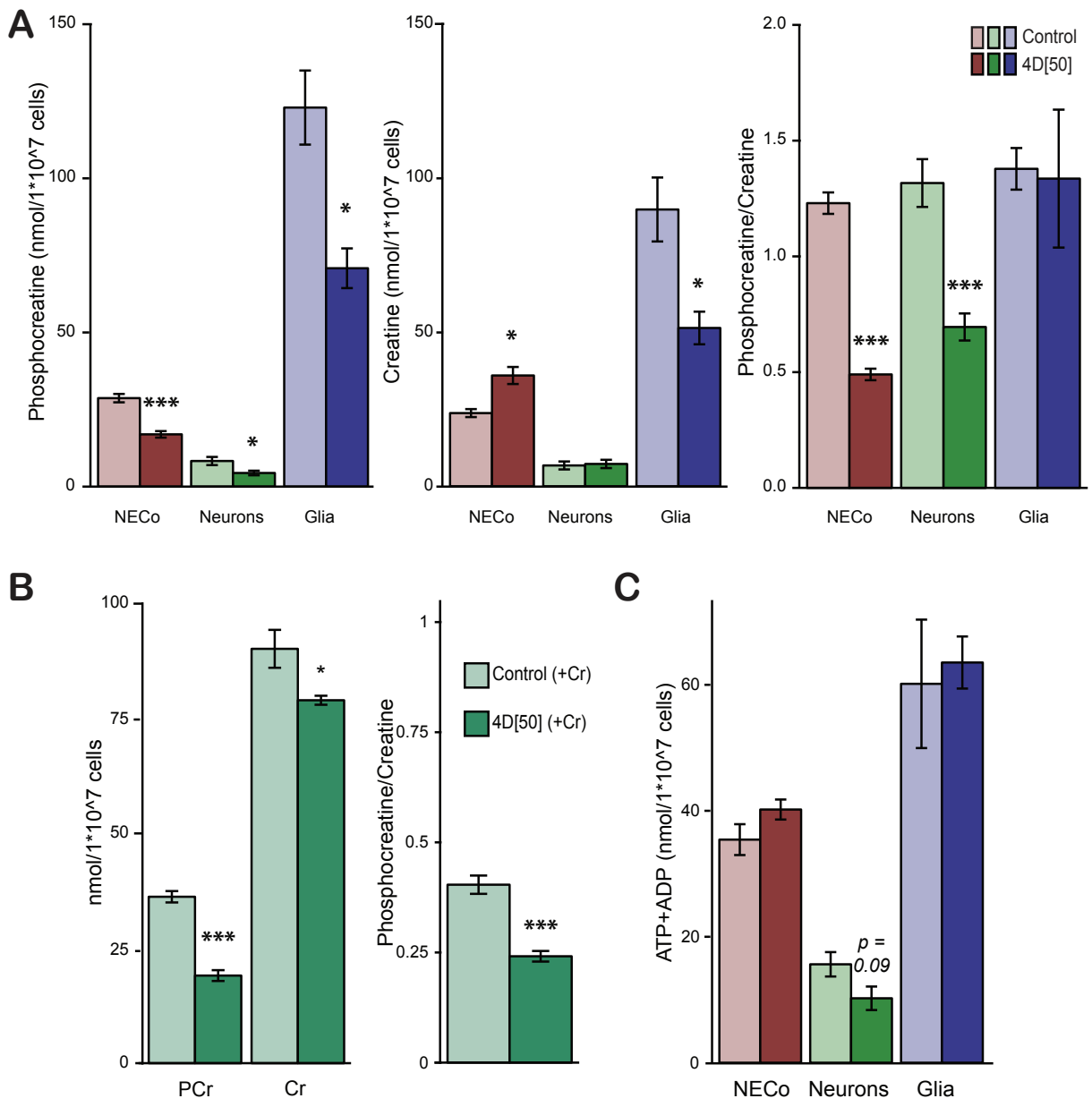

Figure 39. Reduced mitochondrial function decreases neuronal PCr/Cr ratio, and decreases glial tCr.
(A) Phosphocreatine (PCr), creatine (Cr), and PCr/Cr ratio in NECos, neurons, and glia, with and without EtBr. (B) Absolute PCr, Cr, and PCr/Cr ratio in neuronal cultures supplemented with 5 mM Cr 24h before harvest, with and without EtBr. (C) ATP+ADP in NECos, neurons, and glia, with and without EtBr. Error bars reflect +/-SEM. *** = $p < 0.001$; ** = $p < 0.01$; * = $p < 0.05$, compared to respective controls, following Tukey's HSD post-hoc test.

significant reduction in PCr and the PCr/Cr, though no change in Cr (control n = 8, treated n = 9). In glia, PCr and Cr were significantly reduced, with no change in the ratio (n = 5). Because the final step for Cr synthesis is predominantly carried out in glia (Tachikawa et al., 2004), the

neuronal cultures had a low basal concentration of Cr. To ensure that the reduction in PCr is not a phenomenon of low Cr levels, or an artifact due to methodological limitations in the NMR assay, we re-examined the PCr/Cr ratio in neuronal cultures supplemented with 5 mM Cr 24h before harvest (n = 4 – single dissection). While the total amount of Cr and PCr increased considerably, EtBr-treated cultures still had significantly decreased PCr, and a significantly decreased PCr/Cr ratio (Figure 39B). The amount of ATP+ADP was not different after EtBr treatment in any cell type (Figure 39C), which indicates that the reduction in ADP observed in prior experiments does not reflect a change in the total ATP+ADP pool.

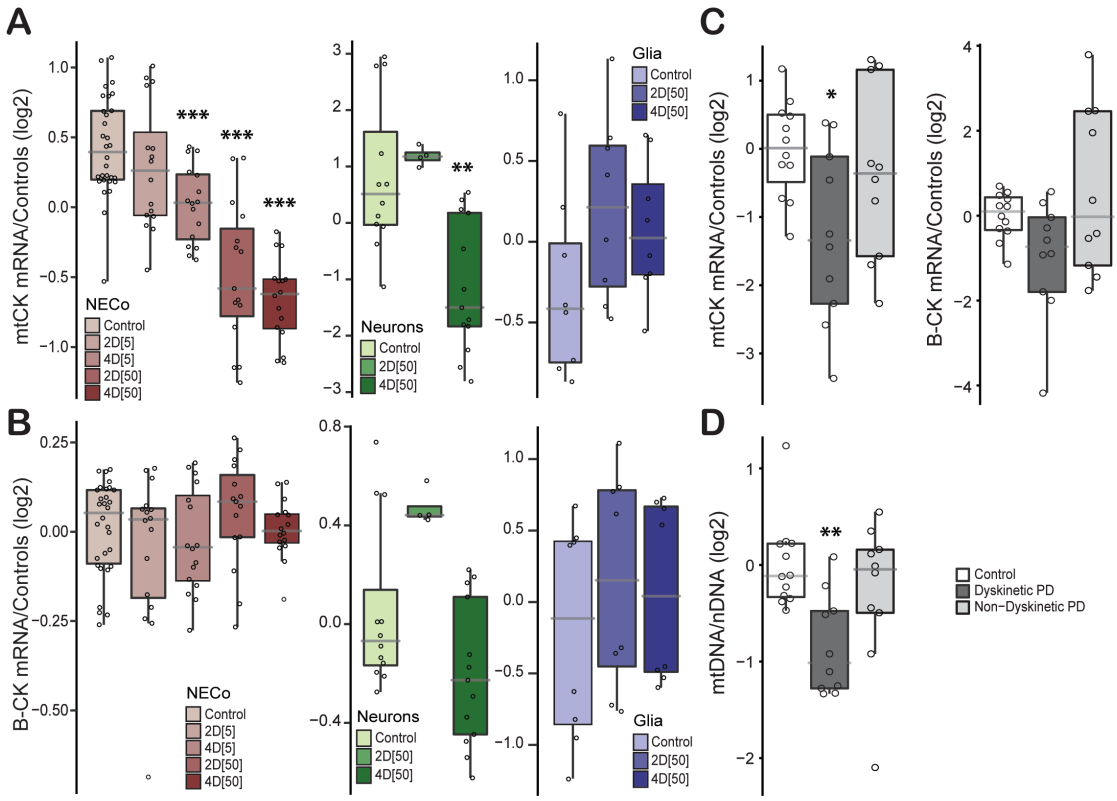

Figure 40. Decreased mtDNA quantity corresponds to decreased expression of mtCK.
(A) mtCK mRNA levels in rat NECos (left), neurons (middle), and glia (right), normalized to reference genes, in the presence and absence of EtBr. (B) B-CK mRNA in rat NECos (left), neurons (middle), and glia (right), normalized to reference genes, in the presence and absence of EtBr. *** = $p < 0.001$; ** = $p < 0.01$, relative to respective controls, following Wilcoxon's post-hoc test. (C) Expression levels of mtCK and B-CK in matched human control subjects, dyskinetic and non-dyskinetic PD patients, normalized to reference genes. Each point represents an independent sample, though the same samples were used across genes. (D) Relative mtDNA quantity from the same cohort as in (C), normalized to nDNA (Naydenov et al., 2010). ** = $p < 0.01$, * = $p < 0.05$, following Tukey's HSD post-hoc test.

We further examined the expression of the genes involved in the regulation of the PCr/Cr pool – mtCK and B-CK. EtBr treatment decreased expression of mtCK in NECos (KW = 52.28, $p < 0.0001$), and neuron cultures (KW = 13.6, $p < 0.0001$), but not in glia (Figure 40A). B-CK was not altered in any of the three cultures (Figure 40B). Despite reports of the segregation of mtCK into neurons, and B-CK into glia (Lowe et al., 2013; Tachikawa et al., 2004), we detected expression of both genes in both culture types, which may also be a consequence of the early developmental stage of these cultures.

We were able to examine mRNA expression in the putamen of PD patients with LID, and found significantly decreased mtCK levels compared to controls ($F = 3.722$, $p = 0.03$), (Figure 40C, left), and no significant change in B-CK (Figure 40C, right). In contrast, neither gene was significantly different from control in non-dyskinetic PD patients. LID patients also showed a reduction in mtDNA levels (Figure 40D) ($F = 5.546$, $p < 0.01$), (partial sample overlap with previously published data (Naydenov et al., 2010)).

4. Discussion

We previously identified decreased mtDNA in PD patients who developed LID (Naydenov et al., 2010), and here present a mechanism that shows the effects of mtDNA reduction on energy homeostasis of striatal neurons and glia. We also observed a relationship between mtDNA, mtCK expression, and PCr levels in neurons, and were able to show that the decrease in mtCK expression observed after mtDNA loss is also observed in PD patients with LID, who have significantly lower mtDNA levels. As PCr can be measured *in vivo* with magnetic resonance spectroscopy (MRS) it would not be difficult to envision using PCr as a biomarker to identify PD patients most susceptible to LID development (Barbiroli et al., 1993; Saneto et al., 2008; Ren et al., 2015).

4.1. The utility of EtBr in modeling suppression of mtDNA and mtRNA quantity

EtBr accumulates in mitochondria, where it intercalates into mtDNA and interferes with replication (Leibowitz, 1971) and transcription (Zylbee et al., 1969). Though this unique property is typically employed to generate rho0 cell lines (Desjardins et al., 1985; Armand et al., 2004; Yu et al., 2007), it is also a powerful and rapid means to manipulate mtDNA and mtRNA quantities in primary cultures. In our experiments, glial mtDNA was less sensitive to EtBr than neuronal mtDNA, as higher doses were required to significantly reduce mtDNA in glia (Supplemental Figure 2). However, mtRNA was reduced in glia even at the lower EtBr concentration, most likely because the occlusion of mtDNA by EtBr renders it inaccessible to mtRNA polymerase (Leibowitz, 1971). Interestingly, the degree of mtRNA downregulation varied correspondingly with the distance of the gene from the heavy chain promoter, with the closest gene the least downregulated, and the most distal gene the most downregulated. This difference can be explained by the polycistronic nature of mtRNA transcription; POLRMT transcribes the entire mtDNA plasmid, and individual mtRNAs are cleaved in subsequent steps (Mercer et al., 2011; Rorbach and Minczuk, 2012; Haute et al., 2015). By intercalating into mtDNA, EtBr might cause premature transcription cessation, which would more dramatically affect mtRNAs that are further from the promoter.

4.2. Decreased mtDNA and mtRNA reduces mitochondrial respiration and increases glycolytic flux in glia

Basal, maximum, and leak respiration were reduced after EtBr treatment in all culture conditions. Despite the lower sensitivity of glial mtDNA to EtBr, the reduction in mtRNA was enough to reduce mitochondrial OCR. The net reduction in all measured aspects of mitochondrial oxygen consumption suggests that the effect of EtBr was not specific for a particular RC complex. Rather, the significant reduction in leak OCR indicates a reduction in the proton pumping activity

of complexes I-IV. Despite the reduction in OCR function, all cultures remained viable throughout the experiment, suggesting that neurons and glia have compensatory mechanisms to deal with bioenergetic stress.

Glial basal respiration was equal to its maximum, in contrast to neurons, which reserved a significant spare capacity. This difference has also been previously observed (Damiano et al., 2014), and may be a consequence of the greater metabolite transport burden in glia. Following EtBr treatment, glia basal respiration was significantly lower than its maximum, a reclamation of spare capacity that was unexpected but could be a consequence of the switch to alternative metabolic pathways. ATP production in glia was shunted away from mitochondrial respiration toward an increase in glycolytic flux, demonstrated by an increase in glial ECAR, an increase in NADH, and an increase in glucose consumption (Supplemental Figure 1). This supports previous observations of the capacity of glia to increase the rate of glycolysis, which has been shown to be a function of cell-type specific expression of PFKFB3 (Herrero-Mendez et al., 2009; Bolaños et al., 2010). Increased expression of this enzyme increases production of fructose-2,6-bisphosphate, which stimulates phosphofructokinase, a rate-limiting enzyme in glycolysis. In neurons, however, PFKFB3 is constitutively degraded, which precludes upregulation of glycolysis (Herrero-Mendez et al., 2009), and other compensatory mechanisms are employed.

4.3. Reduced mtDNA in neurons diminishes PCr levels

Mitochondrial function is vital for maintaining intracellular phosphate balance, which is particularly important for neurons (Kann and Kovács, 2007). Our results suggest that decreased mtDNA reduces mitochondrial oxygen consumption, most likely via a reduction in the number of functional RC units, which would constrain ATP production. To compensate for the loss of ATP, neurons diminish their reserves.

One of the first targets of mitochondrially-generated ATP is mtCK, which is complexed with the adenine nucleotide transporter, in charge of exchanging ATP and ADP across the inner mitochondrial membrane (Dolder et al., 2003). mtCK resides in the intermembrane space of mitochondria where it transfers a phosphate from ATP to Cr to form PCr. PCr is shuttled to sites of use (Wallimann and Hemmer, 1994; Schlattner et al., 2006; Wallimann et al., 2011), where B-CK regenerates Cr and ATP (Schlattner et al., 2016). Under high glycolytic ATP production, B-CK may function as a kinase as well as a phosphatase in the cytosol, interconverting Cr and PCr (Schlattner et al., 2016). In contrast, the high concentration of ATP near mtCK renders its function almost exclusively unidirectional as kinase. A downregulation of mtCK should consequently decrease the levels of PCr, whereas changes in B-CK expression could have more complex effects on the PCr/Cr ratio. Accordingly, we detected a reduction in PCr that coincided with a decrease in mtCK.

Most cases of compromised energy state lead to an upregulation of mtCK [50]. For example, in certain mtDNA mutation disorders (MELAS, MERRF, CPEO), the sarcomeric isoform of mtCK is upregulated. However, downregulation of mtCK has been observed in a number of cancers – particularly in the myocyte to sarcoma transition (Patra et al., 2012; Yan, 2016). As tumorigenesis progresses, increased energetic demand may require the immediate use of all ATP and disfavor the synthesis of PCr. Interestingly, this may mirror the pattern of activity observed in LID, as the flood of L-DOPA-derived DA on a DA-deprived system, and subsequent high flux through various signaling pathways, is energetically costly.

The Cr-PCr system functions as a temporal and spatial energy buffer of vital importance for synaptic activity, membrane polarization, and general cellular maintenance. CK is associated with synapses and with membrane ATPases such as ion pumps in the plasma membrane, where it can quickly convert PCr to Cr and ATP to maintain network activity (Andres et al., 2008). A

shortage of PCr at sites of high ATP demand may contribute to the deregulation of MSNs, as it becomes more difficult to regulate ion channels, Δψ, and vesicle releases (Du et al., 2008).

4.4. Creatine phosphorylation as a biomarker for LID susceptibility

A few observations from previous studies point to deregulation of the PCr/Cr system as a potential mechanism in LID. A study of the 6-OHDA/L-DOPA model of LID in rats identified a decrease in mtCK and in GAMT, an enzyme involved in Cr synthesis, as a factor differentiating dyskinetic from nondyskinetic rats (Konradi et al., 2004). A subsequent proteomic analysis of this 6-OHDA/L-DOPA rat model re-identified GAMT downregulation in rats with LID (Valastro et al., 2007). Since GAMT is a key enzyme in Cr biosynthesis, these rats will likely have decreased amounts of Cr and PCr, and a concomitant perturbation in mtCK expression may further reduce PCr. Analogously, we observed that EtBr-treated glia cultures had significant reductions in both Cr and PCr, and neurons had a reduction in PCr/Cr ratio and mtCK and B-CK expression.

Our findings support a clinical relevance of PCr/Cr for LID. Although a recent clinical trial with oral Cr supplementation did not slow the progression of PD (Kieburtz et al., 2015), this study did not examine the effect of Cr on dyskinesia. We hypothesize that reduced PCr availability could be a critical component in the progression of LID. Moreover, PCr/Cr may serve as a diagnostic marker for LID susceptibility. As we have shown here and previously (Naydenov et al., 2010), dyskinetic PD patients have lower mtDNA levels. We now advance these findings by showing that reducing mtDNA levels leads to decreased mtCK and to reduced availability of PCr in primary striatal neurons. Moreover, we show that dyskinetic PD patients also have reduced mtCK expression. PCr, which plays a central role in brain health, is also one of the few compounds detectable in *in vivo* ^{31}P-MRS (Barbiroli et al., 1993; Saneto et al., 2008; Ren et al., 2015). Therefore, Cr phosphorylation capacity in PD patients can be used as a biomarker for risk of LID development, and help clinicians to target therapeutic options to individual PD patients.

5. Conclusion

Maintenance of mitochondrial function is important for the brain and for neurons with their high demand for ATP. Our prior studies demonstrated that patients with LID have less mtDNA in the putamen than their non-dyskinetic counterparts. Because post-mortem studies preclude functional analyses, the exact cellular consequences of that finding were unknown. mtDNA encodes several critical subunits of the RC, but the extent to which mtDNA quantity affects striatal mitochondrial function has not been resolved. We now demonstrate that decreasing mtDNA in rat primary cultures decreases mtRNA and respiration, increases glycolysis in glia, and perturbs the neuronal phosphate balance by decreasing mtCK expression and Cr phosphorylation in neurons. Importantly, we also demonstrate that mtCK is significantly downregulated in patients with LID. These observations enhance our understanding of how decreased mtDNA in the putamen may contribute to LID. Moreover, the reduction in Cr phosphorylation can serve as a non-invasive, MRS-detectable biomarker to assess which PD patients are at greater risk for LID.

6. Supplemental Figures

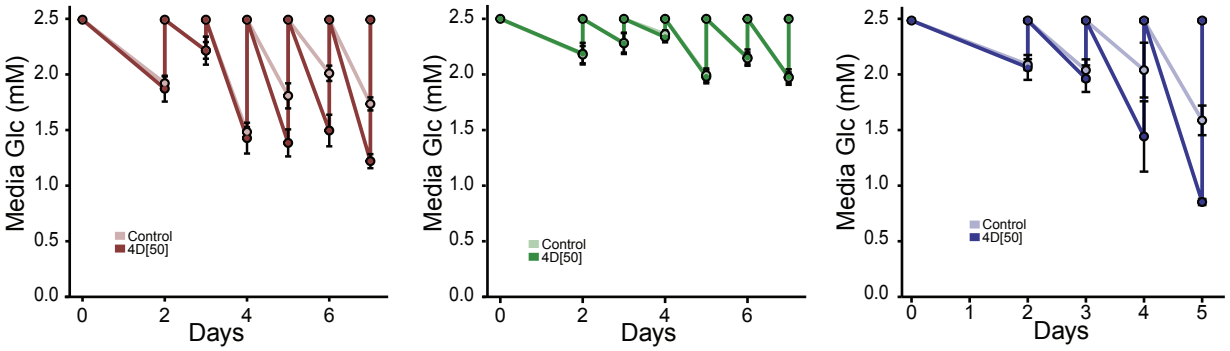

Supplemental Figure 1. EtBr treatment increases NECo and glia glucose consumption.
Representative traces from single dissections of NECo (left), neuron (middle), and glia (right) media glucose concentrations from plating until harvest. Beginning DIV2, media glucose was monitored daily and restored to 2.5 mM. Glucose concentrations decreased more rapidly in glia and NECo cultures under EtBr treatment. NECo – control n = 10, treated n = 11; neuron – control n = 11, treated n = 12; glia – n = 6. Error bars reflect +/-SEM.

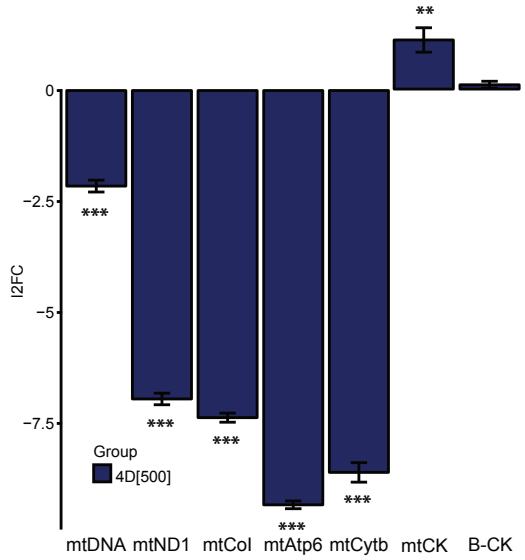

Supplemental Figure 2. A high dose of EtBr significantly reduces glia mtDNA, mtRNA, and increases mtCK.
Log2-fold change in mtDNA and mtRNA quantity in glial cultures in response to 500 ng/mL EtBr for 4 days (4D[500]). Single dissection, n=6. Expression was normalized to nDNA (for mtDNA) or reference genes (for mtRNA). ** = $p < 0.01$; *** = $p < 0.001$, relative to controls. Error bars reflect delta-method propagated +/-SEM. Baseline (0 on y-axis) reflects control levels.

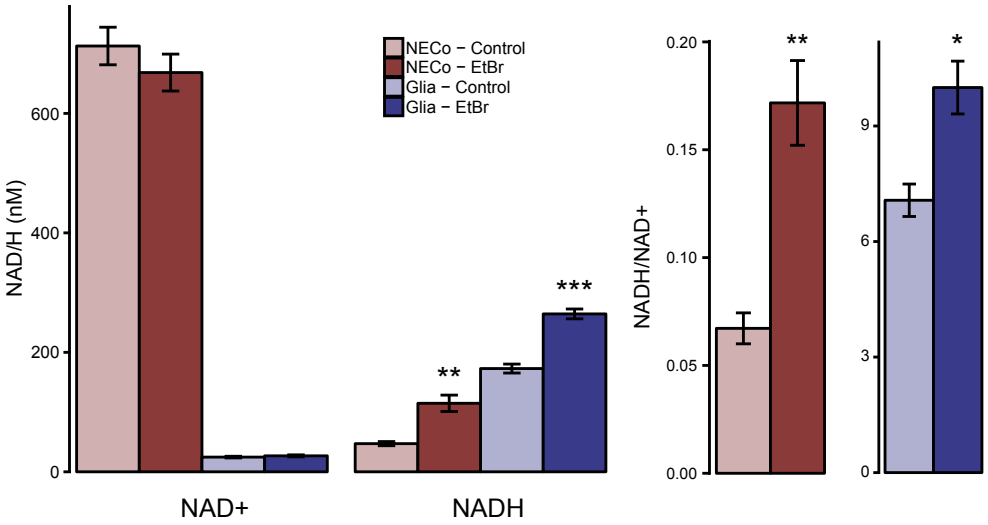

Supplemental Figure 3. EtBr decreases NAD+ and increases NADH and NADH/NAD+ ratio in NECos and glia.

Left, Absolute NAD+ and NADH concentration in NECo and glia cultures (nM); Right, NADH/NAD+ ratio for NECo and glia cultures. Both experiments are from a single dissection, NECo n = 5; glia n = 6. * = $p < 0.05$; ** = $p < 0.01$; *** = $p < 0.001$, relative to controls. Error bars reflect +/- SEM.

CHAPTER VI

DISCUSSION

1. Summary

As the causes of dopaminergic denervation and disease progression in PD remain poorly defined, so too are the underlying causes of the development of LID. The focus of this work has been to examine the contributions mtDNA quantity in the striatum to the pathogenesis of LID. Previous work in our lab identified mtDNA quantity in the putamen as a factor differentiating age- and L-DOPA dose-matched dyskinetic PD patients from non-dyskinetic PD patients (Naydenov et al., 2010), and though this finding was observed post-mortem, we hypothesized that this difference may have contributed to the segregation of these two groups. We speculated that PD patients with mtDNA quantity that had randomly been reduced more dramatically through the aging process than others may be more susceptible to developing LID in response to L-DOPA therapy. This study has refined a model for mtDNA depletion in primary neuronal cultures, described molecular alterations in response to mtDNA depletion that may contribute to the pathogenesis of LID, and demonstrated a relationship between mtDNA and mtCK expression, which could eventually provide a method for the in vivo detection of brain mtDNA quantity.

1.1. The utility of ethidium bromide in establishing a model of mtDNA depletion in primary striatal cultures

The first objective of this study was to determine a reproducible method of reducing mtDNA quantity in a culture system that sufficiently mimics the *in vivo* physiology of the striatum. Though we attempted to use gene knockdowns to reduce mtDNA quantity by impeding the function of the mtDNA replisome in cell lines, we found that this approach did not consistently reduce mtDNA quantity, particularly over successive cell divisions. This is likely because cells

with a high degree of knockdown and low mtDNA quantity were selected against, and consequently the degree of temporal separation between gene knockdown, mtDNA quantity reduction, and the subsequent physiological effects we were attempting to evaluate was too great to make this model practical. The low MOI of the lentiviral system and requirement for post-transfection antibiotic selection made this system unsuitable for a primary culture system as well, as an insufficient quantity of neurons survived this procedure to be used for molecular analyses.

In order to increase reproducibility and to more tightly control the degree of mtDNA depletion, we turned to treatment with EtBr, where we could directly regulate the exposure dose and duration. Interestingly, this method was also ineffective in our cell line experiments, as we found EtBr treatment did not consistently reduce mtDNA in this system across multiple cell divisions. As EtBr has been extensively used to reduce mtDNA (Schroeder et al., 2008; Kao et al., 2012; Nacarelli et al., 2014), and has even been used to create ρ0 cells which completely lack mtDNA (Fukuyama et al., 2002; Kukat et al., 2008; Schon et al., 2012), this approach was unexpectedly unsuccessful in our hands. We may not have used sufficiently high doses of EtBr for our probed cell lines, or, similarly to our lack of success with the gene knockdown approach, multiple passages may have selected against cells with significant reductions in mtDNA quantity. Instead, EtBr was very effective at the reduction of mtDNA in primary striatal cultures. We observed consistent reduction of mtDNA in both mouse and rat primary striatal neuron and glia co-cultures, and this reduction was correlated with both EtBr dose and the duration of EtBr exposure, which allowed us to probe different degrees of mtDNA reduction.

In rat cultures, we also demonstrated that isolated primary striatal neurons are more sensitive to mtDNA reduction than isolated primary glia, as at the dose used for the majority of our experiments (four days of 50ng/mL exposure with no washout – 4D[50]) did not significantly reduce glial mtDNA. Curiously, the 4D[50] dose consistently reduced mtDNA to a greater degree in cocultures than in isolated neuronal cultures (reduced to approximately 70% of control and to 50% of control, respectively). This likely indicates that neuron and glia cocultures can sustain

lower levels of mtDNA before inducing apoptosis in contrast to neuronal cultures; indeed, in some of our experiments we observed a small amount of cell loss in isolated neuron cultures, which may suggest that isolated neurons begin to die when mtDNA is depleted below 50% of control.

In addition to mtDNA, in rat cultures we observed that EtBr also dose- and time-dependently reduces mtRNA expression. This reduction was much more dramatic than the reduction in mtDNA, as for example, a reduction in mtDNA to approximately 50% of control was accompanied by an mtRNA reduction to 1-6% of control, depending on the transcript. We also discovered that though low doses of EtBr (i.e., 2D[5] and 4D[5]) did not affect mtDNA quantity, it did significantly reduce the expression of some mtRNA transcripts. This exaggerated reduction likely has two major causes: first, mtRNA is transcribed more frequently than mtDNA is replicated, so the inhibitory effects of EtBr would be more readily visible in mtRNA quantity, and second, as the mechanism of action of EtBr is its intercalation into dsDNA, it interferes with the action of Polγ, but also POLRMT, which should reduce transcription. Though this difference was useful for examining different degrees of inhibition of mitochondrial function, it is also important for considering the future applications of the results of this study, as we may have observed a greater reduction in mitochondrial function than the degree of mtDNA reduction would suggest. This dual inhibition may go some way to account for the discrepancy between some of our results and those typically reported in the literature, as we observed significant reductions in mitochondrial function following as little as a 30% reduction in mtDNA quantity. This contrasts with the known 'threshold effect' of mtDNA mutations (Rossignol et al., 2003; Stewart and Chinnery, 2015), which suggests that mtDNA mutations do not typically become pathogenic until they are present in >80% of mtDNA plasmids. However, there is less of a consensus about the level of mtDNA depletion required to observe an effect on mitochondrial function, and this level may vary more across model systems. For example, West et al., 2015 observed little effect on OCR in a Tfam+/- mouse embryonic fibroblast cell line with 50% mtDNA reduction, Lin et al., 2016 observed about a 40% reduction in OCR following a 30% reduction in mtDNA in a Tfam knockdown renal cell

carcinoma cell line, and Guha et al., 2013 observed a selective reduction in maximum but not basal OCR following EtBr-mediated mtDNA reduction of a breast cancer cell line by 70%. Though the degree of mtDNA reduction and its correlation to physiological effects may not be directly translatable for future studies, we believe the present work still accurately reflects pathways and processes perturbed by changes in mtDNA quantity.

1.2. The metabolic shifts induced by mtDNA reduction in striatal cultures

Having established a model of mtDNA (and mtRNA) reduction in primary striatal neuron, glia, and neuron and glia cocultures, we next investigated the impact of this reduction on cellular physiology. The protein-coding genes of mtDNA form the subunits of the mitochondrial RC, which establishes and utilizes an electrochemical gradient to generate ATP. This process consumes oxygen, and consequently activity of this RC is linked to OCR. As discussed above, mtDNA quantity and OCR do not necessarily correspond, so we investigated this relationship in our cultures.

In this study, we found that mtDNA depletion through EtBr treatment was sufficient to significantly reduce all measured forms of mitochondrially-linked oxygen consumption. This suggests that the EtBr-mediated reduction in mtDNA also translates to a net reduction in the number of functional RCs, and that this reduction did not specifically impact a single complex. Though in all types of primary cultures EtBr dose-dependently reduced OCR, as it had dose-dependently reduced mtDNA, the magnitude of mtDNA reduction did not directly correlate with the reduction in oxygen consumption. This discrepancy was especially apparent when comparing EtBr response in glia and neurons. Though glial mtDNA was not significantly affected by EtBr (though some mtRNA transcripts were reduced), OCR was reduced. This reduction was similar in magnitude to the EtBr-mediated reduction in oxygen consumption in both neuron and cocultures. We have hypothesized that this discrepancy suggests that glial mitochondrial

respiratory function may be differentially regulated in response to mtDNA replication inhibition than neurons. This may arise from two different mechanisms. First, there may be different rates in transcript turnover between neurons and glia – i.e., if glial mtRNA is less frequently synthesized, a small reduction in its quantity would be more likely to impact the synthesis of mitochondrial RC proteins, and reduce its function. Second, glia may have higher metabolic demands than unstimulated neurons, and are capable of undergoing a metabolic switch from oxidative phosphorylation to primarily glycolytic metabolism. This possibility was supported in multiple ways by our data. Glial basal oxygen consumption was much higher than that of either neurons or cocultures, and relevantly, was essentially equivalent to its maximum, ATP—synthesis uncoupled respiration, indicating no 'spare capacity.' Neurons, in contrast, had a substantial 'spare capacity', which may be a property of reserving an activity-dependent 'spare capacity' to accommodate stimulation. This suggests that under basal conditions, glial metabolic demands are sufficient to require full mitochondrial capacity. Even small reductions in mitochondrial respiratory function may then require the upregulation of alternate metabolic pathways for the generation of ATP, such as glycolysis.

In our glial and co-culture systems, we observed several hallmarks of glycolytic upregulation. First, we discovered that in these two culture conditions, EtBr treatment increased media glucose consumption, as measured from residual media glucose on each day of treatment. Measured concurrently with OCR, we discovered that EtBr treatment elevated the basal ECAR of glia and cocultures. This likely reflects increased production of lactic acid; a metabolic shunt for glycolysis wherein pyruvate is converted into lactate to regenerate NAD+, which disinhibits increased substrate flux through glycolysis for the additional production of ATP. This transition from mitochondria-dependent energy production to glycolytic metabolism may be mediated by AMPK activation as the AMP/ATP ratio rises with falling mitochondrial function (Doménech et al., 2015), though importantly, glia may be predominantly glycolytic *in vivo* (Kasischke et al., 2004; Bélanger et al., 2011; Volkenhoff et al., 2015). In concert with elevated ECAR, EtBr treatment

also increased NADH and increased the ATP/ADP ratio. Increased NADH supports our hypothesis that glycolytic activity is increased, as this indicates more NADH is being produced than is being used to fuel the mitochondrial RC. Interestingly, this also suggests that the increased pyruvate to lactate conversion does not sufficiently restore the NADH/NAD+ ratio. 1H-NMR analysis allowed us to determine that despite the increased ATP/ADP ratio, there was no net change in the total quantity of adenine nucleotides between conditions (see Figure 41). In this case, we hypothesized that the increased ratio may instead be another hallmark of increased glycolytic metabolism, and decreased mitochondrial activity. This is also supported by comparing the ATP/ADP ratios of untreated glia and neuronal cultures, as the more endogenously glycolytic glia have a much higher ATP/ADP ratio than the mitochondria-dependent neurons.

Indeed, the experiments performed in isolated primary neurons instead demonstrated a distinct lack of glycolytic upregulation. EtBr-treatment of neurons did not increase media glucose consumption, alter the ATP/ADP ratio, nor did it increase available reducing equivalents (likely NADH). Together, these findings support previously mentioned studies that have proposed glia are predominantly glycolytic, while neuron metabolism is more dependent on mitochondrial function. Our studies especially support recent work (Herrero-Mendez et al., 2009; Bolaños et al., 2010) indicating neurons are incapable of upregulating glycolysis (due to inhibition of a key mechanism for increasing the activity of PFK), and further these findings to demonstrate that even a reduction of mtDNA is not sufficient to remove this metabolic brake. Our results in glia also indicate that while they have a greater glycolytic capacity than neurons, in basal conditions they also have high mitochondrial activity, and in a cell:cell comparison, this activity is even higher than that of neurons. The differential adaptations of these two cell types to mtDNA depletion will be important to consider for future studies of neurological mitochondria-related disorders.

1.3. The contributions of mtDNA depletion to DAergic signaling

In a majority of studies, LID is examined through the lens of the molecular mechanisms through which L-DOPA treatment transitions from providing beneficial, symptom-alleviating therapy to producing highly detrimental side effects. Through these studies, a number of molecular mediators of LID have been identified (Cenci and Konradi, 2010; Santini et al., 2012). The majority of these changes are attributable to a hypersensitization of the D_1R signaling cascade, as following the onset of dyskinesia, several downstream effectors are hyperactivated during DA or L-DOPA treatment. Although other pathways and neurotransmitters have been implicated in the pathophysiology of LID (Huot et al., 2013), we chose to focus on members of this pathway to determine if mtDNA depletion and the resulting mitochondrial dysfunction could affect dopaminergic signaling in a manner that might mimic the processes of LID. We hypothesized that reduced mtDNA might sufficiently compromise mitochondrial function such that Ca^{2+} buffering would be impaired, which might raise cytosolic Ca^{2+} (Nicholls, 2009), and elevate the activity of the Ca^{2+}-sensitive D1 cascade.

Unfortunately, this study did not conclusively demonstrate if reduced mtDNA could hyperactivate D_1 signaling. Initial experiments using mouse primary cultures suggested that mtDNA reduction increased basal ERK1/2 phosphorylation and increased DA-mediated IEG expression, which parallel observations of signaling changes following the induction of dyskinesia (Murer and Moratalla, 2011). We also observed an increase in basal H4K8 acetylation, which while contrasting with the finding of reduced total H4 acetylation in LID (Nicholas et al., 2008), nonetheless suggests that reduced mtDNA perturbs this system. However, we found that our mouse cultures' magnitude of response to DA was highly inconsistent from dissection to dissection, which made it difficult to evaluate any alterations to this response. With this in mind, we moved these experiments to rat primary cultures, which we found were generally more consistent. However, we observed few differences in either basal or DA (or D_1/D_2 agonist) stimulated ERK1/2 phosphorylation between control and EtBr-treated cultures, and none of these

findings supported our earlier observations in mouse. Similarly, we were unable to reproduce our observation that mtDNA reduction increased DA-mediated induction of cfos expression – instead, we discovered that the D_1-mediated induction of cfos and egr was actually suppressed in EtBr-treated cultures. We did however observe some increased basal histone acetylation following mtDNA reduction, at residues H3K9 and H3K27, which was conceptually consistent with the increase in H4K8 acetylation in mouse cultures. This may indicate that mtDNA reduction increases the number of actively transcribed gene sites, though the relevance of this difference to LID must be counterbalanced with the point that primary culture uses an embryonic system, with fundamentally different neuron differentiation and growth gene programs than those used in the adult brain. Nonetheless, multiple studies have shown that LID induction is accompanied by a variety of changes in gene transcription (Konradi et al., 2004; Heiman et al., 2014), and both dMSNs and iMSNs undergo considerable spine remodeling (Moratalla et al., 2017). It may be informative for future studies to examine the gene programs activated by the increased acetylation we have observed, to determine if this mechanism has relevance for LID.

This study suggests that reduced mtDNA may affect the activity of the D_1 signaling pathway. Whereas copious efforts have identified mechanisms through which extracellularly-initiated signaling cascades impact mitochondrial function, these data add to a small but increasing body of work investigating the reciprocal impact of mitochondrial function on the activity of various signaling pathways. The impact of mitochondrial Ca^{2+} buffering on other Ca^{2+}-dependent signaling pathways has long been appreciated (Billups and Forsythe, 2002; Parekh, 2003), as has the importance of energy homeostasis (i.e. the AMP/ATP ratio) on AMPK and mTOR acitivty (Sarbassov et al., 2005; Hardie, 2014), and even redox status (i.e. the NAD+/NADH ratio) on the activity of the sirtuin family of deacetylases (Huang et al., 2010; Verdin et al., 2010). However, these findings are infrequently extrapolated to the activity of canonical GPCR signaling pathways, like those that are perturbed in LID. Due to the considerable species disparity in our results, further experiments would be necessary to confirm or refute our previous

results, but our findings do suggest that additional studies addressing the impact of compromised mitochondrial function on D_1 signaling may be fruitful.

1.4. The impact of mtDNA quantity on mitochondrial dynamics

The genes and proteins regulating mitochondrial fission and fusion are essential for ensuring the appropriate distribution of mitochondria within the cell – particularly important for highly polarized cells such as neurons with high local energy requirements (Chen and Chan, 2009). These processes are dynamically regulated by a number of extracellular and intracellular signals, including oxidative, nutrient, and stimulation-mediated stressors. Maintenance of mitochondrial fission and fusion is also essential for the distribution and segregation of 'heathy' and dysfunctional mtDNA plasmids, respectively (Nunnari et al., 1997; Twig et al., 2008). Excess mitochondrial fission can reduce mtDNA quantity, while excess mitochondrial fusion can interfere with the segregation of damaged mitochondria for mitophagy (Ono et al., 2001; Parone et al., 2008; Chen et al., 2010). Little is known about the inverse relationship between mtDNA quantity and mitochondrial dynamics, however. This study addressed mitochondrial dynamics gene regulation following mtDNA depletion with EtBr treatment.

We found that mtDNA depletion may promote mitochondrial fusion through the upregulation of Opa1. In mouse cultures, this pro-fusion response was enhanced by a downregulation of Dnm1l and Fis1, two fission genes, but in rat cultures we instead observed a concomitant upregulation of both Opa1 and Dnm1l. To address this discrepancy, we attempted to quantify changes in mitochondrial morphology by examining mitochondrial area, length, and distance from the nucleus in rat glia identified in images of rat cocultures. We used glia, and not neurons (or ideally both) to quantify differences in mitochondrial morphology because of a convergence of unique features – glia mitochondria were clearly defined discrete objects at a magnification that also permitted the visualization of the entire glial cell body. In contrast, though

we could visualize distinct neuronal mitochondria, we were not able to do this at a magnification that simultaneously depicted the full neuronal dendritic and axonal arbor and distinct mitochondria. Additionally, as plating density affects neuronal outgrowths and maturity in cultures, we attempted to use the same plating density used in our molecular assays, and this density precluded the assignment of most visualized neuronal processes to separate cell types, which prevented the measurement of the distance between these mitochondria and the nucleus. Using glial mitochondria, we determined that mtDNA depletion increased mitochondrial area and length, which supports our hypothesis that mtDNA depletion may promote mitochondrial fusion. Importantly, lower doses of EtBr that did not reduce mtDNA also increased mitochondrial area, but only the highest tested dose of EtBr increased both area and length. We did not observe a consistent relationship between EtBr dose or exposure to mitochondrial distance from the nucleus, so we were unable to reach a conclusion about the relevance of this putative increase in mitochondrial fusion to intracellular mitochondrial distribution. However, these data suggest that mtDNA depletion may promote mitochondrial fusion, which could be probed in future studies.

1.5. The relationship between mtDNA quantity and phosphocreatine

A novel finding from the present study was the association between neuronal mtDNA quantity, mtCK expression, and the abundance of PCr. Though ATP is the primary form of cellular 'energy' used for a host of intracellular processes, it is synthesized within the mitochondrial matrix, and with its three terminal phosphates is fairly bulky and highly polar molecule. In highly energetic cell types such as neurons, myocytes, and cardiomyocytes, efficient distribution of this cellular energy and ATP-derived phosphate relies on the CK system (Wallimann et al., 2011). Comprised of two dual function kinase/phosphatases, this shuttle transfers a terminal phosphate from ATP to Cr, a low weight organic acid, by mtCK and then locally regenerates ATP from PCr by B-CK. We discovered that in rat neurons and cocultures, EtBr treatment significantly decreases mtCK

expression, with little effect on the expression of B-CK. As we saw no change in mtCK expression in glia treated with the same (4D[50]) dose of EtBr, we initially hypothesized that mtCK expression might be tethered to mtDNA quantity, as this dose of EtBr does not reduce mtDNA in glia. Treatment with a higher dose of EtBr (4D[500]), which does reduce mtDNA in this cell type, increased mtCK expression. As a result, we believe this relationship between mtDNA depletion and depression of mtCK expression may be a neuron-specific effect.

Perturbations in the CK system have been previously implicated in multiple neurological disorders (Schlattner et al., 2006). Proteomic analyses of an animal of LID also identified mtCK as one of many genes deregulated following the induction of LID (Valastro et al., 2007). We were then encouraged to discover that in a cohort of control, dyskinetic-PD, and nondyskinetic-PD patients, mtCK was significantly downregulated in the dyskinetic-PD group. This cohort of patients overlapped considerably with the cohort we initially used to identify the specific reduction of mtDNA, and so we are confident to report an association between these two phenomena. Interestingly, we also observed a reduction of B-CK in the dyskinetic-PD group, and an increase in B-CK in the nondyskinetic-PD group, but due to the high heterogeneity of the post-mortem human samples, neither effect reached significance. Nonetheless, this paralleled reduction in mtCK in human LID lends considerable translational impact to our model, and presents a mechanism through which mtDNA reduction may compromise the energetic capacity of the striatum.

We further report that reduction in the expression of mtCK reduces both the PCr/Cr ratio and the total quantity of PCr in striatal neuron cultures and cocultures. We observed significant reductions in the absolute quantity of PCr in both systems, which in cocultures was accompanied by a proportional increase in the quantity of Cr, suggesting little effect on total Cr quantity. As isolated neuron cultures have low endogenous Cr, we also supplemented these cultures with 5mM Cr. While the total Cr we detected in these cells increased approximately 10-fold, PCr quantity was still deficient in EtBr-treated cells. In contrast, though we observed no changes in

the PCr/Cr ratio in glia, we instead observed a significant reduction in both Cr and PCr. While we were unable to identify the source of this reduction in the present study, this cell-type difference presents an interesting direction for future studies examining the relationship between mitochondrial function and the Cr-PCr shuttle.

The expression and function of the Cr shuttle is as yet poorly defined in the brain, despite the long-standing appreciation for its function in this organ (Bessman and Carpenter, 1985; Chen et al., 1995). This shuttle may be compartmentalized in the brain, with B-CK expression constricted to glia, and mtCK expression limited to neurons (Tachikawa et al., 2004; Schlattner et al., 2016). This cell type segregation of these raises interesting questions about the function of the shuttle in the brain, and suggests an additional layer of complexity of Cr transport. Brain Cr is primarily synthesized locally (Defalco and Davies, 1961; Braissant et al., 2005, 2010), and remains distinct from the systemic pool synthesized in the liver and kidneys, but the segregation of its synthesis between brain cell types is less clear. Reportedly, the CrT (SLC6A8) is more or less exclusively expressed in neurons (and oligodendrocytes) (Braissant et al., 2010), suggesting a mechanism in which glia synthesize Cr, utilize B-CK for local PCr synthesis, or export it to neurons where mtCK performs this synthesis. However, the absence of B-CK in neurons to perform the reverse reaction poses a considerable complication for this model. A recent study (Schlattner et al., 2016) reported that though these two enzymes are segregated in most brain regions, MSNs are some of the only neuronal subtypes that abundantly express both enzymes, though the purpose of this selective dual expression remains unclear. In the present study, we readily detected the expression of both enzymes in both neuronal and glial cultures, though this may be an effect of the early developmental stage of this culture system. Nonetheless, this putative enzyme segregation may partially explain the specific neuronal downregulation of mtCK in response to mtDNA depletion, as these enzymes are likely already under cell-type specific regulation mechanisms.

To our knowledge, no studies have previously identified a direct relationship between mtDNA quantity and mtCK expression in the brain. Typically, mtDNA mutation-related disorders (i.e. CPEO, MERRF, MELAS, see Chapter I) are associated with a compensatory upregulation of mtCK, which can even become pathological as mtCK can oligomerize to form crystalline mitochondrial inclusion bodies, which are enzymatically deficient (Schlattner et al., 2006). Importantly, development of these inclusions has primarily been observed with the sarcomeric isoform of mtCK, but this phenomenon still presents a curious question as to the differential mechanisms of mtCK expression in response to mtDNA depletion. Inactivation of mtCK through ROS/RNS disruption of its octameric structure has been proposed as a common mechanism in some neurodegenerative disorders (Stachowiak et al., 1998; Wendt et al., 2003; Li et al., 2006; Eliuk et al., 2007; Laar et al., 2008), but this mechanism occurs independently of changes in gene regulation. Instead, mtCK downregulation has been detected in some forms of cancer, which may be a consequence of the Warburg effect. However, multiple other forms of cancer upregulate mtCK, calling the 'intent' of the directionality of this regulation into question (Patra et al., 2012). We posit that our findings present a novel direct relationship between mtDNA quantity and mtCK expression, which may improve the understanding of the mechanisms underlying Cr shuttle in the brain, particularly in cases of compromised mitochondrial function.

2. Future Directions

In the present study, we have established a model of consistent mtDNA reduction in primary striatal cultures, described multiple resulting physiological changes in both neurons and glia, and identified several pathways through which mtDNA reduction may create dyskinesiogenic conditions in the striatum. These results lay the groundwork for a host of additional experiments that could further advance the understanding and appreciation of the connection between mtDNA quantity, mitochondrial function, and their relationship to the development of dyskinesia.

2.1. Alternative approaches to current experiments

Though the EtBr treatment model works efficiently and reproducibly in the short term for primary cultures, it has some limitations that could be addressed in future experiments examining the effects of reduced mtDNA. First, in this model, we have used a single application of EtBr to reduce mtDNA with no washout. This means that EtBr is increasingly taken up by mitochondria over time, and as it intercalates with mtDNA, further mtDNA and mtRNA replication and transcription is inhibited. We have exploited this kinetic process to examine the effects of different degrees of mtDNA reduction, but we cannot conclusively correlate the degree of mtDNA reduction with the magnitude of physiological effect. For instance, assuming that EtBr inhibition of mtDNA replication occurs more rapidly than the propagated effects of reduced mtDNA, we are likely observing the physiological effects of a lesser degree of mtDNA reduction than what we quantified with qPCR. However, as previously noted, we are likely also overestimating the effects of this degree of mtDNA reduction due to the combinatorial effect of EtBr on mtRNA. A model of consistent mtDNA reduction would be more physiologically relevant, though due to its constant replication and mitophagic mechanisms, this is difficult to accomplish chemically. Genetic models may be more successful in some cases, as the Tfam heterozygous mouse has been reported to have a consistent reduction in mtDNA quantity (Larsson et al., 1998) but this reduction is not entirely consistent across tissues, and Tfam also facilitates the initiation of mtRNA transcription (Kelly and Scarpulla, 2004). Potentially, a conditional knockout mouse wherein Tfam or polymerase gamma is selectively reduced in the neurons and/or glia of the mouse striatum may create sufficiently stable mtDNA reduction in this region. This conditional knockout mouse could then be used in models of PD and LID, to directly determine if reduced striatal mtDNA potentiates the development of LID.

As the present study yielded mostly contradictory results about the impact of mtDNA quantity on dopaminergic signaling, further experiments will be necessary to make conclusive observations. First, it may be useful to determine if reduced mtDNA increases cytosolic Ca^{2+},

either basally or following stimulation. An even more nuanced approach would be to ascertain if mtDNA reduction impairs mitochondrial Ca^{2+} loading capacity, before opening of the mPTP is triggered. These may help solidify our hypothesis that reduced mitochondrial function contributes to the hyperactivation of dopaminergic signaling through reduced Ca^{2+} buffering activity. Next, it may be more useful to take a kinetic approach to analyzing the activation of effectors such as ERK1/2 and ppd. While elevations in either the phosphorylation or expression of these effectors are hallmarks of the onset of LID, the extended duration of their activation has also been observed (Murer and Moratalla, 2011). Considering the variability in the magnitude of response to DA observed in these cultures across dissections, it may be more prudent to instead assess the duration of increased phosphorylation or expression, as this may be a more robust measure of increased signal intensity. This approach could also be taken to more comprehensively measure alterations in histone acetylation (and other modifications), both at baseline and in response to DA stimulation. While our present results do suggest that some residues, typically markers of highly active gene transcription sites, have increased acetylation following mtDNA reduction, these are preliminary findings and would need to be reproduced. A more comprehensive analysis of different histone modifications may be useful to thoroughly assess the impact of mtDNA depletion, and more recent techniques such as ChIP-seq may then be used to identify the profiles of genes transcriptionally regulated by these modifications.

Similarly small adjustments to our current approach may also be useful for further analysis of shifts in mitochondrial morphology following mtDNA reduction. Though we observed a slight increase in mitochondrial size (area and length) in response to EtBr treatment, we were only able to perform this quantification in glial cultures. In future experiments, a few different approaches may facilitate the visualization of mitochondria in neurons. One popular approach is the use of lower density neuronal cultures, but this does impact the degree of neuronal arborization in cultures. Instead, a different approach may be the use of transient transfection with mito-RFP under a neuron-specific promoter, combined with transfection of a neuronal GFP marker. Ideally

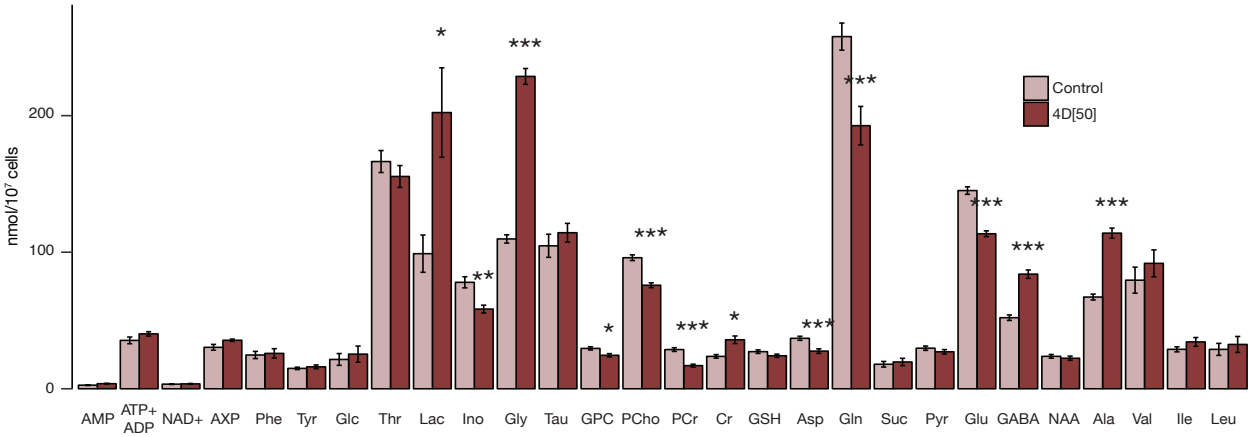

Figure 41. ^{1}H-NMR quantifiable metabolites in primary striatal neuron-enriched cocultures. nmol metabolite/10^7 cells in control or EtBr-treated cells. Two dissections, n = 16. *** = $p < 0.001$, ** = $p < 0.01$, * = $p < 0.05$; Student's t-test following Benjamini-Hochberg correction. Error bars reflect +/- SEM. See Figure 38 for corresponding peak positions. AXP = ATP + ADP + AMP; Phe = phenylalanine; Tyr = tyrosine; Glc = glucose; Thr = threonine; Lac = lactate; Ino = *myo*-inositol, Gly = glycine; Tau = taurine; GPC = glycerophosphocholine; PCho = phosphocholine; PCr = phosphocreatine; Cr = creatine; GSH = glutathione; Asp = aspartate; Gln = glutamine; Suc = succinate; Pyr = pyruvate; Glu = glutamate; GABA = 4-aminobutyrate; NAA = N-acetylaspartate; Ala = alanine; Val = valine; Ile = isoleucine; Leu = leucine.

at low doses, the combination of these two markers would permit us to visualize a fraction of the neurons in culture and their mitochondria, allowing the quantification of mitochondrial distribution within single cells, eliminating the density-dependent problems of the approach in the current study. Additionally, using the transient transfection of mito-RFP would also create an opportunity for live-cell imaging, which could provide information about the impact of mtDNA quantity on the kinetics of mitochondrial distribution in neuronal processes, which may be more dramatically impacted by a small increase in mitochondrial fusion. Finally, as our study observed many differences between glial and neuronal mitochondrial metabolism, it may also be illustrative to observe the interaction between these two populations of mitochondria in cocultures. This could be accomplished using neuronal promoter-dependent mitoGFP in concert with glial promoter-dependent mitoRFP, though transgenic animals expressing different fluorescent markers for neuron and glia cell bodies may also be necessary to visualize a sufficient quantity of these cell types. It may also be informative to examine the effects of DA signaling on mitochondrial trafficking, and how this may be affected by mtDNA quantity. Dnm1l activity, which mediates

mitochondrial fusion, is suppressed by PKA phosphorylation, and this interaction is enhanced by GSK3β scaffolding (Loh et al., 2015), pointing to mechanisms through which both D_1R and D_2R activation may regulate mitochondrial dynamics.

2.2. Further implications of the present study

In the present study, we used ^{1}H-NMR to quantify Cr and PCr, and detected a significant reduction in PCr in neurons and cocultures following the addition of EtBr. However, due to the unselective nature of ^{1}H-NMR spectroscopy, using a targeted metabolomic approach we were able to identify a total of 28 metabolites (Figure 38). As we detected significant changes in a majority of these metabolites, we hypothesize that this data may provide useful information for future studies investigating the impact of mtDNA reduction. To contextualize these data, we grouped these metabolites into four major pathways – canonical glycolysis and TCA cycle, the lactate-alanine shuttle, the glutamate-glutamine GABA cycle, and, for lack of a better grouping system, 'other.' Of course, many of these compounds are involved in multiple metabolic pathways, but we created a simplified schematic for reference (Figure 42). Unfortunately, due to the limits of detection we were unable to detect most of the components of the glycolytic pathway and TCA cycle. However, of the quantifiable elements (glucose, pyruvate, and succinate), we did not observe any significant differences between control and EtBr-treated groups.

In contrast, we observed significant increases in lactate and alanine quantity, both of which are generated from non-oxidative reactions from pyruvate (Adeva-Andany et al., 2014; Bak et al., 2006). Some studies have indicated that lactate and alanine exchange between neurons and glia may play an important role in ammonia transfer, or for supplying neurons with lactate as a metabolic substrate. Elevations in both indicate decreased respiratory activity, and in the case of lactate, a need to extra-mitochondrially regenerate NAD+. Plasma increases in both are clinical signs of mitochondrial disease (Haas et al., 2008). Though not directly part of lactate-alanine

exchange, the observed reduction in aspartate further reflects this decrease in mitochondrial function, as aspartate is produced by conversion from OAA, a TCA intermediate, but requires electron acceptors (i.e. NAD+) for this production (Sullivan et al., 2015).

An unexpected finding of this study was the observed increase in GABA, despite the coincident decrease in glutamate and glutamine. Glutamine and glutamate are derived at least in part from TCA activity (Hertz, 2013), and their reduction may further support decreased flux through this pathway. GABA is only produced directly from glutamate via GAD, making its elevation in the face of the reduction in both glutamate and glutamine surprising. We hypothesize that there are a few likely possibilities for this increase, which may warrant future investigation. All three metabolites form a complex network of interactions between neurons and glia known as the glutamate/GABA-glutamine cycle (Bak et al., 2006; Hertz, 2013; Schousboe et al., 2013; Morken et al., 2014; Brekke et al., 2015). In this cycle, TCA substrate αKG is converted into glutamate, which is converted into glutamine exclusively in glia. This glutamine is exported into neurons, which in neurons can be directly converted back into glutamate. In GABAergic neurons such as the MSNs of the striatum, this glutamate can be converted into GABA, which can be packaged into vesicles and released. GABA itself can be taken up by either neurons or glia, and be re-used as a neurotransmitter or oxidized into succinate to re-enter the TCA cycle. While these pathways have not been definitively characterized in the striatum, we may still hypothesize that disruption of one or more of these steps may result in the increase in GABA we observed. First, in order for GABA to be oxidized in either neurons or glia, it must be imported into mitochondria before its conversion to succinyl semi-aldehyde, as the necessary enzyme to perform this is strictly mitochondrial. It is possible that the decreased number of functional RCs may impair the glial mitochondrial ability to import GABA. Alternately, if we can assume that the rest of our data support a perturbation in TCA cycle, this may decrease demand for influx of succinate into the cycle, and disfavor the conversion of GABA. Finally, the increase in GABA may also reflect a

decrease in neurotransmitter release – another process which is very energetically demanding and thus may be destabilized by mtDNA depletion.

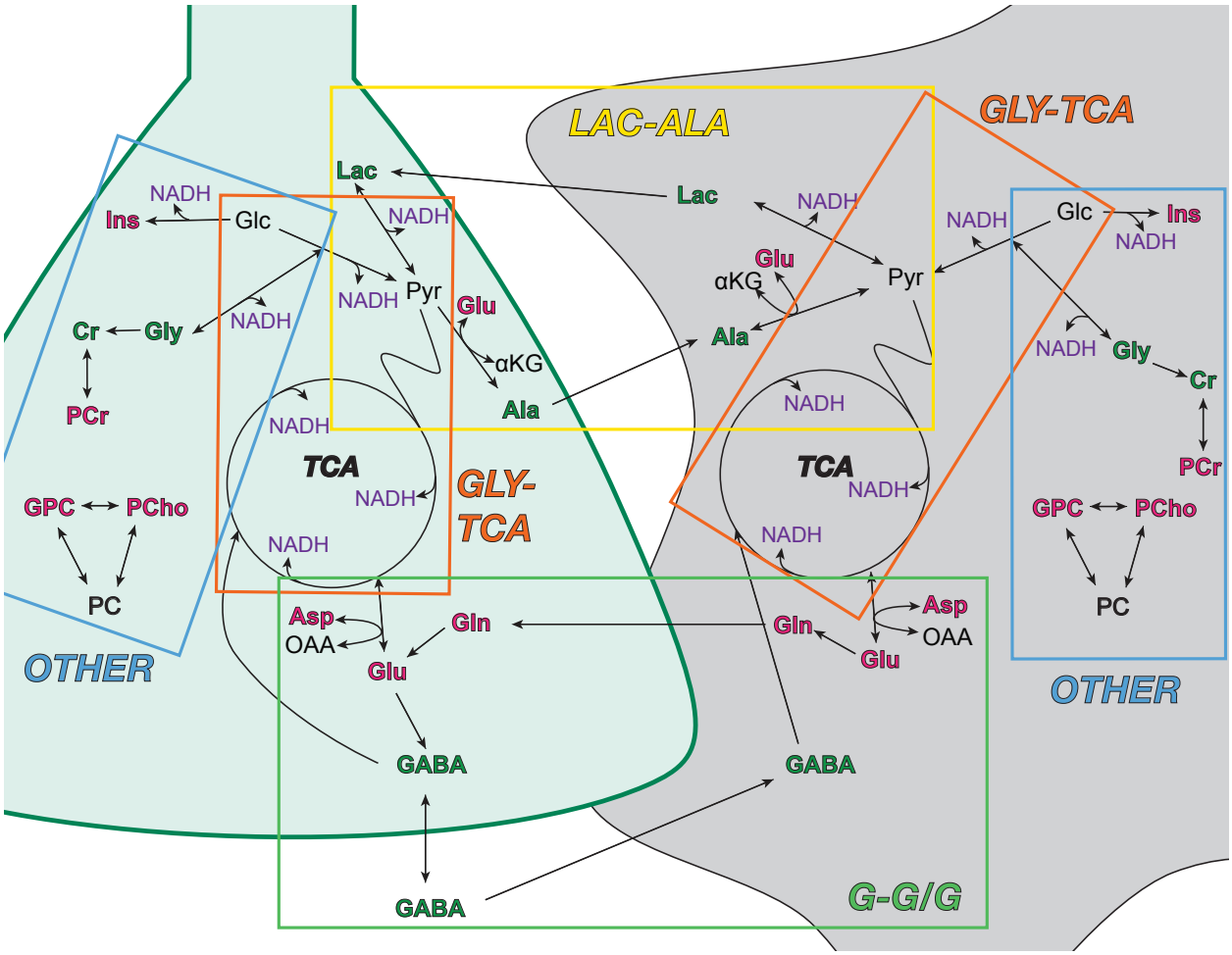

Figure 42. Schema of major examined glucose metabolic pathways between neurons and glia. In both cell types (neuron, green; glia, grey), glucose is oxidatively metabolized to pyruvate, which is incorporated into the TCA cycle for further oxidation. Using this framework, we contextualized the 1H-NMR-detectable metabolites determined to be altered by EtBr treatment (See Figure 41). Elevated metabolites are in green, reduced metabolites are in magenta. We grouped these pathways and their offshoots into four major subsets for discussion: Glycolysis-TCA cycle, orange box; lactate-alanine shuttle, yellow box; glutamine-glutamate/GABA cycle, green box; other metabolites; blue box. For clarity, some enzymatic steps, intermediates, and alternate pathways are not shown. However, we included NADH-producing steps or pathways where relevant (purple).

In addition, we observed a number of other unexpected perturbations. First, we observed a large increase in glycine, which may be partially attributable to the decrease in glial total Cr production, as it is a precursor in Cr biosynthesis (Wyss and Kaddurah-Daouk, 2000). However, the magnitude of glycine increase far exceeds the decrease in Cr, which suggests additional

perturbations in its metabolic pathway. Interestingly, glycine and serine are interconverted in a cycle that passes through the mitochondria – serine is converted to glycine in the cytosol in an NADH-consuming reaction, but glycine is converted back to serine in a reaction that produces NADH (Kikuchi et al., 2008; Locasale, 2013). As our data already demonstrate an increase in NADH in EtBr-treated cells, this condition likely favors glycine production. Similarly, we also noted a significant decrease in myo-inositol, which is typically synthesized from glucose-6 phosphate in a process that generates NADH (Livermore et al., 2016). This reduction in inositol may disrupt a number of signaling pathways, though further studies may be required to determine if this reduction sufficiently affects the obligate signaling pool. Signaling may be further disrupted due to reductions in phosphocholine and glycerophosphocholine, which are both possible precursors of phosphatidylcholine (Fagone and Jackowski, 2013), which can itself be converted into DAG or arachidonic acid (Exton, 1990). However, this pathway has many more intermediates, and further analysis would be necessary to determine how this pathway is impaired.

These data present a number of interesting avenues for further investigation. In addition to impairing the Cr-PCr shuttle, mtDNA reduction also appears to interfere with multiple biosynthetic pathways, including amino acids and membrane lipid precursors. Many of these alterations support previous observations about reduced mitochondrial function, but another interesting commonality between some of these balances emerges. Broadly, production of some of the metabolites increased by EtBr treatment (i.e. glycine, lactate) favor the regeneration of NAD+, while synthesis of those reduced (i.e. glutamate, glutamine, aspartate, inositol) favor the production of NADH. It is possible that the increased NADH we observed as a consequence of increased glial glycolytic activity may further perturb biosynthetic pathways within neurons and glia. While mitochondrial dysfunction in neurons is most commonly associated with oxidative stress, these interactions present an interesting possibility of reductive stress, which could be an avenue for further investigations into neuron and glia metabolic coupling, and the effects of impaired mitochondrial function.

The observed elevations in glycine and GABA are directly relevant for LID. Though these are intracellular measurements, and thus not directly informative about potential changes at the synapse, elevations in these metabolites may have disease relevance. LID is primarily linked to hyperactivity of GABAergic dMSNs, and elevated GABA release has been observed in the SNr following the onset of dyskinesia. Local increases in glycine may also have multiple effects - NMDA receptors are co-activated by glutamate and glycine, and high concentrations of glycine do increase NMDA activity (Newell et al., 1997). Increased striatal glycine simulates DA release, which may contribute to non-phsyiological elevations of DA that contribute to the pathogenesis of LID (Yadid et al., 1993). Together elevations in these two neurotransmitters could be an important link between mitochondrial dysfunction and LID, though future studies would likely need to consider the effects of neuronal stimulation on this mechanism.

2.3. Applications for animal experiments and clinical translatability

Our findings that mtDNA depletion reduces mtCK expression and PCr availability, and that human dyskinetic PD patients also have reduced mtDNA and mtCK expression, have a number of applications for future experiments. These can be grouped into two major directions – assessing the consistency of the relationship between these two, and determining the pathogenicity of depleted PCr and/or mtDNA in LID and other neurodegenerative disorders.

An immediate next step could be to verify the relationship between mtDNA and mtCK expression. Though this relationship appears robust in neurons in our system, there are many other models of mtDNA reduction that could be probed. In particular, more stable models of mtDNA reduction may be necessary, in light of how in cases of mitochondrial DNA related diseases, (sarcomeric) mtCK is typically upregulated (Schlattner et al., 2006). Transgenic animals (like the Tfam heterozygous mice) could be used to determine if other sources of mtDNA reduction similarly reduce mtCK expression. Careful analysis is needed to determine if this is a striatum or

brain specific mechanism, one that is linked to developmental stage, or an *in vitro* artifact. Furthermore, additional studies are needed to determine the mechanistic link between mtDNA reduction and mtCK downregulation.

No major changes in nuclear-encoded mitochondrial genes have been detected in animal models of LID, though mtDNA quantity has not been thoroughly probed. Independently of mtDNA, mtCK activity and PCr availability may still be relevant for LID. mtCK has been previously identified as a gene and protein downregulated in dyskinetic animals (Valastro et al., 2007), though the magnitude of this effect is typically small. However, this effect has not been pursued at the level of comparing the PCr/Cr ratio, or examining phosphorylation capacity. It may be informative to determine if PCr is reduced in these animals, and to further pursue the mechanisms by which this deficiency may contribute to the development of LID.

It is possible that mtDNA reduction is only relevant in human LID, as gradual increase in mutation and deletion load may require the human time course of the disease. If mtDNA reduction does consistently reduce neuronal mtCK activity and PCr availability, there is an intriguing mechanism by which L-DOPA treatment may exacerbate this phenomenon. Human L-DOPA treatment frequently causes an additional side effect, hyperhomocysteinemia (Blandini et al., 2001), which itself may contribute to the increased incidence of cognitive impairment and dementia in PD (Zoccolella et al., 2010). The bulk of homocysteine synthesis is tethered to Cr synthesis (Mudd et al., 1980), and Cr supplementation has been exploited to attempt to reduce plasma homocysteine in a number of disease contexts (Deminice and Rosa, 2016). This raises the possibility that L-DOPA-elevated homocysteine may reduce Cr synthesis, which may contribute to the development of LID. This mechanism may converge with the reduced mtCK activity caused by mtDNA reduction, which could create a severe bioenergetic deficiency that potentiates the development of LID.

Finally, if the relationship between neuronal mtDNA quantity and mtCK expression holds, and if reduced mtDNA (and/or PCr) does contribute to the pathogenesis of LID, this may open up

the possibility of a biomarker for LID risk. Cr and PCr are both measurable *in vivo* using MRS, or a combination of MRS and MRI (MRSI), and multiple studies have examined PD patients for alterations in PCr and ATP (Hoang et al., 1998; Rango et al., 2006; Weiduschat et al., 2013) or total Cr (Holshouser et al., 1995; Cruz et al., 1997; Taylor-Robinson et al., 1999; Gröger and Berg, 2012). These techniques have been explored extensively to attempt to identify a biomarker for PD (Rango, 2015; Tuite, 2016), and while one study has proposed decreases in the NAA/total Cr ratio as an indicator of dopaminergic degeneration (Seraji-Bozorgzad et al., 2015), this field is in its infancy. We hypothesize that LID risk may be a function of a reduced PCr/Cr ratio due to reduced mtCK function, which is currently technically challenging (though possible) to measure. Constant advances in higher field strength magnets and the development of different techniques such as Chemical Exchange Saturation Transfer (Kogan et al., 2013; Haris et al., 2014) may facilitate this process.

3. Conclusion

Mitochondrial dysfunction has long been implicated as a contributing factor in the etiology of idiopathic PD. In contrast, its contribution to the development of LID is underappreciated; though the hypothesis that energetic differences may underlie the differential distribution of dyskinetic and non-dyskinetic PD patients has some support. As our lab previously identified putamenal mtDNA quantity as a factor differentiating these two groups, this work has focused on identifying mechanisms through which changes in mtDNA levels may contribute to the striatal pathology of LID. We created a model of *in vitro* primary striatal mtDNA reduction, and demonstrated that this reduction may derange dopaminergic signaling and mitochondrial dynamics. More conclusively, we have presented novel evidence of a direct relationship between mtDNA quantity, mtCK expression, and PCr abundance in striatal neurons. We have also demonstrated that mtDNA quantity and mtCK expression are simultaneously and selectively

reduced in dyskinetic PD patients, relative to non-dyskinetic PD patients. Substantial work remains to establish the mechanisms by which mtDNA quantity may affect mtCK, and to further determine the pathogenicity of both reduced mtDNA and mtCK. However, this study lends support to the role of both mitochondrial dysfunction and the Cr system in LID. If deregulation of the Cr system proves to be a valid biomarker for the development of LID, this could be a method to identify which patients may be better served by initial therapy with dopaminergic agents instead of L-DOPA, a serious unmet clinical need. Understanding the contributions of mitochondrial and metabolic perturbations in the pathophysiology of LID may also lead to the development of disease-modifying therapies in the future.

REFERENCES

Abou-Sleiman P, Healy D, Quinn N, Lees A, Wood N (2003) The role of pathogenic DJ-1 mutations in Parkinson's disease. Ann Neurol 54:283–286.

Adachi K, Oiwa K, Yoshida M, Nishizaka T, Jr K (2012) Controlled rotation of the F1-ATPase reveals differential and continuous binding changes for ATP synthesis. Nat Commun 3:1022.

Adam-Vizi V, Tretter L (2013) The role of mitochondrial dehydrogenases in the generation of oxidative stress. Neurochem Int 62:757–763.

Adeva-Andany M, López-Ojén M, Funcasta-Calderón R, Ameneiros-Rodríguez E, Donapetry-García C, Vila-Altesor M, Rodríguez-Seijas J (2014) Comprehensive review on lactate metabolism in human health. Mitochondrion 17:76–100.

Ahlskog JE, Muenter MD (2001) Frequency of levodopa-related dyskinesias and motor fluctuations as estimated from the cumulative literature. Mov Disord 16:448–458.

Ahmed M, Berthet A, Bychkov E, Porras G, Li Q, Bioulac B, Carl Y, Bloch B, Kook S, Aubert I, Dovero S, Doudnikoff E, Gurevich V, Gurevich E, Bezard E (2010) Lentiviral overexpression of GRK6 alleviates L-Dopa–Induced Dyskinesia in experimental Parkinson's disease. Sci Transl Med 2:28ra28–28ra28.

Ahmed M, Bychkov E, Li L, Gurevich V, Gurevich E (2015) GRK3 suppresses L-DOPA-Induced Dyskinesia in the rat model of Parkinson's disease via its RGS homology domain. Sci Rep 5:10920.

Akbarian S, Smith MA, Jones EG (1995) Editing for an AMPA receptor subunit RNA in prefrontal cortex and striatum in Alzheimer's disease, Huntington's disease and schizophrenia. Brain Res 699:297–304.

Alano C, Beutner G, Dirksen R, Gross R, Sheu S (2002) Mitochondrial permeability transition and calcium dynamics in striatal neurons upon intense NMDA receptor activation. J Neurochem 80:531–538.

Aldridge J, Horibe T, Hoogenraad N (2007) Discovery of genes activated by the mitochondrial unfolded protein response (mtUPR) and cognate promoter elements. PloS ONE:e874.

Alston C, Rocha M, Lax N, Turnbull D, Taylor R (2017) The genetics and pathology of mitochondrial disease. J Pathol 241:236–250.

Amuthan G, Biswas G, Zhang S, Klein-Szanto A, Vijayasarathy, Avadhani N (2001) Mitochondria-to-nucleus stress signaling induces phenotypic changes, tumor progression and cell invasion. Embo J 20:1910–1920.

Anand R, Wai T, Baker M, Kladt N, Schauss A, Rugarli E, Langer T (2014) The i-AAA protease YME1L and OMA1 cleave OPA1 to balance mitochondrial fusion and fission. J Cell Biol 204:919–929.

Anderson C, Swanson R (2000) Astrocyte glutamate transport: Review of properties, regulation, and physiological functions. Glia 32:1–14.

Anderson, Bankier, Barrell, de Bruijn, Coulson, Drouin, Eperon, Nierlich, Roe, Sanger, Schreier, Smith, Staden, Young (1981) Sequence and organization of the human mitochondrial genome. Nature 290:457–465.

Andersson, Hilbertson, Cenci MA (1999) Striatal fosB Expression Is Causally Linked with l-DOPA-Induced Abnormal Involuntary Movements and the Associated Upregulation of Striatal Prodynorphin mRNA in a Rat Model of Parkinson's Disease. Neurobiol Dis 6:461–474.

Andersson, Konradi, Cenci (2001) cAMP response element-binding protein is required for dopamine-dependent gene expression in the intact but not the dopamine-denervated striatum. J Neurosci 21:9930–9943.

Andres RH, Ducray AD, Schlattner U, Wallimann T, Widmer H (2008) Functions and effects of creatine in the central nervous system. Brain Res Bull 76:329–343.

Andreyev AY, Kushnareva YE, Murphy AN, Starkov AA (2015) Mitochondrial ROS metabolism: 10 Years later. Biochemistry (Mosc) 80:517–531.

Andreyev AY, Kushnareva YE, Starkov AA (2005) Mitochondrial metabolism of reactive oxygen species. Biochemistry (Mosc) 70:200–214.

Angelini C, Bello L, Spinazzi M, Ferrati C (2009) Mitochondrial disorders of the nuclear genome. Acta Myol 28:16–23.

Area-Gomez E, del Castillo M, Tambini M, Guardia-Laguarta C, de Groof A, Madra M, Ikenouchi J, Umeda M, Bird T, Sturley S, Schon E (2012) Upregulated function of mitochondria-associated ER membranes in Alzheimer disease. Embo J 31:4106–4123.

Armand R, Channon JY, Kintner J, White KA, Miselis KA, Perez RP, Lewis LD (2004) The effects of ethidium bromide induced loss of mitochondrial DNA on mitochondrial phenotype and ultrastructure in a human leukemia T-cell line (MOLT-4 cells). Toxicol Appl Pharmacol 196:68–79.

Atkins C, Sweatt J (1999) Reactive oxygen species mediate activity-dependent neuron-glia signaling in output fibers of the hippocampus. J Neurosci 19:7241–7248.

Aubert I, Guigoni C, Håkansson K, Li Q, Dovero S, Barthe N, Bioulac B, Gross C, Fisone G, Bloch B, Bezard E (2005) Increased D1 dopamine receptor signaling in levodopa-induced dyskinesia. Ann Neurol 57:17–26.

Babcock D, Herrington J, Goodwin P, Park Y, Hille B (1997) Mitochondrial participation in the intracellular Ca2+ network. J Cell Biol 136:833–844.

Bach, Lan, Johnson, Abell, Bembenek, Kwan, Seeburg, Shih (1988) cDNA cloning of human liver monoamine oxidase A and B: molecular basis of differences in enzymatic properties. Proc Natl Acad Sci USA 85:4934–4938.

Baertling F, Rodenburg R, Schaper J, Smeitink J, Koopman W, Mayatepek E, Morava E, Distelmaier F (2014) A guide to diagnosis and treatment of Leigh syndrome. J Neurol Neurosurg Psychiatry 85:257–265.

Bak L, Schousboe A, Sonnewald U, Waagepetersen H (2006) Glucose is necessary to maintain neurotransmitter homeostasis during synaptic activity in cultured glutamatergic neurons. J Cereb Blood Flow Metab 26:1285–1297.

Bak L, Walls A, Schousboe A, Ring A, Sonnewald U, Waagepetersen H (2009) Neuronal glucose but not lactate utilization is positively correlated with NMDA-induced neurotransmission and fluctuations in cytosolic Ca2+ levels. J Neurochem 109:87–93.

Bak LK, Schousboe A, Waagepetersen HS (2006) The glutamate/GABA-glutamine cycle: aspects of transport, neurotransmitter homeostasis and ammonia transfer. J Neurochem 98:641–653.

Baldeiras I, Santana I, Proença M, Garrucho M, Pascoal R, Rodrigues A, Duro D, Oliveira C (2008) Peripheral oxidative damage in mild cognitive impairment and mild Alzheimer's disease. J Alzheimers Dis 15:117–128.

Bamford NS, Robinson S, Palmiter RD, Joyce JA, Moore C, Meshul CK (2004) Dopamine modulates release from corticostriatal terminals. J Neurosci 24:9541–9552.

Baquer, Hothersall, McLean (1988) Function and regulation of the pentose phosphate pathway in brain. Curr Top Cell Regul 29:265–289.

Barbiroli B, Montagna P, Martinelli P, Lodi R, Iotti S, Cortelli P, Funicello R, Zaniol P (1993) Defective brain energy metabolism shown by in vivo 31P MR spectroscopy in 28 patients with mitochondrial cytopathies. J Cereb Blood Flow Metab 13:469–474.

Barford D (1996) Molecular mechanisms of the protein serine/threonine phosphatases. Trends Biochem Sci 21:407–412.

Bastide M et al. (2015) Pathophysiology of L-dopa-induced motor and non-motor complications in Parkinson's disease. Prog Neurobiol 132:96–168.

Baughman J, Perocchi F, Girgis H, Plovanich M, Belcher-Timme C, Sancak Y, Bao R, Strittmatter L, Goldberger O, Bogorad R, Koteliansky V, Mootha V (2011) Integrative genomics identifies MCU as an essential component of the mitochondrial calcium uniporter. Nature 476:341–345.

Beaulieu J-M, Gainetdinov R (2011) The physiology, signaling, and pharmacology of dopamine Receptors. Pharmacol Rev 63:182–217.

Beaulieu J-M, Gainetdinov RR, Caron MG (2007) The Akt–GSK-3 signaling cascade in the actions of dopamine. Trends in Pharmacol Sci 28:166–172.

Beaulieu J-M, Sotnikova TD, Marion S, Lefkowitz RJ, Gainetdinov RR, Caron MG (2005) An Akt/β-Arrestin 2/PP2A signaling complex mediates dopaminergic neurotransmission and behavior. Cell 122:261–273.

Beckman K, Ames B (1999) Endogenous oxidative damage of mtDNA. Mutat Res 424:51–58.

Bélanger M, Allaman I, Magistretti PJ (2011) Brain energy metabolism: Focus on astrocyte-neuron metabolic cooperation. Cell Metabolism 14:724–738.

Bellou V, Belbasis L, Tzoulaki I, Middleton LT, Ioannidis JP, Evangelou E (2017) Systematic evaluation of the associations between environmental risk factors and dementia: An umbrella review of systematic reviews and meta-analyses. Alzheimers Dement 13:406–418.

Bender T, Martinou J-C (2016) The mitochondrial pyruvate carrier in health and disease: To carry or not to carry? Biochim Biophy Acta 1863:2436–2442.

Benhamou L, Cohen D (2014) Electrophysiological characterization of entopeduncular nucleus neurons in anesthetized and freely moving rats. Frontiers Syst Neurosci 8:7.

Berg D et al. (2011) AFQ056 treatment of levodopa-induced dyskinesias: Results of 2 randomized controlled trials. Mov Disord 26:1243–1250.

Berg D, Postuma R, Bloem B, Chan P, Dubois B, Gasser T, Goetz C, Halliday G, Hardy J, Lang A, Litvan I, Marek K, Obeso J, Oertel W, Olanow W, Poewe W, Stern M, Deuschl G (2014) Time to redefine PD? Introductory statement of the MDS Task Force on the definition of Parkinson's disease. Mov Disord 29:454–462.

Berke, Paletzki, Aronson, Hyman, Gerfen (1998) A complex program of striatal gene expression induced by dopaminergic stimulation. J Neurosci 18:5301–5310.

Bernard V, Normand E, Bloch B (1992) Phenotypical characterization of the rat striatal neurons expressing muscarinic receptor genes. J Neurosci 12:3591–3600.

Bernardi P, Scorrano L, Colonna R, Petronilli V, Lisa F (1999) Mitochondria and cell death. Mechanistic aspects and methodological issues. Eur J Biochem 264:687–701.

Berridge MJ (1998) Neuronal Calcium Signaling. Neuron 21:13–26.

Berthet A, Bezard E (2009) Dopamine receptors and L-DOPA-Induced Dyskinesia. Parkinsonism Relat Disord 4:S8–12.

Bessman S, Carpenter C (1985) The creatine-creatine phosphate energy shuttle. Annu Rev Biochem 54:831–862.

Bezawork-Geleta A, Brodie E, Dougan D, Truscott K (2015) LON is the master protease that protects against protein aggregation in human mitochondria through direct degradation of misfolded proteins. Sci Rep 5:17397.

Bezprozvanny I (2009) Calcium signaling and neurodegenerative diseases. Trends Mol Med 15:89–100.

Bharti S, Sommers J, Zhou J, Kaplan D, Spelbrink J, Mergny J-L, Brosh R (2014) DNA sequences proximal to human mitochondrial DNA deletion breakpoints prevalent in human disease form G-quadruplexes, a class of DNA structures inefficiently unwound by the mitochondrial replicative Twinkle helicase. J Biol Chem 289:29975–29993.

Białecka M, Droździk M, Kłodowska-Duda G, Honczarenko K, Gawrońska-Szklarz B, Opala G, Stankiewicz J (2004) The effect of monoamine oxidase B (MAOB) and catechol-O-methyltransferase (COMT) polymorphisms on levodopa therapy in patients with sporadic Parkinson's disease. Acta Neurol Scand 110:260–266.

Białecka M, Kurzawski M, Kłodowska-Duda G, Opala G, Tan E-KK, Droździk M (2008) The association of functional catechol-O-methyltransferase haplotypes with risk of Parkinson's disease, levodopa treatment response, and complications. Pharmacogenet Genomics 18:815–821.

Billups B, Forsythe ID (2002) Presynaptic mitochondrial calcium sequestration influences transmission at mammalian central synapses. J Neurosci 22:5840–5847.

Bisaglia M, Filograna R, Beltramini M, Bubacco L (2014) Are dopamine derivatives implicated in the pathogenesis of Parkinson's disease? Ageing Res Rev 13:107–114.

Biskup S, Moore D, Celsi F, Higashi S, West A, Andrabi S, Kurkinen K, Yu S, Savitt J, Waldvogel H, Faull R, Emson P, Torp R, Ottersen O, Dawson T, Dawson V (2006) Localization of LRRK2 to membranous and vesicular structures in mammalian brain. Ann Neurol 60:557–569.

Biswas G, Adebanjo O, Freedman B, Anandatheerthavarada H, Vijayasarathy, Zaidi M, Kotlikoff M, Avadhani N (1999) Retrograde Ca2+ signaling in C2C12 skeletal myocytes in response to mitochondrial genetic and metabolic stress: a novel mode of inter-organelle crosstalk. Embo J 18:522–533.

Bittner C, Loaiza A, Ruminot I, Larenas V, Sotelo-Hitschfeld T, Gutiérrez R, Córdova A, Valdebenito R, Frommer W, Barros F (2010) High resolution measurement of the glycolytic rate. Front Neuroenergetics 2:26.

Björklund A, Dunnett SB (2007) Dopamine neuron systems in the brain: An update. Trends Neurosci 30:194–202.

Blackmer T, Larsen EC, Bartleson C, Kowalchyk JA, Yoon E-J, Preininger AM, Alford S, Hamm HE, Martin TF (2005) G protein βγ directly regulates SNARE protein fusion machinery for secretory granule exocytosis. Nat Neurosci 8:421–425.

Blandini F, Fancellu R, Martignoni E, Mangiagalli A, Pacchetti C, Samuele A, Nappi G (2001) Plasma homocysteine and L-DOPA metabolism in patients with Parkinson disease. Clin Chem 47:1102–1104.

Bleazard W, McCaffery M, King E, Bale S, Mozdy A, Tieu Q, Nunnari J, Shaw J (1999) The dynamin-related GTPase Dnm1 regulates mitochondrial fission in yeast. Nat Cell Biol 1:298–304.

Bleier L, Dröse S (2012) Superoxide generation by complex III: From mechanistic rationales to functional consequences. Biochim Biophys Acta 1827:1320–1331.

Boado RJ, Li J, Nagaya M, Zhang C, Pardridge WM (1999) Selective expression of the large neutral amino acid transporter at the blood–brain barrier. Proc Natl Acad Sci USA 96:12079–12084.

Boddum K, Jensen TP, Magloire V, Kristiansen U, Rusakov DA, Pavlov I, Walker MC (2016) Astrocytic GABA transporter activity modulates excitatory neurotransmission. Nat Commun 7:13572.

Bogenhagen DF (2012) Mitochondrial DNA nucleoid structure. Biochim Biophys Acta 1819:914–920.

Bohr V, Stevnsner T, de Souza-Pinto N (2002) Mitochondrial DNA repair of oxidative damage in mammalian cells. Gene 286:127–134.

Boiteux A, Hess B (1981) Design of Glycolysis. Philos Trans R Soc Lond B Biol Sci 293:5–22.

Bolam JP, Hanley JJ, Booth PAC, Bevan MD (2000) Synaptic organisation of the basal ganglia. J Anat 196:527–542.

Bolam P, Pissadaki E (2012) Living on the edge with too many mouths to feed: Why dopamine neurons die. Mov Disord 27:1478–1483.

Bolaños JP (2016) Bioenergetics and redox adaptations of astrocytes to neuronal activity. J Neurochem 139:115–125.

Bolaños JP, Almeida A (2010) The pentose-phosphate pathway in neuronal survival against nitrosative stress. IUBMB Life 62:14–18.

Bolaños JP, Almeida A, Moncada S (2010) Glycolysis: a bioenergetic or a survival pathway? Trends Biochem Sci 35:145–149.

Bolaños JP, Delgado-Esteban M, Herrero-Mendez A, Fernandez-Fernandez S, Almeida A (2008) Regulation of glycolysis and pentose–phosphate pathway by nitric oxide: Impact on neuronal survival. Biochim Biophys Acta 1777:789–793.

Bonawitz N, Clayton D, Shadel G (2006) Initiation and beyond: Multiple functions of the human mitochondrial transcription machinery. Mol Cell 24:813–825.

Bonifati V, Rizzu P, van Baren M, Schaap O, Breedveld G, Krieger E, Dekker M, Squitieri F, Ibanez P, Joosse M, van Dongen J, Vanacore N, van Swieten J, Brice A, Meco G, van Duijn C, Oostra B, Heutink P (2003) Mutations in the DJ-1 gene associated with autosomal recessive early-onset Parkinsonism. Science 299:256–259.

Borden LA (1996) GABA transporter heterogeneity: Pharmacology and cellular localization. Neurochem Int 29:335–356.

Boumezbeur F, Petersen K, Cline G, Mason G, Behar K, Shulman G, Rothman D (2010) The contribution of blood lactate to brain energy metabolism in humans measured by dynamic 13C nuclear magnetic resonance spectroscopy. J Neurosci 30:13983–13991.

Bourgeois JM, Tarnopolsky MA (2004) Pathology of skeletal muscle in mitochondrial disorders. Mitochondrion 4:441–452.

Bouzier-Sore A-K, Pellerin L (2013) Unraveling the complex metabolic nature of astrocytes. Front Cell Neurosci 7:179.

Bowmaker M, Yang M, Yasukawa T, Reyes A, Jacobs H, Huberman J, Holt I (2003) Mammalian mitochondrial DNA replicates bidirectionally from an initiation zone. J Biol Chem 278:50961–50969.

Boyer PD (1997) The ATP synthase - A splendid molecular machine. Annu Rev Biochem 66:717–749.

Braak H, Del Tredici K, Rüb U, de Vos RA, Jansen Steur EN, Braak E (2003) Staging of brain pathology related to sporadic Parkinson's disease. Neurobiol Aging 24:197–211.

Braak H, Tredici K, Bratzke H, Hamm-Clement J, Sandmann-Keil D, Rüb U (2002) Staging of the intracerebral inclusion body pathology associated with idiopathic Parkinson's disease (preclinical and clinical stages). J Neurol 249:1–1.

Braak, Müller, Rüb, Ackermann, Bratzke, de Vos, Tredici D (2006) Pathology associated with sporadic Parkinson's disease--where does it end? J Neural Transm Suppl 70:89–97.

Braidy N, Poljak A, Jayasena T, Guillemin GJ, Sachdev P (2014) Ionotropic receptors in the central nervous system and neurodegenerative disease. In: Handbook of Neurotoxicity, (Kostrzewa RM, ed), pp 1071–1092. New York: Springer.

Braissant O (2012) Creatine and guanidinoacetate transport at blood-brain and blood-cerebrospinal fluid barriers. J Inherit Metab Dis 35:655–664.

Braissant O, Béard E, Torrent C, Henry H (2010) Dissociation of AGAT, GAMT and SLC6A8 in CNS: Relevance to creatine deficiency syndromes. Neurobiol Dis 37:423–433.

Braissant O, Henry H, Villard A-M, Speer O, Wallimann T, Bachmann C (2005) Creatine synthesis and transport during rat embryogenesis: Spatiotemporal expression of AGAT, GAMT and CT1. BMC Dev Biol 5:1–16.

Brami-Cherrier K, Valjent E, Hervé D, Darragh J, Corvol J-C, Pages C, Arthur S, Simon A, Girault J-A, Caboche J (2005) Parsing molecular and behavioral effects of cocaine in mitogen- and stress-activated protein kinase-1-deficient mice. J Neurosci 25:11444–11454.

Brand MD, Nicholls DG (2011) Assessing mitochondrial dysfunction in cells. Biochem J 435:297–312.

Brdiczka D, Pette D (1971) Intra- and extramitochondrial Isozymes of (NADP) malate dehydrogenase. Eur J Biochem 19:546–551.

Breckenridge D, Stojanovic M, Marcellus R, Shore G (2003) Caspase cleavage product of BAP31 induces mitochondrial fission through endoplasmic reticulum calcium signals, enhancing cytochrome c release to the cytosol. J Cell Biology 160:1115–1127.

Brekke E, Morken T, Sonnewald U (2015) Glucose metabolism and astrocyte–neuron interactions in the neonatal brain. Neurochem Int 82:33–41.

Bricker D, Taylor E, Schell J, Orsak T, Boutron A, Chen Y-C, Cox J, Cardon C, Vranken J, Dephoure N, Redin C, Boudina S, Gygi S, Brivet M, Thummel C, Rutter J (2012) A

mitochondrial pyruvate carrier required for pyruvate uptake in yeast, Drosophila, and humans. Science 337:96–100.

Bridges TM, Lindsley CW (2008) G-protein-coupled receptors: From classical modes of modulation to allosteric mechanisms. ACS Chem Biol 3:530–541.

Bronstein JM et al. (2011) Deep brain stimulation for Parkinson disease: an expert consensus and review of key issues. Arch Neurol 68:165.

Brosnan J, da Silva R, Brosnan M (2011) The metabolic burden of creatine synthesis. Amino Acids 40:1325–1331.

Brotchie J, Lee J, Venderova K (2005) Levodopa-induced dyskinesia in Parkinson's disease. J Neural Transm (Vienna) 112:359–391.

Brown A (2004) Brain glycogen re-awakened. J Neurochem 89:537–552.

Brown A, Deutch A, Colbran R (2005) Dopamine depletion alters phosphorylation of striatal proteins in a model of Parkinsonism. Eur J Neurosci 22:247–256.

Bruni F, Gramegna P, Oliveira J, Lightowlers R, Chrzanowska-Lightowlers Z (2013) REXO2 Is an oligoribonuclease active in human mitochondria. Plos ONE 8:e64670.

Bruni F, Lightowlers R, Chrzanowska-Lightowlers Z (2017) Human mitochondrial nucleases. FEBS J 284:1767–1777.

Budd S, Nicholls D (1996) Mitochondria, calcium regulation, and acute glutamate excitotoxicity in cultured cerebellar granule cells. J Neurochem 67:2282–2291.

Bunik VI, Fernie AR (2009) Metabolic control exerted by the 2-oxoglutarate dehydrogenase reaction: a cross-kingdom comparison of the crossroad between energy production and nitrogen assimilation. Biochem J 422:405–421.

Burté F, Carelli V, Chinnery P, Yu-Wai-Man P (2015) Disturbed mitochondrial dynamics and neurodegenerative disorders. Nat Rev Neurol 11:11–24.

Butow R, Avadhani N (2004) Mitochondrial signaling: The retrograde response. Mol Cell 14:1–15.

Bychkov E, Zurkovsky L, Garret MB, Ahmed MR, Gurevich EV (2012) Distinct cellular and subcellular distributions of G protein-coupled receptor kinase and arrestin isoforms in the striatum. PLoS ONE 7:e48912.

Cagin U, Duncan O, Gatt A, Dionne M, Sweeney S, Bateman J (2015) Mitochondrial retrograde signaling regulates neuronal function. Proc Natl Acad Sci USA 112:E6000–E6009.

Calabresi P, Centonze D, Gubellini P, Pisani A, Bernardi G (1998) Endogenous ACh enhances striatal NMDA-responses via M1-like muscarinic receptors and PKC activation. Eur J Neurosci 10:2887–2895.

Calabresi P, Picconi B, Tozzi A, Ghiglieri V, Filippo M (2014) Direct and indirect pathways of basal ganglia: a critical reappraisal. Nat Neurosci 17:1022–1030.

Calon F, Morissette M, Ghribi O, Goulet M, Grondin R, Blanchet P, Bédard P, DiPaolo T (2002) Alteration of glutamate receptors in the striatum of dyskinetic 1-methyl-4-phenyl-1,2,3,6-tetrahydropyridine-treated monkeys following dopamine agonist treatment. Prog Neuropsychopharmacol Biol Psychiatry 26:127–138.

Calvo SE, Mootha VK (2010) The mitochondrial proteome and human disease. Annu Rev Genomics Hum Genet 11:25–44.

Camps M, Carozzi A, Schnabel P, Scheer A, Parker PJ, Gierschik P (1992) Isozyme-selective stimulation of phospholipase C-β2 by G protein βγ-subunits. Nature 360:684–686.

Canet-Avilés RM, Wilson MA, Miller DW, Ahmad R, McLendon C, Bandyopadhyay S, Baptista MJ, Ringe D, Petsko GA, Cookson MR (2004) The Parkinson's disease protein DJ-1 is neuroprotective due to cysteine-sulfinic acid-driven mitochondrial localization. Proc Natl Acad Sci USA 101:9103–9108.

Cansev M, Wurtman RJ (2007) Aromatic Amino Acids in the Brain. In: Amino Acids and Peptides in the Nervous System. (Lajtha A, Oja SS, Schousboe A, Saransaari P, eds), pp 59–97. Handbook of Neurochemistry and Molecular Neurobiology. Springer.

Cao X, Yasuda T, Uthayathas S, Watts R, Mouradian M, Mochizuki H, Papa S (2010) Striatal overexpression of ΔFosB reproduces chonic Levodopa-induced involuntary movements. J Neurosci 30:7335–7343.

Carlsson A, Rasmussen BE, Kristjansen P (1959) The urinary excretion of adrenaline and noradrenaline by schizophrenic patients during reserpine treatment. J Neurochem 4:318–320.

Carta AR, Frau L, Pontis S, Pinna A, Morelli M (2008) Direct and indirect striatal efferent pathways are differentially influenced by low and high dyskinetic drugs: Behavioural and biochemical evidence. Parkinsonism Relat Disord 14:S165–S168.

Cartoni R, Martinou J-C (2009) Role of mitofusin 2 mutations in the physiopathology of Charcot–Marie–Tooth disease type 2A. Exp Neurol 218:268–273.

Case J, Wallace D (1981) Maternal inheritance of mitochondrial DNA polymorphisms in cultured human fibroblasts. Somat Cell Genet 7:103–108.

Cecchini G (2003) Function and structure of Complex II of the respiratory chain. Annu Rev Biochem 72:77–109.

Cenci A (2014) Presynaptic mechanisms of L-DOPA-Induced Dyskinesia: The findings, the debate, and the therapeutic implications. Front Neurol 5:242.

Cenci MA (2007) L-DOPA-Induced Dyskinesia: Cellular mechanisms and approaches to treatment. Parkinsonism Relat Disord 13:S263–S267.

Cenci MA (2017) Molecular Mechanisms of L-DOPA-Induced Dyskinesia. In: Handbook of Basal Ganglia Structure and Function, 2nd ed. (Steiner H, Tseng KY, eds), pp 857-871. Handbook of Behavioral Neuroscience. Academic Press.

Cenci MA, Konradi C (2010) Maladaptive striatal plasticity in L-DOPA-induced dyskinesia. Prog Brain Res 183:209–233.

Cenci MA, Ohlin EK (2009) Rodent models of treatment-induced motor complications in Parkinson's disease. Parkinsonism Relat Disord 15:S13–S17.

Cepeda C, Buchwald N, Levine M (1993) Neuromodulatory actions of dopamine in the neostriatum are dependent upon the excitatory amino acid receptor subtypes activated. Proc Natl Acad Sci USA 90:9576–9580.

Cepeda C, Levine MS (1998) Dopamine and N-Methyl-D-Aspartate receptor interactions in the neostriatum. Dev Neurosci 20:1–18.

Cerson E, Kunji E (2012) Substrate binding in the mitochondrial ADP/ATP carrier. Biochim Biophys Acta 1817:S33.

Chan D (2012) Fusion and fission: Interlinked processes critical for mitochondrial health. Annu Rev Genet 46:265–287.

Chan NC, Chan DC (2011) Parkin uses the UPS to ship off dysfunctional mitochondria. Autophagy 7:771–772.

Chan S, Guzman J, Ilijic E, Mercer J, Rick C, Tkatch T, Meredith G, Surmeier J (2007) “Rejuvenation” protects neurons in mouse models of Parkinson’s disease. Nature 447:1081–1086.

Chance B, Williams G (1955) A simple and rapid assay of oxidative phosphorylation. Nature 175:1120–1121.

Chandel N (2015) Evolution of mitochondria as signaling organelles. Cell Metab 22:204–206.

Chang C-R, Blackstone C (2007) Cyclic AMP-dependent protein kinase phosphorylation of Drp1 regulates its GTPase activity and mitochondrial morphology. J Biol Chem 282:21583–21587.

Chao J-R, Parganas E, Boyd K, Hong C, Opferman J, Ihle J (2008) Hax1-mediated processing of HtrA2 by Parl allows survival of lymphocytes and neurons. Nature 452:98–102.

Chapuis S, Ouchchane L, Metz O, Gerbaud L, Durif F (2005) Impact of the motor complications of Parkinson’s disease on the quality of life. Mov Disord 20:224–230.

Chassain, Eschalier, Durif (2003) Antidyskinetic effect of magnesium sulfate in MPTP-lesioned monkeys. Exp Neurol 182:490–496.

Chaudhuri KR, Odin P, Antonini A, Martinez-Martin P (2011) Parkinson’s disease: the non-motor issues. Parkinsonism Relat Disord 17:717–723.

Chaudhuri R, Bhidayasiri R, van Laar T (2016) Unmet needs in Parkinson’s disease: New horizons in a changing landscape. Parkinsonism Relat Disord 33:S2–S8.

Chen H, Chan DC (2009) Mitochondrial dynamics--fusion, fission, movement, and mitophagy--in neurodegenerative diseases. Hum Mol Genet 18:R169–R176.

Chen H, Chomyn A, Chan D (2005) Disruption of fusion results in mitochondrial heterogeneity and dysfunction. J Biol Chem 280:26185–26192.

Chen H, Detmer S, Ewald A, Griffin E, Fraser S, Chan D (2003) Mitofusins Mfn1 and Mfn2 coordinately regulate mitochondrial fusion and are essential for embryonic development. J Cell Biol 160:189–200.

Chen H, McCaffery M, Chan D (2007) Mitochondrial fusion protects against neurodegeneration in the cerebellum. Cell 130:548–562.

Chen H, Vermulst M, Wang YE, Chomyn A, Prolla TA, McCaffery MJ, Chan DC (2010) Mitochondrial fusion is required for mtDNA stability in skeletal muscle and tolerance of mtDNA mutations. Cell 141:280–289.

Chen J, Swope D (2007) Pharmacotherapy for Parkinson’s disease. Pharmacotherapy 27:161S–173S.

Chen L, Roberts R, Friedman DL (1995) Expression of brain-type creatine kinase and ubiquitous mitochondrial creatine kinase in the fetal rat brain: Evidence for a nuclear energy shuttle. J Comp Neurol 363:389–401.

Chinnery P, Thorburn D, Samuels D, White S, Dahl H-H, Turnbull D, Lightowlers R, Howell N (2000) The inheritance of mitochondrial DNA heteroplasmy: random drift, selection or both? Trends Genet 16:500–505.

Chinnery PF, Schon EA (2003) Mitochondria. J Neurol Neurosurg Psychiatry 74:1188–1199.

Chinta S, Mallajosyula J, Rane A, Andersen J (2010) Mitochondrial alpha-synuclein accumulation impairs complex I function in dopaminergic neurons and results in increased mitophagy in vivo. Neurosci Lett 486:235–239.

Choi D (1985) Glutamate neurotoxicity in cortical cell culture is calcium dependent. Neurosci Lett 58:293–297.

Choi DW (1988) Calcium-mediated neurotoxicity: relationship to specific channel types and role in ischemic damage. Trends Neurosci 11:465–469.

Choi T, Pardridge W (1986) Phenylalanine transport at the human blood-brain barrier. Studies with isolated human brain capillaries. J Biol Chem 261:6536–6541.

Chotibut T, Apple D, Jefferis R, Salvatore M (2012) Dopamine transporter loss in 6-OHDA Parkinson's model is unmet by parallel reduction in dopamine uptake. Plos One 7:e52322.

Christian B, Spremulli L (2012) Mechanism of protein biosynthesis in mammalian mitochondria. Biochim Biophys Acta 1819:1035–1054.

Chrivia, Kwok, Lamb, Hagiwara, Montminy, Goodman (1993) Phosphorylated CREB binds specifically to the nuclear protein CBP. Nature:855–859.

Cicchetti F, Drouin-Ouellet J, Gross RE (2009) Environmental toxins and Parkinson's disease: what have we learned from pesticide-induced animal models? Trends Pharmacol Sci 30:475–483.

Cilenti L, Soundarapandian M, Kyriazis G, Stratico V, Singh S, Gupta S, Bonventre J, Alnemri E, Zervos A (2004) Regulation of HAX-1 anti-apoptotic protein by Omi/HtrA2 protease during cell death. J Biol Chem 30:50295–50301.

Cipolat S, Rudka T, Hartmann D, Costa V, Serneels L, Craessaerts K, Metzger K, Frezza C, Annaert W, D'Adamio L, Derks C, Dejaegere T, Pellegrini L, D'Hooge R, Scorrano L, Strooper B (2006) Mitochondrial rhomboid PARL regulates cytochrome c release during apoptosis via OPA1-dependent cristae remodeling. Cell 126:163–175.

Cipolat, de Brito, Zilio D, Scorrano (2004) OPA1 requires mitofusin 1 to promote mitochondrial fusion. Proc Natl Acad Sci USA 30:15927–15932.

Clarke C (2004) Neuroprotection and pharmacotherapy for motor symptoms in Parkinson's disease. Lancet Neurol 3:466–474.

Clausen T, Kaiser M, Huber R, Ehrmann M (2011) HTRA proteases: regulated proteolysis in protein quality control. Nat Rev Mol Cell Bio 12:152–162.

Clay HB, Sillivan S, Konradi C (2011) Mitochondrial dysfunction and pathology in bipolar disorder and schizophrenia. Int J Dev Neurosci 29:311–324.

Clayton D (1982) Replication of animal mitochondrial DNA. Cell 28:693–705.

Clayton D (2000) Transcription and replication of mitochondrial DNA. Hum Reprod 15:11–17.

Clayton D (2003) Mitochondrial DNA replication: What we know. IUBMB Life 55:213–217.

Cline SD (2012) Mitochondrial DNA damage and its consequences for mitochondrial gene expression. Biochim Biophys Acta 1819:979–991.

Cogliati S, Frezza C, Soriano M, Varanita T, Quintana-Cabrera R, Corrado M, Cipolat S, Costa V, Casarin A, Gomes L, Perales-Clemente E, Salviati L, Fernandez-Silva P, Enriquez J, Scorrano L (2013) Mitochondrial cristae shape determines respiratory chain supercomplexes assembly and respiratory efficiency. Cell 155:160–171.

Cole AR (2012) GSK3 as a sensor determining cell fate in the brain. Front Mol Neurosci 5:4.

Cole RL, Konradi C, Douglass J, Hyman SE (1995) Neuronal adaptation to amphetamine and dopamine: Molecular mechanisms of prodynorphin gene regulation in rat striatum. Neuron 14:813–823.

Colombini M (2012) Mitochondrial outer membrane channels. Chem Rev 112:6373–6387.

Comi C, Ferrari M, Marino F, Magistrelli L, Cantello R, Riboldazzi G, Bianchi M, Bono G, Cosentino M (2017) Polymorphisms of dopamine receptor genes and risk of L-DOPA–Induced Dyskinesia in Parkinson's disease. Int J Mol Sci 18:242.

Conn JP, Battaglia G, Marino MJ, Nicoletti F (2005) Metabotropic glutamate receptors in the basal ganglia motor circuit. Nat Rev Neurosci 6:787–798.

Contreras L (2015) Role of AGC1/aralar in the metabolic synergies between neuron and glia. Neurochem Int 88:38–46.

Conway K, Harper J, Lansbury P (1998) Accelerated in vitro fibril formation by a mutant α-synucleinlinked to early-onset Parkinson disease. Nat Med 4:1318–1320.

Cooper AJ (2013) Quantitative analysis of neurotransmitter pathways under steady state conditions – A perspective. Front Endocrinol 4:179.

Copeland W, Longley M (2014) Mitochondrial genome maintenance in health and disease. DNA Repair 19:190–198.

Copeland WC (2010) The Mitochondrial DNA polymerase in health and disease. In: Genome Stability and Human Diseases, vol 50. (Nasheuer HP, eds) pp 211–222 Subcellular Biochemistry. Springer.

Corvol J-C, Muriel M-P, Valjent E, Féger J, Hanoun N, Girault J-A, Hirsch E, Hervé D (2004) Persistent increase in olfactory type G-protein α subunit levels may underlie D1 receptor functional hypersensitivity in Parkinson disease. J Neurosci 24:7007–7014.

Cowell R, Blake K (2007) Localization of the transcriptional coactivator PGC-1α to GABAergic neurons during maturation of the rat brain. Journal of Comp Neurol 502:1–18.

Crane, Sols (1954) The non-competitive inhibition of brain hexokinase by glucose-6-phosphate and related compounds. J Biol Chem 210:597–606.

Cribbs T, Strack S (2007) Reversible phosphorylation of Drp1 by cyclic AMP-dependent protein kinase and calcineurin regulates mitochondrial fission and cell death. Embo Rep 8:939–944.

Crittenden J, Cantuti-Castelvetri I, Saka E, Keller-McGandy C, Hernandez L, Kett L, Young A, Standaert D, Graybiel A (2009) Dysregulation of CalDAG-GEFI and CalDAG-GEFII predicts the severity of motor side-effects induced by anti-parkinsonian therapy. Proc Natl Acad Sci USA 106:2892–2896.

Crossman AR (2000) Functional anatomy of movement disorders. J Anat 196:519–525.

Cruz C, Aminoff M, Meyerhoff D, Graham S, Weiner M (1997) Proton MR spectroscopic imaging of the striatum in Parkinson's disease. Magn Reson Imaging 15:619–624.

Csordás G, Várnai P, Golenár T, Roy S, Purkins G, Schneider T, Balla T, Hajnóczky G (2010) Imaging interorganelle contacts and local calcium dynamics at the ER-Mitochondrial interface. Mol Cell 39:121–132.

Cui H, Kong Y, Zhang H (2012) Oxidative stress, mitochondrial dysfunction, and aging. J Signal Transduct 2012:646354.

Cullen PJ, Lockyer PJ (2002) Integration of calcium and RAS signalling. Nat Rev Mol Cell Biol 3:339–348.

Dall T, Gallo P, Chakrabarti R, West T, Semilla A, Storm M (2013) An aging population and growing disease burden will require a large and specialized health care workforce by 2025. Health Aff 32:2013–2020.

Damiano M, Gautier CA, Bulteau A-L, Ferrando-Miguel R, Gouarne C, Paoli M, Pruss R, Auchère F, L'Hermitte-Stead C, Bouillaud F, Brice A, Corti O, Lombès A (2014) Tissue- and cell-specific mitochondrial defect in parkin-deficient mice. PLoS ONE 9:e99898.

Datler C, Pazarentzos E, Mahul-Mellier A-L, Chaisaklert W, Hwang M-S, Osborne F, Grimm S (2014) CKMT1 regulates the mitochondrial permeability transition pore in a process that provides evidence for alternative forms of the complex. J Cell Sci 127:1816–1828.

David G, Talbot J, Barrett EF (2003) Quantitative estimate of mitochondrial [Ca2+] in stimulated motor nerve terminals. Cell Calcium 33:197–206.

Davidson M, Walker W, Hernandez-Rosa E (2009) The m.3243A>G mtDNA mutation is pathogenic in an in vitro model of the human blood brain barrier. Mitochondrion 9:463–470.

Davie CA (2008) A review of Parkinson's disease. Br Med Bull 81:109–127.

Dawson AP (1997) Calcium signalling: How do IP3 receptors work? Curr Biol 7:R544–R547.

De Brito O, Scorrano L (2010) An intimate liaison: spatial organization of the endoplasmic reticulum–mitochondria relationship. Embo J 29:2715–2723.

De Lau LM, Breteler M (2006) Epidemiology of Parkinson's disease. Lancet Neurol 5:525–535.

DeBalsi K, Hoff K, Copeland W (2017) Role of the mitochondrial DNA replication machinery in mitochondrial DNA mutagenesis, aging and age-related diseases. Ageing Res Rev 33:89–104.

Defalco A, Davies R (1961) The synthesis of creatine by the brain of the intact rat. J Neurochem 7:308–312.

Deister C, Chan S, Surmeier J, Wilson C (2009) Calcium-activated SK channels influence voltage-gated ion channels to determine the precision of firing in globus pallidus neurons. J Neurosci 29:8452–8461.

Dekundy A, Lundblad M, Danysz W, Cenci A (2007) Modulation of L-DOPA-Induced abnormal involuntary movements by clinically tested compounds: Further validation of the rat dyskinesia model. Behav Brain Res 179:76–89.

Deloulme JC, Helies, Ledig, Lucas, Sensenbrenner (1997) A comparative study of the distribution of α- and γ-enolase subunits in cultured rat neural cells and fibroblasts. Int J Dev Neurosci 15:183–194.

Deminice R, Rosa F (2016) Creatine supplementation decreased homocysteine plasma levels in rats but not humans: A critical review with meta-analysis. Journal of Nutr Intermed Metab 3:50–57.

Denton, Randle, Martin (1972) Stimulation by calcium ions of pyruvate dehydrogenase phosphate phosphatase. Biochem J 128:161–163.

Denton, Richards, Chin (1978) Calcium ions and the regulation of NAD+-linked isocitrate dehydrogenase from the mitochondria of rat heart and other tissues. Biochem J 176:899–906.

Desjardins P, Frost E, Morais R (1985) Ethidium bromide-induced loss of mitochondrial DNA from primary chicken embryo fibroblasts. Mol Cell Biol 5:1163–1169.

Devine MJ, Birsa N, Kittler JT (2016) Miro sculpts mitochondrial dynamics in neuronal health and disease. Neurobiol Dis 90:27–34.

DeWire SM, Ahn S, Lefkowitz RJ, Shenoy SK (2007) β-Arrestins and cell signaling. Annu Rev Physiol 69:483–510.

Dexter, Carter, Wells, Javoy-Agid, Agid, Lees, Jenner, Marsden (1989) Basal lipid peroxidation in Substantia Nigra is increased in Parkinson's disease. J Neurochem 52:381–389.

Di Monte DA (2003) The environment and Parkinson's disease: Is the nigrostriatal system preferentially targeted by neurotoxins? Lancet Neurol 2:531–538.

Diaz-Ruiz R, Rigoulet M, Devin A (2011) The Warburg and Crabtree effects: On the origin of cancer cell energy metabolism and of yeast glucose repression. Biochim Biophys Acta 1807:568–576.

Dienel G (2012) Brain lactate metabolism: The discoveries and the controversies. J Cereb Blood Flow Metabolism 32:1107–1138.

DiMauro S, Schon E (2003) Mitochondrial respiratory-chain diseases. N Engl J Med 348:2656–2668.

Divac N, Prostran M, Jakovcevski I, Cerovac N (2014) Second-generation antipsychotics and extrapyramidal adverse effects. Biomed Res Int 2014:656370.

Dodson M, Guo M (2007) Pink1, Parkin, DJ-1 and mitochondrial dysfunction in Parkinson's disease. Curr Opin Neurobiol 17:331–337.

Dolder M, Walzel B, Speer O, Schlattner U, Wallimann T (2003) Inhibition of the mitochondrial permeability transition by creatine kinase substrates. J Biol Chem 278:17760–17766.

Dölle C, Flønes I, Nido G, Miletic H, Osuagwu N, Kristoffersen S, Lilleng P, Larsen J, Tysnes O-B, Haugarvoll K, Bindoff L, Tzoulis C (2016) Defective mitochondrial DNA homeostasis in the substantia nigra in Parkinson disease. Nat Commun 7:13548.

Dolphin AC (2003) G protein modulation of voltage-gated calcium channels. Pharmacol Rev 55:607–627.

Doménech E, Maestre C, Esteban-Martínez L, Partida D, Pascual R, Fernández-Miranda G, Seco E, Campos-Olivas R, Pérez M, Megias D, Allen K, López M, Saha AK, Velasco G, Rial E, Méndez R, Boya P, Salazar-Roa M, Malumbres M (2015) AMPK and PFKFB3 mediate glycolysis and survival in response to mitophagy during mitotic arrest. Nat Cell Biology 17:1304–1316.

Douglass, McKinzie, Pollock (1994) Identification of multiple DNA elements regulating basal and protein kinase A-induced transcriptional expression of the rat prodynorphin gene. Mol Endocrinol 8:333–344.

Drechsel D, Patel M (2010) Respiration-dependent H2O2 removal in brain mitochondria via the thioredoxin/peroxiredoxin system. J Biol Chem 285:27850–27858.

Dröge W (2002) Free radicals in the physiological control of cell function. Physiol Rev 82:47–95.

Du F, Zhu X-H, Zhang Y, Friedman M, Zhang N, Uğurbil K, Chen W (2008) Tightly coupled brain activity and cerebral ATP metabolic rate. Proc Natl Acad Sci USA 105:6409–6414.

Duarte JM, Gruetter R (2012) Cerebral Glucose Transport and Homeostasis. In: Neural Metabolism In Vivo, vol 4 (Choi IY, Gruetter R, eds), pp 655–673 Advances in Neurobiology. Springer.

Duchen MR (2012) Mitochondria, calcium-dependent neuronal death and neurodegenerative disease. Pflügers Arch 464:111–121.

Dudman JT, Eaton ME, Rajadhyaksha A, Macías W, Taher M, Barczak A, Kameyama K, Huganir R, Konradi C (2003) Dopamine D1 receptors mediate CREB phosphorylation via phosphorylation of the NMDA receptor at Ser897–NR1. J Neurochem 87:922–934.

Dunah, Wang, Yasuda, Kameyama, Huganir, Wolfe, Standaert (2000) Alterations in subunit expression, composition, and phosphorylation of striatal N-methyl-D-aspartate glutamate receptors in a rat 6-hydroxydopamine model of Parkinson's disease. Mol Pharmacol 57:342–352.

Dzeja P, Terzic A (2003) Phosphotransfer networks and cellular energetics. J Exp Biology 206:2039–2047.

Edvardson S, Korman S, Livne A, Shaag A, Saada A, Nalbandian R, Allouche-Arnon H, Gomori M, Katz-Brull R (2010) L-arginine:glycine amidinotransferase (AGAT) deficiency: Clinical presentation and response to treatment in two patients with a novel mutation. Mol Genet Metab 101:228–232.

Eeden S, Tanner C, Bernstein A, Fross R, Leimpeter A, Bloch D, Nelson L (2003) Incidence of Parkinson's disease: variation by age, gender, and race/ethnicity. Am J Epidemiol 157:1015–1022.

Efremov R, Baradaran R, Sazanov L (2010) The architecture of respiratory complex I. Nature 465:441–445.

Eguchi Y, Shimizu S, Tsujimoto Y (1997) Intracellular ATP levels determine cell death fate by apoptosis or necrosis. Cancer Res 57:1835–1840.

Ehses S, Raschke I, Mancuso G, Bernacchia A, Geimer S, Tondera D, Martinou J-C, Westermann B, Rugarli E, Langer T (2009) Regulation of OPA1 processing and mitochondrial fusion by m-AAA protease isoenzymes and OMA1. J Cell Biol 187:1023–1036.

El-Hattab A, Adesina A, Jones J, Scaglia F (2015) MELAS syndrome: Clinical manifestations, pathogenesis, and treatment options. Mol Genet Metab 116:4–12.

Elgass K, Pakay J, Ryan M, Palmer C (2013) Recent advances into the understanding of mitochondrial fission. Biochim Biophys Acta 1833:150–161.

Eliuk SM, Renfrow MB, Shonsey EM, Barnes S, Kim H (2007) Active site modifications of the brain isoform of creatine kinase by 4-hydroxy-2-nonenal correlate with reduced enzyme activity: Mapping of modified sites by Fourier transform-ion cyclotron resonance mass spectrometry. Chem Res Toxicol 20:1260–1268.

Engelman HS, MacDermott AB (2004) Presynaptic ionotropic receptors and control of transmitter release. Nat Rev Neurosci 5:135–145.

Ennis SR, Kawai N, Ren X, Abdelkarim GE, Keep RF (1998) Glutamine uptake at the blood-brain barrier is mediated by N-system transport. J Neurochem 71:2565–2573.

Erecińska M, Silver I (1989) ATP and Brain Function. J Cereb Blood Flow Metab 9:2–19.

Erickson J, Joiner M, Guan X, Kutschke W, Yang J, Oddis C, Bartlett R, Lowe J, O'Donnell S, Aykin-Burns N, Zimmerman M, Zimmerman K, Ham A-J, Weiss R, Spitz D, Shea M, Colbran R, Mohler P, Anderson M (2008) A dynamic pathway for calcium-independent activation of CaMKII by methionine oxidation. Cell 133:462–474.

Evans R, Herin G, Hawes S, Blackwell K (2015) Calcium-dependent inactivation of calcium channels in the medial striatum increases at eye opening. Journal of Neurophysiology 113:2979–2986.

Exner N, Lutz A, Haass C, Winklhofer K (2012) Mitochondrial dysfunction in Parkinson's disease: molecular mechanisms and pathophysiological consequences. Embo J 31:3038–3062.

Exton J (1990) Signaling through phosphatidylcholine breakdown. J Biol Chem 265:1–4.

Fabbrini G, Brotchie J, Grandas F, Nomoto M, Goetz C (2007) Levodopa-Induced Dyskinesias. Mov Disord 22:1379–1389.

Fagone P, Jackowski S (2013) Phosphatidylcholine and the CDP–choline cycle. Biochim Biophys Acta 1831:523–532.

Fahn S (2003) Description of Parkinson's disease as a clinical syndrome. Ann NY Acad Sci:1–14.

Falkenberg M, Larsson N-G, Gustafsson C (2007) DNA replication and transcription in mammalian mitochondria. Annu Rev Biochem 76:679–699.

Fasano S, D'Antoni A, Orban P, Valjent E, Putignano E, Vara H, Pizzorusso T, Giustetto M, Yoon B, Soloway P, Maldonado R, Caboche J, Brambilla R (2009) Ras-guanine nucleotide-releasing factor 1 (Ras-GRF1) controls activation of extracellular signal-regulated kinase (ERK) signaling in the striatum and long-term behavioral responses to cocaine. Biol Psychiatry 66:758–768.

Feig (2011) Regulation of neuronal function by Ras-GRF exchange factors. Genes Cancer 2:306–319.

Fernandez-Fernandez S, Almeida A, Bolaños JP (2012) Antioxidant and bioenergetic coupling between neurons and astrocytes. The Biochemical Journal 433:3–11.

Fernández-Vizarra E, Tiranti V, Zeviani M (2009) Assembly of the oxidative phosphorylation system in humans: What we have learned by studying its defects. Biochim Biophys Acta 1793:200–211.

Ferre S, Ciruela F, Borycz J, Solinas M, Quarta D, Antoniou K, Quiroz C, Justinova Z, Lluis C, Franco R, Goldberg SR (2008) Adenosine A1-A2A receptor heteromers: new targets for caffeine in the brain. Front Biosci 13:2391.

Feyder M, Bonito-Oliva A, Fisone G (2011) L-DOPA-Induced Dyskinesia and abnormal signaling in striatal medium spiny neurons: Focus on Dopamine D1 receptor-mediated transmission. Front Behav Neurosci 5:71.

Feyder M, Södersten E, Santini E, Vialou V, LaPlant Q, Watts EL, Spigolon G, Hansen K, Caboche J, Nestler EJ, Fisone G (2016) A role for mitogen- and stress-activated kinase 1 in L-DOPA–Induced Dyskinesia and ΔFosB expression. Biol Psychiatry 79:362–371.

Fieblinger T, Sebastianutto I, Alcacer C, Bimpisidis Z, Maslava N, Sandberg S, Engblom D, Cenci A (2014) Mechanisms of Dopamine D1 receptor-mediated ERK1/2 activation in the parkinsonian striatum and their modulation by metabotropic glutamate receptor type 5. J Neurosci 34:4728–4740.

Fields TA, Casey PJ (1997) Signalling functions and biochemical properties of pertussis toxin-resistant G-proteins. Biochem J 321:561–571.

Fienberg A et al. (1998) DARPP-32: regulator of the efficacy of dopaminergic neurotransmission. Science 281:838–842.

Firth JD, Ebert BL, Ratcliffe PJ (1995) Hypoxic regulation of Lactate Dehydrogenase A: Interaction between Hypoxia-Inducible Factor 1 and cAMP Response Elements. J Biol Chem 270:21021–21027.

Fish J, Raule N, Attardi G (2004) Discovery of a major D-Loop replication origin reveals two modes of human mtDNA synthesis. Science 306:2098–2101.

Fisone G, Håkansson K, Borgkvist A, Santini E (2007) Signaling in the basal ganglia: postsynaptic and presynaptic mechanisms. Physiol Behav 92:8–14.

Fliss M, Usadel H, Caballero O, Wu L, Buta M, Eleff S, Jen J, Sidransky D (2000) Facile detection of mitochondrial DNA mutations in tumors and bodily fluids. Science 287:2017–2019.

Foehring, Zhang, Lee JCF, Callaway (2009) Endogenous calcium buffering capacity of Substantia Nigral dopamine neurons. J Neurophysiol 102:2326–2333.

Frank M, Duvezin-Caubet S, Koob S, Occhipinti A, Jagasia R, Petcherski A, Ruonala M, Priault M, Salin B, Reichert A (2012) Mitophagy is triggered by mild oxidative stress in a mitochondrial fission dependent manner. Biochim Biophys Acta 1823:2297–2310.

Fransson Å, Ruusala A, Aspenström P (2006) The atypical Rho GTPases Miro-1 and Miro-2 have essential roles in mitochondrial trafficking. Biochem Biophys Res Commun 344:500–510.

Frederick AL, Yano H, Trifilieff P, Vishwasrao HD, Biezonski D, Mészáros J, Urizar E, Sibley DR, Kellendonk C, Sonntag KC, Graham DL, Colbran RJ, Stanwood GD, Javitch JA (2015) Evidence against dopamine D1/D2 receptor heteromers. Mol Psychiatry 20:1373–1385.

Frezza C, Cipolat S, de Brito O, Micaroni M, Beznoussenko G, Rudka T, Bartoli D, Polishuck R, Danial N, Strooper B, Scorrano L (2006) OPA1 controls apoptotic cristae remodeling independently from mitochondrial fusion. Cell 126:177–189.

Friedman J (2011) The role of free radicals in the nervous system. In: Oxidative Stress and Free Radical Damage in Neurology (Gadoth N., Göbel H, eds), pp 1–17. Oxidative Stress in Applied Basic Research and Clinical Practice. Humana Press.

Friedman J, Lackner L, West M, DiBenedetto J, Nunnari J, Voeltz G (2011) ER tubules mark sites of mitochondrial division. Science 334:358–362.

Friel, Tsien (1989) Voltage-gated calcium channels: direct observation of the anomalous mole fraction effect at the single-channel level. Proc Natl Acad Sci 86:5207–5211.

Fryer, Appleton, Sweeney, Rosenbloom, Harding (1994) Mitochondrial DNA 8993 (NARP) mutation presenting with a heterogeneous phenotype including “cerebral palsy”. Arch Dis Child 71:419–422.

Fuchs T, Ozelius LJ (2013) Genetics in dystonia: An update. Curr Neurol Neurosci Rep 13:410.

Fuke S, Suo S, Takahashi N, Koike H, Sasagawa N, Ishiura S (2001) The VNTR polymorphism of the human dopamine transporter (DAT1) gene affects gene expression. Pharmacogenomics J 1:152–156.

Fukui M, Zhu B (2010) Mitochondrial superoxide dismutase SOD2, but not cytosolic SOD1, plays a critical role in protection against glutamate-induced oxidative stress and cell death in HT22 neuronal cells. Free Radic Bio Med 48:821–830.

Fukuyama R, Nakayama A, Nakase T, Toba H, Mukainaka T, Sakaguchi H, Saiwaki T, Sakurai H, Wada M, Fushiki S (2002) A newly established neuronal ρ0 cell line highly susceptible to oxidative stress accumulates iron and other metals: Relevance to the origin of metal ion deposits in brains with neurodegenerative disorders. J Biol Chem 277:41455–41462.

Gabriel M, Litchfield DW (2013) Protein Kinase CK2: At the Crossroads of Pathways Controlling Cell Proliferation and Survival. In: Protein Kinase CK2 (Pinna LA, eds), pp 169–189. John Wiley and Sons.

Gajer, Furdas, Gründer, Gothwal, Heinicke, Keller, Colland, Fulda, Pahl, Fichtner, Sippl, Jung (2015) Histone acetyltransferase inhibitors block neuroblastoma cell growth in vivo. Oncogenesis 9:e137.

Galimov E, Chernyak B, Sidorenko A, Tereshkova A, Chumakov P (2014) Prooxidant properties of p66shc are mediated by mitochondria in human cells. Plos ONE 9:e86521.

Gao A, Houtkooper R (2014) Mitochondrial fission: Firing up mitochondria in brown adipose tissue. Embo J 33:401–402.

Garcia-Olivares J, Torres-Salazar D, Owens WA, Baust T, Siderovski DP, Amara SG, Zhu J, Daws LC, Torres GE (2013) Inhibition of dopamine transporter activity by G Protein βγ subunits. PLoS ONE 8:e59788.

Gardner P, Raineri I, Epstein L, White C (1995) Superoxide radical and iron modulate aconitase activity in mammalian cells. J Biol Chem 270:13399–13405.

Garone C, Tadesse S, Hirano M (2011) Clinical and genetic spectrum of mitochondrial neurogastrointestinal encephalomyopathy. Brain 134:3326–3332.

Gaspari M, Falkenberg M, Larsson N, Gustafsson C (2004) The mitochondrial RNA polymerase contributes critically to promoter specificity in mammalian cells. Embo J 23:4606–4614.

Gautron L, Layé S (2005) Glucose metabolism in the brain. Psychoneuroendocrinology 30:116–118.

Geier EG, Schlessinger A, Fan H, Gable JE, Irwin JJ, Sali A, Giacomini KM (2013) Structure-based ligand discovery for the Large-neutral Amino Acid Transporter 1, LAT-1. Proc Natl Acad Sci USA 110:5480–5485.

Gerachshenko T, Blackmer T, Yoon E-J, Bartleson C, Hamm HE, Alford S (2005) Gβγ acts at the C terminus of SNAP-25 to mediate presynaptic inhibition. Nat Neurosci 8:597–605.

Gerard, Schachter (1932) Glucose Utilization by Brain. Exp Biol M 29:525–528.

Gerdes F, Tatsuta T, Langer T (2012) Mitochondrial AAA proteases — Towards a molecular understanding of membrane-bound proteolytic machines. Biochim Biophys Acta 1823:49–55.

Gerfen (2000) Molecular effects of dopamine on striatal-projection pathways. Trends Neurosci 23:S64–70.

Gerfen C (2003) D1 dopamine receptor supersensitivity in the dopamine-depleted striatum animal model of Parkinson's disease. The Neuroscientist 9:455–462.

Gerfen CR, Bolam JP (2017) The neuroanatomical organization of the basal ganglia. In: Handbook of Basal Ganglia Structure and Function, 2nd ed. (Steiner H, Tseng KY, eds), pp 3–32. Handbook of Behavioral Neuroscience. Academic Press.

Gerfen, Engber, Mahan, Susel, Chase, Monsma, Sibley (1990) D1 and D2 dopamine receptor-regulated gene expression of striatonigral and striatopallidal neurons. Science 250:1429–1432.

Gertz M, Steegborn C (2010) The lifespan-regulator p66Shc in mitochondria: redox enzyme or redox sensor? Antioxid Redox Signal 13:1417–1428.

Ghiglieri V, Bagetta V, Pendolino V, Picconi B, Calabresi P (2012) Corticostriatal plastic changes in experimental L-DOPA-Induced Dyskinesia. Parkinsons Dis 2012:358176.

Giacco F, Brownlee M (2010) Oxidative stress and diabetic complications. Circ Res 107:1058–1070.

Gibb, Lees (1988) The relevance of the Lewy body to the pathogenesis of idiopathic Parkinson's disease. J Neurol Neurosurg Psychiatry 51:745–752.

Gibbs M, Anderson D, Hertz L (2006) Inhibition of glycogenolysis in astrocytes interrupts memory consolidation in young chickens. Glia 54:214–222.

Gibson G, Starkov A, Blass J, Ratan R, Beal F (2010) Cause and consequence: Mitochondrial dysfunction initiates and propagates neuronal dysfunction, neuronal death and behavioral abnormalities in age-associated neurodegenerative diseases. Biochim Biophys Acta 1802:122–134.

Giladi N, Weitzman N, Schreiber S, Shabtai H, Peretz C (2007) New onset heightened interest or drive for gambling, shopping, eating or sexual activity in patients with Parkinson's disease: the role of dopamine agonist treatment and age at motor symptoms onset. J Psychopharmacol 21:501–506.

Giles, Blanc, Cann, Wallace (1980) Maternal inheritance of human mitochondrial DNA. Proc Natl Acad Sci USA 77:6715–6719.

Ginés S, Paoletti P, Alberch J (2010) Impaired TrkB-mediated ERK1/2 activation in Huntington Disease knock-in striatal cells involves reduced p52/p46 shc expression. J Biol Chem 285:21537–21548.

Ginovart N, Farde L, Halldin C, Swahn C (1999) Changes in striatal D2-receptor density following chronic treatment with amphetamine as assessed with pet in nonhuman primates. Synapse 31:154–162.

Giorgio M, Migliaccio E, Orsini F, Paolucci D, Moroni M, Contursi C, Pelliccia G, Luzi L, Minucci S, Marcaccio M, Pinton P, Rizzuto R, Bernardi P, Paolucci F, Pelicci P (2005) electron transfer between cytochrome c and p66shc generates reactive oxygen species that trigger mitochondrial apoptosis. Cell 122:221–233.

Glinka, Gassen, Youdim (1997) Mechanism of 6-hydroxydopamine neurotoxicity. J Neural Transm Suppl 50:55–66.

Goetz C et al. (2008) Movement Disorder Society-sponsored revision of the Unified Parkinson's Disease Rating Scale (MDS-UPDRS): Scale presentation and clinimetric testing results. Mov Disord 23:2129–2170.

Goker-Alpan O, Schiffmann R, Park JK, Stubblefield BK, Tayebi N, Sidransky E (2003) Phenotypic continuum in neuronopathic Gaucher disease: an intermediate phenotype between type 2 and type 3. J Pediatr 143:273–276.

Gold S, Hoang C, Potts B, Porras G, Pioli E, Kim K, Nadjar A, Qin C, LaHoste G, Li Q, Bioulac B, Waugh J, Gurevich E, Neve R, Bezard E (2007) RGS9–2 negatively modulates l-3,4-Dihydroxyphenylalanine-Induced Dyskinesia in experimental Parkinson's disease. J Neurosci 27:14338–14348.

Golenar T, Bansaghi S, Csordas G, Yule D, Joseph S, Hajnoczky G (2010) Dependence of ER-Mitochondria calcium transfer on different IP3 receptor isoforms. Biophys J 98:381a.

Gomes L, Benedetto G, Scorrano L (2011) During autophagy mitochondria elongate, are spared from degradation and sustain cell viability. Nat Cell Biol 13:589–598.

Goren N, Manzano A, Riera L, Ambrosio S, Ventura F, Bartrons R (2000) 6-Phosphofructo-2-kinase/fructose-2,6-bisphosphatase expression in rat brain during development. Mol Brain Res 75:138–142.

Goto Y, Nonaka I, Horai S (1990) A mutation in the tRNALeu(UUR) gene associated with the MELAS subgroup of mitochondrial encephalomyopathies. Nature 348:651–653.

Goudreau J, Pérez A, Aminoff M, Boyd J, Burau K, Christine C, Leehey M, Morgan J, Investigators N-P (2016) Choice of dopaminergic therapy among early, mild Parkinson disease subjects in North America. J Neurol Sci 366:74–81.

Grandas, Galiano M, Tabernero C (1999) Risk factors for Levodopa-Induced Dyskinesias in Parkinson's disease. J Neurol 246:1127–1133.

Graybiel AM (2005) The basal ganglia: learning new tricks and loving it. Curr Opin Neurobiol 15:638–644.

Greber BJ, Ban N (2015) Structure and function of the mitochondrial ribosome. Annu Rev Biochem 85:1–30.

Greer PL, Greenberg ME (2008) From synapse to nucleus: Calcium-dependent gene transcription in the control of synapse development and function. Neuron 59:846–860.

Greif GJ, Lin YJ, Liu JC, Freedman JE (1995) Dopamine-modulated potassium channels on rat striatal neurons: specific activation and cellular expression. J Neurosci 15:4533–4544.

Grenier K, McLelland G-L, Fon E (2013) Parkin- and PINK1-Dependent Mitophagy in Neurons: Will the Real Pathway Please Stand Up? Front Neurol 4:100.

Griffiths EJ, Rutter GA (2009) Mitochondrial calcium as a key regulator of mitochondrial ATP production in mammalian cells. Biochim Biophys Acta 1787:1324–1333.

Grimsby, Chen, Wang, Lan, Shih (1991) Human monoamine oxidase A and B genes exhibit identical exon-intron organization. Proc Natl Acad Sci USA 88:3637–3641.

Gröger A, Berg D (2012) Does structural neuroimaging reveal a disturbance of iron metabolism in Parkinson's disease? Implications from MRI and TCS studies. J Neural Transm (Vienna) 119:1523–1528.

Groth RD, Dunbar RL, Mermelstein PG (2003) Calcineurin regulation of neuronal plasticity. Biochem Biophys Res Commun 311:1159–1171.

Guha M, Srinivasan S, Ruthel G, Kashina A, Carstens R, Mendoza A, Khanna C, Winkle VT, Avadhani N (2013) Mitochondrial retrograde signaling induces epithelial–mesenchymal transition and generates breast cancer stem cells. Oncogene 33:5238–5250.

Guigoni C, Bezard E (2009) Involvement of canonical and non-canonical D1 dopamine receptor signalling pathways in L-DOPA-Induced Dyskinesia. Parkinsonism Relat Disord 3:S64–7.

Guigoni, Aubert, Li, Gurevich, Benovic, Ferry, Mach, Stark, Leriche, Håkansson, Bioulac B, Gross C, Sokoloff P, Fisone G, Gurevich, Bloch B, Bezard E (2005) Pathogenesis of Levodopa-Induced Dyskinesia: Focus on D1 and D3 dopamine receptors. Parkinsonism Relat Disord 15:S25–9.

Guillot TS, Miller GW (2009) Protective actions of the vesicular monoamine transporter 2 (VMAT2) in monoaminergic neurons. Mol Neurobiol 39:149–170.

Gurevich E, Gurevich V (2006) Arrestins: ubiquitous regulators of cellular signaling pathways. Genome Biol 7:236.

Gurevich E, Gurevich V (2010) Dopamine receptors and the treatment of Parkinson's disease. In: The Dopamine Receptors 2nd ed. (Neve KA, ed)., pp 525–584. The Receptors. Humana Press.

Gustafsson C, Falkenberg M, Larsson N-G (2015) Maintenance and expression of mammalian Mitochondrial DNA. Annu Rev Biochem 85:1–28.

Guzman J, Sánchez-Padilla J, Chan S, Surmeier J (2009) Robust pacemaking in substantia nigra dopaminergic neurons. J Neurosci 29:11011–11019.

Haas RH, Parikh S, Falk MJ, Saneto RP, Wolf NI, Darin N, Wong L-J, Cohen BH, Naviaux RK (2008) The in-depth evaluation of suspected mitochondrial disease. Mol Genet Metab 94:16–37.

Habas A, Hahn J, Wang X, Margeta M (2013) Neuronal activity regulates astrocytic Nrf2 signaling. Proc Natl Acad Sci USA 110:18291–18296.

Hahn K, Salomons G, Tackels-Horne D, Wood T, Taylor H, Schroer R, Lubs H, Jakobs C, Olson R, Holden K, Stevenson R, Schwartz C (2002) X-linked mental retardation with seizures and carrier manifestations is caused by a mutation in the creatine-transporter gene (SLC6A8) located in Xq28. Am J Hum Genet 70:1349–1356.

Håkansson K, Galdi S, Hendrick J, Snyder G, Greengard P, Fisone G (2006) Regulation of phosphorylation of the GluR1 AMPA receptor by dopamine D2 receptors. J Neurochem 96:482–488.

Halestrap A, Brenner C (2003) The adenine nucleotide translocase: A central component of the mitochondrial permeability transition pore and key player in cell death. Curr Med Chem 10:1507–1525.

Hamanaka R, Chandel N (2010) Mitochondrial reactive oxygen species regulate cellular signaling and dictate biological outcomes. Trends Biochem Sci 35:505–513.

Hansson M, Persson T, Friberg H, Keep M, Rees A, Wieloch T, Elmér E (2003) Powerful cyclosporin inhibition of calcium-induced permeability transition in brain mitochondria. Brain Res 960:99–111.

Haque MD, Elmore KB, Tripathy A, Koc H, Koc EC, Spremulli LL (2010) Properties of the C-terminal tail of human mitochondrial inner membrane protein Oxa1L and its interactions with mammalian mitochondrial ribosomes. J Biol Chem 285:28353–28362.

Hardie G, Ross F, Hawley S (2012) AMPK: a nutrient and energy sensor that maintains energy homeostasis. Nat Rev Mol Cell Biol 13:251–262.

Hardie GD (2014) AMPK—Sensing energy while talking to other signaling pathways. Cell Metab 20:939–952.

Harding H, Zhang Y, Ron D (1999) Protein translation and folding are coupled by an endoplasmic-reticulum-resident kinase. Nature:271–274.

Hardman C, Henderson J, Finkelstein D, Horne M, Paxinos G, Halliday G (2002) Comparison of the basal ganglia in rats, marmosets, macaques, baboons, and humans: Volume and neuronal number for the output, internal relay, and striatal modulating nuclei. J Comp Neurol 445:238–255.

Haris M, Singh A, Cai K, Kogan F, McGarvey J, Debrosse C, Zsido GA, Witschey WR, Koomalsingh K, Pilla JJ, Chirinos JA, Ferrari VA, Gorman JH, Hariharan H, Gorman RC, Reddy R (2014) A technique for in vivo mapping of myocardial creatine kinase metabolism. Nature medicine 20:209–214.

Harman D (1972) The biologic clock: The mitochondria? J Am Geriatr Soc 20:145–147.

Harman D (1981) The aging process. Proc Natl Acad Sci USA 78:7124–7128.

Harvey BH, Shahid M (2012) Metabotropic and ionotropic glutamate receptors as neurobiological targets in anxiety and stress-related disorders: focus on pharmacology and preclinical translational models. Pharmacol Biochem Behav 100:775–800.

Hattori Y, Akimoto K, Nishikimi T, Matsuoka H, Kasai K (2006) Activation of AMP-activated protein kinase enhances Angiotensin ii–induced proliferation in cardiac fibroblasts. Hypertension 47:265–270.

Hauptmann N, Grimsby J, Shih J, Cadenas E (1996) The metabolism of tyramine by monoamine oxidase a/b causes oxidative damage to mitochondrial DNA. Arch Biochem Biophys 335:295–304.

Hauser RA, McDermott MP, Messing S (2006) Factors associated with the development of motor fluctuations and dyskinesias in Parkinson disease. Arch Neurol 63:1756–1760.

Haute L, Pearce SF, Powell CA, D'Souza AR, Nicholls TJ, Minczuk M (2015) Mitochondrial transcript maturation and its disorders. J Inherit Metab Dis 38:655–680.

Haynes C, Petrova K, Benedetti C, Yang Y, Ron D (2007) ClpP mediates activation of a mitochondrial unfolded protein response in C. elegans. Dev Cell 13:467–480.

Haynes C, Ron D (2010) The mitochondrial UPR – protecting organelle protein homeostasis. J Cell Sci 123:3849–3855.

Hebert L, Weuve J, Scherr P, Evans D (2013) Alzheimer disease in the United States (2010–2050) estimated using the 2010 census. Neurology 80:1778–1783.

Hedskog L, Pinho C, Filadi R, Rönnbäck A, Hertwig L, Wiehager B, Larssen P, Gellhaar S, Sandebring A, Westerlund M, Graff C, Winblad B, Galter D, Behbahani H, Pizzo P, Glaser E, Ankarcrona M (2013) Modulation of the endoplasmic reticulum–mitochondria interface in Alzheimer's disease and related models. Proc Natl Acad Sci USA 110:7916–7921.

Heikkila R, Manzino L, Cabbat F, Duvoisin R (1984) Protection against the dopaminergic neurotoxicity of 1-methyl-4-phenyl-1,2,5,6-tetrahydropyridine by monoamine oxidase inhibitors. Nature 311:467–469.

Heiman M, Heilbut A, Francardo V, Kulicke R, Fenster R, Kolaczyk E, Mesirov J, Surmeier D, Cenci M, Greengard P (2014) Molecular adaptations of striatal spiny projection neurons during levodopa-induced dyskinesia. Proc Natl Acad Sci USA 111:4578–4583.

Hellemans J, Mortier G, De Paepe A, Speleman F, Vandesompele J (2007) qBase relative quantification framework and software for management and automated analysis of real-time quantitative PCR data. Genome Biology 8:R19.

Henneberry R (1989) The role of neuronal energy in the neurotoxicity of excitatory amino acids. Neurobiol Aging 10:611–613.

Heo J-M, Ordureau A, Paulo J, Rinehart J, Harper W (2015) The Pink1-parkin mitochondrial ubiquitylation pathway drives a program of OPTN/NDP52 recruitment and TBK1 activation to promote mitophagy. Mol Cell 60:7–20.

Herlitze S, Garcia DE, Mackie K, Hille B, Scheuer T, Catterall WA (1996) Modulation of Ca2+ channels by G-protein βγ subunits. Nature 380:258–262.

Hernandez-Lopez S, Tkatch T, Perez-Garci E, Galarraga E, Bargas J, Hamm H, Surmeier D (2000) D2 dopamine receptors in striatal medium spiny neurons reduce L-type Ca2+ currents and excitability via a novel PLCβ1-IP3-calcineurin-signaling cascade. J Neurosci 20:8987–8995.

Herrero-Mendez A, Almeida A, Fernández E, Maestre C, Moncada S, Bolaños JP (2009) The bioenergetic and antioxidant status of neurons is controlled by continuous degradation of a key glycolytic enzyme by APC/C–Cdh1. Nat Cell Biol 11:747–752.

Hertz L (2004) Intercellular metabolic compartmentation in the brain: past, present and future. Neurochem Int 45:285–296.

Hertz L (2011) Brain glutamine synthesis requires neuronal aspartate: A commentary. J Cereb Blood Flow Metab 31:384–387.

Hertz L (2013) The glutamate–glutamine (GABA) cycle: Importance of late postnatal development and potential reciprocal interactions between biosynthesis and degradation. Front Endocrinol 4:59.

Hertz L, Peng L, Dienel G (2007) Energy metabolism in astrocytes: High rate of oxidative metabolism and spatiotemporal dependence on glycolysis/glycogenolysis. J Cereb Blood Flow Metab 27:219–249.

Hertz L, Rothman DL (2017) Glutamine-glutamate cycle flux is similar in cultured astrocytes and brain and both glutamate production and oxidation are mainly catalyzed by aspartate aminotransferase. Biology 6:E17.

Hervé D, Lévi-Strauss M, Marey-Semper I, Verney C, Tassin J, Glowinski J, Girault J (1993) G(olf) and Gs in rat basal ganglia: possible involvement of G(olf) in the coupling of dopamine D1 receptor with adenylyl cyclase. J Neurosci 13:2237–2248.

Herzig S, Raemy E, Montessuit S, Veuthey J-L, Zamboni N, Westermann B, Kunji ER, Martinou J-C (2012) Identification and functional expression of the mitochondrial pyruvate carrier. Science 337:93–96.

Higley MJ, Sabatini BL (2008) Calcium signaling in dendrites and spines: Practical and functional considerations. Neuron 59:902–913.

Hirano M, DiMauro S (1996) Clinical features of mitochondrial myopathies and encephalomyopathies. In: Handbook of Muscle Disease (Lane RJM, ed), pp 479–504. Marcel Dekker Inc.

Hirano M, Pavlakis S (1994) Topical review: mitochondrial myopathy, encephalopathy, lactic acidosis, and strokelike episodes (MELAS): Current concepts. J Child Neurol 9:4–13.

Hirano, Silvestri, Blake, Lombes, Minetti, Bonilla, Hays, Lovelace, Butler, Bertorini, Threlkeld, Mitsumoto, Salberg, Rowland, DiMauro (1994) Mitochondrial neurogastrointestinal encephalomyopathy (MNGIE): Clinical, biochemical, and genetic features of an autosomal recessive mitochondrial disorder. Neurology 44:721–727.

Hirsch E, Graybiel A, Agid Y (1988) Melanized dopaminergic neurons are differentially susceptible to degeneration in Parkinson's disease. Nature 334:345–348.

Hoang T, Bluml S, Dubowitz D, Moats R, Kopyov O, Jacques D, Ross B (1998) Quantitative proton-decoupled 31P MRS and 1H MRS in the evaluation of Huntington's and Parkinson's diseases. Neurology 50:1033–1040.

Hofmann (1976) The significance of phosphofructokinase to the regulation of carbohydrate metabolism. Rev Physiol Bioch P 75:1–68.

Hollenbeck P, Saxton W (2005) The axonal transport of mitochondria. J Cell Sci 118:5411–5419.

Holmström K, Finkel T (2014) Cellular mechanisms and physiological consequences of redox-dependent signalling. Nat Rev Mol Cell Bio 15:411–421.

Holness MJ, Sugden MC (2003) Regulation of pyruvate dehydrogenase complex activity by reversible phosphorylation. Biochem Soc T 31:1143–1151.

Holshouser BA, Komu M, Möller HE, Zijlmans J, Kolem H, Hinshaw DB, Sonninen P, Vermathen P, Heerschap A, Masur H, Rinne UK, Koster A, Tosk JM (1995) Localized proton NMR spectroscopy in the striatum of patients with idiopathic Parkinson's disease: a multicenter pilot study. Magn Reson Med 33:589–594.

Hong X, Song R, Song H, Zheng T, Wang J, Liang Y, Qi S, Lu Z, Song X, Jiang H, Liu L, Zhang Z (2013) PTEN antagonises Tcl1/hnRNPK-mediated G6PD pre-mRNA splicing which contributes to hepatocarcinogenesis. Gut 63:1635-1647

Hoyle G, Mercer E, Palmiter R, Brinster R (1994) Cell-specific expression from the human dopamine beta-hydroxylase promoter in transgenic mice is controlled via a combination of positive and negative regulatory elements. J Neurosci 15:2455–2463.

Hu D, Serrano F, Oury T, Klann E (2006) Aging-dependent alterations in synaptic plasticity and memory in mice that overexpress extracellular superoxide dismutase. J Neurosci 26:3933–3941.

Huang J-Y, Hirschey MD, Shimazu T, Ho L, Verdin E (2010) Mitochondrial sirtuins. Biochim Biophys Acta 1804:1645–1651.

Hume S, Myers R, Bloomfield P, Opacka-Juffry J, Cremer J, Ahier R, Luthra S, Brooks D, Lammertsma A (1992) Quantitation of Carbon-11-labeled raclopride in rat striatum using positron emission tomography. Synapse 12:47–54.

Hunn B, Cragg S, Bolam P, Spillantini M-G, Wade-Martins R (2015) Impaired intracellular trafficking defines early Parkinson's disease. Trends Neurosci 38:178–188.

Huot P, Johnston TH, Koprich JB, Fox SH, Brotchie JM (2013) The pharmacology of L-DOPA-induced dyskinesia in Parkinson's disease. Pharmacol Rev 65:171–222.

Hur JH, Cho J, Walker DW (2010) Aging: Dial M for mitochondria. Aging 2:69–73.

Hurley M, Jackson M, Smith L, Rose S, Jenner P (2014) Proteomic analysis of striatum from mptp-treated marmosets (Callithrix jacchus) with L-DOPA-Induced Dyskinesia of differing severity. J Mol Neurosci 52:302–312.

Hurley MJ, Dexter DT (2012) Voltage-gated calcium channels and Parkinson's disease. Pharmacol Ther 133:324–333.

Hurley, Mash, Jenner (2001) Dopamine D(1) receptor expression in human basal ganglia and changes in Parkinson's disease. Brain Res Mol Brain Res 87:271–279.

Hutchison CA, Newbold JE, Potter SS, Edgell M (1974) Maternal inheritance of mammalian mitochondrial DNA. Nature 251:536–538.

Ichas F, Jouaville L, Mazat J-P (1997) Mitochondria are excitable organelles capable of generating and conveying electrical and calcium signals. Cell 89:1145–1153.

Iderberg, McCreary AC, Varney MA, Cenci MA, Newman-Tancredi (2015) Activity of serotonin 5-HT1A receptor “biased agonists” in rat models of Parkinson’s disease and L-DOPA-induced dyskinesia. Neuropharmacology 93:52–67.

Ikeda SR (1996) Voltage-dependent modulation of N-type calcium channels by G-protein βγ subunits. Nature 380:255–258.

Ingerman E, Perkins E, Marino M, Mears J, McCaffery M, Hinshaw J, Nunnari J (2005) Dnm1 forms spirals that are structurally tailored to fit mitochondria. J Cell Biol 170:1021–1027.

Iravani MM, McCreary AC, Jenner P (2012) Striatal plasticity in Parkinson’s disease and L-DOPA induced dyskinesia. Parkinsonism Relat Disord 18:S123–S125.

Ishihara N, Eura Y, Mihara K (2004) Mitofusin 1 and 2 play distinct roles in mitochondrial fusion reactions via GTPase activity. J Cell Sci 117:6535–6546.

Ishihara N, Nomura M, Jofuku A, Kato H, Suzuki S, Masuda K, Otera H, Nakanishi Y, Nonaka I, Goto Y, Taguchi N, Morinaga H, Maeda M, Takayanagi R, Yokota S, Mihara K (2009) Mitochondrial fission factor Drp1 is essential for embryonic development and synapse formation in mice. Nat Cell Biol 11:958–966.

Ishihara N, Otera H, Oka T, Mihara K (2012) Regulation and physiologic functions of GTPases in mitochondrial fusion and fission in mammals. Antioxidants Redox Signal 19:389–399.

Itoh Y, Esaki T, Shimoji K, Cook M, Law M, Kaufman E, Sokoloff L (2003) Dichloroacetate effects on glucose and lactate oxidation by neurons and astroglia in vitro and on glucose utilization by brain in vivo. Proc Natl Acad Sci USA 100:4879–4884.

Janavs JL, Aminoff MJ (1998) Dystonia and chorea in acquired systemic disorders. J Neurology Neurosurg Psychiatry 65:436–445.

Jankovic (2008) Parkinson’s disease: clinical features and diagnosis. J Neurology Neurosurg Psychiatry 79:368–376.

Jankovic J (2005) Motor fluctuations and dyskinesias in Parkinson’s disease: Clinical manifestations. Mov Disord 20:S11–6.

Janssen-Heininger Y, Mossman B, Heintz N, Forman H, Kalyanaraman B, Finkel T, Stamler J, Rhee S, van der Vliet A (2008) Redox-based regulation of signal transduction: Principles, pitfalls, and promises. Free Radic Biol Med 45:1–17.

Jellinger K (2012) The role of α-synuclein in neurodegeneration — An update. Transl Neurosci 3:75-122.

Jenner P (2008) Molecular mechanisms of L-DOPA-induced dyskinesia. Nat Rev Neurosci 9:665–677.

Jiang P, Du W, Wu M (2014) Regulation of the pentose phosphate pathway in cancer. Protein Cell 5:592–602.

Jiang Z, North R (1992) Pre- and postsynaptic inhibition by opioids in rat striatum. J Neurosci 12:356–361.

Jin S, Youle R (2013) The accumulation of misfolded proteins in the mitochondrial matrix is sensed by PINK1 to induce PARK2/Parkin-mediated mitophagy of polarized mitochondria. Autophagy 9:1750–1757.

Jo, Son, Koh, Lee, Song, Kim, Lee, Jeong, Kim, Park, Song, Huh, Huhe (2001) Control of mitochondrial redox balance and cellular defense against oxidative damage by mitochondrial NADP+-dependent isocitrate dehydrogenase. J Biol Chem 276:16168–16176.

John J (2014) The control of mtDNA replication during differentiation and development. Biochim Biophys Acta 1840:1345–1354.

Johnston I, Williams B (2016) Evolutionary inference across eukaryotes identifies specific pressures favoring mitochondrial gene retention. Cell Syst 2:101–111.

Johnston JP (1968) Some observations upon a new inhibitor of monoamine oxidase in brain tissue. Biochem Pharmacol 17:1285–1297.

Johnston T, Fox S, McIldowie M, Piggott M, Brotchie J (2010) Reduction of L-DOPA-Induced Dyskinesia by the selective metabotropic glutamate receptor 5 antagonist 3-[(2-methyl-1,3-thiazol-4-yl)ethynyl]pyridine in the 1-methyl-4-phenyl-1,2,3,6-tetrahydropyridine-lesioned macaque model of Parkinson's disease. J Pharmacol Exp Ther 333:865–873.

Jolivet R, Allaman I, Pellerin L, Magistretti P, Weber B (2010) Comment on recent modeling studies of astrocyte–neuron metabolic interactions. J Cereb Blood Flow Metab 30:1982–1986.

Jope RS, Johnson G (2004) The glamour and gloom of glycogen synthase kinase-3. Trends Biochem Sci 29:95–102.

Jouaville L, Ichas F, Mazat J-P (1998) Modulation of cell calcium signals by mitochondria. Mol Cell Biochem 184:371–376.

Jouaville L, Pinton P, Bastianutto C, Rutter G, Rizzuto R (1999) Regulation of mitochondrial ATP synthesis by calcium: Evidence for a long-term metabolic priming. Proc Natl Acad Sci USA 96:13807–13812.

Kaakkola S (2000) Clinical pharmacology, therapeutic use and potential of COMT inhibitors in Parkinson's disease. Drugs 59:1233–1250.

Kai Y, Takamatsu C, Tokuda K, Okamoto M, Irita K, Takahashi S (2006) Rapid and random turnover of mitochondrial DNA in rat hepatocytes of primary culture. Mitochondrion 6:299–304.

Kaila V, Verkhovsky M, Wikström M (2010) Proton-coupled electron transfer in cytochrome oxidase. Chem Rev 110:7062–7081.

Kaiser R, Hofer A, Grapengiesser A, Gasser T, Kupsch A, Roots I, Brockmöller J (2003) L -dopa-induced adverse effects in PD and dopamine transporter gene polymorphism. Neurology 60:1750–1755.

Kalia L, Lang A (2004) Parkinson's disease. Lancet 386:896–912.

Kamer K, Mootha V (2015a) MICU1 and MICU2 Operate Together to Regulate the Uniporter. Biophys J 108:567a.

Kamer K, Mootha V (2015b) The molecular era of the mitochondrial calcium uniporter. Nat Rev Mol Cell Bio 16:545–553.

Kandel E, Schwartz J, Jessell T (2000) Principles of Neural Science, 4th ed. New York: McGraw-Hill.

Kane L, Lazarou M, Fogel A, Li Y, Yamano K, Sarraf S, Banerjee S, Youle R (2014) PINK1 phosphorylates ubiquitin to activate Parkin E3 ubiquitin ligase activity. J Cell Biol 205:143–153.

Kang D, Nishida J, Iyama A, Nakabeppu Y, Furuichi M, Fujiwara T, Sekiguchi M, Takeshige K (1995) Intracellular localization of 8-oxo-dGTPase in human cells, with special reference to the role of the enzyme in mitochondria. J Biol Chem 270:14659–14665.

Kann O, Kovács R (2007) Mitochondria and neuronal activity. Am J Physiol Cell Physiol 292:C641–C657.

Kao L-P, Ovchinnikov D, Wolvetang E (2012) The effect of ethidium bromide and chloramphenicol on mitochondrial biogenesis in primary human fibroblasts. Toxicol Appl Pharmacol 261:42–49.

Kaplan N, Vituri A, Korczyn AD, Cohen OS, Inzelberg R, Yahalom G, Kozlova E, Milgrom R, Laitman Y, Friedman E, Rosset S, Hassin-Baer S (2014) Sequence variants in SLC6A3, DRD2, and BDNF genes and time to levodopa-induced dyskinesias in Parkinson's disease. J Mol Neurosci 53:183–188.

Karmodiya K, Krebs A, Oulad-Abdelghani M, Kimura H, Tora L (2012) H3K9 and H3K14 acetylation co-occur at many gene regulatory elements, while H3K14ac marks a subset of inactive inducible promoters in mouse embryonic stem cells. BMC genomics:424.

Kasischke KA, Vishwasrao HD, Fisher PJ, Zipfel WR, Webb WW (2004) Neural activity triggers neuronal oxidative metabolism followed by astrocytic glycolysis. Science 305:99–103.

Kawasaki H, Springett G, Toki S, Canales J, Harlan P, Blumenstiel J, Chen E, Bany A, Mochizuki N, Ashbacher A, Matsuda M, Housman D, Graybiel A (1998) A Rap guanine nucleotide exchange factor enriched highly in the basal ganglia. Proc Natl Acad Sci USA 95:13278–13283.

Keefe K, Gerfen C (1996) D1 dopamine receptor-mediated induction of zif268 andc-fos in the dopamine-depleted striatum: Differential regulation and independence from NMDA receptors. J Comp Neurol 367:165–176.

Keefe KA, Horner KA (2017) Neurotransmitter regulation of striatal gene expression. In: Handbook of Basal Ganglia Structure and Function, 2nd ed. (Steiner H, Tseng KY, eds), pp 609-637. Handbook of Behavioral Neuroscience. Academic Press.

Keller MF et al. (2012) Using genome-wide complex trait analysis to quantify "missing heritability" in Parkinson's disease. Hum Mol Genet 21:4996–5009.

Kelly DP, Scarpulla RC (2004) Transcriptional regulatory circuits controlling mitochondrial biogenesis and function. Genes Dev 18:357–368.

Kelly R, Mahmud A, McKenzie M, Trounce I, John J (2012) Mitochondrial DNA copy number is regulated in a tissue specific manner by DNA methylation of the nuclear-encoded DNA polymerase gamma A. Nucleic Acids Res 40:10124–10138.

Kennedy MB, McGuinness T, Greengard P (1983) A calcium/calmodulin-dependent protein kinase from mammalian brain that phosphorylates Synapsin I: partial purification and characterization. J Neurosci 3:818–831.

Kennedy S, Salk J, Schmitt M, Loeb L (2013) Ultra-sensitive sequencing reveals an age-related increase in somatic mitochondrial mutations that are inconsistent with oxidative damage. PLoS Genet 9:e1003794.

Kessler R, Bleichert F, Warnke J-P, Eschrich K (2008) 6-Phosphofructo-2-kinase/fructose-2,6-bisphosphatase (PFKFB3) is up-regulated in high-grade astrocytomas. J Neurooncol 86:257–264.

Khan NA, Auranen M, Paetau I, Pirinen E, Euro L, Forsström S, Pasila L, Velagapudi V, Carroll CJ, Auwerx J, Suomalainen A (2014) Effective treatment of mitochondrial myopathy by nicotinamide riboside, a vitamin B3. EMBO Mol Med 6:721–731.

Kikuchi G, Morokawa Y, Yoshida T, Hiraga K (2008) Glycine cleavage system: reaction mechanism, physiological significance, and hyperglycinemia. Proc Jpn Acad Ser B Phys Biol Sci 84:246–263.

Kim J, Tchernyshyov I, Semenza G, Dang C (2006) HIF-1-mediated expression of pyruvate dehydrogenase kinase: A metabolic switch required for cellular adaptation to hypoxia. Cell Metab 3:177–185.

Klein C, Schlossmacher MG (2006) The genetics of Parkinson disease: Implications for neurological care. Nat Clin Pract Neurol 2:136–146.

Klein C, Westenberger A (2012) Genetics of Parkinson's Disease. Cold Spring Harb Perspect Med 2:a008888.

Kleman AM, Yuan JY, Aja S, Ronnett GV, Landree LE (2008) Physiological glucose is critical for optimized neuronal viability and AMPK responsiveness in vitro. J Neurosci Methods 167:292–301.

Klepac, Relja, Klepac, Hećimović, Babić, Trkulja (2007) Oxidative stress parameters in plasma of Huntington's disease patients, asymptomatic Huntington's disease gene carriers and healthy subjects. J Neurol 254:1676–1683.

Knoll, Magyar (1972) Some puzzling pharmacological effects of monoamine oxidase inhibitors. Adv Biochem Psychoph 5:393–408.

Kogan F, Haris M, Singh A, Cai K, Debrosse C, Nanga R, Hariharan H, Reddy R (2013) Method for high-resolution imaging of creatine in vivo using chemical exchange saturation transfer. Magn Reson Med 71:164–172.

Kohan A, Talukdar I, Walsh C, Salati L (2009) A role for AMPK in the inhibition of glucose-6-phosphate dehydrogenase by polyunsaturated fatty acids. Biochem Biophys Res Commun 388:117–121.

Kohout TA, Lefkowitz RJ (2003) Regulation of G protein-coupled receptor kinases and arrestins during receptor desensitization. Mol Pharmcol 63:9–18.

Konradi C (1998) The molecular basis of dopamine and glutamate interactions in the striatum. Adv Pharmacol 42:729–733.

Konradi C, Cole R, Heckers S, Hyman S (1994) Amphetamine regulates gene expression in rat striatum via transcription factor CREB. J Neurosci 14:5623–5634.

Konradi C, Cole RL, Green D, Senatus P, Leveque J, Pollack AE, Grossbard SJ, Hyman SE (1995) Analysis of the proenkephalin second messenger-inducible enhancer in rat striatal cultures. J Neurochem 65:1007–1015.

Konradi C, Heckers S (1995) Haloperidol-induced Fos expression in striatum is dependent upon transcription factor cyclic AMP response element binding protein. Neuroscience 65:1051–1061.

Konradi C, Kobierski LA, Nguyen TV, Heckers S, Hyman SE (1993) The cAMP-response-element-binding protein interacts, but Fos protein does not interact, with the proenkephalin enhancer in rat striatum. Proc Natl Acad Sci USA 90:7005–7009.

Konradi C, Leveque J, Hyman S (1996) Amphetamine and dopamine-induced immediate early gene expression in striatal neurons depends on postsynaptic NMDA receptors and calcium. J Neurosci 16:4231–4239.

Konradi C, Macías W, Dudman JT, Carlson RR (2003) Striatal proenkephalin gene induction: coordinated regulation by cyclic AMP and calcium pathways. Brain Res Mol Brain Res 115:157–161.

Konradi C, Westin JE, Carta M, Eaton ME, Kuter K, Dekundy A, Lundblad M, Cenci AM (2004) Transcriptome analysis in a rat model of L-DOPA-induced dyskinesia. Neurobiol Dis 17:219–236.

Kornblum C et al. (2013) Loss-of-function mutations in MGME1 impair mtDNA replication and cause multisystemic mitochondrial disease. Nat Genet 45:214–219.

Koshiba T, Detmer S, Kaiser J, Chen H, McCaffery M, Chan D (2004) Structural basis of mitochondrial tethering by mitofusin complexes. Science 305:858–862.

Kostrzewa R, Jacobowitz D (1974) Pharmacological actions of 6-hydroxydopamine. Pharmacol Rev 26:199–288.

Kostrzewa RM (2007) The blood-brain barrier for catecholamines — Revisited. Neurotox Res 11:261–271.

Koutsopoulos O, Laine D, Osellame L, Chudakov D, Parton R, Frazier A, Ryan M (2010) Human Miltons associate with mitochondria and induce microtubule-dependent remodeling of mitochondrial networks. Biochim Biophys Acta 1803:564–574.

Kouzarides T (2007) Chromatin modifications and their function. Cell 128:693–705.

Kowal S, Dall T, Chakrabarti R, Storm M, Jain A (2013) The current and projected economic burden of Parkinson's disease in the United States. Mov Disord 28:311–318.

Kravitz A, Freeze B, Parker P, Kay K, Thwin M, Deisseroth K, Kreitzer A (2010) Regulation of parkinsonian motor behaviours by optogenetic control of basal ganglia circuitry. Nature 466:622-626

Kujawa K, Leurgans S, Raman R, Blasucci L, Goetz CG (2000) Acute orthostatic hypotension when starting dopamine agonists in Parkinson's disease. Arch Neurol 57:1461–1463.

Kujoth, Hiona, Pugh, Someya, Panzer, Wohlgemuth, Hofer, Seo, Sullivan, Jobling, Morrow, Remmen V, Sedivy, Yamasoba, Tanokura, Weindruch, Leeuwenburgh, Prolla (2005) Mitochondrial DNA mutations, oxidative stress, and apoptosis in mammalian aging. Science 309:481–484.

Kukat A, Kukat C, Brocher J, Schäfer I, Krohne G, Trounce IA, Villani G, Seibel P (2008) Generation of rho0 cells utilizing a mitochondrially targeted restriction endonuclease and comparative analyses. Nucleic Acids Res 36:e44.

Kumar JM, Nicholls DG, Andersen JK (2003) Oxidative α-ketoglutarate dehydrogenase inhibition via subtle elevations in monoamine oxidase B levels results in loss of spare respiratory capacity: implications for Parkinson's disease. J Biol Chem 278:46432–46439.

Kumar R, Agarwal A, Seth P (1995) Free radical-generated neurotoxicity of 6-hydroxydopamine. J Neurochem 64:1703–1707.

Kumer SC, Vrana KE (1996) Intricate regulation of tyrosine hydroxylase activity and gene expression. J Neurochem 67:443–462.

Kunji E (2004) The role and structure of mitochondrial carriers. FEBS Lett 564:239–244.

Kushnareva Y, Mury AN, Andreyev A (2002) Complex I-mediated reactive oxygen species generation: modulation by cytochrome c and NAD(P)+ oxidation–reduction state. Biochem J 368:545–553.

Kvamme E, Torgner I, Roberg B (2001) Kinetics and localization of brain phosphate activated glutaminase. J Neurosci Res 66:951–958.

Kwon J, Lee S-R, Yang K-S, Ahn Y, Kim Y, Stadtman ER, Rhee S (2004) Reversible oxidation and inactivation of the tumor suppressor PTEN in cells stimulated with peptide growth factors. Proc Natl Acad Sci USA 101:16419–16424.

Laar VS, Dukes AA, Cascio M, Hastings TG (2008) Proteomic analysis of rat brain mitochondria following exposure to dopamine quinone: Implications for Parkinson disease. Neurobiol Dis 29:477–489.

Lake N, Compton A, Rahman S, Thorburn D (2015) Leigh syndrome: One disorder, more than 75 monogenic causes. Ann Neurol 79:190–203.

Lanciego JL, Luquin N, Obeso JA (2012) Functional Neuroanatomy of the Basal Ganglia. Cold Spring Harb Perspect Med 2:a009621.

Langston JW, Ballard P, Tetrud JW, Irwin I (1983) Chronic Parkinsonism in humans due to a product of meperidine-analog synthesis. Science 219:979–980.

Langston W (2017) The MPTP Story. J Park Dis 7:S11–S22.

Lapuente-Brun E, Moreno-Loshuertos R, Acín-Pérez R, Latorre-Pellicer A, Colás C, Balsa E, Perales-Clemente E, Quirós P, Calvo E, Rodríguez-Hernández, Navas P, Cruz R, Carracedo Á, López-Otín C, Pérez-Martos A, Fernández-Silva P, Fernández-Vizarra E, Enríquez J (2013) Supercomplex assembly determines electron flux in the mitochondrial electron transport chain. Science 340:1567–1570.

Larsson N-G (2010) Somatic mitochondrial DNA mutations in mammalian aging. Annu Rev Biochem 79:683–706.

Larsson N, Wang J, Wilhelmsson H, Oldfors A, Rustin P, Lewandoski M, Barsh G, Clayton D (1998) Mitochondrial transcription factor A is necessary for mtDNA maintenance and embryogenesis in mice. Nat Genet 18:231–236.

Larsson, Tulinius, Holme, Oldfors, Andersen, Wahlström, Aasly (1992) Segregation and manifestations of the mtDNA tRNA(Lys) A-->G(8344) mutation of myoclonus epilepsy and ragged-red fibers (MERRF) syndrome. Am J Hum Genet 51:1201–1212.

Lee D, Clayton D (1998) Initiation of mitochondrial DNA replication by transcription and R-loop processing. J Biol Chem 273:30614–30621.

Lee J-YY, Cho J, Lee E-KK, Park S-SS, Jeon BS (2011) Differential genetic susceptibility in diphasic and peak-dose dyskinesias in Parkinson's disease. Mov Disord 26:73–79.

Lee, Johnson, Gough, Donoghue, Cagnone, Vaghjiani, Brown, Johns, John S (2015) Mitochondrial DNA copy number is regulated by DNA methylation and demethylation of POLGA in stem and cancer cells and their differentiated progeny. Cell Death Dis 6:e1664.

Lefkowitz RJ, Shenoy SK (2005) Transduction of receptor signals by β-Arrestins. Science 308:512–517.

Leibowitz RD (1971) The effect of ethidium bromide on mitochondrial DNA synthesis and mitochondrial DNA structure in HeLa cells. J Cell Biol 51:116–122.

Lenaz G, Genova M (2010) Structure and organization of mitochondrial respiratory complexes: A new understanding of an old subject. Antioxid Redox Signal 12:961–1008.

Lerner J (1987) Acidic amino acid transport in animal cells and tissues. Comp Biochem Physiol B 87:443–457.

Leslie N, Bennett D, Lindsay Y, Stewart H, Gray A, Downes CP (2003) Redox regulation of PI 3-kinase signalling via inactivation of PTEN. Embo J 22:5501–5510.

Levey A, Kitt C, Simonds W, Price D, Brann M (1991) Identification and localization of muscarinic acetylcholine receptor proteins in brain with subtype-specific antibodies. J Neurosci 11:3218–3226.

Levin B, Cheng H, Reeder D (1999) A human mitochondrial DNA standard reference material for quality control in forensic identification, medical diagnosis, and mutation detection. Genomics 55:135–146.

Lezza A (2012) Mitochondrial transcription factor A (TFAM): One actor for different roles. Front Biol 7:30–39.

Li K, Reichmann H, Ziemssen T (2015) Recognition and treatment of autonomic disturbances in Parkinson's disease. Expert Rev Neurother 15:1189–1203.

Li X, Bürklen T, Yuan X, Schlattner U, Desiderio DM, Wallimann T, Homayouni R (2006) Stabilization of ubiquitous mitochondrial creatine kinase preprotein by APP family proteins. Mol Cell Neurosci 31:263–272.

Li, Hu, Wang, Man, Ren, Wen, Nukina, Fei, Wang (2010) Omi/HtrA2 is a positive regulator of autophagy that facilitates the degradation of mutant proteins involved in neurodegenerative diseases. Cell Death Differ 17:1773–1784.

Limbird L (2005) Cell Surface Receptors - A Short Course on Theory and Methods, 3rd ed. Springer US.

Lin C-S, Lee H-T, Lee M-H, Pan S-C, Ke C-Y, Chiu A, Wei Y-H (2016) Role of mitochondrial DNA copy number alteration in human renal cell carcinoma. Int J Mol Sci 17:814.

Lin J, Handschin C, Spiegelman B (2005) Metabolic control through the PGC-1 family of transcription coactivators. Cell Metab 1:361–370.

Lin M, Beal F (2006) Mitochondrial dysfunction and oxidative stress in neurodegenerative diseases. Nature 443:787–795.

Lindgren H, Andersson D, Lagerkvist S, Nissbrandt H, Cenci A (2010) L-DOPA-induced dopamine efflux in the striatum and the substantia nigra in a rat model of Parkinson's disease: temporal and quantitative relationship to the expression of dyskinesia. J Neurochem 112:1465–1476.

Lindgren H, Ohlin E, Cenci A (2009) Differential involvement of D1 and D2 dopamine receptors in L-DOPA-induced angiogenic activity in a rat model of Parkinson's disease. Neuropsychopharmacol 34:2477–2488.

Liu P, Qian L, Sung J-S, de Souza-Pinto N, Zheng L, Bogenhagen D, Bohr V, Wilson D, Shen B, Demple B (2008) Removal of oxidative DNA damage via FEN1-dependent long-patch base excision repair in human cell mitochondria. Mol Cell Biol 28:4975–4987.

Liu Z, Brown A, Fisher D, Wu Y, Warren J, Cui X (2016) Tissue specific expression of Cre in rat tyrosine hydroxylase and dopamine active transporter-positive neurons. PLoS ONE 11:e0149379.

Livermore T, Azevedo C, Kolozsvari B, Wilson M, Saiardi A (2016) Phosphate, inositol and polyphosphates. Biochem Soc Trans 44:253–259.

Llorente-Folch I, Sahún I, Contreras L (2013) AGC1-malate aspartate shuttle activity is critical for dopamine handling in the nigrostriatal pathway. J Neurochem 124:347-362

Loane C, Politis M (2011) Positron emission tomography neuroimaging in Parkinson's disease. Am J Transl Res 3:323–341.

Locasale JW (2013) Serine, glycine and one-carbon units: cancer metabolism in full circle. Nat Rev Cancer 13:572–583.

Logothetis D, Kurachi Y, Galper J, Neer E, Clapham D (1987) The beta gamma subunits of GTP-binding proteins activate the muscarinic K+ channel in heart. Nature 325:321–326.

Loh J-K, Lin C-C, Yang M-C, Chou C-H, Chen W-S, Hong M-C, Cho C-L, Hsu C-M, Cheng J-T, Chou A-K, Chang C-H, Tseng C-N, Wang C-H, Lieu A-S, Howng S-L, Hong Y-R (2015) GSKIP- and GSK3-mediated anchoring strengthens cAMP/PKA/Drp1 axis signaling in the regulation of mitochondrial elongation. Biochim Biophys Acta 1853:1796–1807.

Longley M, Humble M, Sharief F, Copeland W (2010) Disease variants of the human mitochondrial DNA helicase encoded by C10orf2 differentially alter protein stability, nucleotide hydrolysis, and helicase activity. J Biol Chem 285:29690–29702.

Lopert P, Patel M (2014a) Nicotinamide nucleotide transhydrogenase (Nnt) links the substrate requirement in brain mitochondria for hydrogen peroxide removal to the thioredoxin/peroxiredoxin (Trx/Prx) System. J Biol Chem 289:15611–15620.

Lopert P, Patel M (2014b) Brain mitochondria from DJ-1 knockout mice show increased respiration-dependent hydrogen peroxide consumption. Redox Biology 2:667–672.

Lovinger DM, Mathur BN (2012) Endocannabinoids in striatal plasticity. Parkinsonism Relat Disord 18:S132–S134.

Lowe M, Faull R, Christie D, Waldvogel H (2015) Distribution of the creatine transporter throughout the human brain reveals a spectrum of creatine transporter immunoreactivity. J Comp Neurol 523:699–725.

Lowe MT, Kim EH, Faull RL, Christie DL, Waldvogel HJ (2013) Dissociated expression of mitochondrial and cytosolic creatine kinases in the human brain: A new perspective on the role of creatine in brain energy metabolism. J Cereb Blood Flow Metab 33:1295–1306.

Lu B, Lee J, Nie X, Li M, Morozov YI, Venkatesh S, Bogenhagen DF, Temiakov D, Suzuki CK (2013) Phosphorylation of human TFAM in mitochondria impairs DNA binding and promotes degradation by the AAA+ Lon protease. Mol Cell 49:121–132.

Luk K, Kehm V, Carroll J, Zhang B, O'Brien P, Trojanowski J, Lee V (2012) Pathological α-synuclein transmission initiates Parkinson-like neurodegeneration in nontransgenic mice. Science 338:949–953.

Lund T, Risa Ø, Sonnewald U, Schousboe A, Waagepetersen H (2009) Availability of neurotransmitter glutamate is diminished when β-hydroxybutyrate replaces glucose in cultured neurons. J Neurochem 110:80–91.

Luo Y, Bond J, Ingram V (1997) Compromised mitochondrial function leads to increased cytosolic calcium and to activation of MAP kinases. Proc Natl Acad Sci USA 94:9705–9710.

Luthman, Fredriksson, Sundström, Jonsson, Archer (1989) Selective lesion of central dopamine or noradrenaline neuron systems in the neonatal rat: motor behavior and monoamine alterations at adult stage. Behav Brain Res 33:267–277.

Lyytinen J, Kaakkola S, Ahtila S, Tuomainen P, Teräväinen H (1997) Simultaneous MAO-B and COMT inhibition in L-DOPA-treated patients with Parkinson's disease. Movement Disord 12:497–505.

MacAskill A, Rinholm J, Twelvetrees A, Arancibia-Carcamo L, Muir J, Fransson A, Aspenstrom P, Attwell D, Kittler J (2009) Miro1 Is a calcium sensor for glutamate receptor-dependent localization of mitochondria at synapses. Neuron 61:541–555.

MacDermott AB, Role LW, Siegelbaum SA (1999) Presynaptic ionotropic receptors and the control of transmitter release. Annu Rev Neurosci 22:443–485.

MacDonald ML, Naydenov A, Chu M, Matzilevich D, Konradi C (2006) Decrease in creatine kinase messenger RNA expression in the hippocampus and dorsolateral prefrontal cortex in bipolar disorder. Bipolar Disord 8:255–264.

MacVicar T, Langer T (2016) OPA1 processing in cell death and disease – the long and short of it. J Cell Sci 129:2297–2306.

Magistretti PJ (2006) Neuron–glia metabolic coupling and plasticity. J Exp Biol 209:2304–2311.

Magistretti, Pellerin, Rothman, Shulman (1999) Energy on demand. Science 283:496–497.

Magrinelli F, Picelli A, Tocco P, Federico A, Roncari L, Smania N, Zanette G, Tamburin S (2016) Pathophysiology of motor dysfunction in Parkinson's disease as the rationale for drug treatment and rehabilitation. Parkinsons Dis 2016:9832839.

Makino M, Horai S, Goto Y, Nonaka I (2000) Mitochondrial DNA mutations in Leigh syndrome and their phylogenetic implications. J Hum Genet 45:69–75.

Man, Turnbull, Chinnery (2002) Leber hereditary optic neuropathy. J Med Genet 39:162–169.

Mandel H, Szargel R, Labay V, Elpeleg O, Saada A, Shalata A, Anbinder Y, Berkowitz D, Hartman C, Barak M, Eriksson S, Cohen N (2001) The deoxyguanosine kinase gene is mutated in individuals with depleted hepatocerebral mitochondrial DNA. Nat Genet 29:337–341.

Mangia S, DiNuzzo M, Giove F, Carruthers A, Simpson I, Vannucci S (2011) Response to "Comment on recent modeling studies of astrocyte—neuron metabolic interactions": Much ado about nothing. J Cereb Blood Flow Metabolism 31:1346–1353.

Mangiavacchi S, Wolf ME (2004) D1 dopamine receptor stimulation increases the rate of AMPA receptor insertion onto the surface of cultured nucleus accumbens neurons through a pathway dependent on protein kinase A. J Neurochem 88:1261–1271.

Manoharan S, Guillemin G, Abiramasundari R, Essa M, Akbar M, Akbar M (2016) The role of reactive oxygen species in the pathogenesis of Alzheimer's disease, Parkinson's disease, and Huntington's disease: A mini review. Oxid Med Cell Longev 2016:8590578.

Manson A, Stirpe P, Schrag A (2012) Levodopa-induced-dyskinesias clinical features, incidence, risk factors, management and impact on quality of life. J Parkinsons Dis 2:189–198.

Mansour A, Fox CA, Akil H, Watson SJ (1995) Opioid-receptor mRNA expression in the rat CNS: anatomical and functional implications. Trends Neurosci 18:22–29.

Mansuy IM, Shenolikar S (2006) Protein serine/threonine phosphatases in neuronal plasticity and disorders of learning and memory. Trends Neurosci 29:679–686.

Marchese A, Paing MM, Temple B, Trejo J (2008) G protein–coupled receptor sorting to endosomes and lysosomes. Annu Rev Pharmacol Toxicol 48:601–629.

Marchi S, Patergnani S, Pinton P (2014) The endoplasmic reticulum–mitochondria connection: One touch, multiple functions. Biochim Biophys Acta 1837:461–469.

Marchington, Hartshorne, Barlow, Poulton (1997) Homopolymeric tract heteroplasmy in mtDNA from tissues and single oocytes: support for a genetic bottleneck. Am J Hum Genet 60:408–416.

Marrif H, Juurlink B (1999) Astrocytes respond to hypoxia by increasing glycolytic capacity. Jl of Neurosci Res 57:255–260.

Marroquin L, Hynes J, Dykens J, Jamieson J, Will Y (2007) Circumventing the Crabtree Effect: Replacing media glucose with galactose increases susceptibility of HepG2 cells to mitochondrial toxicants. Toxicol Sci 97:539–547.

Marsh S, Blurton-Jones M (2012) Examining the mechanisms that link β-amyloid and α-synuclein pathologies. Alzheimers Res Ther 4:11.

Martin M, Cho J, Cesare A, Griffith J, Attardi G (2005) Termination factor-mediated DNA loop between termination and initiation sites drives mitochondrial rRNA synthesis. Cell 123:1227–1240.

Martinez-Martin P, Jeukens-Visser M, Lyons KE, Rodriguez-Blazquez C, Selai C, Siderowf A, Welsh M, Poewe W, Rascol O, Sampaio C, Stebbins GT, Goetz CG, Schrag A (2011) Health-related quality-of-life scales in Parkinson's disease: critique and recommendations. Mov Disord 26:2371–2380.

Martinez-Martin et al. (2015) Assessing the non-motor symptoms of Parkinson's disease: MDS-UPDRS and NMS Scale. Eur J Neurol 22:37–43.

Masuda-Suzukake M, Nonaka T, Hosokawa M, Oikawa T, Arai T, Akiyama H, Mann D, Hasegawa M (2013) Prion-like spreading of pathological α-synuclein in brain. Brain 136:1128–1138.

Mathupala, Ko, Pedersen (2006) Hexokinase II: Cancer's double-edged sword acting as both facilitator and gatekeeper of malignancy when bound to mitochondria. Oncogene 25:4777–4786.

Mathupala, Rempel, Pedersen (1997) Aberrant glycolytic metabolism of cancer cells: a remarkable coordination of genetic, transcriptional, post-translational, and mutational events that lead to a critical role for type II hexokinase. J Bioenerg Biomembr 29:339–343.

Matsuda N (2016) Phospho-ubiquitin: upending the PINK–Parkin–ubiquitin cascade. J Biochem 159:379–385.

Matsuda W, Furuta T, Nakamura K, Hioki H, Fujiyama F, Arai R, Kaneko T (2009) Single nigrostriatal dopaminergic neurons form widely spread and highly dense axonal arborizations in the neostriatum. J Neurosci 29:444–453.

Matsumine et al. (1997) Localization of a gene for an autosomal recessive form of juvenile Parkinsonism to chromosome 6q25.2-27. Am J Hum Genet 60:588–596.

Matsushima Y, Goto Y, Kaguni LS (2010) Mitochondrial Lon protease regulates mitochondrial DNA copy number and transcription by selective degradation of mitochondrial transcription factor A (TFAM). Proc Natl Acad Sci USA 107:18410–18415.

Mátyás F, Yanovsky Y, Mackie K, Kelsch W, Misgeld U, Freund TF (2006) Subcellular localization of type 1 cannabinoid receptors in the rat basal ganglia. Neuroscience 137:337–361.

Maurel A, Hernandez C, Kunduzova O, Bompart G, Cambon C, Parini A, Francés B (2002) Age-dependent increase in hydrogen peroxide production by cardiac monoamine oxidase A in rats. Am J Physiol Heart Circ Physiol 284:H1460–7.

Mayford M (2007) Protein kinase signaling in synaptic plasticity and memory. Curr Opin Neurobiol 17:313–317.

McCormack J, Denton R (1990) Intracellular calcium ions and intramitochondrial Ca2+ in the regulation of energy metabolism in mammalian tissues. Proc Nutr Soc 49:57–75.

McCormack, Denton (1979) The effects of calcium ions and adenine nucleotides on the activity of pig heart 2-oxoglutarate dehydrogenase complex. Biochem J 180:533–544.

McIntyre CC, Anderson RW (2016) Deep brain stimulation mechanisms: the control of network activity via neurochemistry modulation. J Neurochem 139 Suppl 1:338–345.

McKenna M, Waagepetersen H, Schousboe A, Sonnewald U (2006) Neuronal and astrocytic shuttle mechanisms for cytosolic-mitochondrial transfer of reducing equivalents: Current evidence and pharmacological tools. Biochem Pharmacol 71:399–407.

McKenna MC, Dienel GA, Sonnewald U, Waagepetersen HS, Schousboe A (2012) Energy Metabolism of the Brain. In: Basic Neurochemistry, 8th ed., pp 200–231. Academic Press.

Mears J, Lackner L, Fang S, Ingerman E, Nunnari J, Hinshaw J (2010) Conformational changes in Dnm1 support a contractile mechanism for mitochondrial fission. Nat Struct Mol Biology 18:20–26.

Meiser J, Weindl D, Hiller K (2013) Complexity of dopamine metabolism. Cell Commun Signal 11:1–18.

Meisinger C, Sickmann A, Pfanner N (2008) The mitochondrial proteome: From inventory to function. Cell 134:22–24.

Mellor H, Parker PJ (1998) The extended protein kinase C superfamily. Biochem J 332:281–292.

Meng T-C, Fukada T, Tonks N (2002) Reversible oxidation and inactivation of protein tyrosine phosphatases in vivo. Mol Cell 9:387–399.

Ménnistó PT (1994) Clinical potential of catechol-o-methyltransferase (COMT) inhibitors as adjuvants in Parkinson's disease. CNS Drugs 1:172–179.

Mercer TR, Neph S, Dinger ME, Crawford J, Smith MA, Shearwood A-MJ, Haugen E, Bracken CP, Rackham O, Stamatoyannopoulos JA, Filipovska A, Mattick JS (2011) The human mitochondrial transcriptome. Cell 146:645–658.

Mérida I, Ávila-FLores A, Merino E (2008) Diacylglycerol kinases: at the hub of cell signalling. Biochem J 410:631–631.

Metman L, Del Dotto P, van den Munckhof P, Fang, Mouradian MM, Chase TN (1998) Amantadine as treatment for dyskinesias and motor fluctuations in Parkinson's disease. Neurology 50:1323–1326.

Meulener M, Whitworth A, Armstrong-Gold C, Rizzu P, Heutink P, Wes P, Pallanck L, Bonini N (2005) Drosophila Dj-1 mutants are selectively sensitive to environmental toxins associated with Parkinson's disease. Curr Biol 15:1572–1577.

Mishra P (2016) Interfaces between mitochondrial dynamics and disease. Cell Calcium 60:190–198.

Mishra P, Chan D (2014) Mitochondrial dynamics and inheritance during cell division, development and disease. Nat Rev Mol Cell Bio 15:634–646.

Misko A, Jiang S, Wegorzewska I, Milbrandt J, Baloh R (2010) Mitofusin 2 is necessary for transport of axonal mitochondria and interacts with the Miro/Milton complex. J Neurosci 30:4232–4240.

Mitsumoto A, Nakagawa Y (2001) DJ-1 is an indicator for endogenous reactive oxygen species elicited by endotoxin. Free Radic Res 35:885–893.

Moiseeva O, Bourdeau V, Roux A, Deschênes-Simard X, Ferbeyre G (2009) Mitochondrial dysfunction contributes to oncogene-induced senescence. Mol Cell Biol 29:4495–4507.

Montier LLC, Deng J, Bai Y (2009) Number matters: control of mammalian mitochondrial DNA copy number. J Genet Genomics 36:125–131.

Montminy M (1997) Transcriptional regulation by cyclic AMP. Annu Rev Biochem 66:807–822.

Montminy MR, Bilezikjian LM (1987) Binding of a nuclear protein to the cyclic-AMP response element of the somatostatin gene. Nature 328:175–178.

Montoya, Christianson, Levens, Rabinowitz, Attardi (1982) Identification of initiation sites for heavy-strand and light-strand transcription in human mitochondrial DNA. Proc Natl Acad Sci USA 79:7195–7199.

Moratalla R, Solís O, Suárez L (2017) Morphological plasticity in the striatum associated with dopamine dysfunction. In: Handbook of Basal Ganglia Structure and Function, 2nd ed. (Steiner H, Tseng KY, eds), pp 755–770 Handbook of Behavioral Neuroscience. Academic Press.

Morelli M, Paolo T, Wardas J, Calon F, Xiao D, Schwarzschild MA (2007) Role of adenosine A2A receptors in parkinsonian motor impairment and L-DOPA-induced motor complications. Prog Neurobiol 83:293–309.

Moriya (1993) Single-stranded shuttle phagemid for mutagenesis studies in mammalian cells: 8-oxoguanine in DNA induces targeted G.C-->T.A transversions in simian kidney cells. Proc Natl Acad Sci USA 90:1122–1126.

Morken T, Brekke E, Håberg A, Widerøe M, Brubakk A-M, Sonnewald U (2014) Neuron–astrocyte interactions, pyruvate carboxylation and the pentose phosphate pathway in the neonatal rat brain. Neurochem Res 39:556–569.

Mráček T, Drahota Z, Houštěk J (2013) The function and the role of the mitochondrial glycerol-3-phosphate dehydrogenase in mammalian tissues. Biochim Biophys Acta 1827:401–410.

Mudd S, Ebert M, Scriver C (1980) Labile methyl group balances in the human: the role of sarcosine. Metabolism 29:707–720.

Muñoz M, Ponce E (2003) Pyruvate kinase: current status of regulatory and functional properties. Comp Biochem Physiol Part B Biochem Mol Biol 135:197–218.

Murer M, Moratalla R (2011) Striatal signaling in L-DOPA-Induced Dyskinesia: Common mechanisms with drug abuse and long term memory involving D1 dopamine receptor stimulation. Front Neuroanat 5:51.

Murphy JA, Stein IS, Lau GC, Peixoto RT, Aman TK, Kaneko N, Aromolaran K, Saulnier JL, Popescu GK, Sabatini BL, Hell JW, Zukin SR (2014) Phosphorylation of Ser1166 on GluN2B by PKA Is critical to synaptic NMDA receptor function and Ca2+ signaling in spines. J Neurosci 34:869–879.

Nacarelli T, Azar A, Sell C (2014) Inhibition of mTOR prevents ROS production initiated by ethidium bromide-induced mitochondrial DNA depletion. Front Endocrinol 5:122.

Nałęcz KA (2016) Solute carriers in the blood–brain barier: Safety in abundance. Neurochem Res 42:795–809.

Nalls MA et al. (2014) Large-scale meta-analysis of genome-wide association data identifies six new risk loci for Parkinson's disease. Nat Genet 46:989–993.

Naon D, Scorrano L (2014) At the right distance: ER-mitochondria juxtaposition in cell life and death. Biochim Biophys Acta 1843:2184–2194.

Napolitano A, Manini P, d' Ischia M (2011) Oxidation chemistry of catecholamines and neuronal degeneration: An update. Curr Med Chem 18:1832–1845.

Narendra D, Jin S, Tanaka A, Suen D-F, Gautier C, Shen J, Cookson M, Youle R (2010) PINK1 is selectively stabilized on impaired mitochondria to activate Parkin. PLoS Biol 8:e1000298.

Narendra D, Tanaka A, Suen D-F, Youle R (2008) Parkin is recruited selectively to impaired mitochondria and promotes their autophagy. J Cell Biol 183:795–803.

Nass M, Nass, Afzelius (1965) The general occurrence of mitochondrial DNA. Exp Cell Res 37:516–539.

Navab M, Reddy S, Lenten B, Fogelman A (2011) HDL and cardiovascular disease: atherogenic and atheroprotective mechanisms. Nat Rev Cardiol 8:222–232.

Navailles S, Deurwaerdère P (2011) Presynaptic control of serotonin on striatal dopamine function. Psychopharmacology 213:213–242.

Naydenov A, Vassoler F, Luksik A, Kaczmarska J, Konradi C (2010) Mitochondrial abnormalities in the putamen in Parkinson's disease dyskinesia. Acta Neuropathol 120:623–631.

Nelson DL, Cox MM (2004) Lehninger Principles of Biochemistry, 4th ed. W. H. Freeman.

Nestler EJ (2001) Molecular basis of long-term plasticity underlying addiction. Nat Rev Neurosci 2:119–128.

Neupert W, Herrmann JM (2007) Translocation of proteins into mitochondria. Annu Rev Biochem 76:723–749.

Newell DW, Barth A, Ricciardi TN, Malouf AT (1997) Glycine causes increased excitability and neurotoxicity by activation of NMDA receptors in the hippocampus. Exp Neurol 145:235–244.

Nicholas A, Lubin F, Hallett P (2008) Striatal histone modifications in models of Levodopa-Induced Dyskinesia. J Neurochem 106:486–494.

Nicholls D, Budd S (2000) Mitochondria and neuronal survival. Physiol Rev 80:315–360.

Nicholls D, Ward M (2000) Mitochondrial membrane potential and neuronal glutamate excitotoxicity: mortality and millivolts. Trends Neurosci 23:166–174.

Nicholls D (2005) Mitochondria and calcium signaling. Cell Calcium 38:311–317

Nicholls DG (2009) Mitochondrial calcium function and dysfunction in the central nervous system. Biochim Biophys Acta 1787:1416–1424.

Nicholls DG, Ferguson SJ (2013) Bioenergetics, 4th ed. Cambridge, MA: Academic Press.

Nicholls DG, Ferguson SJ (2013) Chapter 8: Transporters. In Bioenergetics, 4th ed., pp 221–251. Academic Press.

Nishi A, Kuroiwa M, Shuto T (2011) Mechanisms for the modulation of dopamine D1 receptor signaling in striatal neurons. Front Neuroanat 5:43.

Nishi, Snyder, Greengard (1997) Bidirectional regulation of DARPP-32 phosphorylation by dopamine. J Neurosci 17:8147–8155.

Nishino I, Spinazzola A, Hirano M (1999) Thymidine phosphorylase gene mutations in MNGIE, a human mitochondrial disorder. Science 283:689–692.

Noyes K, Liu H, Holloway R, Dick A (2007) Accuracy of medicare claims data in identifying Parkinsonism cases: Comparison with the medicare current beneficiary survey. Mov Disord 22:509–514.

Nunnari J, Marshall W, Straight A, Murray A, Sedat J, Walter P (1997) Mitochondrial transmission during mating in Saccharomyces cerevisiae is determined by mitochondrial fusion and fission and the intramitochondrial segregation of mitochondrial DNA. Mol Biol Cell 8:1233–1242.

Nutt J, Woodward W, Anderson J (1985) The effect of carbidopa on the pharmacokinetics of intravenously administered levodopa: The mechanism of action in the treatment of parkinsonism. Ann Neurol 18:537–543.

Nuytemans K, Theuns J, Cruts M, Broeckhoven C (2010) Genetic etiology of Parkinson disease associated with mutations in the SNCA, PARK2, PINK1, PARK7, and LRRK2 genes: a mutation update. Hum Mutat 31:763–780.

Oertel W, Schulz JB (2016) Current and experimental treatments of Parkinson's disease: A guide for neuroscientists. J Neurochem 139:325–337.

Oh J, Geller A, Zhang G, Chase T (2003) Gene transfer of constitutively active protein kinase C into striatal neurons accelerates onset of levodopa-induced motor response alterations in parkinsonian rats. Brain Res 971:18–30.

Okun MS (2012) Deep-brain stimulation for Parkinson's disease. N Engl J Med 367:1529–1538.

Okuno D, Iino R, Noji H (2011) Rotation and structure of FoF1-ATP synthase. J Biochem 149:655–664.

Olanow W, Brundin P (2013) Parkinson's disease and alpha synuclein: Is Parkinson's disease a prion-like disorder? Mov Disord 28:31–40.

Olanow W, Kieburtz K, Rascol O, Poewe W, Schapira A, Emre M, Nissinen H, Leinonen M, Stocchi F, in in Investigators S (2013) Factors predictive of the development of Levodopa-induced dyskinesia and wearing-off in Parkinson's disease. Movt Disord 28:1064–1071.

Oliveri RL, Annesi G, Zappia M, Civitelli D, De Marco EV, Pasqua AA, Annesi F, Spadafora P, Gambardella A, Nicoletti G, Branca D, Caracciolo M, Aguglia U, Quattrone A (2000) The dopamine D2 receptor gene is a susceptibility locus for Parkinson's disease. Mov Disord 15:127–131.

Olmsted JB, Carlson K, Klebe R, Ruddle F, Rosenbaum J (1970) Isolation of microtubule protein from cultured mouse neuroblastoma cells. Proc Natl Acad Sci USA 65:129–136.

Olson PA, Tkatch T, Hernandez-Lopez S, Ulrich S, Ilijic E, Mugnaini E, Zhang H, Bezprozvanny I, Surmeier JD (2005) G-protein-coupled receptor modulation of striatal CaV1.3 L-Type Ca2+ channels is dependent on a shank-binding domain. J Neurosci 25:1050–1062.

Ono T, Isobe K, Nakada K, Hayashi J-I (2001) Human cells are protected from mitochondrial dysfunction by complementation of DNA products in fused mitochondria. Nat Genet 28:272–275.

Orr A, Li S, Wang C-E, Li H, Wang J, Rong J, Xu X, Mastroberardino P, Greenamyre T, Li X-J (2008) N-terminal mutant huntingtin associates with mitochondria and impairs mitochondrial trafficking. J Neurosci 28:2783–2792.

Ouattara, Hoyer, Grégoire, Morissette, Gasparini, Gomez-Mancilla, Paolo D (2010) Changes of AMPA receptors in MPTP monkeys with levodopa-induced dyskinesias. Neuroscience 167:1160–1167.

Owen O, Kalhan S, Hanson R (2002) The key role of anaplerosis and cataplerosis for citric acid cycle function. J Biol Chem 277:30409–30412.

Palmer C, Elgass K, Parton R, Osellame L, Stojanovski D, Ryan M (2013) Adaptor proteins MiD49 and MiD51 can act independently of Mff and Fis1 in Drp1 recruitment and are specific for mitochondrial fission. J Biol Chem 288:27584–27593.

Palmieri F (2004) The mitochondrial transporter family (SLC25): physiological and pathological implications. Pflügers Arch 447:689–709.

Palmieri F (2013) The mitochondrial transporter family SLC25: Identification, properties and physiopathology. Mol Aspects Med 34:465–484.

Pankiv S, Clausen T, Lamark T, Brech A, Bruun J-A, Outzen H, Øvervatn A, Bjørkøy G, Johansen T (2007) p62/SQSTM1 binds directly to Atg8/LC3 to facilitate degradation of ubiquitinated protein aggregates by autophagy. J Biol Chem 282:24131–24145.

Panov A, Dikalov S, Shalbuyeva N, Hemendinger R, Greenamyre J, Rosenfeld J (2007) Species- and tissue-specific relationships between mitochondrial permeability transition and generation of ROS in brain and liver mitochondria of rats and mice. Am J Physiol Cell Physiol 292:C708–C718.

Papa, Francavilla, Paradies, Meduri (1971) The transport of pyruvate in rat liver mitochondria. FEBS Lett 12:285–288.

Paramasivam A, Meena A, Pedaparthi L, Jyothi V, Uppin M, Jabeen S, Sundaram C, Thangaraj K (2016) Novel mutation in C10orf2 associated with multiple mtDNA deletions, chronic progressive external ophthalmoplegia and premature aging. Mitochondrion 26:81–85.

Parekh A (2003) Mitochondrial regulation of intracellular Ca2+ signaling: More than just simple Ca2+ buffers. Physiology 18:252–256.

Parihar MS, Parihar A, Fujita M, Hashimoto M, Ghafourifar P (2008) Mitochondrial association of alpha-synuclein causes oxidative stress. Cell Mol Life Sci 65:1272–1284.

Parkinson J 1817. An essay on the shaking palsy. Whittingham and Rowland for Sherwood, Needly and Jones, London

Parone P, Cruz S, Tondera D, Mattenberger Y, James D, Maechler P, Barja F, Martinou J-C (2008) Preventing mitochondrial fission impairs mitochondrial function and leads to loss of mitochondrial DNA. PLoS ONE 3:e3257.

Paschen W, Djuricic B (1994) Extent of RNA editing of glutamate receptor subunit GluR5 in different brain regions of the rat. Cell Mol Neurobiol 14:259–270.

Passonneau J, Lowry O (1964) The role of phosphofructokinase in metabolic regulation. Adv Enzyme Regul 2:265–274.

Patel M (2017) Inheritance: Male mtDNA just can’t catch a break. Curr Biol 27:R264–R266.

Patel, Korotchkina LG (2006) Regulation of the pyruvate dehydrogenase complex. Biochem Soc T 34:217–222.

Pathak D, Shields L, Mendelsohn B, Haddad D, Lin W, Gerencser A, Kim H, Brand M, Edwards R, Nakamura K (2015) The role of mitochondrially derived ATP in synaptic vesicle recycling. J Biol Chem 290:22325–22336.

Patra S, Ghosh A, Roy S, Bera S, Das M, Talukdar D, Ray S, Wallimann T, Ray M (2012) A short review on creatine–creatine kinase system in relation to cancer and some experimental results on creatine as adjuvant in cancer therapy. Amino Acids 42:2319–2330.

Pebay-Peyroula E, Dahout-Gonzalez C, Kahn R, Trézéguet V, Lauquin G, Brandolin G (2003) Structure of mitochondrial ADP/ATP carrier in complex with carboxyatractyloside. Nature 426:39–44.

Pekkurnaz G, Trinidad J, Wang X, Kong D, Schwarz T (2014) Glucose Regulates Mitochondrial Motility via Milton Modification by O-GlcNAc Transferase. Cell 158:54–68.

Pellegrino M, Nargund A, Haynes C (2013) Signaling the mitochondrial unfolded protein response. Biochim Biophys Acta 1833:410–416.

Pellerin L, Magistretti P (2012) Sweet Sixteen for ANLS. J Cereb Blood Flow Metabolism 32:1152–1166.

Penit-Soria, Durand, Besson, Herve (1997) Levels of stimulatory G protein are increased in the rat striatum after neonatal lesion of dopamine neurons. Neuroreport 8:829–833.

Perez, Anne, Debruxelles, Menegon, Lambrecq, Lacombe, Martin-Negrier ML, Brochet, Goizet (2009) Leber's optic neuropathy associated with disseminated white matter disease: A case report and review. Clin Neurol Neurosur 111:83–86.

Pernas L, Scorrano L (2015) Mito-morphosis: Mitochondrial fusion, fission, and cristae remodeling as key mediators of cellular function. Annu Rev Physiol 78:1–27.

Pfaffl MW, Tichopad A, Prgomet C, Neuvians TP (2004) Determination of stable housekeeping genes, differentially regulated target genes and sample integrity: BestKeeper–Excel-based tool using pair-wise correlations. Biotechnol Lett 26:509–515.

Pfeffer G, Sirrs S, Wade K, Mezei M (2011) Multisystem disorder in late-onset chronic progressive external ophthalmoplegia. Can J Neurol Sci 38:119–123.

Picconi B, Centonze D, Håkansson K, Bernardi G, Greengard P, Fisone G, Cenci A, Calabresi P (2003) Loss of bidirectional striatal synaptic plasticity in L-DOPA–induced dyskinesia. Nat Neurosci 6:501–506.

Pickrell A, Youle R (2015) The Roles of PINK1, Parkin, and Mitochondrial Fidelity in Parkinson's Disease. Neuron 85:257–273.

Pinton P, Rimessi A, Marchi S, Orsini F, Migliaccio E, Giorgio M, Contursi C, Minucci S, Mantovani F, Wieckowski M, Sal G, Pelicci P, Rizzuto R (2007) Protein Kinase C β and Prolyl Isomerase 1 regulate mitochondrial effects of the life-span determinant p66Shc. Science 315:659–663.

Pissadaki E, Bolam P (2013) The energy cost of action potential propagation in dopamine neurons: clues to susceptibility in Parkinson's disease. Front Comput Neurosc 7:13.

Pitcher, Inglese, Higgins, Arriza, Casey, Kim, Benovic, Kwatra, Caron, Lefkowitz (1992) Role of beta gamma subunits of G proteins in targeting the beta-adrenergic receptor kinase to membrane-bound receptors. Science 257:1264–1267.

Pitter JG, Maechler, Wollheim CB, Spät (2002) Mitochondria respond to Ca2+ already in the submicromolar range: correlation with redox state. Cell Calcium 31:97–104.

Pivovarova N, Andrews B (2010) Calcium-dependent mitochondrial function and dysfunction in neurons. Febs J 277:3622–3636.

Pivovarova N, Nguyen H, Winters C, Brantner C, Smith C, Andrews B (2004) Excitotoxic calcium overload in a subpopulation of mitochondria triggers delayed death in hippocampal neurons. J Neurosci 24:5611–5622.

Polymeropoulos MH et al. (1997) Mutation in the alpha-synuclein gene identified in families with Parkinson's disease. Science 276:2045–2047.

Porras G, Li Q, Bezard E (2012) Modeling Parkinson's disease in primates: The MPTP Model. Cold Spring Harb Perspect Med 2:a009308.

Poston C, Krishnan S, Bazemore-Walker C (2013) In-depth proteomic analysis of mammalian mitochondria-associated membranes (MAM). J Proteomics 79:219–230.

Pryde KR, Hirst J (2011) Superoxide is produced by the reduced flavin in mitochondrial complex I: A single, unified mechanism that applies during both forward and reverse electron transfer. J Biol Chem 286:18056–18065.

Przedborski S, Levivier M, Raftopoulos C, Naini A, Hildebrand J (1995) Peripheral and central pharmacokinetics of apomorphine and its effect on dopamine metabolism in humans. Mov Disord 10:28–36.

Puopolo M, Raviola E, Bean B (2007) Roles of subthreshold calcium current and sodium current in spontaneous firing of mouse midbrain dopamine neurons. J Neurosci 27:645–656.

Pyle A, Anugrha H, Kurzawa-Akanbi M, Yarnall A, Burn D, Hudson G (2016) Reduced mitochondrial DNA copy number is a biomarker of Parkinson's disease. Neurobiol Aging 38:216.e7–216.e10.

Quilty MC, King AE, Gai W-P, Pountney DL, West AK, Vickers JC, Dickson TC (2006) Alpha-synuclein is upregulated in neurones in response to chronic oxidative stress and is associated with neuroprotection. Exp Neurol 199:249–256.

Quinlan C, Gerencser A, Treberg J, Brand M (2011) The mechanism of superoxide production by the antimycin-inhibited mitochondrial Q-cycle. J Biol Chem 286:31361–31372.

Quirós P, Langer T, López-Otín C (2015) New roles for mitochondrial proteases in health, ageing and disease. Nat Rev Mol Cell Bio 16:345–359.

Quirós P, Mottis A, Auwerx J (2016) Mitonuclear communication in homeostasis and stress. Nat Rev Mol Cell Bio 17:213–226.

Rajadhyaksha A, Barczak A, Macías W, Leveque J, Lewis S, Konradi C (1999) L-Type Ca(2+) channels are essential for glutamate-mediated CREB phosphorylation and c-fos gene expression in striatal neurons. J Neurosci 19:6348–6359.

Rajadhyaksha, Leveque J-C, Macías, Barczak, Konradi (1998) Molecular components of striatal plasticity: The various routes of cyclic AMP pathways. Dev Neurosci 20:204–215.

Rambold A, Kostelecky B, Lippincott-Schwartz J (2011) Together we are stronger. Autophagy 7:1568–1569.

Ramonet D et al. (2011) Dopaminergic neuronal loss, reduced neurite complexity and autophagic abnormalities in transgenic mice expressing G2019S mutant LRRK2. PLoS One 6:e18568.

Ramsay R, Salach J, Dadgar J, Singer T (1986) Inhibition of mitochondrial NADH dehydrogenase by pyridine derivatives and its possible relation to experimental and idiopathic parkinsonism. Biochem Bioph Res Co 135:269–275.

Rango M (2015) Parkinson's disease: in vivo brain metabolomics by MRS. Int Rev Neurobiol 122:81–94.

Rango M, Bonifati C, Bresolin N (2006) Parkinson's disease and brain mitochondrial dysfunction: A functional phosphorus magnetic resonance spectroscopy study. J Cereb Blood Flow Metab 26:283–290.

Rascol O, Brooks D, Korczyn A, Deyn P, Clarke C, Lang A, Abdalla M (2006) Development of dyskinesias in a 5-year trial of ropinirole and L-dopa. Mov Disord 21:1844–1850.

Rascol O, Brooks DJ, Korczyn AD, Deyn PP, Clarke CE, Lang AE (2000) A five-year study of the incidence of dyskinesia in patients with early Parkinson's disease who were treated with ropinirole or levodopa. N Engl J Med 342:1484–1491.

Redgrave P, Rodriguez M, Smith Y, Rodriguez-Oroz M, Lehericy S, Bergman H, Agid Y, DeLong M, Obeso J (2010) Goal-directed and habitual control in the basal ganglia: implications for Parkinson's disease. Nat Rev Neurosci 11:760–772.

Reeve AK, Simcox EM, Duchen MR, Turnbull DM (2016) Mitochondrial dysfunction in neurodegenerative disorders, 2nd ed. Springer International Publishing.

Rehling P, Wiedemann N, Pfanner N, Truscott KN (2001) The mitochondrial import machinery for preproteins. Crit Rev Biochem Mol Biol 36:291–336.

Reitman Z, Yan H (2010) Isocitrate Dehydrogenase 1 and 2 mutations in cancer: Alterations at a crossroads of cellular metabolism. J Natl Cancer Inst 102:932–941.

Remmen H, Salvador C, Yang H, Huang T, Epstein C, Richardson A (1999) Characterization of the antioxidant status of the heterozygous manganese superoxide dismutase knockout mouse. Arch Biochem Biophys 363:91–97.

Ren J, Sherry DA, Malloy CR (2015) 31P-MRS of healthy human brain: ATP synthesis, metabolite concentrations, pH, and T1 relaxation times. NMR in Biomedicine 28:1455–1462.

Riachi N, Behmand R, Harik S (1991) Correlation of MPTP neurotoxicity in vivo with oxidation of MPTP by the brain and blood-brain barrier in vitro in five rat strains. Brain Res 555:19–24.

Rice S, Gelfand V (2006) Paradigm lost: Milton connects kinesin heavy chain to miro on mitochondria. J Cell Biol 173:459–461.

Richfield E, Thiruchelvam M, Cory-Slechta D, Wuertzer C, Gainetdinov R, Caron M, Monte D, Federoff H (2002) Behavioral and neurochemical effects of wild-type and mutated human α-synuclein in transgenic mice. Exp Neurol 175:35–48.

Richter-Dennerlein R, Dennerlein S, Rehling P (2015) Integrating mitochondrial translation into the cellular context. Nat Rev Mol Cell Bio 16:586–592.

Richter-Dennerlein R, Oeljeklaus S, Lorenzi I, Ronsör C, Bareth B, Schendzielorz A, Wang C, Warscheid B, Rehling P, Dennerlein S (2016) Mitochondrial protein synthesis adapts to influx of nuclear-encoded protein. Cell 167:471–483.e10.

Rieck M, Schumacher-Schuh AF, Altmann V, Francisconi CL, Fagundes PT, Monte TLL, Callegari-Jacques SM, Rieder CR, Hutz MH (2012) DRD2 haplotype is associated with dyskinesia induced by levodopa therapy in Parkinson's disease patients. Pharmacogenomics 13:1701–1710.

Riss TL, Moravec RA, Niles AL, Duellman S, Benink HA, Worzella TJ, Minor L (2016) Cell Viability Assays. In Assay Guidance Manual (Sittampalam GS, Coussens NP, Brimacombe K, Grossman A, Arkin M, Auld D, Austin C, Baell J, Bejcek B, Chung TDY, Dahlin JL, Devanaryan

V, Foley TL, Glicksman M, Hall MD, Hass JV, Ingless J, Iversen PW, Kahl SD, Kales SC, Lal-Nag M, Li Z, McGee J, McManus O, Riss T, Trask OJ Jr, Weidner JR, Xia M, Xu X, eds). Bethesda, MD: Eli Lilly & Company and the National Center for Advancing Translational Sciences.

Rizk A, Paul G, Incardona P, Bugarski M, Mansouri M, Niemann A, Ziegler U, Berger P, Sbalzarini I (2014) Segmentation and quantification of subcellular structures in fluorescence microscopy images using Squassh. Nat Protoc 9:586–596.

Rizzuto, Brini, Murgia, Pozzan (1993) Microdomains with high Ca2+ close to IP3-sensitive channels that are sensed by neighboring mitochondria. Science 262:744–747.

Robertson HA, Peterson MR, Murphy, Robertson GS (1989) D1-dopamine receptor agonists selectively activate striatal c-fos independent of rotational behaviour. Brain Res 503:346–349.

Robinson A, Overy C, Kunji E (2008) The mechanism of transport by mitochondrial carriers based on analysis of symmetry. Proc Natl Acad Sci USA 105:17766–17771.

Rojo, Campos, Sánchez, Bonaventura, Aguilar, García, González, Rey, Arenas, Olivé, Ferrer (2006) NARP-MILS syndrome caused by 8993 T > G mitochondrial DNA mutation: a clinical, genetic and neuropathological study. Acta Neuropathol 111:610–616.

Rorbach J, Minczuk M (2012) The post-transcriptional life of mammalian mitochondrial RNA. Biochem J 444:357–373.

Roselli F, Caroni P (2015) From intrinsic firing properties to selective neuronal vulnerability in neurodegenerative diseases. Neuron 85:901–910.

Roskoski R (2012) ERK1/2 MAP kinases: Structure, function, and regulation. Pharmacol Res 66:105–143.

Roskoski R (2012b) MEK1/2 dual-specificity protein kinases: Structure and regulation. Biochem Biophys Res Commun 417:5–10.

Rossignol R, Faustin B, Rocher C, Malgat M, Mazat J-P, Letellier T (2003) Mitochondrial threshold effects. Biochem J 370:751–762.

Rossignol R, Gilkerson R, Aggeler R, Yamagata K, Remington SJ, Capaldi RA (2004) Energy substrate modulates mitochondrial structure and oxidative capacity in cancer cells. Cancer Res 64:985–993.

Rothman D, Sibson N, Hyder F, Shen J, Behar K, Shulman R (1999) In vivo nuclear magnetic resonance spectroscopy studies of the relationship between the glutamate--glutamine neurotransmitter cycle and functional neuroenergetics. Philos Trans R Soc Lond B Biol Sci 354:1165–1177.

Rötig A, Poulton J (2009) Genetic causes of mitochondrial DNA depletion in humans. Biochim Biophys Acta 1792:1103–1108.

Rowland A, Voeltz G (2012) Endoplasmic reticulum–mitochondria contacts: Function of the junction. Nat Rev Mol Cell Bio 13:607–625.

Runswick MJ, Powell SJ, Nyren P, Walker JE (1987) Sequence of the bovine mitochondrial phosphate carrier protein: structural relationship to ADP/ATP translocase and the brown fat mitochondria uncoupling protein. EMBO J 6:1367–1373.

Ruszkiewicz J, Albrecht J (2015) Changes in the mitochondrial antioxidant systems in neurodegenerative diseases and acute brain disorders. Neurochem Int 88:66–72.

Rydström J (2006) Mitochondrial NADPH, transhydrogenase and disease. Biochim Biophys Acta 1757:721–726.

Rylander D, Iderberg H, Li Q, Dekundy A, Zhang J, Li H, Baishen R, Danysz W, Bezard E, Cenci A (2010) A mGluR5 antagonist under clinical development improves L-DOPA-induced dyskinesia in parkinsonian rats and monkeys. Neurobiol Dis 39:352–361.

Saada A, Shaag A, Mandel H, Nevo Y, Eriksson S, Elpeleg O (2001) Mutant mitochondrial thymidine kinase in mitochondrial DNA depletion myopathy. Nat Genet 29:342–344.

Salomons G, van Dooren S, Verhoeven N, Cecil K, Ball W, Degrauw T, Jakobs C (2007) X-linked creatine-transporter gene (SLC6A8) defect: A new creatine-deficiency syndrome. Am J Hum Genetics 68:1497–1500.

Samadi P, Grégoire L, Morissette M, Calon F, Tahar A, Dridi M, Belanger N, Meltzer L, Bédard P, Paolo T (2008) mGluR5 metabotropic glutamate receptors and dyskinesias in MPTP monkeys. Neurobiol Aging 29:1040–1051.

Samuels D, Schon E, Chinnery P (2004) Two direct repeats cause most human mtDNA deletions. Trends Genet 20:393–398.

Sancak Y, Markhard A, Kitami T, Kovács-Bogdán E, Kamer K, Udeshi N, Carr S, Chaudhuri D, Clapham D, Li A, Calvo S, Goldberger O, Mootha V (2013) EMRE Is an essential component of the mitochondrial calcium uniporter complex. Science 342:1379–1382.

Sánchez-Lemus E, Arias-Montaño J-AA (2006) M1 muscarinic receptors contribute to, whereas M4 receptors inhibit, dopamine D1 receptor-induced [3H]-cyclic AMP accumulation in rat striatal slices. Neurochem Res 31:555–561.

Sanders L, Laganière J, Cooper O, Mak S, Vu J, Huang A, Paschon D, Vangipuram M, Sundararajan R, Urnov F, Langston W, Gregory P, Zhang S, Greenamyre T, Isacson O, Schüle B (2014) LRRK2 mutations cause mitochondrial DNA damage in iPSC-derived neural cells from Parkinson's disease patients: Reversal by gene correction. Neurobiol Dis 62:381–386.

Saneto R, Cohen B, Copeland W, Naviaux R (2013) Alpers-Huttenlocher Syndrome. Pediatr Neurol 48:167–178.

Saneto RP, Friedman SD, Shaw D (2008) Neuroimaging of mitochondrial disease. Mitochondrion 8:396–413.

Santini E, Alcacer C, Cacciatore S (2009) L-DOPA activates ERK signaling and phosphorylates histone H3 in the striatonigral medium spiny neurons of hemiparkinsonian mice. J Neurochem 108:621–633.

Santini E, Feyder M, Gangarossa G, Bateup H, Greengard P, Fisone G (2012) Dopamine- and cAMP-regulated phosphoprotein of 32-kDa (DARPP-32)-dependent activation of Extracellular Signal-regulated Kinase (ERK) and Mammalian Target of Rapamycin Complex 1 (mTORC1) signaling in experimental Parkinsonism. J Biol Chem 287:27806–27812.

Santini E, Heiman M, Greengard P, Valjent E, Fisone G (2009) Inhibition of mTOR signaling in Parkinson's Disease prevents L-DOPA–Induced Dyskinesia. Sci Signal 2:ra36–ra36.

Santini E, Valjent E, Fisone G (2008) Parkinson's disease: Levodopa-induced dyskinesia and signal transduction. FEBS Journal 275:1392–1399.

Santini E, Valjent E, Usiello A, Carta M, Borgkvist A, Girault J-AA, Hervé D, Greengard P, Fisone G (2007) Critical involvement of cAMP/DARPP-32 and extracellular signal-regulated protein kinase signaling in L-DOPA-induced dyskinesia. J Neurosci 27:6995–7005.

Sarbassov DD, Ali SM, Sabatini DM (2005) Growing roles for the mTOR pathway. Curr Opin Cell Biol 17:596–603.

Sarraf SA, Raman M, Guarani-Pereira V, Sowa ME, Huttlin EL, Gygi SP, Harper JW (2013) Landscape of the PARKIN-dependent ubiquitylome in response to mitochondrial depolarization. Nature 496:372–376.

Sassone-Corsi P (2012) The Cyclic AMP Pathway. Cold Spring Harb Perspect Biol 4:a011148.

Sauvanet C, Duvezin-Caubet S, di Rago J-P, Rojo M (2010) Energetic requirements and bioenergetic modulation of mitochondrial morphology and dynamics. Semin Cell Dev Biol 21:558–565.

Savtchenko L, Megalogeni M, Rusakov DA, Walker MC, Pavlov I (2015) Synaptic GABA release prevents GABA transporter type-1 reversal during excessive network activity. Nat Commun 6:6597.

Scarpulla R (2008) Transcriptional paradigms in mammalian mitochondrial biogenesis and function. Physiol Rev 88:611–638.

Scarpulla R (2011) Metabolic control of mitochondrial biogenesis through the PGC-1 family regulatory network. Biochim Biophys Acta 1813:1269–1278.

Scarpulla R (2012) Nucleus-encoded regulators of mitochondrial function: Integration of respiratory chain expression, nutrient sensing and metabolic stress. Biochim Biophys Acta 1819:1088–1097.

Schaefer C, Schäfer K-H, Löffler (2010) Region-specific distribution of dihydroorotate dehydrogenase in the rat central nervous system points to pyrimidine de novo synthesis in neurons. Nucleosides Nucleotides Nucleic Acids 29:476–481.

Schatz, Haslbrunner, Tuppy (1964) Deoxyribonucleic acid associated with yeast mitochondria. Biochem Bioph Res Co 15:127–132.

Schiavo G, Greensmith L, Hafezparast M, Fisher E (2013) Cytoplasmic dynein heavy chain: the servant of many masters. Trends in Neurosci 36:641–651.

Schieber M, Chandel N (2014) ROS function in redox signaling and oxidative stress. Curr Biol 24:R453–R462.

Schiemann J, Schlaudraff F, Klose V, Bingmer M, Seino S, Magill P, Zaghloul K, Schneider G, Liss B, Roeper J (2012) K-ATP channels in dopamine substantia nigra neurons control bursting and novelty-induced exploration. Nat Neurosci 15:1272–1280.

Schindelin J, Arganda-Carreras I, Frise E, Kaynig V, Longair M, Pietzsch T, Preibisch S, Rueden C, Saalfeld S, Schmid B, Tinevez J-Y, White D, Hartenstein V, Eliceiri K, Tomancak P, Cardona A (2012) Fiji: an open-source platform for biological-image analysis. Nat Methods 9:676–682.

Schlattner U, Klaus A, Rios S, Guzun R, Kay L, Tokarska-Schlattner M (2016) Cellular compartmentation of energy metabolism: creatine kinase microcompartments and recruitment of B-type creatine kinase to specific subcellular sites. Amino Acids 48:1751–1774.

Schlattner U, Tokarska-Schlattner M, Wallimann T (2006) Mitochondrial creatine kinase in human health and disease. Biochim Biophys Acta 1762:164–180.

Schlattner U, Tokarska-Schlattner M, Wallimann T (2006) Mitochondrial creatine kinase in human health and disease. Biochim Biophys Acta 1762:164–180.

Schmidt O, Pfanner N, Meisinger C (2010) Mitochondrial protein import: from proteomics to functional mechanisms. Nat Rev Mol Cell Bio 11:655–667.

Schneggenburger R, Neher E (2005) Presynaptic calcium and control of vesicle fusion. Curr Opin Neurobiol 15:266–274.

Schon E, Area-Gomez E (2013) Mitochondria-associated ER membranes in Alzheimer's disease. Mol Cell Neurosci 55:26–36.

Schon E, DiMauro S, Hirano M (2012) Human mitochondrial DNA: roles of inherited and somatic mutations. Nat Rev Genet 13:878–890.

Schon, Rizzuto, Moraes, Nakase, Zeviani, DiMauro (1989) A direct repeat is a hotspot for large-scale deletion of human mitochondrial DNA. Science 244:346–349.

Schousboe A, Bak LK, Waagepetersen HS (2013) Astrocytic control of biosynthesis and turnover of the neurotransmitters glutamate and GABA. Front Endocrinol 4:102.

Schousboe A, Sickmann H, Walls A, Bak L, Waagepetersen H (2010) Functional importance of the astrocytic glycogen-shunt and glycolysis for maintenance of an intact intra/extracellular glutamate gradient. Neurotox Res 18:94–99.

Schroeder P, Gremmel T, Berneburg M, Krutmann J (2008) Partial depletion of mitochondrial DNA from human skin fibroblasts induces a gene expression profile reminiscent of photoaged skin. J Invest Dermatol 128:2297–2303.

Schuldiner S, Liu Y, Edwards R (1993) Reserpine binding to a vesicular amine transporter expressed in Chinese hamster ovary fibroblasts. J Biol Chem 268:29–34.

Schulze A, Bachert P, Schlemmer H, Harting I, Polster T, Salomons G, Verhoeven N, Jakobs C, Fowler B, Hoffmann G, Mayatepek E (2003) Lack of creatine in muscle and brain in an adult with GAMT deficiency. Ann Neurol 53:248–251.

Schwarz T (2013) Mitochondrial Trafficking in Neurons. Cold Spring Harb Perspect Biol 5:a011304.

Schwarzschild MA, Agnati L, Fuxe K, Chen J-F, Morelli M (2006) Targeting adenosine A2A receptors in Parkinson's disease. Trends Neurosci 29:647–654.

Sena L, Chandel N (2012) Physiological roles of mitochondrial reactive oxygen species. Mol Cell 48:158–167.

Sengupta N, Seto E (2004) Regulation of histone deacetylase activities. J Cell Biochem 93:57–67.

Seraji-Bozorgzad N, Bao F, George E, Krstevska S, Gorden V, Chorostecki J, Santiago C, Zak I, Caon C, Khan O (2015) Longitudinal study of the substantia nigra in Parkinson disease: A high-field 1H-MR spectroscopy imaging study. Mov Disord 30:1400–1404.

Shadel G, Horvath T (2015) Mitochondrial ROS signaling in organismal homeostasis. Cell 163:560–569.

Shan L, Diaz O, Zhang Y, Ladenheim B, Cadet J-L, Chiang Y-H, Olson L, Hoffer B, Bäckman C (2015) L-Dopa induced dyskinesias in Parkinsonian mice: Disease severity or L-Dopa history. Brain Res 1618:261–269.

Shen W, Plokin JL, Zhai S, Surmeier DJ (2017) Dopaminergic modulation of glutamatergic signaling in striatal spiny projection neurons. In: Handbook of Basal Ganglia Structure and Function, 2nd ed. (Steiner H, Tseng KY, eds), pp 179–196 Handbook of Behavioral Neuroscience. Academic Press.

Shen WC, Ballou B, Ryser HJ, Hakala TR (1986) Targeting, internalization, and cytotoxicity of methotrexate-monoclonal anti-stage-specific embryonic antigen-1 antibody conjugates in cultured F-9 teratocarcinoma cells. Cancer research 46:3912–3916.

Sheng, McFadden, Greenberg (1990) Membrane depolarization and calcium induce c-fos transcription via phosphorylation of transcription factor CREB. Neuron 4:571–582.

Shoffner, Lott, Voljavec, Soueidan, Costigan, Wallace (1989) Spontaneous Kearns-Sayre/chronic external ophthalmoplegia plus syndrome associated with a mitochondrial DNA deletion: a slip-replication model and metabolic therapy. Proc Natl Acad Sci USA 86:7952–7956.

Shokolenko I, Venediktova N, Bochkareva A, Wilson GL, Alexeyev MF (2009) Oxidative stress induces degradation of mitochondrial DNA. Nucleic Acids Res 37:2539–2548.

Shoshan-Barmatz V, Mizrachi D (2012) VDAC1: From structure to cancer therapy. Frontiers Oncol 2:164.

Sidhu A, Wersinger C, Moussa C, Veier I (2004) The role of α-synuclein in both neuroprotection and neurodegeneration. Ann N Y Acad Sci 1035:250–270.

Sidransky E, Lopez G (2012) The link between the GBA gene and parkinsonism. Lancet Neurol 11:986–998.

Silva JP, Larsson N-G (2002) Manipulation of mitochondrial DNA gene expression in the mouse. Biochim Biophys Acta 1555:106–110.

Silver IA, Erecińska M (1994) Extracellular glucose concentration in mammalian brain: continuous monitoring of changes during increased neuronal activity and upon limitation in oxygen supply in normo-, hypo-, and hyperglycemic animals. J Neurosci 14:5066–5076.

Simon M, Strathmann M, Gautam N (1991) Diversity of G proteins in signal transduction. Science 252:802–808.

Simpson JN, McGinty JF (1995) Forskolin induces preproenkephalin and preprodynorphin mRNA in rat striatum as demonstrated by in situ hybridization histochemistry. Synapse 19:151–159.

Simpson P, Russell J (1996) Mitochondria support inositol 1,4,5-trisphosphate-mediated Ca2+ waves in cultured oligodendrocytes. J Biol Chem 271:33493–33501.

Smith KE, Gustafson EL, Borden LA, Dhar MT, Durkin MM, Vaysse P, Branchek TA, Gluchowski C, Weinshank RL (1996) Heterogeneity of brain GABA transporters. In: GABA: Receptors, Transporters and Metabolism, pp 63–72 Advances in Pharmacological Sciences. Birkhäuser Basel.

Smith W, Jiang H, Pei Z, Tanaka Y, Morita H, Sawa A, Dawson V, Dawson T, Ross C (2005) Endoplasmic reticulum stress and mitochondrial cell death pathways mediate A53T mutant alpha-synuclein-induced toxicity. Hum Mol Genet 14:3801–3811.

Smith Y, Surmeier DJ, Redgrave P, Kimura M (2011) Thalamic contributions to basal ganglia-related behavioral switching and reinforcement. J Neurosci 31:16102–16106.

Smith, Bevan, Shink, Bolam (1998) Microcircuitry of the direct and indirect pathways of the basal ganglia. Neuroscience 86:353–387.

Smrcka A (2008) G protein βγ subunits: Central mediators of G protein-coupled receptor signaling. Cell Mole Life Sci 65:2191–2214.

Soane, Solenski, Fiskum (2007) Mitochondrial Mechanisms of Oxidative Stress and Apoptosis. In: Brain Energetics. Integration of Molecular and Cellular Processes, 3rd ed. (Lajtha A, Gibson GE, Dienel GA, eds), pp 703-734 Handbook of Neurochemistry and Molecular Neurobiology. Springer US.

Soderling TR (1999) The Ca2+–calmodulin-dependent protein kinase cascade. Trends Biochem Sci 24:232–236.

Soghomonian J, Laprade N (1997) Glutamate decarboxylase (GAD67 and GAD65) gene expression is increased in a subpopulation of neurons in the putamen of parkinsonian monkeys. Synapse 27:122–132.

Soldner F, Stelzer Y, Shivalila CS, Abraham BJ, Latourelle JC, Barrasa MI, Goldmann J, Myers RH, Young RA, Jaenisch R (2016) Parkinson-associated risk variant in distal enhancer of α-synuclein modulates target gene expression. Nature 533:95–99.

Song M, Mihara K, Chen Y, Scorrano L, Dorn G (2015) Mitochondrial fission and fusion factors reciprocally orchestrate mitophagic culling in mouse hearts and cultured fibroblasts. Cell Metab 21:273–285.

Song Z, Chen H, Fiket M, Alexander C, Chan D (2007) OPA1 processing controls mitochondrial fusion and is regulated by mRNA splicing, membrane potential, and Yme1L. J Cell Biol 178:749–755.

Spelbrink J et al. (2001) Human mitochondrial DNA deletions associated with mutations in the gene encoding Twinkle, a phage T7 gene 4-like protein localized in mitochondria. Nat Genet 28:223–231.

Spillantini MG, Schmidt ML, Lee VM, Trojanowski JQ, Jakes R, Goedert M (1997) α-Synuclein in Lewy bodies. Nature 388:839–840.

Stachowiak O, Dolder M, Wallimann T, Richter C (1998) Mitochondrial creatine kinase is a prime target of peroxynitrite-induced modification and inactivation. J Biol Chem 273:16694–16699.

Stanton R (2012) Glucose-6-phosphate dehydrogenase, NADPH, and cell survival. IUBMB Life 64:362–369.

Starkov A (2013) An update on the role of mitochondrial α-ketoglutarate dehydrogenase in oxidative stress. Mol Cell Neurosci 55:13–16.

Starkov A, Fiskum G, Chinopoulos C, Lorenzo B, Browne S, Patel M, Beal F (2004) Mitochondrial α-Ketoglutarate Dehydrogenase Complex Generates Reactive Oxygen Species. J Neurosci 24:7779–7788.

Steece-Collier K, Collier T, Danielson P, Kurlan R, Yurek D, Sladek J (2003) Embryonic mesencephalic grafts increase levodopa-induced forelimb hyperkinesia in parkinsonian rats. Mov Disord 18:1442–1454.

Stefani D, Raffaello A, Teardo E, Szabò I, Rizzuto R (2011) A forty-kilodalton protein of the inner membrane is the mitochondrial calcium uniporter. Nature 476:336–340.

Stephens L, Smrcka A, Cooke F, Jackson T, Sternweis P, Hawkins P (1994) A novel phosphoinositide 3 kinase activity in myeloid-derived cells is activated by G protein beta gamma subunits. Cell 77:83–93.

Stephens, Mueller AJ, Shering AF, Hood SH, Taggart, Arbuthnott GW, Bell JE, Kilford, Kingsbury AE, Daniel SE, Ingham CA (2005) Evidence of a breakdown of corticostriatal connections in Parkinson's disease. Neuroscience:741–754.

Stepien, Torroni, Chung, Hodge, Wallace (1992) Differential expression of adenine nucleotide translocator isoforms in mammalian tissues and during muscle cell differentiation. J Biological Chem 267 132:14592–14597.

Stewart JB, Chinnery PF (2015) The dynamics of mitochondrial DNA heteroplasmy: implications for human health and disease. Nat Rev Genet 16:530–542.

Stewart JB, Larsson N-G (2014) Keeping mtDNA in Shape between Generations. PLoS Genetics 10:e1004670.

Stiburek L, Cesnekova J, Kostkova O, Fornuskova D, Vinsova K, Wenchich L, Houstek J, Zeman J (2012) YME1L controls the accumulation of respiratory chain subunits and is required for apoptotic resistance, cristae morphogenesis, and cell proliferation. Mol Biol Cell 23:1010–1023.

Stiburek L, Fornuskova D, Wenchich L, Pejznochova M, Hansikova H, Zeman J (2007) Knockdown of human Oxa1l impairs the biogenesis of F1Fo-ATP Synthase and NADH:Ubiquinone Oxidoreductase. J Mol Biol 374:506–516.

Stocker M (2004) Ca2+-activated K+ channels: molecular determinants and function of the SK family. Nat Rev Neurosci 5:758–770.

Stowers S, Megeath L, Górska-Andrzejak J, Meinertzhagen I, Schwarz T (2002) Axonal transport of mitochondria to synapses depends on milton, a novel Drosophila protein. Neuron 36:1063–1077.

Stuart JA, Bourque BM, de Souza-Pinto NC, Bohr VA (2005) No evidence of mitochondrial respiratory dysfunction in OGG1-null mice deficient in removal of 8-oxodeoxyguanine from mitochondrial DNA. Free Radic Bio Med 38:737–745.

Stuart JA, Maddalena LA, Merilovich M, Robb EL (2014) A midlife crisis for the mitochondrial free radical theory of aging. Longev Healthspan 3:1–15.

Stumpf J, Copeland W (2011) Mitochondrial DNA replication and disease: Insights from DNA polymerase γ mutations. Cell Mol Life Sci 68:219–233.

Sudhof T (2004) The synaptic vesicle cycle. Annu Rev Neurosci 27:509–547.

Sullivan LB, Gui DY, Hosios AM, Bush LN, Freinkman E, Vander Heiden MG (2015) Supporting aspartate biosynthesis is an essential function of respiration in proliferating cells. Cell 162:552–563.

Sulzer D, Bogulavsky J, Larsen KE, Behr G, Karatekin E, Kleinman MH, Turro N, Krantz D, Edwards RH, Greene LA, Zecca L (2000) Neuromelanin biosynthesis is driven by excess cytosolic catecholamines not accumulated by synaptic vesicles. Proc Natl Acad Sci USA 97:11869–11874.

Sulzer D, Zecca L (2000) Intraneuronal dopamine-quinone synthesis: a review. Neurotox Res 1:181–195.

Sun F, Huo X, Zhai Y, Wang A, Xu J, Su D, Bartlam M, Rao Z (2005) Crystal structure of mitochondrial respiratory membrane protein complex II. Cell 121:1043–1057.

Suomalainen A, Isohanni P (2010) Mitochondrial DNA depletion syndromes – Many genes, common mechanisms. Neuromuscular Disord 20:429–437.

Surmeier J, Guzman J, Sanchez-Padilla J (2010) Calcium, cellular aging, and selective neuronal vulnerability in Parkinson's disease. Cell Calcium 47:175–182.

Surmeier JD, Ding J, Day M, Wang Z, Shen W (2007) D1 and D2 dopamine-receptor modulation of striatal glutamatergic signaling in striatal medium spiny neurons. Trends Neurosci 30:228–235.

Suzuki A, Stern S, Bozdagi O, Huntley G, Walker R, Magistretti P, Alberini C (2011) Astrocyte-neuron lactate transport is required for long-term memory formation. Cell 144:810–823.

Svenningsson P, Fienberg A, Allen P, Moine C, Lindskog M, Fisone G, Greengard P, Fredholm B (2000) Dopamine D1 receptor-induced gene transcription is modulated by DARPP-32. J Neurochem 75:248–257.

Svenningsson P, Nishi A, Fisone G, Girault J-A, Nairn AC, Greengard P (2004) DARPP-32: An integrator of neurotransmission. Annu Rev Pharmacol Toxicol 44:269–296.

Świerczek M, Cieluch E, Sarewicz M, Borek A, Moser C, Dutton L, Osyczka A (2010) An Electronic Bus Bar Lies in the Core of Cytochrome bc1. Science 329:451–454.

Swulius MT, Waxham MN (2008) Ca2+/Calmodulin-dependent Protein Kinases. Cellular and Molecular Life Sciences 65:2637–2657.

Szabadkai G, Rizzuto R (2004) Participation of endoplasmic reticulum and mitochondrial calcium handling in apoptosis: more than just neighborhood? FEBS Lett 567:111–115.

Szabadkai, Simoni AM, Bianchi, Stefani D, Leo, Wieckowski MR, Rizzuto (2006) Mitochondrial dynamics and Ca2+ signaling. Biochim Biophys Acta 1763:442–449.

Szczesny B, Tann A, Longley M, Copeland W, Mitra S (2008) Long patch base excision repair in mammalian mitochondrial genomes. J Biol Chem 283:26349–26356.

Taanman J-W (1999) The mitochondrial genome: structure, transcription, translation and replication. Biochim Biophys Acta 1410:103–123.

Tachikawa M, Fukaya M, Terasaki T, Ohtsuki S, Watanabe M (2004) Distinct cellular expressions of creatine synthetic enzyme GAMT and creatine kinases uCK-Mi and CK-B suggest a novel neuron–glial relationship for brain energy homeostasis. Eur J Neurosci 20:144–160.

Tachikawa M, Hosoya K (2011) Transport characteristics of guanidino compounds at the blood-brain barrier and blood-cerebrospinal fluid barrier: relevance to neural disorders. Fluids Barriers CNS 8:1–12.

Taguchi N, Ishihara N, Jofuku A, Oka T, Mihara K (2007) Mitotic phosphorylation of dynamin-related GTPase Drp1 participates in mitochondrial fission. J Biol Chem 282:11521–11529.

Tang BL (2015) Miro GTPases in mitochondrial transport, homeostasis and pathology. Cells 5:E1.

Tang W, Gilman A (1991) Type-specific regulation of adenylyl cyclase by G protein beta gamma subunits. Science 254:1500–1503.

Tanner CM (1989) The role of environmental toxins in the etiology of Parkinson's disease. Trends Neurosci 12:49–54.

Taylor R, Turnbull D (2005) Mitochondrial DNA mutations in human disease. Nat Rev Genet 6:389–402.

Taylor-Robinson S, Turjanski N, Bhattacharya S, Seery J, Sargentoni J, Brooks D, Bryant D, Cox I (1999) A proton magnetic resonance spectroscopy study of the striatum and cerebral cortex in Parkinson's disease. Metab Brain Dis 14:45–55.

Temperley R, Wydro M, Lightowlers R, Chrzanowska-Lightowlers Z (2010) Human mitochondrial mRNAs—like members of all families, similar but different. Biochim Biophys Acta 1797:1081–1085.

Thayer, Miller (1990) Regulation of the intracellular free calcium concentration in single rat dorsal root ganglion neurones in vitro. J Physiology 425:85–115.

Thomas R, Andrews L, Burman J, Lin W-Y, Pallanck L (2014) PINK1-Parkin pathway activity is regulated by degradation of PINK1 in the mitochondrial matrix. PLoS Genetics:e1004279.

Thompson K et al. (2016) Recurrent de novo dominant mutations in SLC25A4 cause severe early-onset mitochondrial disease and loss of mitochondrial DNA copy number. Am J Hum Genetics 99:860–876.

Threlfell S, West AR (2013) Modulation of striatal neuron activity by cyclic nucleotide signalling and phosphodiesterase inhibition. Basal Ganglia 3:137–146.

Tieu K (2011) A guide to neurotoxic animal models of Parkinson's disease. Cold Spring Harbor Perspect Med 1:a009316.

Tondera D, Grandemange S, Jourdain A, Karbowski M, Mattenberger Y, Herzig S, Cruz S, Clerc P, Raschke I, Merkwirth C, Ehses S, Krause F, Chan D, Alexander C, Bauer C, Youle R, Langer T, Martinou J-C (2009) SLP-2 is required for stress-induced mitochondrial hyperfusion. EMBO J 28:1589–1600.

Tornheim, Lowenstein (1976) Control of phosphofructokinase from rat skeletal muscle. Effects of fructose diphosphate, AMP, ATP, and citrate. J Biol Chem 251:7322–7328.

Torres GE, Gainetdinov RR, Caron MG (2003) Plasma membrane monoamine transporters: structure, regulation and function. Nat Rev Neuro 4:13–25.

Treberg J, Quinlan C, Brand M (2011) Evidence for two sites of superoxide production by mitochondrial NADH-ubiquinone oxidoreductase (Complex I). J Biol Chem 286:27103–27110.

Trettel F, Rigamonti D, Hilditch-Maguire P, Wheeler VC, Sharp AH, Persichetti F, Cattaneo E, MacDonald ME (2000) Dominant phenotypes produced by the HD mutation in STHdh(Q111) striatal cells. Hum Mol Genet 9:2799–2809.

Tritsch NX, Sabatini BL (2012) Dopaminergic modulation of synaptic transmission in cortex and striatum. Neuron 76:33–50.

Truscott KN, Brandner K, Pfanner N (2003) Mechanisms of protein import into mitochondria. Curr Biol 13:R326–R337.

Tsai M-F, Jiang D, Zhao L, Clapham D, Miller C (2014) Functional reconstitution of the mitochondrial Ca2+/H+ antiporter Letm1. J Gen Physiol 143:67–73.

Tuite P (2016) Magnetic resonance imaging as a potential biomarker for Parkinson's disease. Trans Res 175:4–16.

Tullo A, Rossmanith W, Imre E, Sbisà E, Saccone C, Karwan M (1995) RNase mitochondrial RNA processing cleaves RNA from the rat mitochondrial displacement loop at the origin of heavy-strand DNA replication. Eur J Biochem 227:657–662.

Turjanski AG, Vaqué JP, Gutkind JS (2007) MAP kinases and the control of nuclear events. Oncogene 26:3240–3253.

Turjanski, Lees, Brooks (1997) In vivo studies on striatal dopamine D1 and D2 site binding in L-Dopa-treated Parkinson's disease patients with and without dyskinesias. Neurology:717–723.

Turner BM (2000) Histone acetylation and an epigenetic code. Bioessays 22:836–845.

Twig G, Elorza A, Molina A, Mohamed H, Wikstrom J, Walzer G, Stiles L, Haigh S, Katz S, Las G, Alroy J, Wu M, Py B, Yuan J, Deeney J, Corkey B, Shirihai O (2008) Fission and selective fusion govern mitochondrial segregation and elimination by autophagy. Embo J 27:433–446.

Twig G, Hyde B, Shirihai OS (2008) Mitochondrial fusion, fission and autophagy as a quality control axis: The bioenergetic view. Biochim Biophys Acta 1777:1092–1097.

Tyagi R, Azrad A, Degani H, Salomon Y (1996) Simultaneous extraction of cellular lipids and water-soluble metabolites: Evaluation by NMR spectroscopy. Magn Reson Med 35:194–200.

Tymianski M, Charlton M, Carlen P, Tator C (1993) Secondary Ca2+ overload indicates early neuronal injury which precedes staining with viability indicators. Brain Res 607:319–323.

Tzoulis C, Tran G, Coxhead J, Bertelsen B, Lilleng PK, Balafkan N, Payne B, Miletic H, Chinnery PF, Bindoff LA (2014) Molecular pathogenesis of polymerase gamma–related neurodegeneration. Ann Neurol 76:66–81.

Ubersax JA, Ferrell JE (2007) Mechanisms of specificity in protein phosphorylation. Nat Rev Mol Cell Biol 8:530–541.

Ungerstedt U (1968) 6-hydroxy-dopamine induced degeneration of central monoamine neurons. Eur J Pharmacol 5:107–110.

Valastro B, Dekundy A, Krogh M, Lundblad M, James P, Danysz W, Quack G, Cenci M (2007) Proteomic analysis of striatal proteins in the rat model of l-DOPA-induced dyskinesia. J Neurochem 102:1395–1409.

Valavanidis A, Vlachogianni T, Fiotakis C (2009) 8-hydroxy-2′ -deoxyguanosine (8-OHdG): A critical biomarker of oxidative stress and carcinogenesis. J Environ Sci Health C Environ Carcinog Ecotoxicol Rev 27:120–139.

Valente EM, Bentivoglio AR, Dixon PH, Ferraris A, Ialongo T, Frontali M, Albanese A, Wood NW (2001) Localization of a novel locus for autosomal recessive early-onset parkinsonism, PARK6, on human chromosome 1p35-p36. Am J Hum Genet 68:895–900.

Valjent E (2012) Striatal signaling: two decades of progress. Front Neuroanat 16:43.

Valjent, Corvol, Pages, Besson, Maldonado, Caboche (2000) Involvement of the extracellular signal-regulated kinase cascade for cocaine-rewarding properties. J Neurosci 20:8701–8709.

van Spronsen M, Mikhaylova M, Lipka J, Schlager M, van den Heuvel D, Kuijpers M, Wulf P, Keijzer N, Demmers J, Kapitein L, Jaarsma D, Gerritsen H, Akhmanova A, Hoogenraad C (2013) TRAK/Milton motor-adaptor proteins steer mitochondrial trafficking to axons and dendrites. Neuron:485–502.

Vanhoutte P, Barnier J-V, Guibert B, Pagès C, Besson M-J, Hipskind RA, Caboche J (1999) Glutamate induces phosphorylation of Elk-1 and CREB, along with c-fos activation, via an extracellular signal-regulated kinase-dependent pathway in brain slices. Mol Cell Biol 19:136–146.

Vannucci SJ (1994) Developmental expression of GLUT1 and GLUT3 glucose transporters in rat brain. J Neurochem 62:240–246.

Varanita T, Soriano M, Romanello V, Zaglia T, Quintana-Cabrera R, Semenzato M, Menabò R, Costa V, Civiletto G, Pesce P, Viscomi C, Zeviani M, Di Lisa F, Mongillo M, Sandri M, Scorrano L (2015) The Opa1-dependent mitochondrial cristae remodeling pathway controls atrophic, apoptotic, and ischemic tissue damage. Cell Metab 21:834–844.

Varoqui H, Zhu H, Yao D, Ming H, Erickson JD (2000) Cloning and functional identification of a neuronal glutamine transporter. J Biol Chem 275:4049–4054.

Verdin E, Hirschey MD, Finley L, Haigis MC (2010) Sirtuin regulation of mitochondria: energy production, apoptosis, and signaling. Trends Biochem Sci 35:669–675.

Verkhratsky AJ, Petersen OH (1998) Neuronal calcium stores. Cell Calcium 24:333–343.

Vernarecci S, Tosi F, Filetici P (2010) Tuning acetylated chromatin with HAT inhibitors: A novel tool for therapy. Epigenetics 5:105–111.

Vicente A, Galvão-Ferreira P, Tecuapetla F, Costa R (2016) Direct and indirect dorsolateral striatum pathways reinforce different action strategies. Curr Biol 26:R267–R269.

Vizin T, Kos J (2015) Gamma-enolase: a well-known tumour marker, with a less-known role in cancer. Radiol Oncol 49:217–226.

Volkenhoff A, Weiler A, Letzel M, Stehling M, Klämbt C, Schirmeier S (2015) Glial glycolysis is essential for neuronal survival in Drosophila. Cell Metab 22:437–447.

Voloboueva LA, Suh S, Swanson RA, Giffard RG (2007) Inhibition of mitochondrial function in astrocytes: Implications for neuroprotection. J Neurochem 102:1383–1394.

Von Kleist-Retzow J-C, Hornig-Do H-T, Schauen M, Eckertz S, Dinh T, Stassen F, Lottmann N, Bust M, Galunska B, Wielckens K, Hein W, Beuth J, Braun J-M, Fischer JH, Ganitkevich VY, Maniura-Weber K, Wiesner RJ (2007) Impaired mitochondrial Ca2+ homeostasis in respiratory chain-deficient cells but efficient compensation of energetic disadvantage by enhanced anaerobic glycolysis due to low ATP steady state levels. Exp Cell Res 313:3076–3089.

Wakabayashi J, Zhang Z, Wakabayashi N, Tamura Y, Fukaya M, Kensler T, Iijima M, Sesaki H (2009) The dynamin-related GTPase Drp1 is required for embryonic and brain development in mice. J Cell Biol 186:805–816.

Wakayashi K, Takahashi H, Takeda S, Ohama E, Ikuta F (1989) Lewy bodies in the enteric nervous system in Parkinson's disease. Arch Histol and Cytol 52:191–194.

Walaas S, Hemmings H, Greengard P, Nairn A (2011) Beyond the dopamine receptor: Regulation and roles of serine/threonine protein phosphatases. Front Neuroanat 5:50.

Wallace D (1999a) Mitochondrial diseases in man and mouse. Science 283:1482–1488.

Wallace D (2005) A mitochondrial paradigm of metabolic and degenerative diseases, aging, and cancer: A dawn for evolutionary medicine. Genetics 39:359–407.

Wallace D, Lott M, Procaccio V (2013) Mitochondrial medicine: The mitochondrial biology and genetics of metabolic and degenerative diseases, cancer and aging. In: Emery and Rimoin's Principles and Practice of Medical Genetics (Rimoin DL, Pyeritz RE, Korf B, eds) pp 1-153 Elsevier.

Wallace DC (1992) Diseases of the mitochondrial DNA. Annu Rev Biochem 61:1175–1212.

Wallace DC (1999) Mitochondrial diseases in man and mouse. Science 283:1482–1488.

Wallace DC (2010) Mitochondrial DNA mutations in disease and aging. Environ Mol Mutagen 51:440–450.

Wallace DC, Chalkia D (2013) Mitochondrial DNA genetics and the heteroplasmy conundrum in evolution and disease. Cold Spring Harb Perspect Biol 5:a021220.

Wallimann T, Hemmer W (1994) Creatine kinase in non-muscle tissues and cells. Mol Cell Biochem 133:193–220.

Wallimann T, Tokarska-Schlattner M, Schlattner U (2011) The creatine kinase system and pleiotropic effects of creatine. Amino Acids 40:1271–1296.

Wallmichrath I, Szabo B (2002) Analysis of the effect of cannabinoids on GABAergic neurotransmission in the substantia nigra pars reticulata. Naunyn-Schmiedeberg's Arch Pharmacol 365:326–334.

Walters JR (2017) Abnormal activities in cortico-basal ganglia circuits in movement disorders. In: Handbook of Basal Ganglia Structure and Function, 2nd ed. (Steiner H, Tseng KY, eds), pp 741–754 Handbook of Behavioral Neuroscience. Academic Press.

Wamelink, Struys, Jakobs (2008) The biochemistry, metabolism and inherited defects of the pentose phosphate pathway: A review. J Inherit Metab Dis 31:703–717.

Wang D, Shu Z, Lieser S, Chen P-L, Lee W-H (2009) Human mitochondrial SUV3 and polynucleotide phosphorylase form a 330-kDa heteropentamer to cooperatively degrade double-stranded RNA with a 3′-to-5′ directionality. J Biol Chem 284:20812–20821.

Wang G, Chen H-W, Oktay Y, Zhang J, Allen E, Smith G, Fan K, Hong J, French S, McCaffery M, Lightowlers R, Morse H, Koehler C, Teitell M (2010) PNPASE regulates RNA import into mitochondria. Cell 142:456–467.

Wang X, Schwarz T (2009) The mechanism of Ca2+-dependent regulation of kinesin-mediated mitochondrial motility. Cell 136:163–174.

Wang X, Yan M, Fujioka H, Liu J, Wilson-Delfosse A, Chen S, Perry G, Casadesus G, Zhu X (2012) LRRK2 regulates mitochondrial dynamics and function through direct interaction with DLP1. Hum Mol Genet 21:1931–1944.

Wang Z, Zang C, Rosenfeld J, Schones D, Barski A, Cuddapah S, Cui K, Roh T-Y, Peng W, Zhang M, Zhao K (2008) Combinatorial patterns of histone acetylations and methylations in the human genome. Nat Genet 40:897–903.

Warren EB, Sillivan SE, Konradi C (2017) Receptors and second messengers in the basal ganglia. In: Handbook of Basal Ganglia Structure and Function, 2nd ed. (Steiner H, Tseng KY, eds), pp 555–581 Handbook of Behavioral Neuroscience. Academic Press.

Warren EB, Aicher AE, Fessel JP, Konradi C (2017) Mitochondrial DNA depletion by ethidium bromide decreases neuronal mitochondrial creatine kinase: Implications for striatal energy metabolism. PLoS ONE 12(12): e0190456.

Weiduschat N, Mao X, Beal FM, Nirenberg MJ, Shungu DC, Henchcliffe C (2013) Usefulness of proton and phosphorus MR spectroscopic imaging for early diagnosis of Parkinson's disease. J Neuroimaging 25:105–110.

Weintraub D, Koester J, Potenza MN, Siderowf AD, Stacy M, Voon V, Whetteckey J, Wunderlich GR, Lang AE (2010) Impulse control disorders in Parkinson disease: A cross-sectional study of 3090 patients. Arch Neurol 67:589–595.

Weitzman PDJ, Dunmore P (1969) Citrate synthases: Allosteric regulation and molecular size. Biochim Biophys Acta 171:198–200.

Wellstead P, Cloutier M (2011) An energy systems approach to Parkinson's disease. Wiley Interdiscip Rev Syst Biol Med 3:1–6.

Wendt S, Schlattner U, Wallimann T (2003) Differential effects of peroxynitrite on human mitochondrial creatine kinase isoenzymes: Inactivation, octamer destabilization, and identification of involved residues. J Biol Chem 278:1125–1130.

West PA, Khoury-Hanold W, Staron M, Tal MC, Pineda CM, Lang SM, Bestwick M, Duguay BA, Raimundo N, MacDuff DA, Kaech SM, Smiley JR, Means RE, Iwasaki A, Shadel GS (2015) Mitochondrial DNA stress primes the antiviral innate immune response. Nature 520:553–557.

Westergaard, Sonnewald, Schousboe (1995) Metabolic trafficking between neurons and astrocytes: The glutamate/glutamine cycle revisited. Dev Neurosci 17:203–211.

Westermann B (2012) Bioenergetic role of mitochondrial fusion and fission. Biochim Biophys Acta 1817:1833–1838.

Westin JE, Vercammen L, Strome EM, Konradi C, Cenci AM (2007) Spatiotemporal pattern of striatal ERK1/2 phosphorylation in a rat model of L-DOPA–Induced Dyskinesia and the role of dopamine D1 receptors. Biol Psychiatry 62:800–810.

Westin, Andersson, Lundblad, Cenci (2001) Persistent changes in striatal gene expression induced by long-term L-DOPA treatment in a rat model of Parkinson's disease. Eur J Neurosci 14:1171–1176.

Wiedemann N, Pfanner N (2015) Mitochondrial machineries for protein import and assembly. Annu Rev Biochem 86:1–30.

Wiegert SJ, Bading H (2011) Activity-dependent calcium signaling and ERK-MAP kinases in neurons: A link to structural plasticity of the nucleus and gene transcription regulation. Cell Calcium 49:296–305.

Wittich C, Khambatta S, Nguyen D, Beckman T (2014) Kearns–Sayre syndrome: a case series of 35 adults and children. Int J Gen Medicine 7:325–332.

Wong W, Scott JD (2004) AKAP signalling complexes: focal points in space and time. Nat Rev Mol Cell Biol 5:959–970.

Writing Group for the NINDS Exploratory Trials in Parkinson's Disease Investigators (2015) Effect of creatine monohydrate on clinical progression in patients with Parkinson's disease: A randomized clinical trial. JAMA. 313:584-593

Wu S-B, Wei Y-H (2012) AMPK-mediated increase of glycolysis as an adaptive response to oxidative stress in human cells: Implication of the cell survival in mitochondrial diseases. Biochim Biophys Acta 1822:233–247.

Wu SS, Frucht SJ (2005) Treatment of Parkinson's disease: What's on the horizon? CNS Drugs 19:723–743.

Wyss M, Kaddurah-Daouk R (2000) Creatine and creatinine metabolism. Physiol Rev 80:1107–1213.

Xia Z, Storm DR (2005) The role of calmodulin as a signal integrator for synaptic plasticity. Nat Rev Neurosci 6:267–276.

Xie C, Zhang Y-Y, Wang X-D, Chen J, Chen Y-H, Pa J-L, Lin S-Y, Lin H-Z, Wang W-W (2015) Levodopa alone compared with levodopa-sparing therapy as initial treatment for Parkinson's disease: A meta-analysis. Neurol Sci 36:1319–1329.

Y-W-Man, Griffiths, Brown, Howell, Turnbull, Chinnery (2002) The epidemiology of Leber hereditary optic neuropathy in the North East of England. Am J Hum Genet 72:333–339.

Yadid G, Pacak K, Golomb E, Harvey-White J, Lieberman D, Kopin I, Goldstein D (1993) Glycine stimulates striatal dopamine release in conscious rats. British journal of pharmacology 110:50–53.

Yakubovskaya E, Guja K, Eng E, Choi W, Mejia E, Beglov D, Lukin M, Kozakov D, Garcia-Diaz M (2014) Organization of the human mitochondrial transcription initiation complex. Nucleic Acids Res 42:4100–4112.

Yamada M, Yasuhara H (2004) Clinical pharmacology of MAO inhibitors: Safety and future. Neurotoxicology 25:215–221.

Yan Y-B (2016) Creatine kinase in cell cycle regulation and cancer. Amino Acids 48:1775–1784.

Yang C, Kazanietz M (2003) Divergence and complexities in DAG signaling: looking beyond PKC. Trends Pharmacol Sci 24:602–608.

Yang M, Bowmaker M, Reyes A, Vergani L, Angeli P, Gringeri E, Jacobs H, Holt I (2002) Biased incorporation of ribonucleotides on the mitochondrial L-strand accounts for apparent strand-asymmetric DNA replication. Cell 111:495–505.

Ye Y, Li M, Gu L, Chen X, Shi J, Zhang X, Jiang C (2016) Chromatin remodeling during in vivo neural stem cells differentiating to neurons in early Drosophila embryos. Cell Death Differ 24:409–420.

Yoshikawa S, Muramoto K, Shinzawa-Itoh K (2011) Proton-pumping mechanism of cytochrome c oxidase. Annu Rev Biophys 40:205–223.

Youle R, Narendra D (2010) Mechanisms of mitophagy. Nat Rev Mol Cell Bio 12:9–14.

Youle R, van der Bliek A (2012) Mitochondrial fission, fusion, and stress. Science 337:1062–1065.

Young M, Copeland W (2016) Human mitochondrial DNA replication machinery and disease. Curr Opin Genetics Dev 38:52–62.

Yu M, Shi Y, Wei X, Yang Y, Zhou Y, Hao X, Zhang N, Niu R (2007) Depletion of mitochondrial DNA by ethidium bromide treatment inhibits the proliferation and tumorigenesis of T47D human breast cancer cells. Toxicol Lett 170:83–93.

Yuksel C, Du F, Ravichandran C, Goldbach JR, Thida T, Lin P, Dora B, Gelda J, O'Connor L, Sehovic S, Gruber S, Ongur D, Cohen BM (2015) Abnormal high-energy phosphate molecule metabolism during regional brain activation in patients with bipolar disorder. Mol Psychiatry 20:1079–1084.

Zaja-Milatovic, Milatovic, Schantz, Zhang, Montine, Samii, Deutch, Montine (2005) Dendritic degeneration in neostriatal medium spiny neurons in Parkinson disease. Neurology 64:545–547.

Zampese E, Galtieri DJ, Schumacker PT, Surmeier DJ (2017) Chapter 41: Determinants of Selective Vulnerability of Dopamine Neurons in Parkinson's Disease. In: Handbook of Basal Ganglia Structure and Function, 2nd ed. (Steiner H, Tseng KY, eds), pp 821–837. Handbook of Behavioral Neuroscience. Academic Press.

Zesiewicz T, Sullivan K, Hauser R (2007) Levodopa-induced dyskinesia in Parkinson's disease: Epidemiology, etiology, and treatment. Curr Neurol Neurosci Rep 7:302–310.

Zeviani M, Moraes C, DiMauro S, Nakase H, Bonilla E, Schon E, Rowland L (1998) Deletions of mitochondrial DNA in Kearns-Sayre syndrome. Neurology 51:1525-1533

Zhang D (2008) Mechanistic Studies of the Nrf2-Keap1 Signaling Pathway. Drug Metab Rev 38:769–789.

Zhang S-H, Gao F-J, Sun Z-M, Xu P, Chen J-Y (2016) High pressure-induced mtDNA alterations in retinal ganglion cells and subsequent apoptosis. Front Cell Neurosci 10:1–10.

Zhang SF, Hennessey T, Yang L, Starkova NN, Beal MF, Starkov AA (2010) Impaired brain creatine kinase activity in Huntington's Disease. Neurodegener Dis 8:194–201.

Zhao Q, Wang J, Levichkin I, Stasinopoulos S, Ryan M, Hoogenraad N (2002) A mitochondrial specific stress response in mammalian cells. EMBO J 21:4411–4419.

Zheng J (2012) Energy metabolism of cancer: Glycolysis versus oxidative phosphorylation. Oncol Lett 4:1151–1157.

Zickermann V, Wirth C, Nasiri H, Siegmund K, Schwalbe H, Hunte C, Brandt U (2015) Mechanistic insight from the crystal structure of mitochondrial complex I. Science 347:44–49.

Zimprich A et al. (2004) Mutations in LRRK2 cause autosomal-dominant parkinsonism with pleomorphic pathology. Neuron 44:601–607.

Zoccolella S, Lamberti S, Iliceto G, Santamato A, Lamberti P, Logroscino G (2010) Hyperhomocysteinemia in L-dopa treated patients with Parkinson's disease: Potential implications in cognitive dysfunction and dementia? Curr Med Chem 17:3253–3261.

Zylber E, Vesco C, Penman S (1969) Selective inhibition of the synthesis of mitochondria-associated RNA by ethidium bromide. J Mol Biol D44:195–204.